international conference

FT 2021

conference proceedings

Darko Lovrec
Vito Tič
Editors

University of Maribor Press

Fluid Power 2021
Fluidna Tehnika 2021

MARIBOR, 16.–17. SEPTEMBER 2021

University of Maribor
Faculty of Mechanical Engineering

International conference
Fluid Power 2021

Conference Proceedings

Editors
Darko Lovrec
Vito Tič

September 2021

University of Maribor Press

Fluid Power 2021

DARKO LOVREC & VITO TIČ

Abstract The International Fluid Power Conference is a two-day event, intended for all those professionally involved with hydraulic or pneumatic power devices and for all those, wishing to be informed about the 'state of the art', new discoveries and innovations within the field of hydraulics and pneumatics. The gathering of experts at this conference in Maribor has been a tradition since 1995, and is organised by the Faculty of Mechanical Engineering at the University of Maribor, in Slovenia. Fluid Power conferences are organised every second year and cover those principal technical events within the field of fluid power technologies in Slovenia, and throughout this region of Europe. This year's conference is taking place on the 16th and 17th September in Maribor. The main focus of this year's contributions is on the integration of information systems in the field of fluid technology.

Keywords: • fluid power technology • components and systems • control systems • fluids • maintenance and condition monitoring •

CORRESPONDENCE ADDRESS: Darko Lovrec, University of Maribor, Faculty of Mechanical Engineering, Maribor, Slovenia, e-mail: darko.lovrec@um.si. Vito Tič, University of Maribor, Faculty of Mechanical Engineering, Maribor, Slovenia, e-mail: vito.tic@um.si.

Table of Contents

University of Maribor Press

Plenary speak

Potential for Fluid power to Contribute to EU climate Goal 2030

KATHARINA SCHMITZ, YANNICK DUENSING, CHRISTIAN HAAS & GUNNAR MATTHIESEN

Abstract Fluid power drives and systems are an important technology for industrial and mobile applications. Therefore, attention must be drawn to the consequences of worldwide and particular EU climate goals. The chancing climate affects all humans and to reduce serious dangers for our and the next generations greenhouse gas emissions must be dramatically reduced in the next years. In this paper, the EU climate goals are introduced and measures are outlined on how fluid power can contribute to the achievement of the targets. There is still a long way in all industries to go to achieve the goal of zero greenhouse gas emissions, but we need now to think and talk about consequences and challenges for fluid power community.

Keywords: • sustainability • mobile machinery • digitisation • carbon footprint • energy efficiency •

CORRESPONDENCE ADDRESS: Katharina Schmitz, RWTH Aachen University, ifas – Institute for fluid power drives and systems, Campus Boulevard 30, 52074 Aachen, Germany, e-mail: Katharina.schmitz@ifas.rwth-aachen.de. Yannick Duensing, RWTH Aachen University, ifas – Institute for fluid power drives and systems, Campus Boulevard 30, 52074 Aachen, Germany, e-mail: Yannick.duensing@ifas.rwth-aachen.de. Christian Haas, RWTH Aachen University, ifas – Institute for fluid power drives and systems, Campus Boulevard 30, 52074 Aachen, Germany, e-mail: Christian.Haas@ifas.rwth-aachen.de. Gunnar Matthiesen, RWTH Aachen University, ifas – Institute for fluid power drives and systems, Campus Boulevard 30, 52074 Aachen, Germany, e-mail: Gunnar.Matthiesen@ifas.rwth-aachen.de.

1   Introduction

Climate change has become one of the greatest risk factors for humanity in recent decades. Extreme weather and natural disasters have forced societal attitudes to change. Additionally, Regulations of the UN and the federal government provide motivation for all sectors to further develop their current practices not only in terms of economic but also ecological aspects to combat climate change.

Fluid power is an important drive technology when a good controllability of high forces or high torques is required. In general, fluid power can be a very sustainable future technology. But, there are some aspects that need to be solved to contribute to worldwide climate goals and to satisfy sustainability demands.

2   EU Climate Goal 2030

With the Climate Goal 2030 member countries of the EU defined a more detailed, ambitious but also necessary plan to achieve the goals of the Paris Agreement of 2015. The Agreement itself is derived from the Kyoto Protocol, which was first drafted by the United Nations Framework Convention on Climate Change (UNFCCC) in 1992 and adopted in 2005 with the purpose to stabilize the concentration of greenhouse gases in the atmosphere in order to prevent dangerous human-induced disruption of the climate system [1].

2.1   Kyoto protocol and Paris Agreement

Three economic mechanisms were designed in the Kyoto Protocol to help industrialized countries meet their reduction targets: Emissions Trading, Joint Implementation and the Clean Development Mechanism, which are still relevant today. The Clean Development Mechanism allowed well developed countries to help developing countries in implementing climate saving mechanism with the benefit that the emission reductions are credited to themselves. The Emission Trading enabled all countries to trade emission certificates. By achieving and overshooting the set reduction goal of a country, additional certificates could be sold. This was often criticized, as wealthy countries bought certificates to reach their target instead of advancing their reduction efforts, as well as that some of countries with the most emissions and therefore the greatest impact withdrew from the Protocol after the first commitment period.
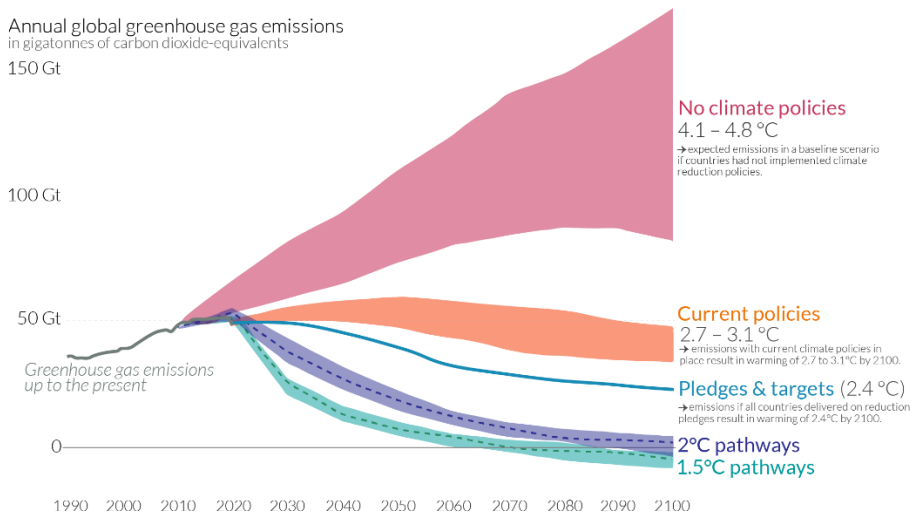
Figure 1: Annual global greenhouse gas emissions [2].

Following the Kyoto Protocol, the Paris Agreement of 2015 was signed by members of the UN Climate Convention with the target to limit the global temperature increase to 1.5 °C over the next 35 years by reduction of climate-damaging emissions such as greenhouse gases like carbon dioxide and nitrogen oxide [3]. In the second half of the century further advances should achieve climate neutrality by reaching an equilibrium between emitted and bound greenhouse gases. Instead of just one common goal for all members like in the Kyoto Protocol, the Paris Agreement also demand for individual intended national determined contribution (NDC) to be included into the international agreement. To ensure transparency, each country reports on its progression every 5 years including newly set ambitious goals to an established committee starting in 2020. As an example Figure 2 displays the graph of the historic and projected emissions under the 2030 emission target for the United States of America [4].
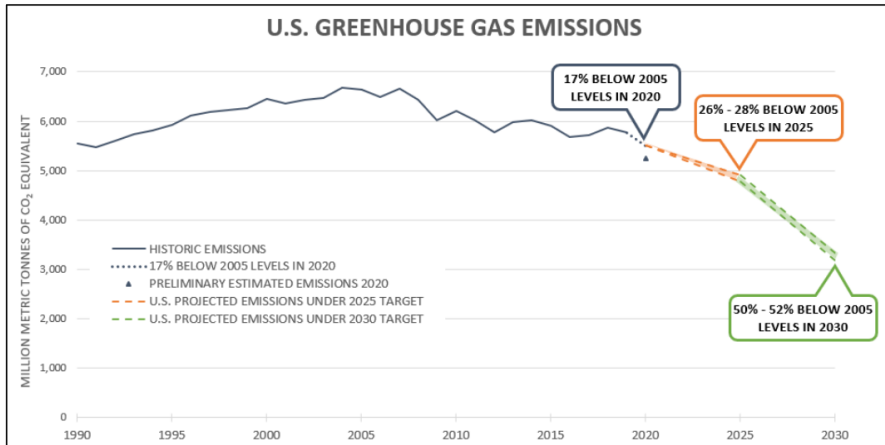
Figure 2: Historic and projected emissions under the 2030 climate target of the United States of America [4]**.**

Additionally the agreement encourages all members to conserve and enhance sinks and reservoirs of greenhouse gases such as forests [3]. Other main objectives worth mentioning are the enhancement of resilience to climate impacts, many of which are unavoidable due to already emitted greenhouse gases and to align financial flows in the wold with the aforementioned objectives [3].

2.2   European Green Deal

Following the Paris Agreement, the European Green Deal aims to make Europe the first climate neutral continent in the world. It is derived from the Paris Agreement, but sets more ambitious goals for its members in a fair, cost effective and competitive way. While still keeping the distant goal of the Paris Agreement to reach global emission neutrality by 2050, all 27 EU members committed to the green new deal, which sets an intermediate target of reducing the greenhouse gas emissions by 55% by 2030 compared to the levels of 1990. Achieving this goal is only possible by simultaneously tackling and investing in sectors like energy, transport, agriculture, finance and regional development, industry as well as research and innovation. All with the greater good of improving the climate, environment and oceans. An overview of the green new deal is given in Figure 3.
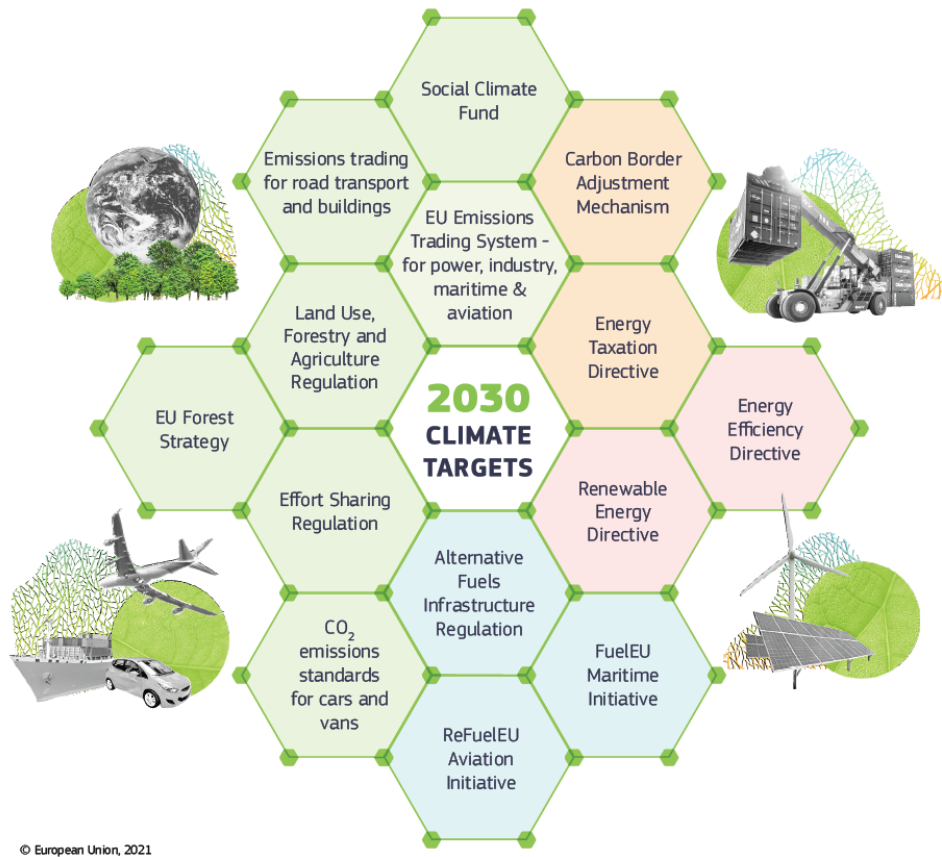
Figure 3: 2030 Climate targets of the European Green Deal [5]**.**

2.3   Emission sources

When trying to reduce the greenhouse gas emissions, it is essential to identify the sectors with the highest impact. Looking at Figure 4 it is clear to see, that the energy sector accounts for the largest share next to agriculture, forestry and land use. Interesting for the scope of this paper is the energy used for operation as well as the energy for manufacturing products and components including the extraction and processing of raw materials such as steel and other metals.
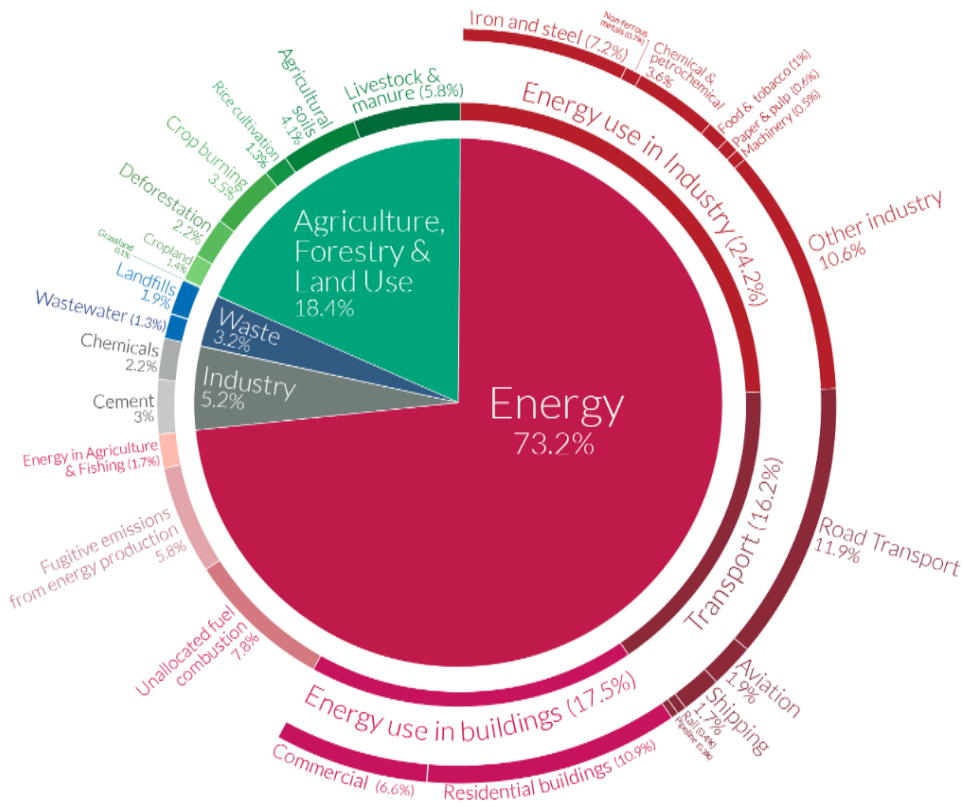
Figure 4: Global greenhouse gas emissions by sector [6]**.**

3   Contribution Potential by Fluid Power

In fluid power industry, three key aspects are of special relevance: 1. Energy consumption of hydraulic and pneumatic systems, 2. Energy and resources needed for manufacturing these components and 3. Overall energy consumption of machines using fluid power drives.

In fact, the emissions linked to the production of hydraulic and pneumatic components only makes up a minor impact as the operation of these components add up to significant greater amounts of greenhouse gas emissions. Previous investigation of a pneumatic drives showed that 99 % of all the entire life cycle emission are due to the energy consumption [7]. Nevertheless, in the future the manufacturing of the products and materials will increase in importance in fighting climate change as the operation

emission will decrease due to the use of electricity from more and more renewable energy sources.

3.1   Sustainable Components & Fluids

When talking about sustainable components, the production of steel and aluminium is a mayor challenge. But, fluid power components have not yet reached the state to only consist of one material that is uncritical to produce. In hydraulics more effort must be set to find better materials for tribological contacts in hydrostatic pumps and motors in order to avoid problematic materials like lead. In previous investigations at ifas, different special alloys were tested to their operation capability in hydrostatic pumps as an alternative to lead. The tribological tests show good behaviour, long endurances and a reduced coefficient of friction [8].

In addition to manufacturing, energy losses in components during operation should be pressed to a minimum. Therefore, new technologies in manufacturing can be useful. One approach is the use of additive manufacturing for the production of fluid power components. This allows the design of smooth flow channels with the benefit of a rigid reduction of pressure losses due to fluid friction. In addition, this allows a more compact design leading to an increase in power density and a reduction of installation space demands. In consequence, this space can then be used in a machine or systems for other components to increase energy saving measures. In Figure 5 an example for an additive manufactured gear pump housing designed at ifas can be seen.

Figure 5: Additive Manufactured Gear Pump [9].

In hydraulics, not only the components such as pumps, motors and valves must be considered but also the pressure media. Standard mineral oil has a CO_2 equivalent of about 3.56 kg for 1 kg oil [10]. In comparison with the overall energy consumption of a fluid power system this can often be neglected, but for the overall goal to reach complete sustainability this aspect needs to be considered in the future.

3.2   Energy efficiency in fluid power systems

The sustainability of fluid power systems and our contribution to worldwide climate goals mainly is a question of energy consumption. In the last decades fluid power community has worked on different measures to decrease energy consumption and to increase energy efficiency. In research, many measures were developed and presented but higher investment costs restricted the extensive use in industry. Nevertheless, the question of energy efficiency will rise in the next years. Special attention should be paid to the overall performance and energy consumption of complete machines and systems. Especially when interacting with other drive technologies like electric motors or diesel engines the overall efficiency is of importance and not only the energy consumption of the fluid power system.

One impressive example for the benefit of a holistic approach is the STEAM project at ifas. There, the hydraulic system of a mobile excavator was optimised in a holistic consideration together with the diesel engine. By using a multipressure hydraulic system and storing some hydraulic energy in accumulators, it was possible to reduce the diesel engine speed from 1800 rpm to 1200 rpm and most power was withdrawal at the optimum operation point of the engine.
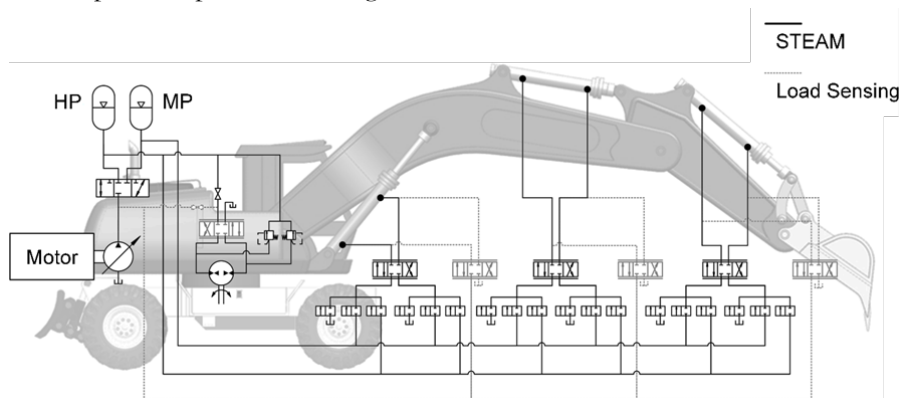
Figure 6: STEAM – Multipressure hydraulic system [11].

In addition, the hydraulic pump was mainly set to a large swivel angle, leading to a higher efficiency of the hydraulic pump. In consequence the measures led to a fuel consumption of -27 % in a standard dig-and-dump cycle [11]. Many more examples like this exist and more effort must be made to decrease energy consumption of fluid power systems and the machines they are used in.

3.3   Smart Fluid Power

The reduction of energy demands in fluid power systems as well as a further increase in operating uptime can be achieved using digital components and approaches. By the use of more sensors inside systems and components, more information of the current state of the system are available. These data can be used for condition monitoring and predictive maintenance approaches leading to reduced downtimes of machines and systems and also allowing longer operation durations with maximal energy efficiency. More research and development is needed here to find efficient and robust ways to extract the required information out of the collected data. Here, machine learning algorithms and artificial intelligence are needed to achieve afore mentioned goals [12], [13].
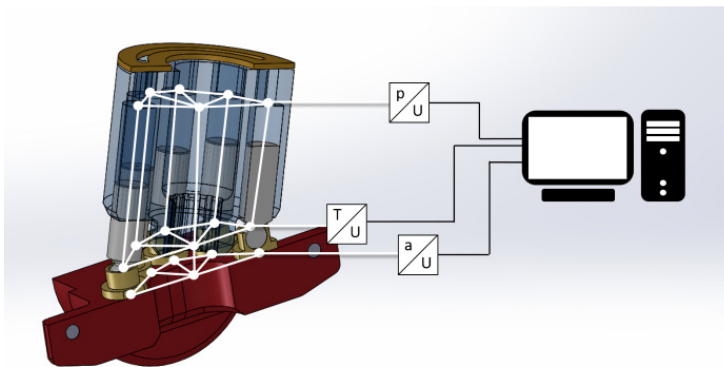
Figure 7: Integrated sensors in a hydraulic pump.

Next to data analysis from components and systems in operation, the further development of virtual representations of both is essential. At ifas, a simulation model was developed that allows for the purely physical modelling of the friction force and the wear of translator seals [14]. Having such simulation tools, the next step could be the implementation of a virtual twin for a component like a rod seal, and the current wear status could be simulated simultaneously to its operation.
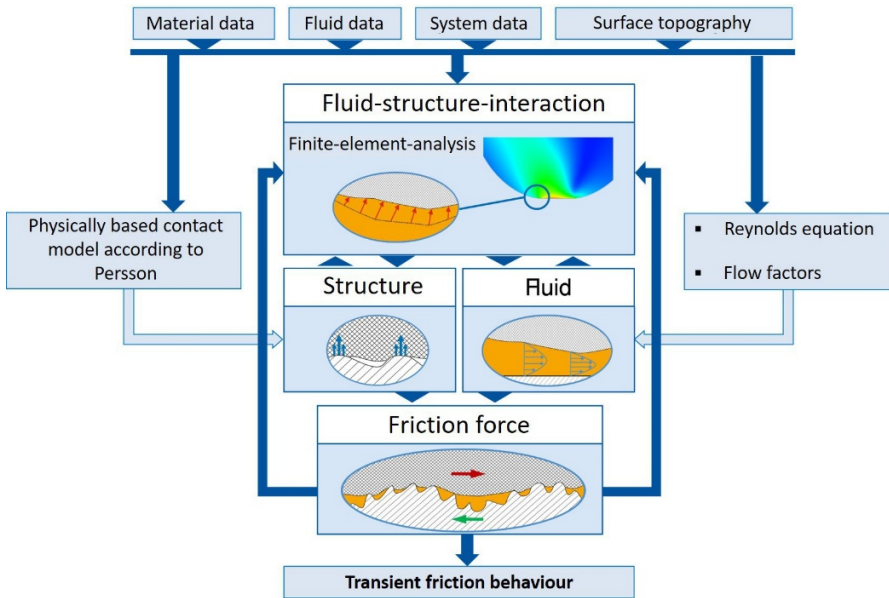
Figure 8: IFAS sealing simulation approach [14]**.**

3.4   Connected Machines

Hydraulic systems are widely used in construction machineries. Therefore it is ineviTable to look at this sector separately. Construction machinery is responsible for a relevant share of global CO_2, NOx and particulate matter emissions. In Germany, construction machinery accounts for ~12 % (123.6 kt p. a.) of all NOx emissions and ~7 % (13.5 kt p. a.) of all particulate matter emissions. Nevertheless, extensive construction activities are necessary for the expansion of renewable energies and for the energy-efficient refurbishment of buildings [15], [16].

At the same time, the construction industry is inefficient in terms of labour productivity compared to other industries, which offers great potential for machine adaptation, including the use of new drive technology or more efficient automated machine operation. In the last decades, the productivity in all industrial sectors increased (world GDP +13 % in last 20 years) due to more automation. In contrast, in the construction sector productivity stagnated [17].

In order to reduce emissions, especially in urban areas, smaller battery-powered construction machines are increasingly being used. However, these are still significantly more expensive than diesel-powered machines and have therefore not yet gained widespread acceptance [18].

Still, to gain more productivity and lower the emissions, energy, and resource consumption the automation of construction machines is a necessity. Since the automation of construction machinery is a major challenge, the first step is to locally remove the operator from the machine itself. The operator controls the machine remotely, first from the construction site itself, then remotely from any distance. By controlling the machine from outside the jobsite environment, employees no longer need to be present on site and are no longer exposed to physically stressful environments, no longer have to travel, which results in direct CO2 savings and can thus be deployed regardless of location [19], [20], [21]. If subtasks are now automated step by step, productivity can be significantly increased until the operator becomes the supervisor of several highly automated, highly efficient construction machines.

In recent years manufacturers of construction machinery developed assisting systems like semi-autonomous digging functions, weighting systems or geo-fencing systems to raise productivity and increase safety for operator, machine and environment. Especially the safety increases are essential as the construction industry is one of the sectors with the highest number of occupational accidents [22].

Besides the improvement of digging functions, e.g. by machine learning motion controllers, linking the interoperation between several machines and gathering and distributing the environmental information is in the focus of current researches. This includes the recording and processing of environmental information, e. g. by LIDAR or camera, the derivation of actions, e.g. by AI or decision trees, as well as advanced communication between construction site members [20], [23], [24].

Beside electrification, automation is a key solution, to make machines more efficient. Automation can help reduce the quantity of resources needed and decrease the energy consumption. These areas offer even more potential for improvement in the future when the machines are interoperable connected. Remote control of machines that cannot be fully automated today allow the reduction of workload on operators, resulting in a less stressful work environment and thus higher morale. Nevertheless, more

research is needed to cope with these highly complex tasks and to reduce the high greenhouse gas emissions and inefficiencies in the energy intensive construction industry.

4   Conclusion

The contribution to worldwide climate goals and EU climate goal in particular is of high relevance for fluid power development and research. The global greenhouse gas emissions must be drastically reduced in the next years.

In this paper different approaches were detected and shown as a starting point for longer discussions and deepening research and development projects how fluid power community can contribute to this mayor human challenge.

References

[1]   United Nations (1998) – Kyoto Protocol to the United Nations Framework Convention on Climate
[2]   Climate Action Tracker (2021) - OurWorldinData.org
[3]   United Nations (2015) – Paris Agreement
[4]   The United States of America (2020) – Nationally Determined Contribution (NDC) – Reducing Greenhouse Gases in the United States: A 2030 Emission Target
[5]   European Comission – Architecture Factsheet: Delivering the European Green Deal, The Decisive Decade - doi: 10.2775/352471
[6]   Ritchie, H., Roser, M. (2020). CO₂ and Greenhouse Gas Emissions - OurWorldInData.org
[7]   Merkelbach, S. (2019) Analysis of the Economic and Ecological Properties of Pneumatic Actuator Systems with Pneumatic Transformers, PhD thesis, RWTH Aachen, Shaker
[8]   Holzer, A., Schmitz, K. (2021). Effizienzsteigerung von Verdrängereinheiten durch optimales Einlaufen, final report of govermental fundated research project, AiF No. 20083 N/1
[9]   Matthiesen, G., et.al, (2020). Design and experimental investigation of an additive manufactured compact drive, Proceedings of the 12th International Fluid Power Conference 12. IFK, Dresden, Germany
[10]   McManus, M. C., Hammond, G. P., Burrows, C. R., (2003). Life-Cycle Assessment of Mineral and Rapeseed Oil in Mobile Hydraulic Systems. In Journal of Industrial Ecology, 2003, 7; S. 163–177.
[11]   Vukovic, M., (2017). Hydraulic Hybrid Systems for Excavators, PhD thesis, RWTH Aachen, Shaker
[12]   Makansi, F., Schmitz, K., (2021). Simulation Based Data Sampling for Condition Monitoring of Fluid Power Drives, Proceedings of the 19th Drive Train Technology Conference (ATK 2021), Aachen, Germany
[13]   Duensing, Y., A. Rodas Rivas, Schmitz, K., (2020). Machine Learning for failure mode detection in mobile machinery, Proceedings of the 11. Kolloquium Mobilhydraulik: Karlsruhe, Germany
[14]   Angerhausen, J, Physikalisch motivierte, (2020). Transiente Modellierung translatorischer Hydraulikdichtungen, PhD thesis, RWTH Aachen, Shaker

[15]   Helms, H., Heidt, C., (2014). Schadstoffemissionenund Belastungsbeitrag mobiler Maschinen in Baden-Württemberg

[16]   Helms, H., Heidt, C., (2014). Erarbeitung eines Konzepts zur Minderung der Umweltbelastung aus NRMM (non road mobile machinery) unter Berücksichtigung aktueller Emissionsfaktoren und Emissionsverminderungsoptionen für den Bestand, ifeu-Institut für Energie- und Umweltforschung, Heidelberg

[17]   Mckinsey Global Institute, (2017). Reinventing construction: A route to higher productivity

[18]   Jansen, S, "Volvo Construction Equipment erwartet auf der elektrischen Baustelle eine Verringerung der CO2-Emissionen um bis zu 95 Prozent", https://www.volvoce.com/deutschland/de-de/about-us/news/2016/elektrische-baustellenloesung/

[19]   Planet Machinery Vehivles, "Doosan demonstrates remote control of construction equipment worldwide using 5G technology", https://www.plantmachineryvehicles.com/equipment/machinery/73195-doosan-demonstrates-remote-control-of-construction-equipment-worldwide-using-5g-technology, 2019

[20]   Dadhich, S., Bodin, U., Andersson, U., (2016). Key challenges in automation of earth-moving machines, Automation in Construction 68

[21]   M. Hutter, T. Braungardt, F. Grigis, G. Hottiger, D. Jud, M. Katz, et al. (2016). IBEX — A tele-operation and training device for walking excavators. In: Kamilo Melo (Hg.): International Symposium on Safety, Security, and Rescue Robotics. EPFL, Lausanne, Switzerland, October 23-27th, 2016. 2016 NJ: IEEE, S. 48–53

[22]   AOK, "Fehlzeitenreport", 2018

[23]   Frese, C., Zube, A., Frey, C., (2020). Workspace monitoring and planning for safe mobile manipulation

[24]   D. Jud , P. Leemann, S. Kerscher , M. Hutter, (2019). Autonomous Free-Form Trenching Using a Walking Excavator. *Ieee Robotics And Automation Letters*, Vol. 4, No. 4, 2019

University of Maribor Press

Plenary speak

Trends in pneumatics – digitalization

HERBERT HUFNAGL, ANDREJ ČEBULAR & MARCUS STEMLER

Abstract The paper presents an overview of the latest technology trends in pneumatic automatization at Festo, focusing on digitalization from a component to a system level. The Festo Motion Terminal (VTEM) is valve terminal, designed for digitalization. Unique valve unit design allows valve functions to be defined by a software and to be changed in a running system very quickly, even on the fly. Model based applications on a valve controller offer many advanced functionalities such as: pneumatic servo positioning, force and torque control of pneumatic drives and pressure or flow regulation in pneumatic systems. VTEM native connectivity with higher order controllers adds a possibility to seamlessly integrate it on all levels, from the field to the cloud. User control logic and/or AI algorithms in a combination with digitalized pneumatics allows new services, such as: auto-commissioning, predictive maintenance, increased energy efficiency, automatic leakage detection within pneumatic systems and many others.

CORRESPONDENCE ADDRESS: Herbert Hufnagl, Festo AG & Co. KG, Ruiter Straße 82, 73734 Esslingen, Germany, e-mail: herbert.hufnagl@festo.com. Andrej Čebular, Festo d.o.o, Blatnica 8, 1236 Trzin, Slovenia, e-mail: andrej.cebular@festo.com. Marcus Stemler, BEng, MA., Festo AG & Co. KG, Ruiter Straße 82, 73734 Esslingen, Germany, e-mail: marcus.stemler@festo.com.

1   Introduction

Digitalization is changing the world; it is penetrating into all aspects of our lives and data is its propellant. Industry has a great potential to benefit from digitalization with clear goals such as: seamless connectivity, increased modularity, higher machine output and productivity, predicting incidents before they happen, predicting and optimizing quality of the produced products, predicting, and minimizing energy losses, preventing machine downtimes due to wear of components.

Modern mechatronic solutions for Industry 4.0 consume raw sensor data and turn it into valuable information. This process is utilized by physical models, AI or combination of both. Transition from a product to a solution requires much more than just analyses of the raw data acquired form the sensors. Data must be interpreted within all possible aspects, that might have an influence on a process. Interconnectivity, interoperability and flexibility of devices and services on a whole scale is a key factor to success.

State-of-the-art hardware for industrial applications should be designed according to the statements listed above.

2   Digitalized pneumatic valves

Introducing piezo technology in pneumatic valves has opened new potentials in design and control, where traditionally solenoid valves were dominant. With clear advantages over the existing technology, such as small footprint, low energy consumption, high switching speed, proportional behaviour, long service life and low cost makes piezo valves ideal for integration as an active drive component in pneumatic valves and valve terminals.

2.1   Piezo element as a bender actuator

Piezoelectricity is a physical phenomenon where materials such as certain crystals, ceramics, polymers, and some biological structures generate measurable electricity when exposed to mechanical strain. The process is reversable, which means that piezoelectric structures deform, when a voltage is applied. This principle is known as inverse piezoelectric effect and is a general principle of any piezo electromechanical transducer. Piezo transducers that generate mechanical motion or oscillations under applied voltage are also known as piezo elements (Figure 1).
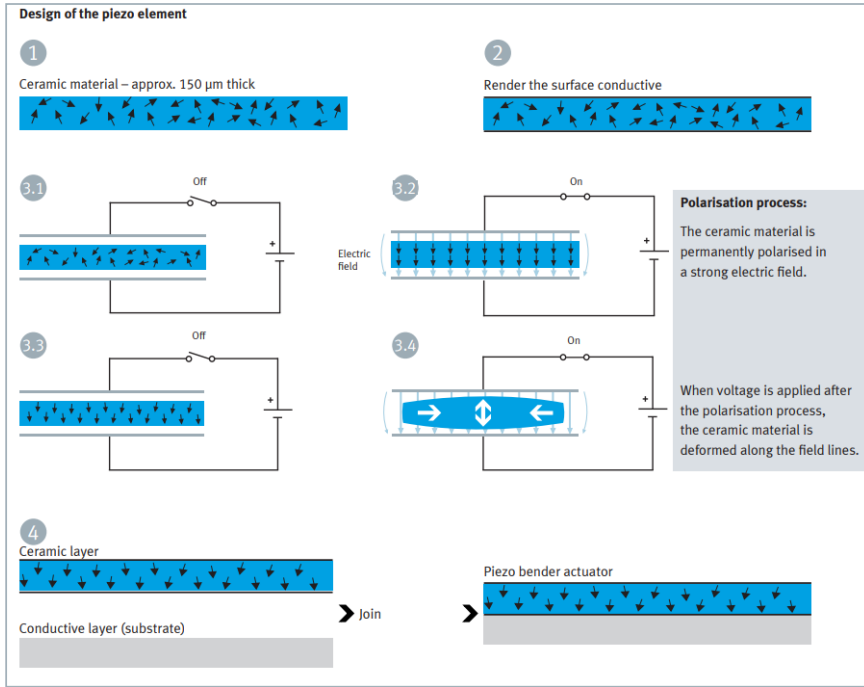
Figure 1: Design of the piezo element [1].

Piezo bender actuator is the fundamental component of a 2/2 piezo valve (Figure 2). When a voltage is applied, the piezo element bends due to a reduction in longitudinal direction, consequently opening a channel for gas medium to flow from inlet towards outlet pneumatic port.
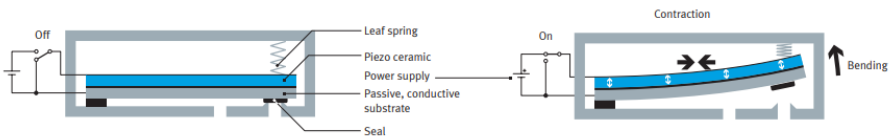
Figure 2: Function of the bender actuator in the piezo valve [1].

Piezo valves are proportional by its design. The more voltage is applied to the bender actuator the wider gap is established between both ports and the bigger medium throughput is established. Compared to solenoid valves, piezo valves need no holding current to maintain a switching state. The higher supply voltage required by piezo valves in

comparison with solenoid valves is of significance only during the switch-on phase. Even then, the switch-on energy consumed is well below the actuation power levels normal in pneumatics.

Piezo transducers are like capacitors from an electrical point of view, energy is needed only in charging phase. Thanks to their capacitive principle, piezo valves require virtually no energy to maintain an active state.

Since ultimately all pneumatic processes in an application are analogue, this is an unbeaTable advantage: there is no need for pulse width modulation and the associated noise problems as a means of trying to achieve a certain proportionality when switching solenoid valves. This means that piezo valves are very resistant to wear and need only minimal energy input. Combined with their short response times, the proportionality of piezo valves makes them ideal actuators for all higher-level control systems [1].
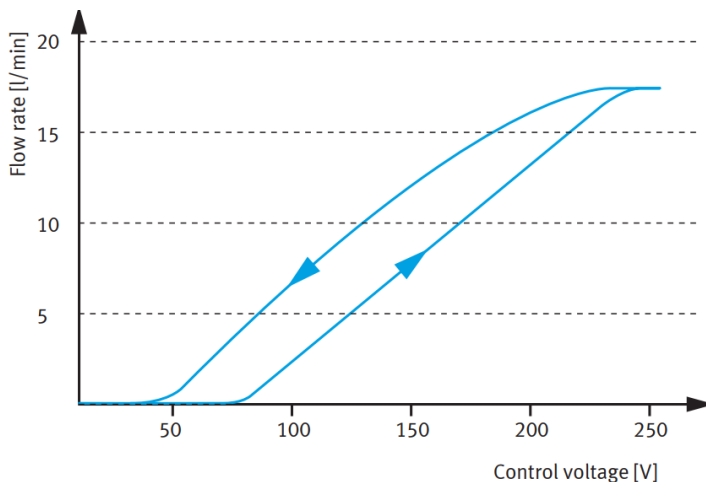
Figure 3: Flow rate as a function of applied voltage in piezo valves – proportional characteristic with hysteresis [1].

2.2   VTEM Motion Terminal – hardware overview

In 2019 company Festo SE & Co. KG introduced VTEM - the pneumatic cyber-physical automation platform (Figure 6). VTEM is a valve terminal with configurable proportional valves, integrated sensors, bus connection and a controller with software-based pneumatic functions [2], [3]. A single unit could cover functionality of more than 50 different

individual pneumatic components including more complex modules such as: flow control valves, directional control valves, proportional regulators.

Pneumatics, sensors, electronics, and software are all integrated on a single piece of hardware, which enables development of advanced applications and services like pneumatic motion, preventive maintenance using condition monitoring, energy efficiency with leakage detection and many others [4].

Every valve unit on Motion Terminal consists of four 2/2-way diaphragm poppet valves, connected in series to form a full bridge. Each of 2/2-way diaphragm poppet valves is position driven by two 2/2-way piezo pilot valves integrated into single cartridge.
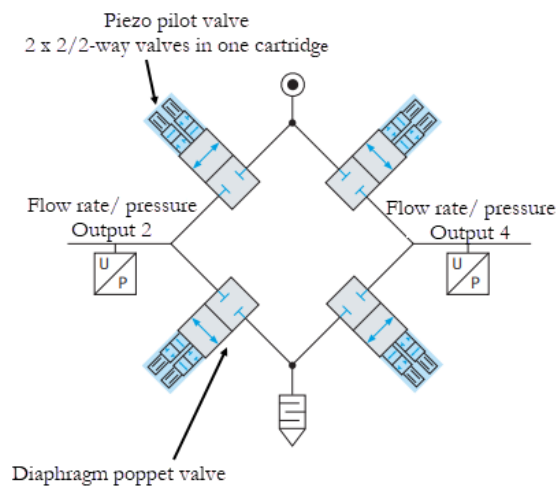
Figure 4: Pneumatic bridge principle [1].

Valve controller is constantly monitoring process parameters such as: 2/2-way diaphragm poppet valves analogue position, analogue pressure at ports 2 and 4 and temperature of the air. Self-learning functions constantly compare the setpoint and actual data and immediately corrects the driven parameters in case of any deviations.

Hardware design (Figure 5) makes VTEM an extremely versatile and flexible pneumatic component which is currently unique on the market. With different control algorithms and software-based models literally any known pneumatic valve function could be implemented on a single valve unit.

Valve electronics with sensors
Integrated stroke, pressure and temperature sensors provide optimal control and transparent condition monitoring.

Four piezo pilot valves
Extremely short switching times, low power consumption, durable and sturdy technology.

Four diaphragm poppet valves
Individual actuation of each poppet valve enables maximum flexibility.

Figure 5: Hardware architecture of VTEM valve unit [1]**.**

With this valve structure, many basic pneumatic functions can be realized without additional mechanical components. The proportional control behaviour allows the mapping of specific sizes or flow rates as well as supply or exhaust air throttles for cylinder drives.

Field bus node

Valve controller

Valves

Input modules
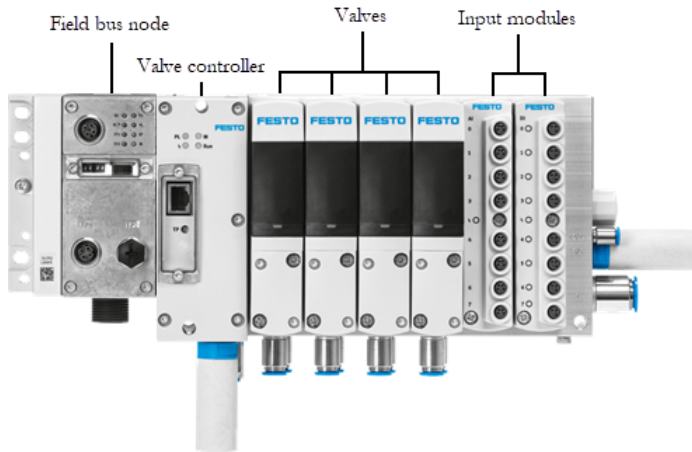
Figure 6: Festo Motion Terminal – layout [1]**.**

2.3 Motion Apps - digitally selecTable valve functions and applications driven by software

Hardware architecture of VTEM allows valve functions to be selected and determined by software. Master system, usually a programmable logic controller (PLC), is communicating with Motion Terminal over integrated fieldbus or Industrial Ethernet node. Communication consists of telegrams, containing information of selected valve function, its dedicated parameters and sensor data [5].

There are several standard valve functions available on VTEM which could be activated via licensees accessible from cloud.

2.3.1 Directional control valve functions

Standard directional control valve functions: 2x2/2 with ports normally closed; 2x3/2 with ports normally closed; 2x3/2 with ports normally opened; 3/2 with ports normally opened + 3/2 with ports normally closed; 4/2 bisTable or monosTable, 4/3 with ports normally closed; 4/3 with ports pressurized; 4/3 with ports exhausted.

Any of these functions could be assigned as often as necessary for example from 4/2-way to 4/3-way or 3/2-way, even during continuous operation.

2.3.2 Proportional directional control valve

Two proportional flow control functions have been integrated in one valve and on one platform. This function enables to use selecTable degree of valve opening between 0 and 100 % on each or both working ports (4/3 or 2 x 3/3). Possible use in industry would be a smooth start-up of a pneumatic drive or a painting application.

2.3.3 Supply and exhaust air flow control

The supply and exhaust air flow control function allows tamperproof software speed adjustment of a pneumatic drive connected to a valve unit. This function eliminates the need for separate flow control valves on the actuator and reduces risk of unauthorized manipulation. It also introduces new motion sequences, such as dynamic flow control adjustments.

2.3.4 Leakage diagnostics

With Leakage diagnostics function system learns characteristics of the process in predetermined diagnostic cycles and allows to set user defined threshold values. Leaks could be individually detected and pinpointed to a specific actuator. It reduces system downtime with preventive maintenance and faster fault detection.

2.3.5 ECO drive

The actuator is operated with the minimum pressure necessary based on the Load and shuts of air supply as soon as the cylinder reached the end position. This eliminates the rise in pressure in the drive chamber at the end of the movement. Energy savings can easily reach values above 70 %. Cylinder limit switches are necessary for the operation.

2.3.6 SelecTable pressure level

Enables the pressure for selected movements to be reset to a reduced level also within a stroke movement. Energy efficient complex movements, such as: quick start-up, smooth travel into the end position, powerful press-fitting and return stroke with reduced pressure are possible. Also enables the speed to be controlled by adjusting the flow control valve setting.

2.3.7 Pre-setting of travel time

The exhaust air flow control function adapts itself to the travel time for retracting and advancing and then maintains it. By continuously comparing the setpoint and actual default values the system automatically adjusts the values in the case of influences such as increased friction due to wear. Cylinder limit switches are necessary for the operation.

2.3.8 Proportional pressure regulation

Pressure and vacuum can be controlled digitally – simultaneously and individually. Each valve unit allows proportional pressure regulation on both working ports independently.

2.3.9   Model-based proportional pressure regulation

By storing fewer boundary parameters for the system, such as tube length, tube diameter and cylinder size, the anticipatory control system ensures maximum accuracy, as the app can compensate for a drop in pressure and volume using the mathematical models in software. No external sensors are needed for that function.

2.3.10   Soft Stop

Highly dynamic, but smooth end-to-end positioning. With analog position transmitters installed only at each end of the pneumatic actuator, drive position is monitored at the end of each stroke. Parameters of a valve unit are adjusted in software control loop to meet the specified setpoint values for a consistent travel time. Active breaking principle is being used to gently stop the drive without any mechanic shock absorbers installed. Eliminating impact shocks at the end of the stroke has a significant impact on increased life span of the pneumatic drive.

2.3.11   Positioning

The pneumatic actuator can be positioned freely along the entire working distance. Positioning task on a pneumatic drive is carried out in a closed loop, so an analogue position transmitter is needed along full stroke. The cylinder movement can be controlled by specifying limits for the parameter of position, speed, acceleration, and jerk. By specifying limit values, the pneumatic drive can travel smoothly to the work area.

2.3.12   Flow control

Flow rate of compressed air and gases up to 600 l/min is digitally regulated for several independent channels at the same time. In general, integrated sensors are sufficient for basic applications. In applications where very precise metering is needed it is possible to add external analogue flow sensors and use their signals as a feedback in the control loop.

Beside all standard applications, that were already mentioned, it is also possible to develop tailored valve functions based on a mathematical or statistical model of a process.

3   Use case from the industry

3.1   Flexible gripping

Robots can perform a wide range of tasks by simply changing the end-of-arm tooling (EOAT), which is equipped with various components. The Motion Terminal offers flexibility during operation: no matter how many different EOATs are used on a robot, they could be controlled centrally from the same hardware. Design and commissioning become much easier while all the changes can be made within software.

3.2   Possible future advanced use of Digitalized pneumatics

3.2.1   Automated Commissioning Process (published by W. Gauchel and W. Wiegand) [6]

Commissioning of pneumatic drives is in theory a very simple process. Connect a defined cylinder chamber to a defined port of the valve terminal with a tube of an adequate length. In reality, this is a complex and difficult process, lots of tubes possibly not marked all look the same. Sometimes the tubes are very long, tubes are channelled e. g. in energy chains, tubes are bundled together, or they run all cross the machine. Thus, the commissioning of pneumatic drives is a time-consuming process which causes substantial costs.

Basic idea: Automated Commissioning Process, connect the end-position switches (or other sensors) electrically to the valve terminal, plug the tubes to any random port of the valve terminal, start a self-identification process: Which tube belongs to which cylinder chamber? Sequential venting of all valve ports, interpreting the signals of the end-position switches (and other sensors). Aim: Faster and error free, thus cost-effective commissioning of pneumatic systems.

Why is the Festo Motion Terminal helpful for automated commissioning?
- It has uniform hardware, only one type of valve slice, it is not necessary to select in advance a defined valve type to control a specific cylinder.
- Proportional valve functionality.
- Different cylinder sizes can easily be controlled by one valve size (only one tube diameter necessary).
- Pressure signal can be used for identification.
- Independent control edges in every valve slice.
- The pneumatic full bridge can be divided into two independent half bridges.

- The two chambers of a double acting cylinder can be connected to half bridges of different valve slices.
-

3.3 Integration of digitalized pneumatics into a higher level systems

Combining digitally driven pneumatic and electric components with AI driven algorithms utilises new concepts in industry. Industrial solutions are now ready to be designed in a way to continuously improve overall equipment effectiveness. Process data from digital components is fed to a system which could detect anomalies based on a model powered by computer learning algorithms (Figure 7).

Figure 7: Anomaly detection and classification, Source: Festo SE & Co. KG.

3.4 Segments in industry, where digitalized pneumatics combined with AI could significantly contribute in OEE rise

3.4.1 Predictive quality

Improves overall production quality by continuously monitoring and analysing production data and detecting quality issues. To ensure the quality of the products is consistent throughout the entire production, it is necessary to permanently monitor and analyse all the relevant parameters and data (via algorithms based on artificial intelligence and machine learning) – technology independent, from component level up to complete machines and production lines. Business Case: Increase yield by reducing number of rejected parts.

3.4.2   Predictive energy

Optimises energy usage by continuously monitoring and analysing energy consumption as well as detecting anomalies.

In order to ensure the lowest possible energy consumption on the shop floor as well as the entire factory, it is necessary to permanently monitor and analyse all of the relevant parameters and data (via algorithms based on artificial intelligence and machine learning) – technology independent, from component level up to complete machines and production lines [8]. Business Case: Cut costs by reducing energy consumption.

3.4.3   Predictive maintenance

Predicts failures and reduces unplanned downtime by continuously monitoring and analysing asset data To ensure the constant performance of components during production, it is necessary to permanently monitor and analyse all of the relevant parameters and data (via algorithms based on artificial intelligence and machine learning) – technology independent, from component level up to complete machines and production lines [9] Business Case: Increase machine uptime by reducing unplanned downtime.

4   Conclusion

Fundamentally different engineering design of a valve terminal has brought an option to define valve functions inside Festo Motion Terminal solely within a software. New generation of pneumatic valves have become flexible cyberphysical systems which are operated digitally by a dedicated integrated controller. Application process data from valve controller and data from integrated sensors are available to higher order control systems through various industrial communication standards. Finally, it is possible to claim that pneumatic components are also ready for Industry 4.0.

References

[1]   Festo AG & Co. KG. White paper: Piezo technology in pneumatic valves, (2017). [Online]. Available: https://www.festo.com/net/SupportPortal/Files/346243/White_Paper_Piezo_EN.pdf.

[2]   Rager, D., Neumann, R., Post, P.,Murrenhoff, H. (2017). Pneumatische Antriebe für Industrie 4.0. *Fachtagung Mechatronik* , 2017

[3]   Festo AG & Co. KG, Weltneuheit Festo Motion Terminal VTEM. (2017).

[4]   Festo SE & Co. KG. Festo Motion Terminal VTEM (2021). [Online]. Available: https://www.festo.com/net/SupportPortal/Files/468005/PSI__Festo_Motion_Terminal_EN.pdf.

[5]   Festo SE & Co. KG. Application Note - Motion Terminal VTEM Quick Reference PLC programming. [Online]. Available: https://www.festo.com/net/SupportPortal/Files/684271/ VTEM_PLC_QuickReference_V1-5a.pdf.

[6]   Gauchel, W., Wiegand, W. (2018). Automated Commissioning of Pneumatic Systems, Universitätsbibliothek der RWTH Aachen,

[7]   Rager D., Doll M, Neumann R., Berner M. (2018). New programmable valve terminal enables flexible and energy-efficient pneumatics for Industry 4.0. *11th International Fluid Power Conference (11. IFK)*, 2020.

[8]   W. T. S. a. Y. W. Gauchel. (2020). Predictive maintenance with a minimum of sensors using pneumatic clamps as an example

[9]   Festo AG & Co. KG. (2017). BionicCobot - Sensitive helper for human-robot collaboration

[10]   Stecki J. S., Davis D. C. (1986). Fluid transmission lines - distributed parameter models part 1: A review of the state of the art. *Proc. Inst. Mech. Eng.*, Part A: *J. Power Energy*, Bd. 200, pp. 215-228,

[11]   Krichel, S. V., , Sawodny, O. (2011). Dynamic modeling of pneumatic transmission lines in Matlab/Simulink. *Fluid Power and Mechatronics (FPM)*, *International Conference on*, 2011

[12]   Rager, D., Neumann, R., Murrenhoff, H. (2015). Simplified Fluid Transmission Line Model for Pneumatic Control Applications. *Proceedings of the Fourteenth Scandinavian International Conference on Fluid Power, SICFP15, Tampere, Finland*

[13]   Rager, D., Neumann, R., Murrenhoff, H. (2016). Remote Pressure Control - Considering Pneumatic Tubes in Controller Design. *10th International Fluid Power Conference (10. IFK)*

[14]   Eckersten, J. Vereinfachte Strömungsberechnung für pneumatische Elemente. *Atlas Copco Deutschland GmbH*, 1977, pp. 62-65

[15]   ISO6358-1. Pneumatic fluid power - Determination of flow-rate characteristics of components using compressible fluids -- Part 1: General rules and test methods for steady-state flow. (2013). *Geneva*

[16]   Bala,H. -P. Durchflussmessungen und strömungstechnische Kenngrößen. (1985) *O+P Ölhydraulik und Pneumatik*, Bd. 29, pp. 541-544, 1985

[17]   Hildebrandt, A. Regelung und Auslegung servopneumatischer Aktuatorsysteme. *Shaker*, 2009.

[18]   Doll, M. (2015). Optimierungsbasierte Strategien zur Steigerung der Energieeffizienz pneumatischer Antriebe.

[19]   Festo AG & Co. KG. (2013). Mehr Produktivität durch optimal gedämpfte Pneumatikzylinder.

[20]   Oertel, H. jr., Böhle, M., Dohrmann, U. (2016). Strömungsmechanik, 4 Hrsg., Vieweg-Verlag

[21]   White, F. M. (2011). Fluid Mechanics, 7 Hrsg., McGraw-Hill, New York

[22]   Chabane S., Sesmat S., Hubert D., Gautier, D., Wartelle, C., Wartelle, Bideaux, E. .Reynolds number-dependent mass flow rate calculation for pneumatic pipes. *Proceedings of the Institution of Mechanical Engineers, Part I: Journal of Systems and Control Engineering*, pp. 419-428, 2015.

[23]   Festo SE & Co. KG. (2021). White paper: Automating on/off process valves," 2020. [Online]. Available:https://www.festo.com/net/SupportPortal/Files/703032/Festo_Automating_Process_Val ves_WhitePaper_EN142460_202005_V01.pdf.

[24]   Festo SE & Co. KG, „Move ahead digitally! With the Festo Motion Terminal!," 11 2020. [Online]. Available: https://www.festo.com/net/SupportPortal/Files/704325/MotionTerminal_brochure_ EN136072_202011_V04.pdf.

[25]   Festo SE & Co. KG. Festo Motion Terminal VTEM - Product information. (2021). [Online]. Available: https://www.festo.com/net/SupportPortal/Files/468005/PSI__Festo_Motion _Terminal_EN.pdf.

[26] Festo SE & Co. KG, „White paper: New ways to increase productivity with smart systems," 2017. [Online]. Available: https://www.festo.com/net/SupportPortal/Files/709735/WP_Digital Simplicity_en_V09_L.pdf.

University of Maribor Press

Research on the water hydraulic pressure relief valve

FRANC MAJDIČ

Abstract Water hydraulics is increasingly becoming a viable alternative to oil hydraulics due to its environmental sustainability. The leakage of water hydraulic components is one of the reasons why water hydraulics is not more widely used. One of the missing water hydraulic components is also the two- stage pressure relief valve. Various valve designs have been investigated. FEM and CFD analyses of the relief valve were performed. Some prototypes were made and tested in the pressure range of 50 to 200 bar at a maximum flow rate of 30 lpm. The functional characteristics of the valve were studied, and the influence of each component was determined. It was found that the manufacture of a two-stage water valve is technologically feasible with appropriate design adjustments.

Keywords: • water hydraulics • relief valves • internal leakage • numerical analyses • measurements •

CORRESPONDENCE ADDRESS: Franc Majdič, University of Ljubljana, Faculty of Mechanical Engineering, Aškerčeva 6, 1000 Ljubljana, Slovenia, e-mail: franc.majdic@fs.uni-lj.si

1   Introduction

Nowadays, we cannot imagine life without technology. It is present everywhere, in medicine, agriculture, forestry, food industry, automobile industry, construction, shipping, aviation etc. We use different principles for energy transmission in technology, from electrical, mechanical, pneumatic to hydraulic transmission. Hydraulic power transmission was used before our era when Ctesibius made the first hydraulic pump. The advantages of hydraulics are the simple design with standard components, the independence of location, the high-power density, the good dynamic behaviour, the simple conversion of rotational to translational movements, the simple change of direction, the stepless change of gear ratio, the simple overload protection, the simple parameter control, and the good possibilities of automation.

From then until the beginning of the 20th century, water was the only hydraulic fluid used. After 1906, mineral hydraulic oil began to gain acceptance due to its many advantages (Figure 1). It is still the most commonly used oil today with a market share of 85 % [1]. The main advantages of using mineral hydraulic oil are its very good lubricating properties, good sealing effect due to its high viscosity and corrosion protection. The disadvantages of using mineral oil are the risk of pollution of the natural environment and drinking water, the strong dependence of viscosity on temperature, the high price, etc.

In 1978, new research was initiated in United Kingdom [2] and Japan [3] on the possibility of using water as a hydraulic fluid. Since then, numerous research have been carried out in the field of water hydraulics [2], [4], [5] and many new components and systems have been developed [6].

Despite the aforementioned development, water hydraulics is still very little used. There are several reasons for this: higher cost of existing water hydraulic components compared to oil hydraulic, problems with freezing of water below 0° C, more expensive production and use of more expensive materials and lack of necessary water hydraulic components to make the whole hydraulic system.

One of the missing components is also pressure relief valve. Despite some research [7] and mass production of water hydraulic pressure relief valves [8], they are missing for flows up to 50 l/min and pressures up to 350 bar. Within the scope of this article, the development of the above-mentioned water-hydraulic two-stage pressure relief valve is presented.
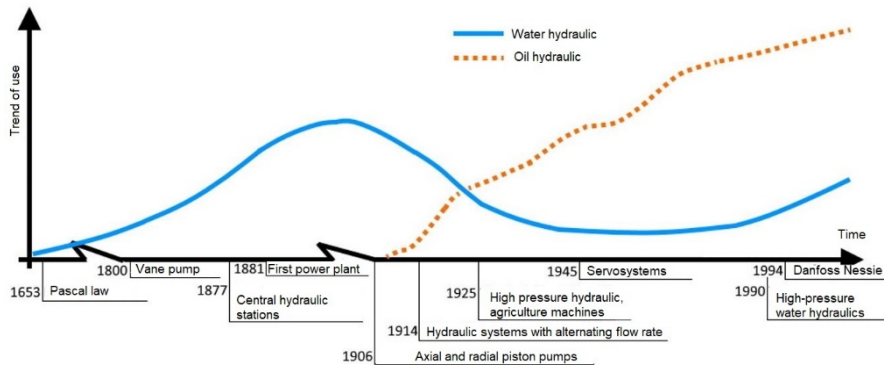
Figure 1: Trend of use of water hydraulics [4].

2   Water as hydraulic fluid

The most important properties of water as a hydraulic pressure medium are power transfer, lubrication, sealing, cooling, kinematic viscosity, compressibility, evaporation pressure, and air consumption [1], [5], [6]. Power transfer is the basic function of a hydraulic fluid. The hydraulic pump transfers the mechanical energy to the hydraulics, which transfers it with fluid through the hydraulic system to the actuators. Water has no significant differences in terms of power transfer compared to the most commonly used hydraulic mineral oil. Lubrication is an important property of a hydraulic fluid as it reduces the friction and wear in sliding contacts inside the hydraulic components. Water has very poor lubrication properties in the contacts of steel surfaces as it is in general used in oil hydraulics. Sealing, which is connected to the kinematic viscosity of the fluid, has an important role in low-gap sliding contacts inside the hydraulic components. Due to the significantly lower kinematics and the viscosity of the water compared to mineral hydraulic oil, the gaps in the water hydraulic components should be at least half the size. The kinematic viscosity of water is fifteen times lower than mineral oil (ISO VG 46 at 50 °C). The cooling properties of water are significantly better than those of mineral hydraulic oil. The compressibility modulus of water is 2.1 10^5 MPa, which is 46 % lower than for hydraulic mineral oil. A very important advantage of water is its availability everywhere in nature and its friendless to the environment (no pollution).

3   Development of pressure relief valve

Pressure-relief valves are primarily used to protect hydraulic systems against overloading, which can lead to failure of the hydraulic system [2], [7]. Almost all relief valves are setTable. For lower flows (in general up to 10 l/min) a one-stage pressure-relief valve is used; higher flows require a two-stage pressure-relief valve. A one-stage valve consists of a conical closing element, a spring, a seat and a valve body. A two-stage pressure-relief valve consists of a one-stage valve on top of its construction, while on the lower part of the valve there is a main body housing with a larger conical closing element and a spring. The advantage of a two-stage pressure-relief valve is good pressure-oscillation damping; the disadvantage is its slower response.

3.1   First design of the valve

A two-stage, water-hydraulics, pressure-relief valve was designed. Figure 2. shows the first tested concept. An external view of the assembled valve in shown on Figure 2a. A cross-section of the two-stage pressure-relief prototype valve is shown in Figure 2b.
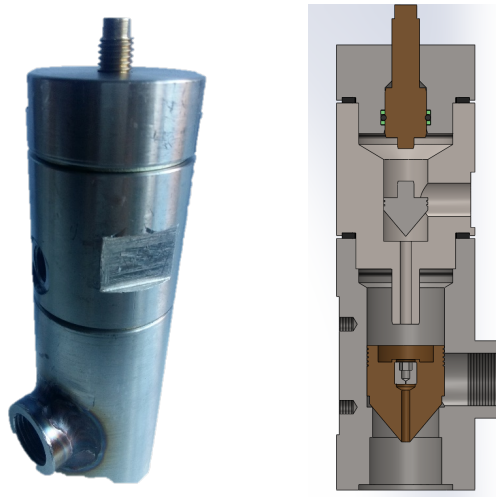
**Figure 2: The first concept of WH pressure-relief valve: prototype (left),
cross-section (Φ50 mm × 175 mm) (right).**

The first concept of a two-stage valve was developed and measurements of its properties were performed (presented in the Results chapter). The first concept was tested with different material pairs (spool/housing). It turned out that the valve did not work as expected, mainly due to manufacturing inaccuracies. Therefore, we developed an improved valve concept.

3.2   The new design of the valve

At the second, improved design of the pressure relief valve (Figure 3), the next modifications were done:

- new housing without welded connector,
- new main spool,
- new control spool,
- new nozzle in the main spool.

a   b
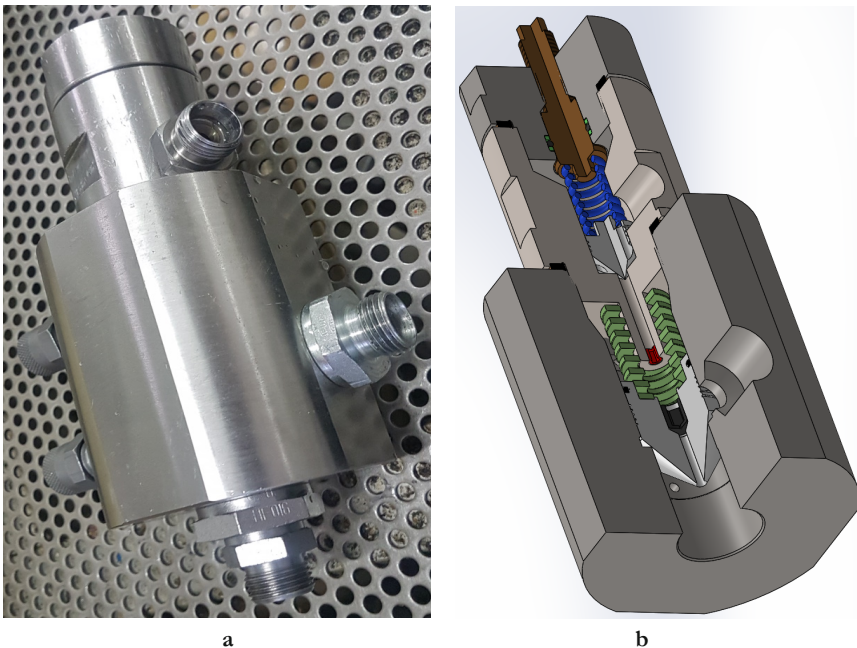
**Figure 3: The second design of water hydraulic pressure relief valve:
a) prototype, b) cross-section (Φ78 mm x 175 mm).**

4   Numerical simulations

To compare the accuracy of the numerical analysis with the analytical calculations, simulations of the fluid flow through the fixed position of each of the spools were also performed. This chapter describes the process of performing an analysis. We started the CFD analysis process by fitting the 3d model in Solidworks. Due to the speed of the simulation and also the correctness of the finite element shape, the model should be simplified as much as possible before using it. Due to the asymmetric shape of the valve, we used a 3d model. Preliminary analysis has shown that the original model has backflow problems at the outlet. This problem is caused by vortices intersected by the boundary surface. The outlet location was therefore moved further away from the valve. We also accounted for changes in the geometry of the tube due to the connections as used in the actual assembly. The spring was excluded from the model due to its complex shape. The distance of the spool from the seat is defined by the distance relationship. The simplified model is used only to define the space occupied by the fluid. Mosaic and polyhedral meshes were used to construct the mesh. Due to the faster convergence of the solution, a polyhedral mesh was used for the final results. Three sides of equilateral elements were added at the contact of the fluid with the walls, allowing a more accurate inventory of the velocity profile near the wall. The inlet mass flow and the outlet pressure were defined in the model, which was zero in all cases. We neglected the pressure due to the height difference with the tank. An anti-slip condition was defined on the valve walls. After comparing the rescue models, the Transition k-kl-ω model was selected for use. The convergence data show the reliability and accuracy of the obtained results. The values depend on the quality of the network and all the settings related to boundary conditions, fluids, choice of rescue models, etc. In general, the residuals in the calculations should be less than 10-4, and for excellent results 10-5. The Transition k-kl-ω model was used because it achieves lower residuals. The success and speed of the rescue were affected by the low viscosity of the water and the associated occurrence of turbulence. Since a total of 18 simulations were performed (three positions of each of the two spools at three different flows), parameterization was used for acceleration. As a key result of the simulations, we defined the average pressure at the inlet face, which represents the pressure drop through the valve at a given flow. Figure 4 shows one of the final results.
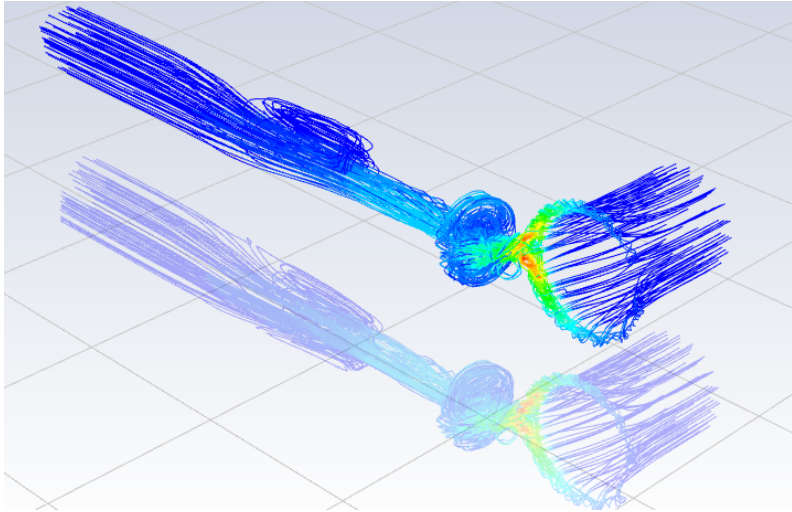
Figure 4: Streamlines from numerical calculations of flow through the valve.

5   Experimental results

All tests and measurements were performed on a dedicated water test rig (Figure 5). The test rig (Figure 6) consists of a high-pressure hydraulic pump, an electric motor, a water tank, a system pressure relief valve, an adjusTable throttle and measuring devices. In addition, there are other components installed on the trolley that were not used in these measurements. The test rig allows pressures up to 300 bar and a maximum flow rate of 30 l/min.
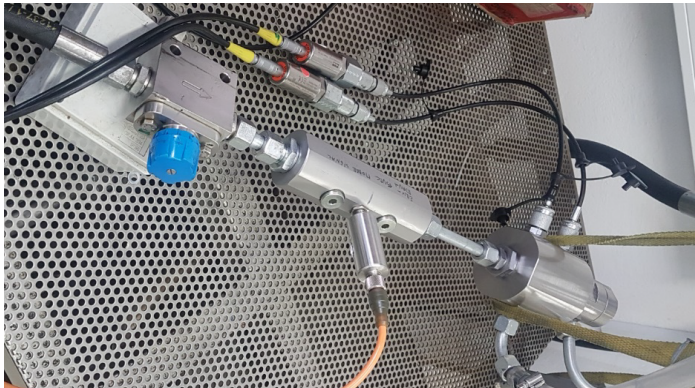
Figure 5: Water hydraulic test rig with specimen.
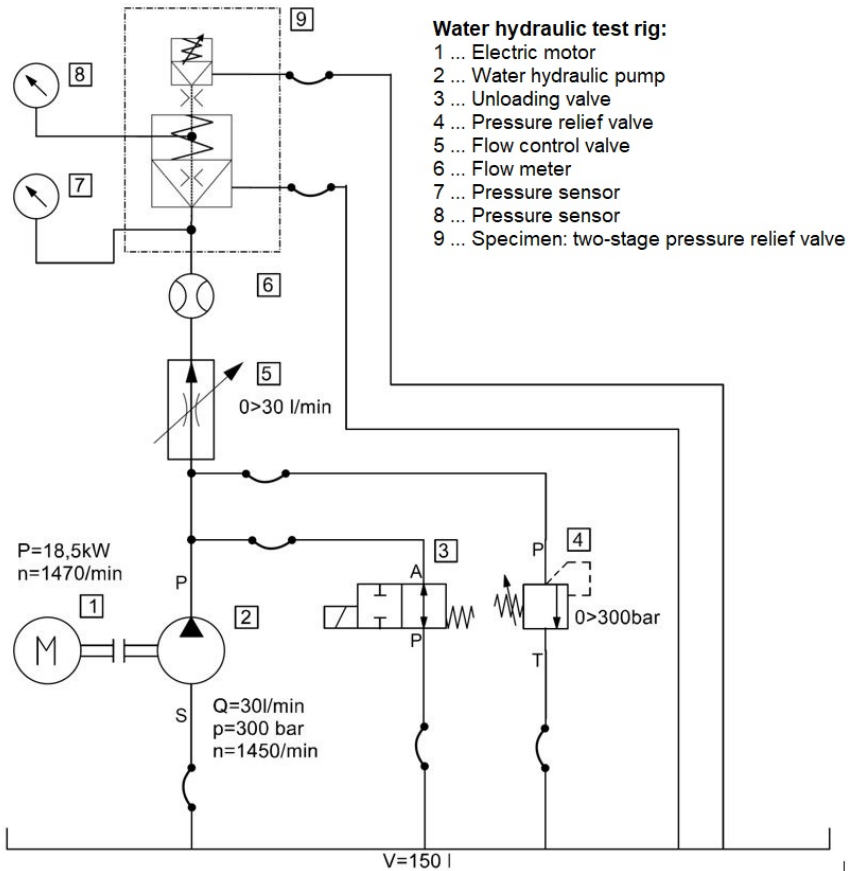
Figure 6: Hydraulic circuit of the water hydraulic test rig with specimen.

6   Results

The test and measurement results of the first prototype showed inadequate performance, so we systematically searched for the faults and produced an improved prototype.

6.1   The first prototype

Figure 7 shows the results of the measurement of the pressure-relief valve containing both spools of the POM polymer. The behaviour of the second configuration of the investigated pressure valve was like the first one. Also, during the second measurement an unaccepTable leakage occurred. The maximum pressure was only 64 bar at a leakage flow rate in the range of 6 litres/min.
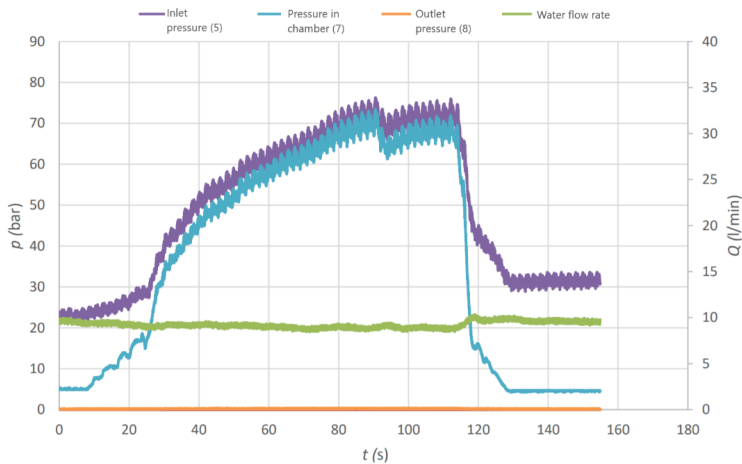
Figure 7: Results with closing conical elements made of PA66GF30.
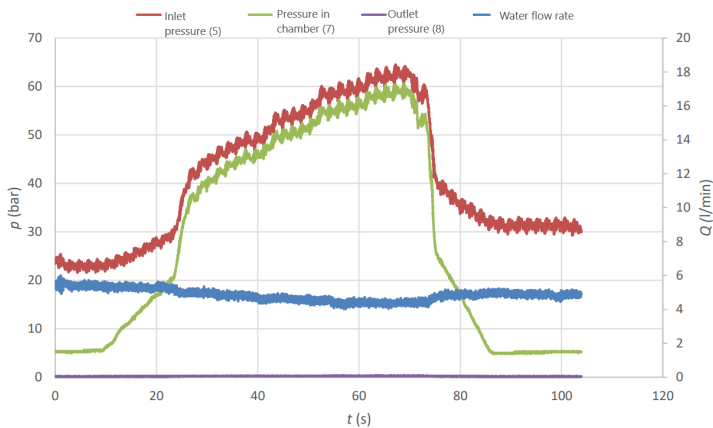
Figure 8: Results with closing the conical element made of POM.

6.2   The second prototype

In final assembly, with all improvements, the valve operates according to its function. Figure 9 shows the process of opening and reclosing the valve at a variable inlet pressure. The valve in the appropriate assembly shows stimulating performance characteristics. From the point of view of the opening process, important features are: Exceeding the set pressure, maintaining stability of the set pressure, internal leakage at an inlet pressure approaching the set pressure, and rapid reclosing of the valve when the inlet pressure falls below the set pressure. Figure 9 shows that in the most successful configuration, the pressure overshoot is less than 10 % of the set pressure. The variation in set pressure is accepTable and the setting does not change over time. Internal leakage at pressures near the setting is significant, but accepTable compared to a standard oil-seat valve. Lowering the inlet pressure abruptly reduces the flow as desired.
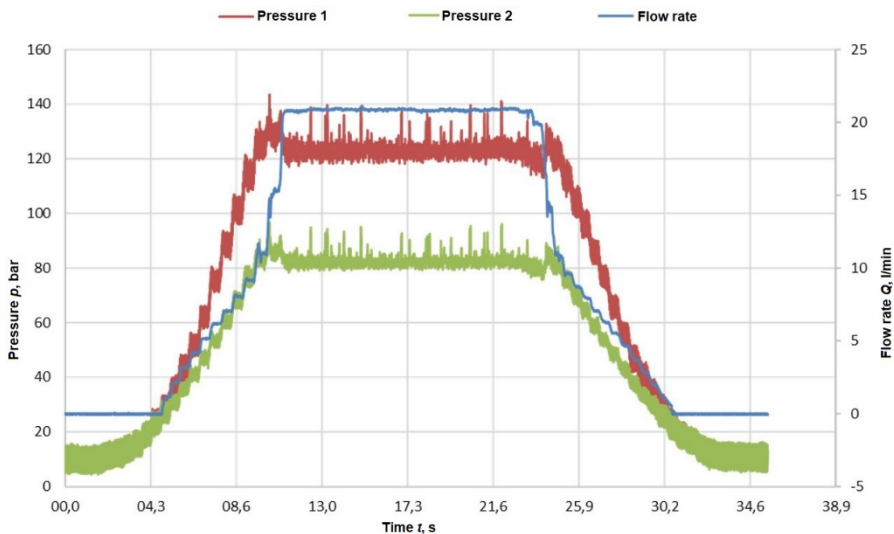
Figure 9: Measurement result of the second valve prototype.

6.3   Numerical simulation in comparison to measurement

The results of the numerical analysis are also accepTable. The results are consistent but differ from the measured values (Figure 10). We estimate that the error could be due to an incorrectly measured spool position during the measurements or to an unintended spool movement. Both the measurements and the numerical analysis show that the

sensitivity of the pressure drop to spool displacement is high. Therefore, even small measurement errors can lead to large deviations.
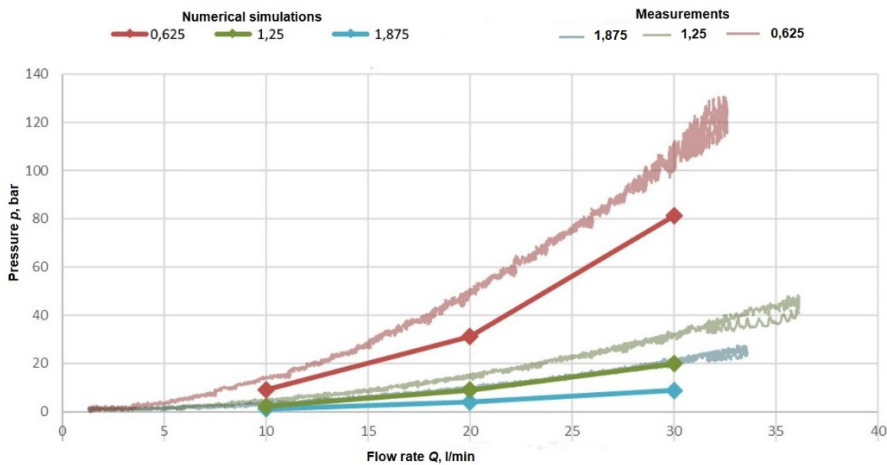
Figure 10: Comparison of the results of numerical calculations and measurements.

7   Conclusions

This paper shows the development of a two-stage water relief valve. The result is a working valve. We started by studying the existing, first prototype valve and the reasons why it did not work. We designed and manufactured new components. Throughout the development, we took measurements and monitored the success and effects of the interventions made. The measurements were also compared with the results of numerical and analytical calculations. After all necessary repairs were made to the valve, we isolated and demonstrated the effects of each of the components that make up a two-stage pressure relief valve with a series of measurements in which we replaced each element individually. Based on the findings from these measurements, we also performed measurements at various pressures, in the most appropriate valve composition.

The main results are:
1) A perfect seal was obtained at the seat of the main spool with a main spool made of polymer. The body was made by conventional turning, without additional technological processes.

2) The sealing of the main spool at the periphery was achieved by using O-rings adapted to the application. No increase in friction or wear of the O-ring was observed when the seal was used.

3) An additional orifice was necessary for proper operation. Installation drastically improved the stability of the valve.

4) Flow downstream of the spool seat must be unobstructed. By changing the geometry of the spool, we were able to get the control portion of the valve to operate properly and maintain the set pressure.

5) By replacing the prototype control section of the valve with a serial single stage valve, we found that the leakage and operation of the control section were accepTable.

6) We found that the valve operated properly in the range of 50 bar to 150 bar when properly assembled. At higher settings, there was a pressure fluctuation in the valve.

7) According to the results of the measurements, the choice of orifice has the most important influence on the operation. An orifice that is too large or too small will cause the valve to malfunction. The soft spring of spool can also cause malfunction of operation. The choice of spool springs does not bring significant differences in performance.

The main contribution of this work is to demonstrate that with suiTable design adjustments, it is possible to produce a satisfactorily operating two-stage water pressure relief valve using simple technological procedures.

References

[1]   Bock, W. (2009). Hydraulik-Fluide als Konstruktionselement. *Vereinigte Fachverlage GmbH*, Mainz

[2]   Trostmann, E. (1996). Water Hydraulics Control Technology. *Lyngby. Technical University of Denmark*, ISBN: 0-8247-9680-2

[3]   Kitagawa, A (1999). Co-operation between Universityes and Water Hydraulic Companies in Japan. *The Sixth Scandinavian International Conference on Fluid Power, SICFP 1999, Tampere, Finland*

[4]   Trostmann, E. Frolund, B., Elesen, B. H., Hilbrecht, B. (2001). Tap Water As A Hydraulic Pressure Medium. *Marcel Dekker, New York*

[5]   Majdič, F. (2010). Voda kot hidravlična kapljevina v pogonsko-krmilni hidravliki. *Doktorska disertacija, Univerza v Ljubljani, Fakulteta za strojništvo*

[6]   Garcia, J., M., Krutz, G., W., Lumkes, J. (2007). Self propelled water hydraulic vechicle. *The Tenth Scandinavian International Conference on Fluid Power, SICFP 2007, Tampere, Finland*

[7]   K. Dasgupta, R. Karmakar (2002). Modelling and dynamics of single-stage pressure relief valve with directional damping. *Simulation Modelling Practice and Theory 10*

[8]   Danfoss (2020). Pressure relief valve VRH 5, VRH 30, VRH 60 VRH 120. *Data sheet, Nordborg, Denmark*

University of Maribor Press

Development of metallic 3d-printed water hydraulic proportional directional control valve

JAN BARTOLJ, ANŽE ČELIK & FRANC MAJDIČ

Abstract New additive metal powder technologies are increasingly used for various prototypes. Different powder materials can be used for very complex shapes. Water hydraulics needs new technologies and new approaches to enable more frequent use by users. A new shape of housing for a water hydraulic proportional directional control valve was designed. FEM and CFD analyses of the valve housing were performed. Based on the results of the initial numerical analyses, topological optimization of the valve housing was performed. The prototype of the valve was fabricated from non-corrosive Inconel powder using 3D printing process. After machining, the valve was assembled and experimentally validated on the water hydraulic test rig. The new 3D-printed Inconel valve housing is more than 3 times lighter than similar housings of industrial valves.

Keywords: • additive technologies • metal 3D print • water hydraulics • numerical analyses • measurements •

CORRESPONDENCE ADDRESS: Jan Bartolj, University of Ljubljana, Faculty of Mechanical Engineering, Aškerčeva 6, 1000 Ljubljana, Slovenia, e-mail: jaan.baartolj99@gmail.com. Anže Čelik, Poclain Hydraulics d.o.o., Industrijska Ulica 2, 4226 Žiri, Slovenia, e-mail: anze.celik@poclain.com. Franc Majdič, University of Ljubljana, Faculty of Mechanical Engineering, Aškerčeva 6, 1000 Ljubljana, Slovenia, e-mail: franc.majdic@fs.uni-lj.si

1.   Introduction

In everyday life, engineers are trying to maximize efficiency of energy transforming processes. The main goal is reducing volume of fossil fuels consumption, either directly (internal combustion engines of mobile machines) or indirectly (thermo-electrical power plants) [1], [2]. In mobile hydraulics engineers can achieve lower consumption of energy sources by reducing mass of final components.

Since a lot of unnecessary material is carried around in form of valve housings, we focused on them. We took an existing water hydraulics 4/3 proportional directional control valve housing [3] and optimized its outer and inner geometry.

2   Basics

As mentioned, we started with commercially available valve of nominal size (CETOP 6). We constructed the valve with potential mass production in mind, so we had to follow the trends of ISO 4401 [1] standard. By following those trends, the valve can replace any other valve of the same nominal size.

We also wanted to achieve that the final product would be able to survive the same pressure and other stress forms as commercially available valves. Final product had to be optimized to stand the pressure of 35 MPa at a flow of 50 l/min. We will satisfy both demands by using FEA and CFD analyses on the CAD model.

3   Development of valve housing

Since we chose metal 3D printing as a manufacturing process (MP), many limitations proposed by conventional MPs were avoided [5], [6]. That allowed us to design complex or organically shaped housing and greatly reduce mass of part.

We used SolidWorks program as software of choice for designing the CAD model. Because additive manufacturing can produce complex outer and especially complex inner geometry, we first constructed the inner chambers that were to be inverted outwards with purposive software function. At first inner chambers were made as basic cylinders, but after some consideration we made them toroidally shaped.

J. Bartolj, A. Čelik, F. Majdič: Development of metallic 3d-printed water hydraulic proportional directional control valve

43

As we decided on the shape of inner chambers, the construction of connectional channels started (Figure 1). At first, the starting and ending shapes were projected on surfaces. Starting profiles were circles. Their locations and biggest possible radiuses are defined in ISO 4401 standard and were made accordingly.
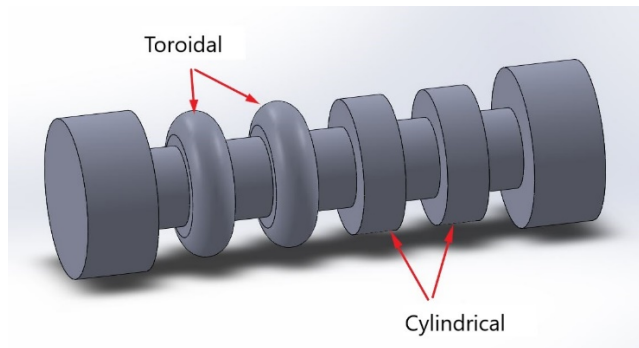
Figure 1: Difference between toroidal and cylindrical geometries (Φ 19 mm x 86 mm).

We projected the ending profiles on toroidal part of inner chambers. Contact surface was greatly increased because we used ellipse shape instead of circle. That will later reveal significantly smaller pressure drop because of smoother change between cavity shapes.

Next step was connecting the two profiles (Figure 2). Since they were not on the same surface neither were they orientated the same, we had to use three dimensional guide curves. This type of curves can be made in several different ways. Because we wanted small changes to be easily implemented to the curves throughout the whole design process, we used the projection technique. This means that each curve is made of two surface based curves, connecting same points stationed in 3D space. Two sketches, of surface based curves were then projected one to another. This gave us easy-to-correct guide curve. We made four guide curves for each of the profiles.
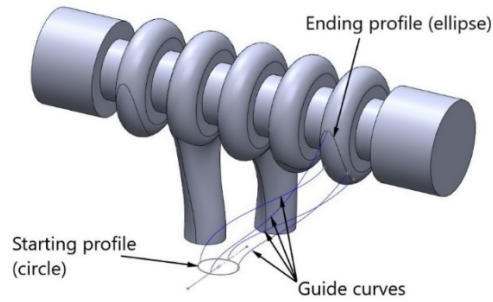
Figure 2: Profiles and guide curves (86 mm x 55 mm x 53 mm).

After finishing all internal cavities, the model was ready to be inverted. We completed this step with command Shell outward. The only needed parameter is wall thickness, which was decided to be 2.8 mm. When completed, we started adding guide holes for mounting bolts. Guide holes locations and bolt sizes are determined by standard. Bolts have to be M5 standard thread and since in hydraulics field are mostly used hexagon socket head cap screws (ISO 4762), we anticipated the usage of those.

We made base plate as adding bottom parallel sketch and extruding it upwards in to the model. Partial result of the design process is shown in Figure 3. This model is named Zeta. We made CAD model without any prior experiences in printing of hydraulic components. This was the first try to reduce mass of the valve housing body and make as smooth transitions between cavities as possible.
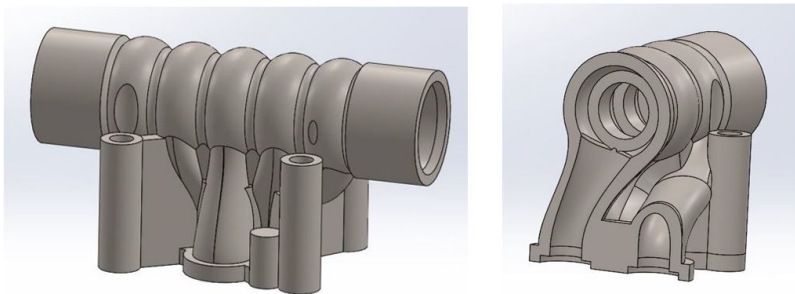
Figure 3: First valve geometry (86 mm x 47 mm x 43 mm).

J. Bartolj, A. Čelik, F. Majdič: Development of metallic 3d-printed water hydraulic proportional directional control valve

45

4 FEA analysis

Since a lot of material was removed, compared to conventional valve housings, we used FEA analyses to confirm the strength of the part.

Analyses were made for different types of stresses. Firstly, we applied forces caused by operating pressure 35 MPa to all internal surfaces that are in contact with fluid. Secondly, we added forces that comes as result of tightening the magnet cores to control the spool valve. After that, the torque of tightening the mounting bolts had to be decided, so that we could applied forces to material. Finally, we defined supports – surfaces on the base plate that are fixed and prevent the structure from moving during the calculation.

Next step was meshing the model where we used second-order tetrahedral finite elements (Figure 4). Since the model has very complicated geometry, meshing was challenging. Some edges and surfaces needed to be removed or changed. After applying basic mesh, we tested to see if everything worked as it should. Once we were confident, we started decreasing size of finite elements and thus increasing their number. As a rule, the more elements, the better the result, and the longer the computation time. After numerous mesh manipulations (i.e. changing mesh size), we compared the results of displacement and stress analyses per elements number. When we saw that results were converging towards specific value, we stopped increasing the count of elements.

Since we were focused on metering edges of housing that are in contact with spool valve, we locally decreased the size of finite elements to prevent unnecessary increase of the calculating time.
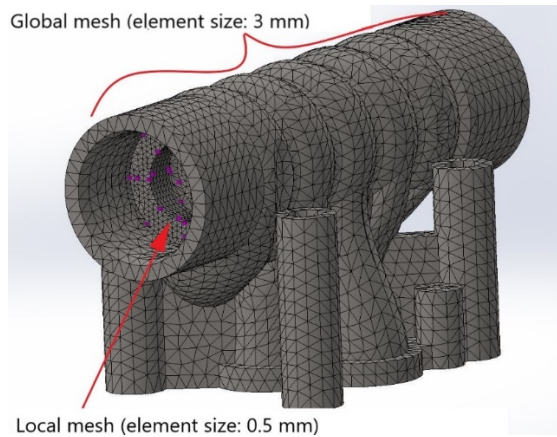
Figure 4: Meshing the CAD model (86 mm x 47 mm x 43 mm).

As a result of FEA analysis we focused on maximal stress through the whole model, maximal global displacement and maximal and minimal metering edges displacement (Figure 5). It was quite clear that stress and global displacement were not an issue for the material given. Major concern were displacements of metering edges. Displacement of metering edges for water hydraulic are expected to be less than 3 microns but were in our case more than four times that value. In aspect of metering edges displacement, we encountered two problems. First: values were much bigger than we wanted; second: in local cylindrical coordinate system we encountered negative displacements. Second problem has to be taken especially carefully. Positive displacements in cylindrical coordinate system mean that the observed radius is increasing its value. But negative values mean that specific radius is closer to the central axis of the coordinate system. So, if values are positive, we are talking about leakage between inner chambers of valve body; but if values are negative, there is the chance of spool collision/jamming.

Both problems are directly related to minimizing the housing body volume and mass. The solution was found adding supports to the most outer metering edges. Those supports connect the base plate with outer cylinders of metering edges in an arcade shape. Just adding those supports reduced the metering edges displacement values to ones that could be tolerated.

J. Bartolj, A. Čelik, F. Majdič: Development of metallic 3d-printed water hydraulic proportional directional control valve

47
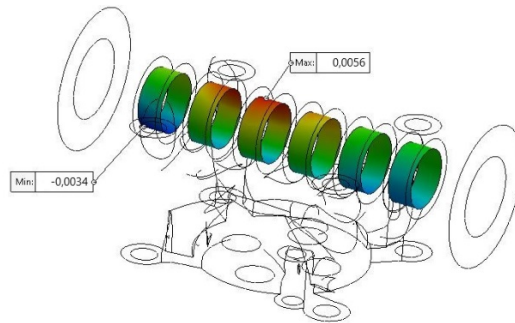
Figure 5: FEA analyses – displacement of the metering edges (86 mm x 47 mm x 43 mm).

5   CFD analysis

Analysing flow characteristics, we came to conclusion, that printed valve housing has significantly lower pressure drop. High flow (from 50 up to 80 l/min) simulations have shown up to 40 bar difference compared to conventional valve characteristics.

Starting parameters were: water temperature 50 °C, fully developed flow, flow rating from 10 to 80 l/min and spool valve offset position. Main points of research were pressure and velocity conditions when fluid was moving through housing.

Similarly to FEA we paid great attention to meshing internal cavities. We chose to make mesh denser locally. Mesh during calculation is shown in Figure 6.
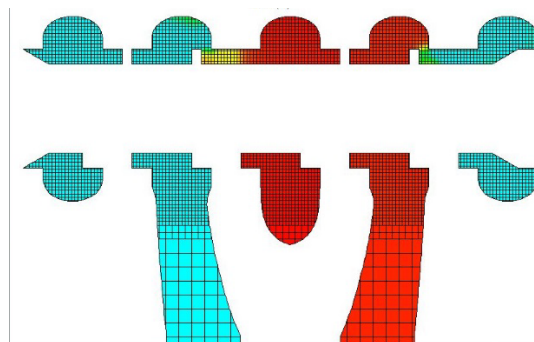
Figure 6: CFD analyses and mesh (86 mm x 47 mm).

When calculating, we focused on cut sections of specific channel. The most interesting was P channel that needed to be corrected. Since flow had a tendency to rotate the spool valve, the shape of channel had to be fixed according to partial results. Corrections to P channel are visible in Figure 7.
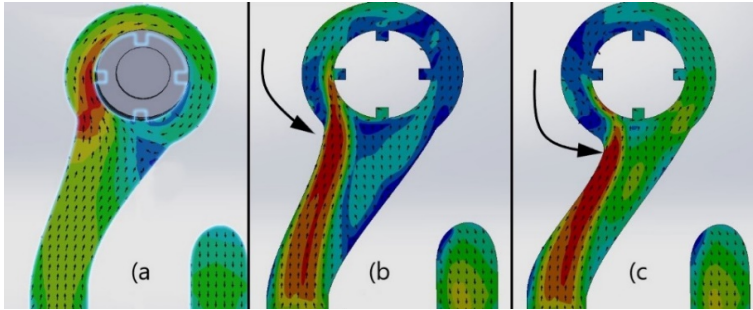
Figure 7: Reshaping the P channel geometry (47 mm x 43 mm).

As can be seen in Figure 7 most of velocity vectors have the same direction clockwise around the spool valve and thus trying to rotate it. If flow is divided in halves, then spool valve has less tendency to rotate.

6   Finished model

According to all the corrections from numerical analyses, we finished a model. Finally, we added small clamping appendixes at the top, and bottom, for final CNC machining. Pockets for O-ring seals were added on bottom end, which required some base plate to be made. Finished model Zeta is shown in Figure 8.
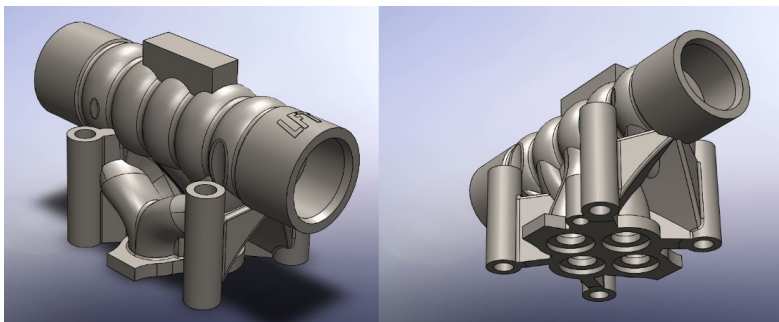
Figure 8: Finished CAD model of the valve housing (86 mm x 47 mm x 43 mm).

J. Bartolj, A. Čelik, F. Majdič: Development of metallic 3d-printed water hydraulic proportional directional control valve

49

7 Valve printing

We printed the valve housing (Figure 9) on the EOS 3D printer with the MS1 [7] material. Maraging steel 1 or tool steel that has great content of nickel and is stainless because of that. This feature is necessary for water hydraulic. Material has yield strength 2010 MPa and ultimate tensile strength 2080 MPa. Material has a density 8.1 g/cm³ and could after heat treatment achieve 50 -57 Rockwell hardness.
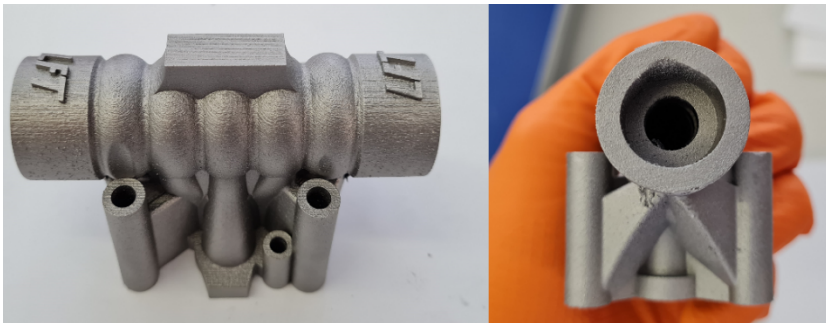
Figure 9: Printed model of the valve housing (86 mm x 47 mm x 43 mm).

After printing, we CNC machined the part to final dimensions. Finally, the hole was honed to exact dimension to accommodate the existing spool valve.

8 Valve testing

We wanted to test the valve to prove that the actual model has similar results to CAD model that was numerically tested. Internal leakage, and Δp-Q characteristics were tested. To ensure as static initial conditions as possible, we kept the water tank temperature at 50 °C using the secondary cooling system.

8.1 Internal leakage

Firstly, we tested the valve housing for internal leakage. We connected the pressure channel of the valve with the water conduit from pump, put the spool valve in centre position and applied 300 bars of pressure. In the period of 1 minute, we measured the

leakage from A and B channels. We repeatedly made three tests and moved the spool valve and returned it to initial position between each repetition to simulate realistic scenario. The tests have shown that in a minute an average of 281 ml of water leaked on A channel and 236 ml on B channel.

8.2   Δ*p-Q* characteristic

Secondly, we experimentally defined the Δ*p-Q* characteristic of the valve (Figure 10). We repeatedly measured the pressure drop between inlet and outlet port of the valve for four different spool valve positions.
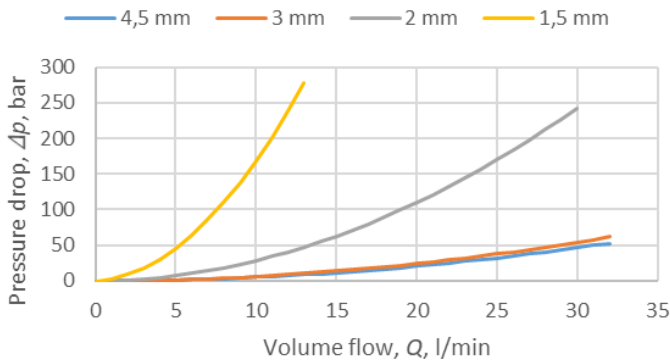
Figure 10: Measured Δ*p-Q* characteristic of the valve.

9   Topology optimization

Lastly, we took the internal cavity of the valve and used topology optimization tool to define outer geometry. We wanted to compare our geometry, to the one that we got from topology optimization, to see, where volume of material was unnecessary and could be taken off the initial model. Variating some parameters gave us various results, between which we had to choose from. We took the best result and started to parameterize it into a model, suiTable for printing. Optimized geometry, could not be directly used for further testing, since number of finite elements meshing the model, should be greatly increased. A model straight out of topology optimization is shown in Figure 11.

J. Bartolj, A. Čelik, F. Majdič: Development of metallic 3d-printed water hydraulic proportional directional control valve

51
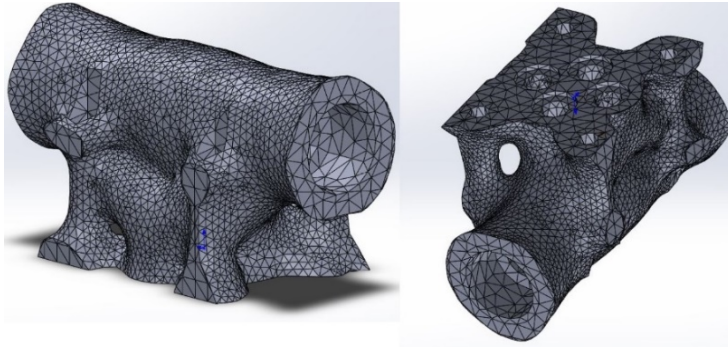
Figure 11: Topologically optimized outer geometry (86 mm x 50 mm x 45 mm).

Model is shaped based on FEA analyses and forces applied. Parameterized finished model is shown in Figure 12.
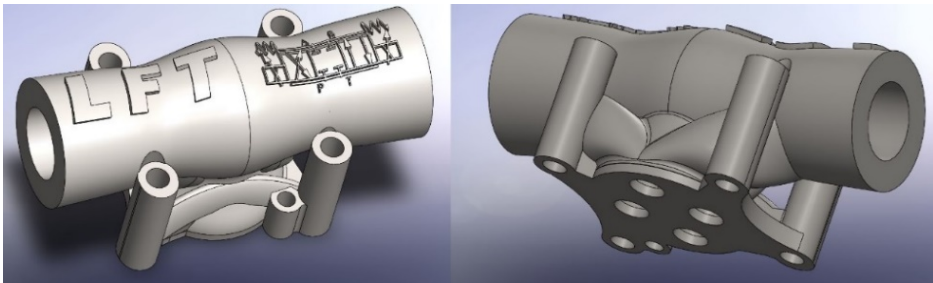
Figure 12: Parametrical finished model of the valve housing (86 mm x 44 mm x 41 mm).

10   Conclusion

3D printing of the parts is a relatively new manufacturing process. It was firstly used just for concept models and small series. In the era where humanity is tending towards a cleaner environment, reduction of mass and lower consumption of energents are crucial for continual development. Metal printing can achieve both of those criteria and can even surpass the competition by lowering the pressure drop because of its internal geometry possibilities.

References

[1]   Majdič, F. (2010). Voda kot hidravlična kapljevina: doktorska disertacija. Ljubljana

[2]   Majdič, F., Pezdirnik J., Kalin, M. (2011). Vodna hidravlika v Sloveniji in pogled v prihodnost. *Fluidna tehnika, Maribor*

[3]   Šenica D. (2015). Proporcionalni potni ventil za vodno hidravliko. Diplomsko delo. Ljubljana

[4]   ISO 4401:2005(E). *Hydraulic fluid power— Four-port directional control valves— Mounting surfaces*

[5]   Vayre, B., Vignat, F., Villeneuve, F. (2012). Metallic additive manufacturing: State-of-the-art review and prospects, Mech. Ind. 13, 89–96. https://doi.org/10.1051/meca/2012003.

[6]   Ngo, T.D., Kashani, A., Imbalzano, G., Nguyen, K.T.Q., Hui, D. (2018)- Additive manufacturing (3D printing): A review of materials, methods, applications and challenges, Compos. Part B Eng. 143, 172–196. https://doi.org/10.1016/j.compositesb.2018.02.012.

[7]   EOS: Material data sheet EOS MaragingSteel MS1. Munchen, 2017

University of Maribor Press

Some special specifics of dimensioning of a hydraulic cylinder as an executive device of an electrohydraulic actuator system

DRAGAN NAUPARAC & NEMANJA VIŠNJIĆ

Abstract The hydraulic cylinder is dimensioned based on a static or dynamic criterion, assuming the desired operating pressure. The paper further analyzes the dimensioning of cylinders according to different load categories. The sizing of the hydraulic cylinder affects the choice of control algorithm parameters but also the stability of the system. How the cylinder dimension and the gain of the distributor affect the choice of the integral constant in the control algorithm in the case when we have the PI control law is especially considered. Then we have by definition an unsTable system 1 / s2 to which we provide stability through feedback.

CORRESPONDENCE ADDRESS: Dragan Nauparac, PPT Inženjering, Bulevar vojvode Mišića, 37-39, 11000 Belgrade, Serbia, dragan.nauparac@ppt-inzenjering.rs. Nemanja Višnjić, Bulevar vojvode Mišića, 37-39, 11000 Belgrade, Serbia, nemanja.visnjic@ppt-inzenjering.rs.

1   Introduction

The calculation and modelling of electrohydraulic actuation systems have been well-known engineering design techniques for many years. Here, in a special way, the calculation and modelling of the hydraulic cylinder as the executive body of the electrohydraulic actuation system and the influence of its basic dimensions on the dynamics of the actuation system are considered separately. It is clear that the hydraulic cylinder itself is a simple motor construction with linear motion and is therefore similarly trated when it comes to calculation and modelling. The matter becomes much more complicated when the cylinder is viewed as a loaded member of the actuation system, which is the only one that is important for design in practice. The cylinder stroke and the corresponding installation measure are not subject to calculation. The calculation of the cylinder basic dimensions is based on the requirements for providing the required force. It is a misinterpretation that the cylinder is dimensioned according to rod speed, because that is always the case with an unloaded cylinder. The cylinder is defined according to the force, where the influence of the speed or the desired flow can be observed within a higher or lower working pressure within the defined nominal pressure.

In this paper, the influence of the diameter of the piston and connecting rod, as the basic parameters of the cylinder on the responsible for obtaining the given dynamic characteristics is considered. The paper does not consider the structural elements of the cylinder structure, such as connecting rod buckling, stresses in the cylinder shell, bearing capacity of threaded joints and the like. The structure of the actuation system is observed by position or by force.

2   Basic elements for the initial calculation

The hydraulic cylinder is characterized by an integral nature, which means that a nominal operating point cannot be defined in an open control circuit. This means that actuation systems with a hydraulic cylinder cannot be modelled by deviations, but only in total coordinates. The cylinder is at the same time a type of oil spring, so that its own frequency depends on the position of the piston within the working stroke. In general calculations, the inertial load of the cylinder is reduced to the end of the connecting rod (reduced mass) and the external force. The first assumption that is adopted in this case is that the natural frequency of

D. *Nauparac & N. Višnjić: Some special specifics of dimensioning of a hydraulic cylinder as an executive device o fan electrohydraulic actuator system*

55

the mechanical parts of the system, the connection of the rod of the cylinder to the load is large, that is, the high stiffness of the mechanical part in relation to the cylinder is assumed. Based on this, we can accept that the hydraulic natural frequency is sufficient for all calculations, i.e. that we do not have a structural load. By structural load we assume an inertial load of low stiffness, so that its natural frequencies can be close to the hydraulic natural frequency, which must be taken into account when calculating and modeling the electrohydraulic actuation system. An example of a structural load for an electrohydraulic actuation system is in flight conrol -the construction of control surfaces which, due to the requirement for the mass to be as small as possible, have a relatively low stiffness. Here, within the basic calculation, we present the initial criteria for defining the dimensions of a hydraulic cylinder:

-   Criterion (1) based on reduced force at the end of the connecting rod

$$\frac{p_s \times \pi (D^2 - d^2)}{4} = F \Rightarrow (D^2 - d^2) = \frac{4F}{p_s \times \pi} = \frac{3D^2}{4} = \frac{4F}{p_s \times \pi} \Rightarrow$$
$$D = \sqrt{\frac{16F}{3(p_s \times \pi)}} \tag{1}$$

-   Criterion (2) on the basis of inertial mass for dynamic requirements with a bandwidth of more than 4 Hz, a cylinder with a double rod [1].

$$A = \frac{(f \times 4)^2 \times \pi^2 \times H \times m}{g \times \beta} \tag{2}$$

-   Criterion (3) based on the known natural frequency of the cylinder with inertial load, selection of an adequate proportional directional control valve or verification of the natural frequency of the actuation system based on a simple mechanical model mass-spring, Figure 1.

$$\omega_h = \sqrt{\frac{4\beta_e A_p^2}{M_t V_t}} \tag{3}$$

In (3) we have the influence of the dimensions of the cylinder on the natural frequency through the work surface and over the stroke (working volume)
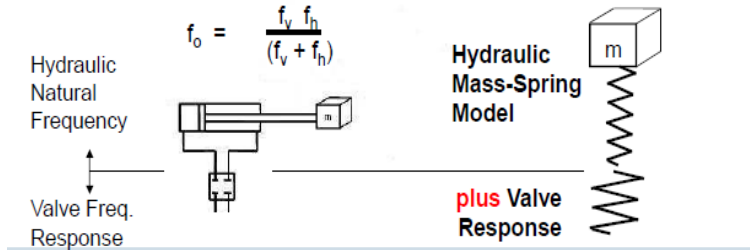
Figure 1: Model for checking the natural frequency of an actuator system without a complete linear model [1].

The hydraulic natural frequency, which depends on the dimensions of the hydraulic cylinder, can also be used for the initial selection of the basic control algorithm in the synthesis of the control system when comparing natural frequency of cylinder with inertial load to the natural frequency of the proportional directional control valve. Based on Table 1, it is possible to determine the initial approach when choosing the initial control algorithm. Of particular interest is case 1, where we have the proportional directional control valve which is "faster" than the cylinder and this leads to the requirement for operation in the state space, because the proportional directional control valve performs a certain destabilization of the actuation system, so stabilization is required and consequently additional feedbacks (load pressure, velocity or by the phase state variables).

Table 1: Initial approach when choosing the initial control algorithm

	Ratio of cylinder natural frequency and directional control valve natural frequency	Recommended control algorithms	Remark
Case 1	$\dfrac{\omega_c}{\omega_R} \approx 0.3$	State variables	Additional feedbacks, pressure and flow (velocity)
Case 2	$\dfrac{\omega_c}{\omega_R} \approx 1$	Proportional control	
Case 3	$\dfrac{\omega_c}{\omega_R} \approx 3$	Proportional-Differential control	

D. Nauparac & N. Višnjić: Some special specifics of dimensioning of a hydraulic cylinder as an executive device o fan electrohydraulic actuator system

57
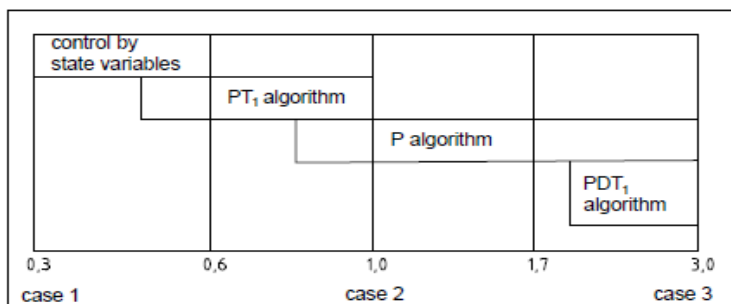
Figure 2: Overview of control algorithms based on Table 1 [1].

3   Standard models of electrohydraulic actuator system

Figure 3 shows a simple structural approach to modelling where we do not have a direct influence of cylinder dimensions, which leads us directly into the state space, which arises from the mechanical analogy that a cylinder with inertial load is represented by a spring-mass model. This approach to modelling, Fig.3, allows us to easily arrive at a force-driven actuation system. This model took into consideration the main nonlinearity of the mathematical type that defines the flow characteristic, the square root type, while other primarily static nonlinearities were not considered.
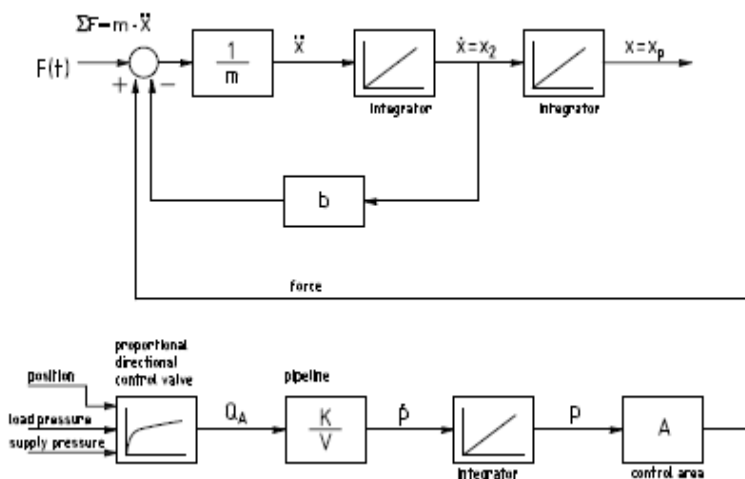
Figure 3: General structural model of EHAS [2].

From Figure 3, we see that we have three integrators in the system, and for that reason that when we use the model from the input-output space for control synthesis, then we choose matching with the so-called " poor integrator", Figure 2.

The model in Figure 4 shows us the approach in which we have an inertial load without additional external force, which gives us the ability to clearly see the value of constant along the integral member, which depends on the working surface of the cylinder and the flow gain. Basically, when we define the PI control algorithm, we have two integrators in the system, the system is unsTable in the open circuit, and we need to design a sTable actuation system in the closed circuit. Here, the value of integral constant of the integrator in the cylinder is important, because it determines the order of value of the integral constant in the PI algorithm, i. e. it should be approximately ten times smaller. We do not have this possibility if we define an external constant or variable force in the actuation system in addition to the inertial load, Figure 5. Then we cannot estimate the order of value of the integral gain in the PI control algorithm at the beginning.
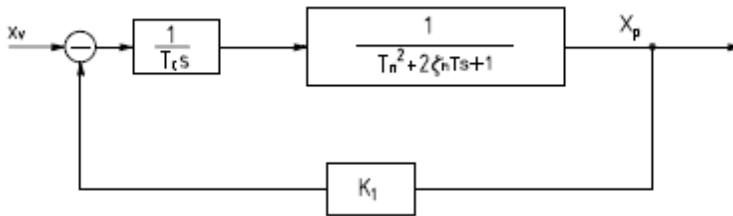
Figure 4: Structure of a mathematical model without external force with positional load and friction [3].

$$T_c = \frac{A_p}{K_{Qx}}$$

$$T_n = \sqrt{\frac{m}{c_1}}$$

$$K_1 = \frac{K_{Qp} \times c}{K_{Qx} \times A_p}, c = 2A_p^2 \frac{E_c}{V_0}$$

(4)

D. Nauparac & N. Višnjić: Some special specifics of dimensioning of a hydraulic cylinder as an executive device o fan electrohydraulic actuator system

59

The models in Figure 3 and Figure 4 refer to throttling control in a hydraulic actuation system. Structurally, the diagram is similar to the variant with volumetric control. Also, feedback gain depends on cylinder working area.
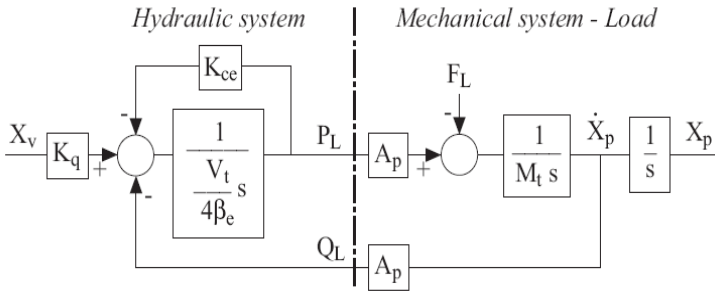
Figure 5: Structure of a mathematical model with external force and inertial load [4].

4   Basic linear model of hydraulic cylinder

A linear model with a load in the form of a transfer function is a third-order transfer function with an integral term. Depending on the degree of damping, we will have a pair of real poles or a pair of conjugate complex poles. We also show one phenomenon, and that is that if we have internal springs for centering in the hydraulic chambers, there is no longer an integral member.

$$W(s) = \frac{K}{s(s^2 + 2\xi\omega s + 1)}, 0 < \xi < 1 \tag{5}$$

$$W(s) = \frac{K}{s(s - a_1)(s - a_2)}, \xi > 1 \tag{6}$$

$$W(s) = \frac{K}{(T_3 s^3 + T_2 s^2 + T_1 s + 1)}, K = \frac{A_p}{c \times r} \tag{7}$$

According to equation (7) the model is with the positional load and the spring in the cylinder. Symbol r is the proportionality factor for the flow and c is the general stiffness.

5   Structural load cylinder model

The structural load of the cylinder means that we have close natural frequencies of the load with the hydraulic natural frequency, for instance of a gate, Figure 6. This means that we have to observe the load through natural frequencies. The model with structural load is given in Figure 7. We see that the structural load increases the order of the model by at least 4. The shape of the model allows us to show the influence of structural load on the connecting rod position or in another form to observe direct displacement of the structure. In addition to the aerodynamic control surfaces in aviation, the structural load for hydraulic cylinders is also represented by the gates within the hydromechanical equipment used on dams, canals and navigation locks in hydropower. With a structural load of this type, we have a significantly higher impact of friction, as we also have sliding friction, sealing rubber and rolling friction, wheels for lateral guide of the gate, where friction can be up to 30 % or more in intensity compared to inertial load, see Figure 6. This is not the case with aerodynamic surfaces where the friction component at the hinge moment is significantly smaller. In this case, we have a variable positional load (dependence of the attack point of the aerodynamic force on the angle of attack), while the gate has a variable force from the water.
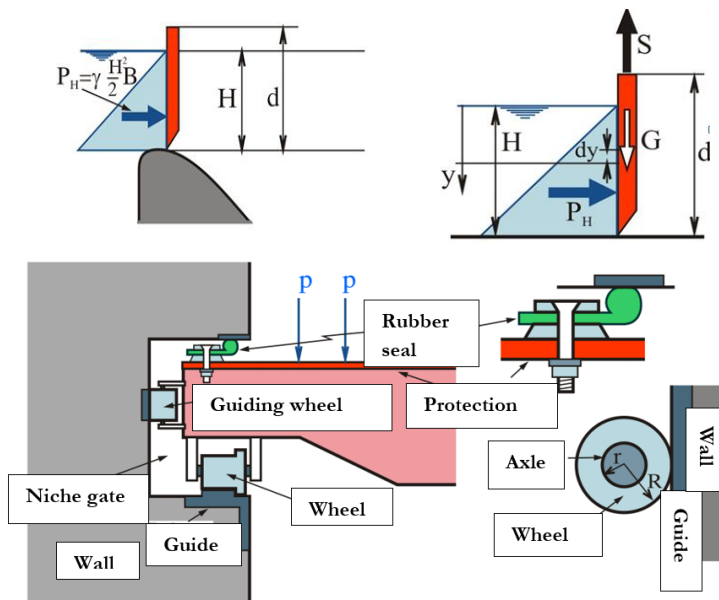
Figure 6: Slide gate model with loads acting on the rod of hydraulic cylinder [5].

D. *Nauparac & N. Višnjić: Some special specifics of dimensioning of a hydraulic cylinder as an executive device o fan electrohydraulic actuator system*

61

The question is how to analyse and model the structural load. One possibility is to use pressure feedback that will prevent the appearance of resonant frequencies when moving the gate, either lifting or lowering. Due to the rationality of making mechanical constructions of gates, they do not have sufficient rigidity, and in the control of their synchronous movement, ever greater dynamic requirements, such as speed of lifting and lowering or the smallest possible synchronous movement error, are constantly required.
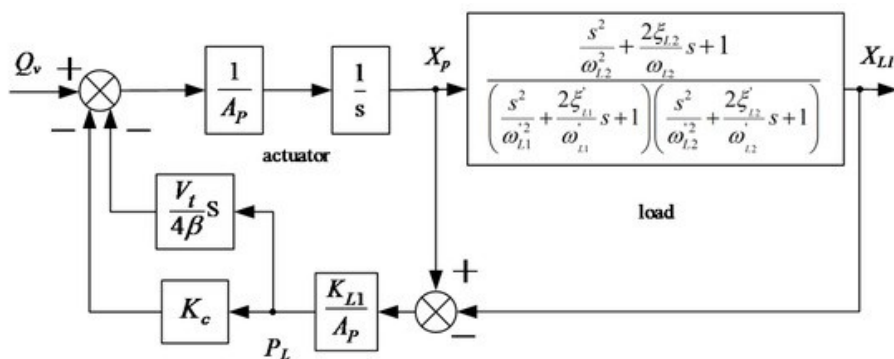
Figure 7: Block diagram of an electrohydraulic actuation system with two masses [6].

Figure 7 shows that the working surface of the hydraulic cylinder appears twice in the block diagram and the working volume of the chambers of the hydraulic cylinder appears once. The structural load model in Figure 7 allows us to easily define the transfer function of the structural load in a linear mathematical model if the previous structural load is calculated by the finite element method (FEM) from which we can directly obtain the frequency of the first harmonic and several higher as well as attenuation degrees. Then we have a complete linear model of high enough order that it can be used for dynamic analysis of the actuation system through which we can check the influence of the dimensions of the hydraulic cylinder on the dynamics of the movement of the gate. Figure 7 shows a dynamic load model with two masses. One mass is the mass of the gate and the other mass is the mass of the moving parts of the cylinder (connecting rod). Figure 7 shows a model of a single cylinder because the gate is symmetrical so that one half of the structure can be observed. The movement of the gate without the dynamics of synchronous movement is observed here.

6　　Conclusion

All steps in the analysis and synthesis of the actuation system are visibly shown, where the dimensions of the hydraulic cylinder have an influence on the dynamic properties of the electrohydraulic actuation system. In this way, the designer of the actuation system, knowing in advance the required dynamic properties of the electrohydraulic actuation system, can consider any change in the dimensions of the cylinder comprehensively within the electrohydraulic system he is designing.

References

[1]　Decker B., Saaski D. (2008). Design & Control of proportional and Servo systems, *Bosch-Rexroth brochure*

[2]　Watter, H. (2007). Hydraulik und Pneumatik, Studium Technik, Wiesbaden

[3]　К.С.Колесников, Машиностроение энциклопедия, Электропривод, Гидро и Виброприводы, Том I-4-2, Машиностроение, Москва, 2012

[4]　Rydberg, K. E. (2008) Hydraulic Systems with Load Dynamics. Linkopings University

[5]　Savić L.. Predavanja-prezentacija Zatvarači 1. (2021). Gradjevinski Fakultet Beograd

[6]　Zaho, S. K., Chen, Y., Ying, G., Yin, C., Xiao, X. (2021). A High Order Load Model and Control Algorithm for an Aerospace Electro Hydraulic Actuator. *IeCAT*

University of Maribor Press

Calculation and analysis hydraulic system for paint mixing machine

ALMIR OSMANOVIĆ, ELVEDIN TRAKIĆ & EDIN OMERAGIĆ

Abstract Paint production and for that colour mixing is an important process which has wide applications in several field. There are various kinds of colour mixing that can be done. It can either be additive colour mixing or subtractive colour mixing. Generally, there are various kinds of paint mixing machines available in the market. They vary in their size, shape, technology and methodologies. The aim of this paper is to present a calculation and analyse of hydraulic system for paint mixing machine. The paint mixing machine has the task of mixing the oil paint components in vessel until the finished mass is obtained. As oil paint is a typical representative of rheological materials where the viscosity depends on the shear rate, it is necessary to mix different paint structures during processing at different speeds - the number of revolutions of the propeller must be changes.

Keywords: • hydraulic system • analysis • simulation • mechatronic • paint mixing machine •

CORRESPONDENCE ADDRESS: Almir Osmanović, University of Tuzla, Faculty of Mechanical Engineering, Urfeta Vejzagića br. 4, 75000 Tuzla, Bosnia and Herzegovina, e-mail: almir.osmanovic@untz.ba. Elvedin Trakić, University of Tuzla, Faculty of Mechanical Engineering, Urfeta Vejzagića br. 4, 75000 Tuzla, Bosnia and Herzegovina, e-mail: elvedin.trakic@untz.ba. Edin Omeragić, B.Eng, University of Tuzla, Faculty of Mechanical Engineering, Urfeta Vejzagića br. 4, 75000 Tuzla, Bosnia and Herzegovina, e-mail: edin.omeragic@gmail.com.

1　　Introduction

The paint mixer has the task of mixing the oil paint components in vessel A until the finished mass is obtained. Oil paint is a typical representative of rheological materials in which the viscosity depends on the shear rate, it is a necessary to mix different paint structures during processing at different speeds. The container with the paint components is pulled on the cart and placed under the propeller (Figure 1). After placing the vessel in the required place, the piston of the hydraulic cylinder C1 drives the mechanism for clamping the vessel with the mixture, and then the piston of the cylinder C2 immerses the propeller in the mixture. The propeller of the mixer is driven by a hydraulic motor of one-way action (M) with regulation of the number of revolutions. The hydraulic system consists of two separate circuits: for the drive of the hydraulic motor M and the system for providing the control drive of the cylinders C1 and C2 (Figure 2).
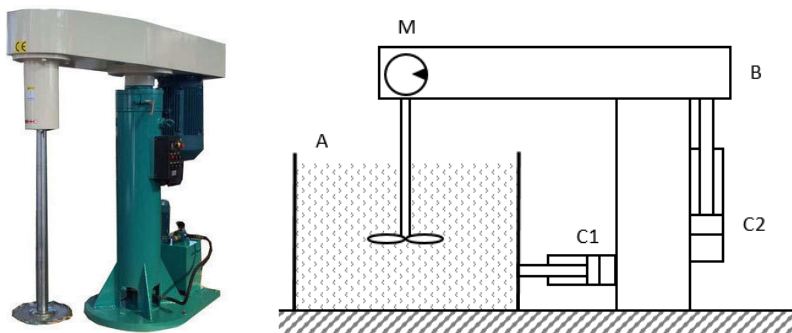
Figure 1: Paint mixing machine and hydraulic components.

Pump P2 with hydraulic regulator drives the hydraulic motor M. The capacity of the pump depends on the pressure of working fluid so that in parallel with its increase. Controlling the position of the regulator is provided by a special branch from the small capacity pump P1. The required pump capacity P2 is controlled by reading the achieved engine speed on the TM tachometer. When the required engine speed is reached, the distribution valve (2) is brought back to the neutral position, and the non-return valve maintains the required pressure in the pump regulator. The pump capacity is kept constant during the further processing of the mixture. If it is necessary to reduce the speed with the production technology, the distribution valves (2) are brought to position (a), the non-return valve is opened, and the control circuit is relieved to the required pressure.
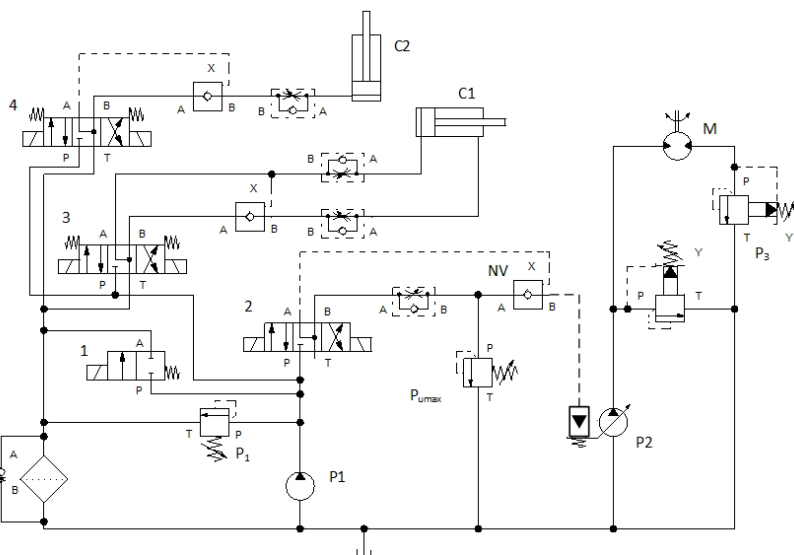
Figure 2: Hydraulic circuit diagram.

The control of the position of the distribution valve (2) is performed, if necessary, by pressing the button placed on the control panel. Cylinder C1 and C2 are supplied by pump P1. The direction of movement of their pistons is controlled by bringing the distribution valves 3 and 4 to the required position, and keeping the pistons in the required position by hydraulically operated non-return valves. The kinematics of the functioning of the hydraulic system is defined by the Table 1 of the solenoid valves.

Table 1: Kinematic functioning of the hydraulic system

System function	1a	2a	2b	3a	3b	4a	4b	
Clamping the container with paint - C2	+	-	-	-	+	-	-	
Lowering the mixer - C1	+	-	-	-	-	+	-	
Increasing the speed - M	+	-	+	-	-	-	-	
Keeping the constant speed - M	-	-	-	-	-	-	-	
Reducing the speed - M	+	+	-	-	-	-	-	
Lifting the mixer - C1	+	-	-	-	-	-	+	
Paint container release - C2	+	-	-	+	-	-	-	
Mixer standstill	-	-	-	-	-	-	-	

2   Calculation of the hydraulic system

Calculation of hydraulic cylinder C1 - for the required clamping force F = 1000 [N] and the adopted cylinder diameter of D = 50 [mm] and connecting rod diameter d = 28 [mm], the required pressure in the cylinder is:

$$F = pA = p_1A_1 = p_2A_2 \tag{1}$$

$$p_1 = \frac{4F}{\pi D^2} = 0.5093 \text{ [MPa]} = 5.093 \text{ [bar]}$$

$$p_2 = \frac{4F}{\pi(D^2-d^2)} = 0.7420 \; [MPa] = 7.420 \text{ [bar]}$$

$$Q = \frac{V_1}{t} = \frac{A_1 l}{l/v} = \; 0.196 \; [l/s] \tag{2}$$

Calculation of hydraulic cylinder C2 - cylinder C2 should enable lifting of platforms of mass m = 500 [kg], speed v = 0.1 [m/s]. Let it takes time to reach this velocity t = 1 [s].

$$F = F_u + G = \; a \cdot m + m \cdot g = \frac{v}{t} \cdot m + m \cdot g = 5000 \text{ [N]} \tag{3}$$

The diameter of the piston D = 100 [mm] is adopted.

$$p_{c2} = \frac{F}{A} = \frac{F}{\pi D^2/4} = 0.637 \text{ [MPa]} = 6.37 \text{ [bar]} \tag{4}$$

Calculation of the required pump capacity:

$$V = Al = 11{,}779{,}500 \text{ [mm}^3\text{]} = 11.7795 \;\; [l] \tag{5}$$

$$Q_p = \frac{V}{t} = 0.784 \text{ [l/s]} = 47[l/min] \tag{6}$$

In order to select a pump of the appropriate specific capacity, it is necessary to select the number of revolutions of the electric motor and the coefficient of volumetric efficiency of the system (n = 1450 [rpm]; η_{vol} = 0.9).

Specific pump capacity:

$$q_p = \frac{Q_p}{n\eta_{vol}} = 36 \text{ [cm}^3\text{/ob]} = \frac{36}{2\pi}\text{[cm}^3\text{/rad]} = 5.72\text{[cm}^3\text{/rad]} \tag{7}$$

A standard axial- piston pump of specific capacity is selected q=36 [cm³/rev] and total capacity Q = 870 [cm³/s].

Selection of pressure and return pipe diameters – according to the pressure, the speed of the fluid in the pressure part of the pipeline is adopted: v = 3.5 [m/s]. The diameter of the pipeline is:

$$Q = vA = v\frac{d^2\pi}{4} \rightarrow d = 1{,}78 \text{ [cm]} \tag{8}$$

A pipeline measuring 25x2.5 [mm], internal diameter d_u = 20 [mm] is adopted.

$$v = \frac{Q}{A} = \frac{4Q}{d^2\pi} = 2.76 \text{ [m/s]} \tag{9}$$

Calculation of the required pump pressure - the required pump pressure is calculated based on the sum of the total pressure losses:

$$p_r = \sum \Delta p_1 + \sum \Delta p_2 + \sum \Delta p_3 + \sum \Delta p_4 + \sum \Delta p_5 + \sum \Delta p_6 + \sum \Delta p_7$$

$$p_v = 1.1 \cdot p_r \tag{10}$$

Where are:
$\Sigma\Delta p_1$ -line resistances in the pipeline from the pump to the cylinder,
$\Sigma\Delta p_2$ - local resistances in the pipeline from the pump to the cylinder,
$\Sigma\Delta p_3$ - resistances in hydraulic components from pump to cylinder,
$\Sigma\Delta p_4$ - line resistances in the pipeline from the cylinder to the tank,
$\Sigma\Delta p_5$ - local resistances in the pipeline from the cylinder to the pump,
$\Sigma\Delta p_6$ - resistances in hydraulic components from cylinder to tank,
$\Sigma\Delta p_7$ - opposing resistances of external forces to the movement of the piston.

The pressure drop of pipeline is equal to:

$$p_{lin} = \sum \Delta p_2 + \sum \Delta p_5 \tag{11}$$

If you want to make an accurate calculation, it is necessary to calculate the pressure drops in all branches in each operation. An accurate calculation is needed to calculate the total heat balance. Often, pressure drops are not calculated in detail, because it is a complicated calculation, especially with complex hydraulic systems. In such situations, only the critical branch is calculated, in which the pressure drop is the largest, and the entire hydraulic system is dimensioned in relation to it.

The pressure drop when lifting the platform is:

$$\Delta p_{lin} = \lambda \cdot \frac{l}{d} \cdot \frac{v^2}{2} \rho = 25084 \ [\text{N/m}^2] = 0.25084 \ [\text{bar}] \tag{12}$$

Local pressure drop - From pump to cylinder we have the following local losses: manifold pressure drop (4) 4/3; pressure drop on throttle valve with non-return valve; pressure drop on non-return valve with hydraulic control. Based on the Q-Δp diagram for the manifold model (Figure 3), the pressure drop for Q = 50 [l/min] is Δp_a = 0.21 [MPa] = 2.1 [bar].
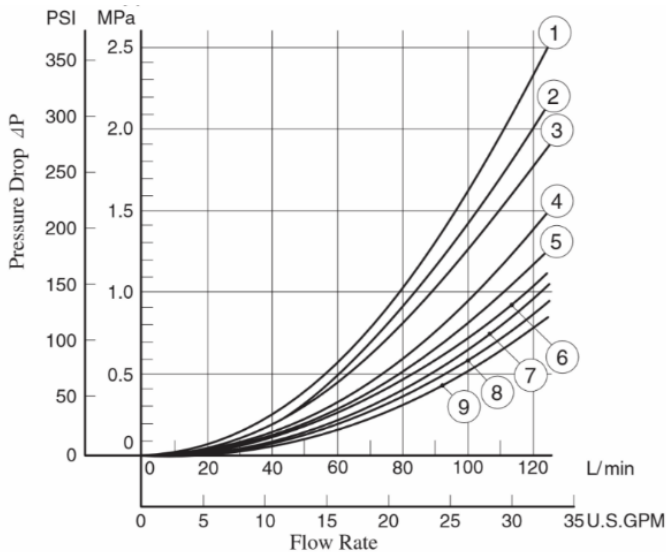
Figure 3: Dependence of manifold pressure drop on flow.

The pressure drop in the non-return valve is given by the diagram Q-Δp (Figure 4) (Δp_b = 0,06 [MPa] = 0,6 [bar]). The pressure drop on the non-return valve with hydraulic control can be determined from the diagram (Figure 5) and for the model the valve model selected is: (Δp_c = 0,3 [MPa] = 3 [bar]).
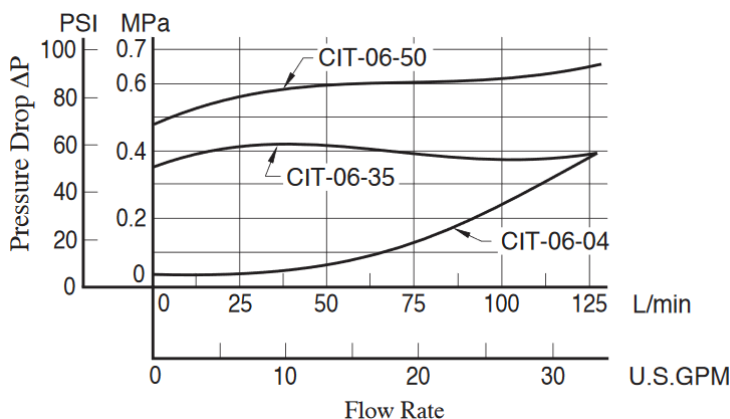
Figure 4: Dependence of non-return valve pressure drop on flow.
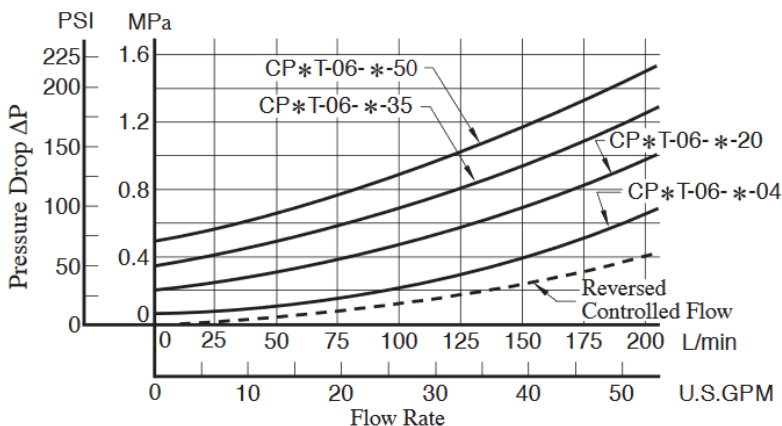
Figure 5: Dependence of pressure drop of non-return valve with hydraulic control.

Pressure drop is:

$$\Delta p = \Delta p_{lin} + \Delta p_a + \Delta p_b + \Delta p_c = 5.95 \text{ [bar]} \tag{13}$$

The total pressure is the pressure drop and the pressure required to overcome the external resistance: $p_r = \Delta p + p_{c2} = 12.32$ [bar] . The pump pressure increases by 10 % and is: $p_p = 1.1 p_r = 13.55$ [bar]. Based on the calculated pressure, the pump with the highest pressure $p_{max} = 20$ [bar] is selected. The pressure relief valve will be set to a pressure of $p_{vop} = 15$ [bar].

Electric motor power calculation - electric motor should enable the pump to start with the following characteristics: maximum pump operating pressure $p_{max} = 20$ [bar], pump capacity $Q = 52.2$ [l/min]. The power of the electric motor of the pump is equal to ($\eta_v = 0.9$-volumetric efficiency coefficient; $\eta_m = 0.85$- mechanical efficiency):

$$N = \frac{p_v Q}{600 \eta_v \eta_m} = 2.27 \text{ [kW]} \tag{14}$$

2.1   Calculation of pump and mixer motor

The estimation of the mixer shaft power (P) required for mixing is based on the application of the following dimensionless correlation:

$$N_p = f(Re_M, Fr_M, \frac{D}{d_m}, \frac{H}{d_m}, \frac{d_3}{d_m}) \tag{15}$$

The installation of the breaker prevents the occurrence of unfavourable vortices and thus eliminates the influence of Freud's number.

$$N_p = f(Re_M, \frac{D}{d_m}, \frac{H}{d_m}, \frac{d_3}{d_m}) \tag{16}$$
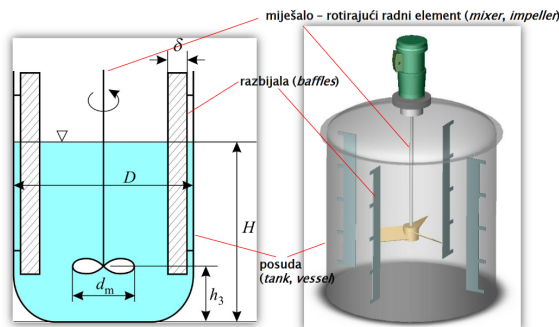
Figure 6: Mixer parameters.

In this case $Re_M = 243$ and the flow is in the transition region between laminar and turbulent. From the power diagram, the power number is about $Np = 1.5$.
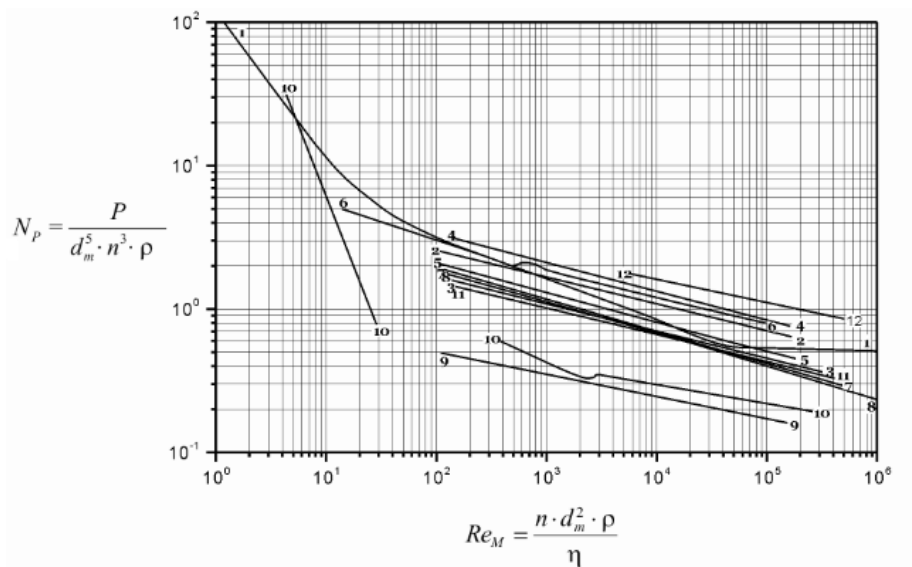
Figure 7: Dimensionless power diagram.

The power on the mixer shaft is:

$$P = N_p \cdot n^3 \cdot d_m^2 \cdot \rho_f = 182 \text{ [kW]} \tag{17}$$

Required torque and specific volume:

$$M = \frac{P}{\omega} = 2896 \text{ [Nm]} \tag{18}$$

$$P = \frac{\Delta p \cdot Q}{600} \rightarrow Q_m = \frac{600 \cdot P}{\Delta p} = 436.8 \text{ [l/min]} \tag{19}$$

$$q_m = \frac{Q_m}{n \cdot \eta_v} = 485 \text{ [cm}^3/\text{ob]} \tag{20}$$

The Rexroth A4FM500 engine is selected based on specific volume, operating pressure and torque. Basic data are given in Table 1.

Table 1: Basic data of A4FM500

Motor		
Specific volume	$q_m = 500 \text{ o/cm}^3$	
Maximum speed	$n = 1800 \text{ o/min}$	
Torque	$M = 2783 \text{ Nm}$	
Pressure drop	$\Delta p = 350 \text{ bar}$	
Volumetric efficiency	$\eta_v = 0.9$	

Fluid flow in the hydraulic circuit of the pump and motor let be $v = 4{,}5$ [m/s]. The diameter of the pipeline is:

$$Q_m = q_m \cdot n \cdot \eta_{vol} = 450 \text{ [l/min]} = 7500 \text{ [cm}^3/\text{s]} \qquad (21)$$

$$d = \sqrt{\frac{4Q}{\pi v}} = 4.6 \text{ [cm]} \qquad (22)$$

The pipeline diameter d = 50 [mm] is adopted.

$$v = \frac{Q}{A} = \frac{4Q}{d^2 \pi} = 3.82 \text{ [m/s]} \qquad (23)$$

Line pressure drop from pump to reservoir:

$$\Delta p_{lin} = \lambda \cdot \frac{l}{d} \cdot \frac{v^2}{2} \rho = 46754 \text{ [N/m}^2\text{]} \qquad (24)$$

The pressure drop on the pressure relief valve is given in the Table and for a flow of 500 [l/min] it is $\Delta p_v = 16$ bar. Working pressure: $\Delta p_r = 266.47$ [bar]. The pump pressure increases by 10% and is: $p_p = 1.1 \Delta p_r = 293$ [bar]. Based on the calculated pressure, the pump with the highest pressure $p_{max} = 350$ [bar] is selected. The pressure relief valve will be set to a pressure of $p_{vop} = 300$ [bar]. Basic data of the used pump are given in Table 2.

Electric motor speed $n_{em} = 950$ [rev/min]. The theoretical flow of the pump is:

$$Q = \frac{q_m \cdot n}{1000} = 475 \text{ [l/min]} \qquad (25)$$

Table 2: Basic data of used pump type AA4CSG 500

Pump (Rexroth AA4CSG 500)		
Specific volume	$q_m = $ 500 o/cm^3	
Maximum speed	$n = $ 1800 o/min	
Torque	$M = $ 2783 Nm	
Pressure drop	$\Delta p = $ 350 bar	
Volumetric efficiency	$\eta_v = $ 0.9	

Pump electric motor power:

$$N = \frac{p_v Q}{600 \eta_v \eta_m} = 362 \text{ [kW]} \tag{26}$$

3 Modelling and simulation of hydraulic system models

The Figure 8 shows the simulation model of the entire system. According to the principle of operation, it can observe three independent parts, so it will analyse the following subsystems separately: raising and lowering the platform; clamping the paint cart; mixing speed control.
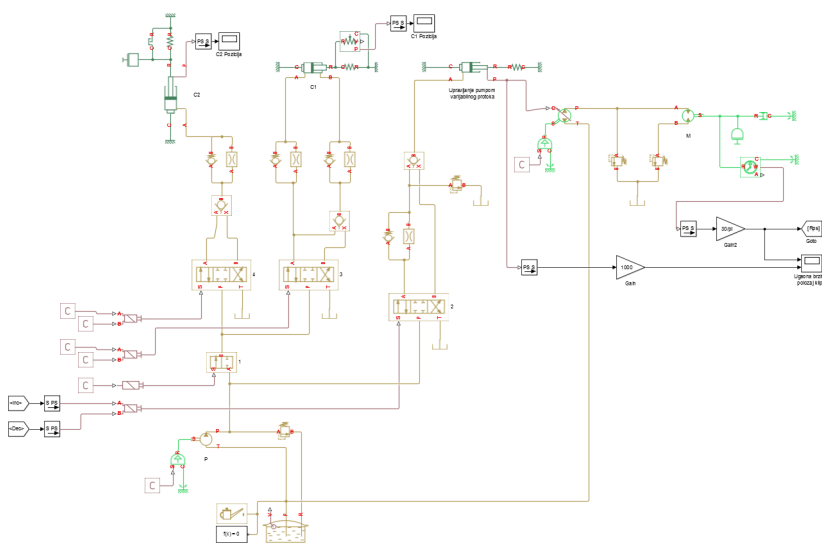
Figure 8: Simulation model of hydraulic system.
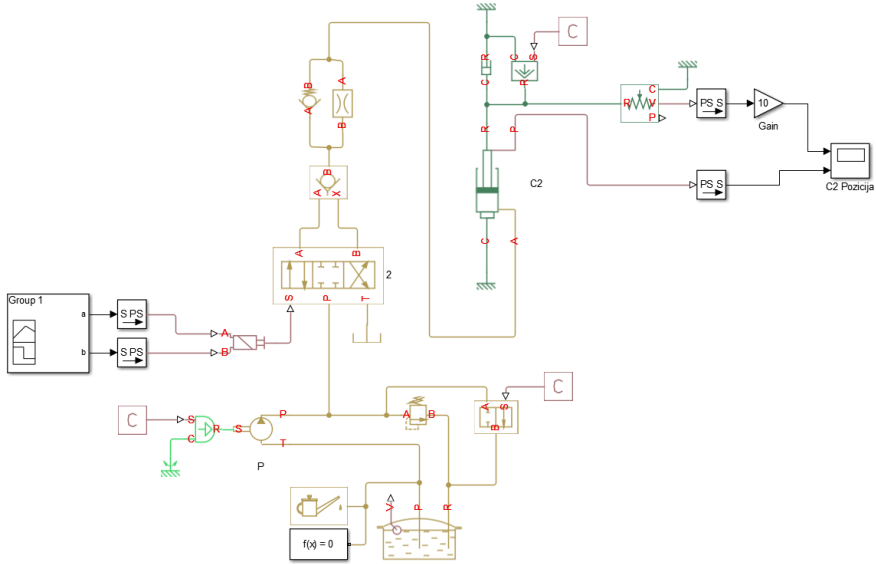
Figure 9: Platform lifting and lowering model.
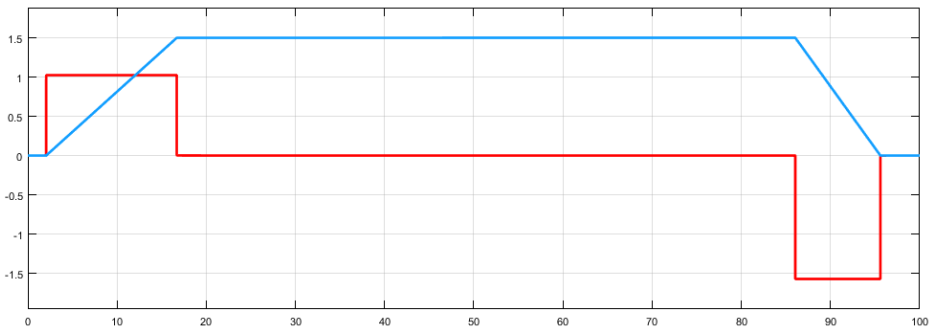
Figure 10: Road and speed diagram.

The following values can be obtained from the diagram:

- Platform boot time T_d = 15 [s].
- Platform lowering time T_s = 10 [s].
- Piston speed when lifting the platform v_d = 0.1 [m/s].
- Piston speed when lowering the platform v_s = 0.16 [m/s].

The values obtained for simulation correspond to the previously calculated values.
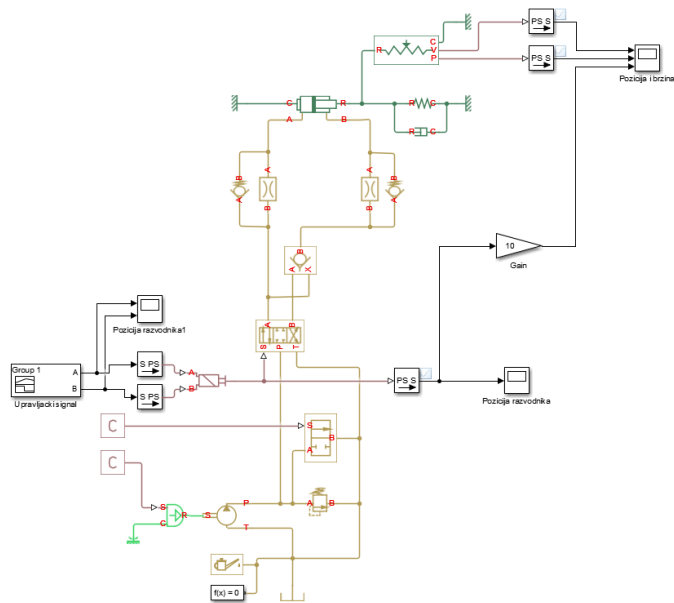
Figure 11: Model of hydraulic circuit for clamping a container with paint.
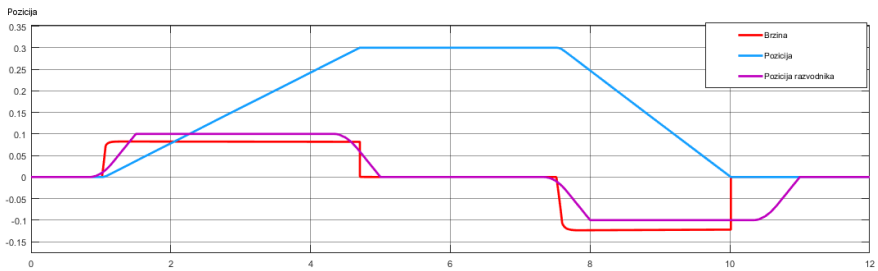
Figure 12: Diagram of the path, speed and position of the valve.
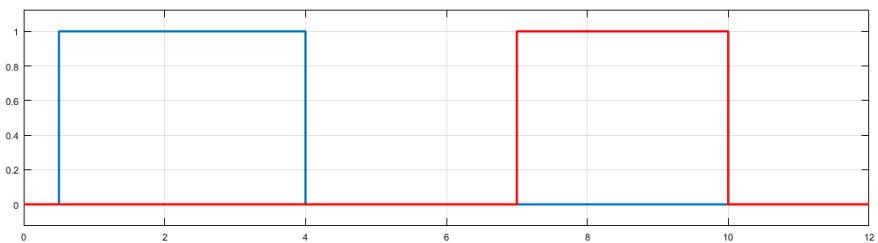
Figure 13: Control signal for valve.
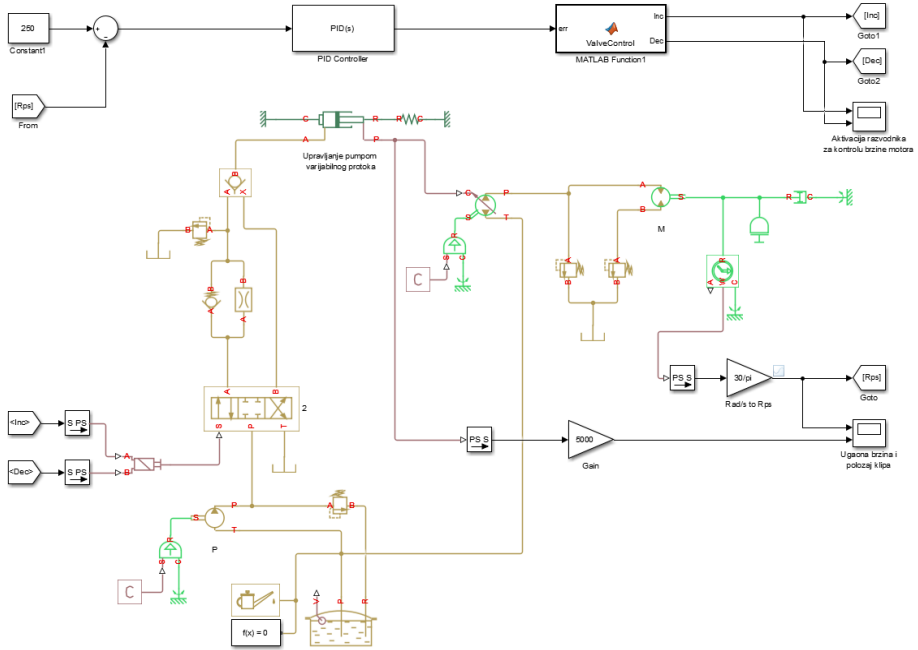
Figure 14: Model of mixing speed control by control of a variable capacity pump.
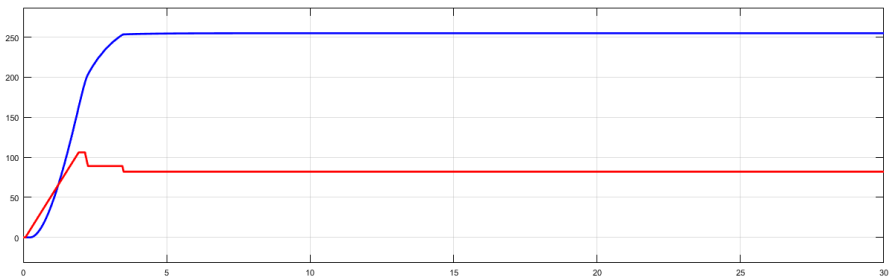
Figure 15: Diagram of angular velocity and position of the connecting rod for pump flow control (PID regulator).

From the values achieved after simulation, it can conclude that the model fully satisfies or that the required parameter is achieved, and that the components, and the model as such can be practically used to create a real system.

3   Conclusion

In this paper work is present calculation and simulation model of the hydraulic system for a paint mixing device. The calculation was performed on the basis of the hydraulic scheme and the principle of operation of the mixing device. The capacity of the mixing device was adopted and on this basis the additional parameters used in the calculation were determined. The outcome of the calculation itself depends on the parameters that are adopted during the calculation, which in a certain way meet the set requirements, e.g. it is possible to reduce the working pressure of the pump by adopting a cylinder with a larger diameter, on the other hand increasing the diameter of the cylinder reduces the speed of the connecting rod which results in choosing a pump with a larger specific volume or increasing the pump speed. Achieving the optimal solution is obtained by setting certain conditions in critical places of the hydraulic system, in this way individual branches of the hydraulic system are solved and the parameters are brought to the working areas. In the second part of the paper, was created model for simulation, which gives a better insight into the behaviour of the whole system. Execution of system simulation is enabled by solving differential equations. Each component of the system is defined by a set of equations, and based on the graph of components. Using appropriate software tools, it provides the ability to simulate the operation of a designed hydraulic system, and it is possible to perform optimization in order to find the most favourable solution, and thus select the components used in the manufacture of hydraulic systems.

References

[1]   Bishop, R. H. (2017). Mechatronic Systems, Sensors, and Actuators: Fundamentals and Modeling. *CRC Press*
[2]   Osmanović, A., Trakić, E. (2021). Hidraulika. Tuzla: Off-set.
[3]   Ramin S. Esfandiari (2018). Modeling and Analysis of Dynamic Systems. *CRC Press*
[4]   Ašković R., Čantrak S., Ćirić M., Radojević Z., Crnojević C., Mirković Lj., Jovanović P., (1986). I knjiga - Hidraulika - razvodnici i ventili. Mašinski fakultet Beograd
[5]   Yousefi H., (2007). On Modeling, System Identification and Control of Servo-Systems with a Flexible Load. Thesis, (PhD), Lappeenranta University of Technology, Finland
[6]   Çetin S., Volkan A.A., (2010). Simulation and hybrid fuzzy-PID control for positioning of a hydraulic system. Nonlinear Dynamics, Vol: 61, Issue: 3, 465-476.
[7]   Dieter W., Norbert G., (2008). Hydraulik - Grundlagen, Komponenten, Schaltungen. Springer Verein Deutscher Ingenieure, Berlin.

University of Maribor Press

Development of direct driven servo hydraulic actuator

TINE JURAK & VITO TIČ

Abstract Direct control of hydraulic cylinders - without use of control valve, represents a newer concept of energy-saving control of cylinders, without damping losses. In order to study this type of drive, it is necessary to design and manufacture a compact model of such device to study the control concepts and to check the operation of the system. We will study the existing implementations of such drives and create our own direct driven servo-hydraulic actuator (hereinafter DD SHA), with which we will move different loads. A servomotor must be attached to a suiTable hydrostatic unit (pump-motor). All the missing components need to be designed and manufactured for completed hydraulic circuit.

Keywords: • hydraulic cylinder • hydraulic actuator • direct driven • servo actuator • PLC control •

CORRESPONDENCE ADDRESS: Tine Jurak, University of Maribor, Faculty of Mechanical Engineering, Maribor, Slovenia, e-mail: tine.jurak@student.um.si. Vito Tič, University of Maribor, Faculty of Mechanical Engineering, Maribor, Slovenia, e-mail: vito.tic@um.si.

1 Introduction

Direct driven servo hydraulic actuators consist a servo motor directly coupled to a hydraulic pump. The positioning of the hydraulic piston, the adjustment of the pressing speed, as well as the force control are accomplished without the use of a directional or proportional valve.

Contrary to this concept the conventional press drive is normally effected via an asynchronous motor running at constant speed and a pump with variable delivery rate that can be adjusted mechanically, and it is controlled by directional or proportional valves.

But still, the new technology cannot be utilised completely without valves. Different valves are required e.g. for safety functions, or for the filling of large cylinder chambers for quick movements. In addition, the maximum pressure in the system is also usually limited by pressure relief valves.

Due to their small size, capacity and versatility, pump-controlled hydraulic systems are very useful in various applications such as bending, moving, compressing, lifting, closing, and steering.

The advantages of such systems are [1]:
  − increased productivity,
  − robustness – long service intervals,
  − overload safety – safety pressure valves,
  − high accuracy and dynamics of the servomotor,
  − possibility of connection – industry 4.0,
  − less necessary components and space,
  − easier maintenance,
  − less hydraulic oil used,
  − mobile system – easy connection and start-up.

There are also very large versions of direct driven (DD) electro hydraulic actuator (EHA) devices used to move turbine gates and flaps in hydropower plants. Such devices are purpose-built and custom-made. The hydraulic cylinders of such devices can reach up to 27 m of working stroke and up to 10,000 kN of working power.

2   Different possibilities of direct driven hydraulic cylinder

There are various systems that use one or two pumps to drive hydraulic cylinders, either through piston rod or differential cylinders. There are also a few different system configurations that use multiple hydraulic pumps to control the differential cylinder.

2.1   Versions with more than one hydraulic pump

Cleasby in Plummer [2] developed and built a prototype of a hydraulic system directly controlled by a pump. It was designed using special one-way hydraulic cylinder with a plane ratio of 1:2 for an aircraft simulator. Each cylinder was connected to a pair of identical constant flow pumps acting as a tandem pump and was connected to an electric servomotor. System also used a hydraulic accumulator which compensated energy of the weight of the load and provides a difference in flow due to the different volumes of the cylinder. This restores some energy and improves the efficiency of the entire hydraulic system.

There are a lot of roller ratios available on the market that are not 1:2, as this ratio is rarely used in practice. In addition, a system that requires two pumps makes the drive assembly heavy, complex, and expensive. Therefore, such systems are not popular in practice.

2.2   Versions with through piston rod and identical areas

Hydraulic cylinders with a through piston rod were developed primarily for the aerospace industry.

In hydraulic systems, hydraulic fluid typically circulates continuously throughout the cycle, including the tank, pump, accumulator, valve, and actuators. In circuits as shown in Figure 1, the hydraulic fluid does not leave the pump and actuator circuit; therefore, it is known as the hydrostatic circuit. However, such a hydraulic cylinder system with a through piston rod is not suiTable for a hydraulic system with a differential cylinder.

Compared to a hydraulic cylinder with a through piston rod, differential cylinders require less space to operate and are therefore more popular in the industry.
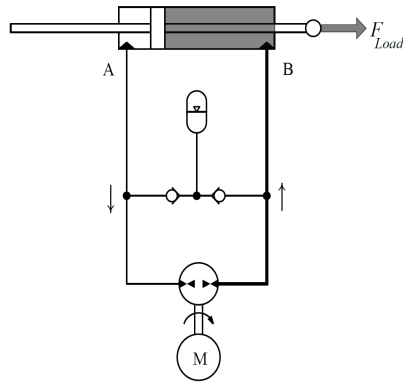
Figure 1: System with through piston rod [1].

2.2   Versions with differential hydraulic cylinders

Allan J. Hewett [3] was the first to patent a single-pump hydraulic system that controlled a single differential hydraulic cylinder. He used a 3/2-way solenoid valve to divert the differential flow of the hydraulic cylinder. The valve directs the differential flow from both sides of the cylinder into the tank. Two non-return valves protect the pump against cavitation.

The force of the load helps to pump to the internal position of the final actuator and calms the uncontrolled movement. Until the solenoid valve changes position, the load will fall uncontrollably. From the moment the solenoid valve changes position, the pump acts as a hydraulic motor.

The hydraulic pump in this circuit operates in four hydraulic quadrants and is able to recover some energy when the load helps operation. The system has been used for some forestry machinery, and the results have shown evidence of uncontrollable load vibrations. Because one side of the cylinder is always connected to the low-pressure side of the hydraulic circuit through the solenoid valve, the circuit is uncontrollable under conditions of sudden load switching.

Rahmfeld and Ivantysynova [4] used a similar idea when they replaced the solenoid valve with two pilot non-return valves. As shown in Figure 2, when the load is resisted, the pump supplies the cylinder terminal B and the piston rod moves outwards. The high pressure at the cylinder connection B is maintained by the closed control valve PCVb

and the non-return valve PCVa remains open. The pump sucks the oil from port A, the excess liquid from port A to pump I is directed to the tank with the open line of the PCVa pilot check valve, and thus pump I operates in pump mode. Because of the support load, the pressure in terminal A rises, the pilot check valve PCVb opens its line, and the piston rod begins to retract. From this point on, the pump works like a hydraulic motor.
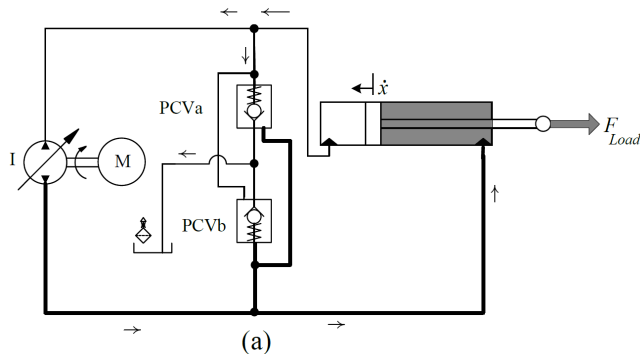
Figure 2: Direct driven differential hydraulic cylinder with two pilot non-return valves [1].

In the systems discussed so far, using a single pump to control the flow of differential hydraulic cylinders, one side of the cylinder is always connected to the low-pressure side of the hydraulic circuit. In the event of a sudden change in load, transient pressures occur, creating unwanted vibrations at the final actuator.

The improved system (Figure 3) consists of a DC electric motor connected to a two-way constant flow hydraulic pump. AdjusTable non-return valves CV1 and CV2 (with the possibility of adjusting the opening pressure) improve the rigidity of the hydraulic cylinder against small support loads by raising the low pressure. The non-return valves PCV1 and PCV2 hold the actuator in its position when the system is idle. Closing the non-return valves PCV3 and PCV4 causes the differential currents of the differential cylinder to be diverted to the tank. The system turns out to be very inefficient due to the use of two adjusTable non-return valves CV1 and CV2 to improve the response of the final actuator to loads that resist movement.
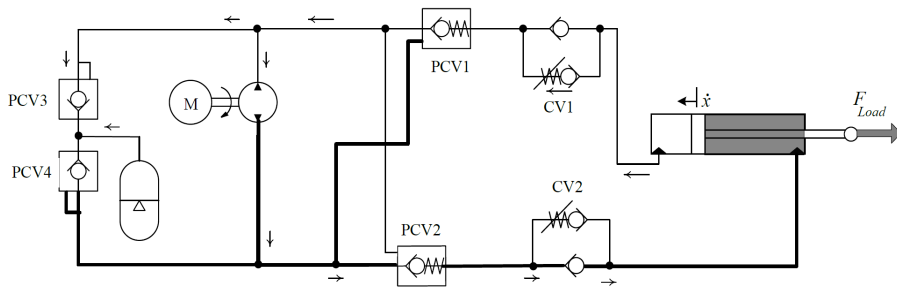
Figure 3: The improved design of direct driven differential hydraulic cylinder [1].

3   Design of our direct driven servo hydraulic actuator

Our goal was to construct and manufacture as simple DD SHA device as possible, which can be loaded as desired. A servomotor and all other hydraulic components had to be attached to a suiTable hydrostatic unit (pump-motor). We decided to choose the already proposed hydraulic scheme for the basic model (Figure 2). It had to be rearranged according to our needs and the shape of the device.

Given that the device will be used in the laboratory for the needs of studies and familiarization with such devices, it was necessary to add connection points for pressure monitoring, safety valves and filters for hydraulic fluid to the existing scheme. We also used a hydraulic accumulator to mitigate or prevent current and pressure peaks (similar to Figure 3). The final hydraulic scheme of designed direct driven servo hydraulic actuator is shown in Figure 4.

DD EHA devices are compact and based on efficiency in terms of device size. Since a lot of hydraulic components are used for our device, the device would be too large if we used classic components and connected them in a classic way - pipes, connections. Therefore, it was necessary to make a hydraulic block in which to install our components. We made a 3D model of the block and the hydraulic block itself, in which we installed the hydraulic components. Figure 5 shows a 3D model of the block with flow channels and connections.
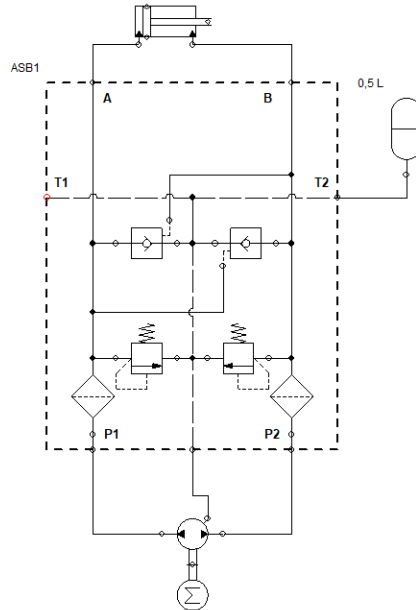
Figure 4: Hydraulic scheme of designed direct driven servo hydraulic actuator.
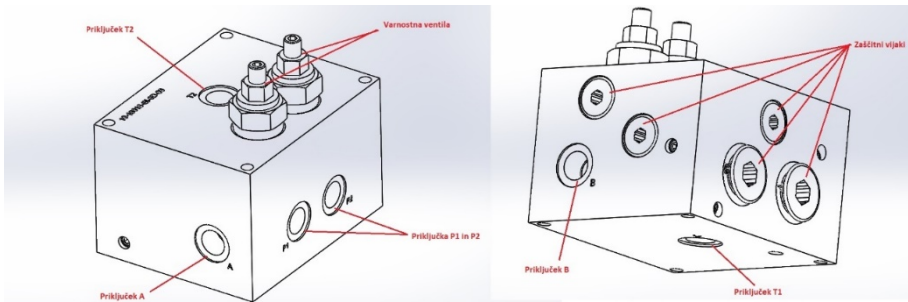
Figure 5: 3D model of the block with flow channels and connections.

3.1   Determination of hydraulic components

Based on the 3D model of the block, we were able to proceed with the construction of the layout of other components of the device and the layout of the device itself.

After the completion of the hydraulic scheme, it was necessary to precisely determine the hydraulic components. Depending on the method of component installation, we

used 2-way screw-in hydraulic valves. Two controlled non-return valves type RHC 21/1 were used. Such valves are characterized by opening with a pressure at the opening connection, which is determined by the ratio of the surfaces inside the valve.

To protect the system against overpressure, we used two safety valves, which are adjusTable from 0 bar to 250 bar.

Because such hydraulic system operate in a closed hydraulic fluid circulation circuit, we used coarse screw-in hydraulic fluid filters. In our case, this is a built-in mesh with the appropriate density of loops (knits).

The final actuator of our device is a differential hydraulic cylinder. The diameter of the piston (d) is 22 mm, and the diameter of the cylinder (D) is 32 mm. The stroke of the cylinder (L) is 315 mm.

The size of the tank was determined according to the difference in chamber volumes in the hydraulic cylinder. The volume of the hydraulic accumulator is also determined. We used a 1-liter hydraulic fluid tank and a 0.75-liter hydraulic accumulator.

The main component of our DD SHA device is the hydraulic pump. A Bosch-Rexroth pump model AZMB-32-4.0UHO02PL was used. The external gear motor/pump, for both directions of rotation, can be used in four-quadrant operation. The size of the pump is 4 cm^3 and the maximum working pressure is 220 bar. The pump has a leakage port on which the maximum permissible pressure can be 3 bar. The pump is driven by a Rexroth Indramat, model MKD071B-061-KG1-KN with built-in absolute encoder, which gives us information about the position of the servomotor. The motor allows us a maximum speed of 4000 min-1 and a maximum torque of 32 Nm.

3.2   Modeling of device and final layout

Modeling of our device began with the connection of a servomotor and a pump. The shafts of both components are connected to the clutch, so it was necessary to make a suiTable flange, which connects the motor and the pump.
This was followed by planning the installation of the hydraulic block and other components.

Considering the fact that the air in the liquids always appears at the highest point of the system, it made sense to place the hydraulic accumulator in the highest position. Due to gravity, we ensured a constant pressure of the hydraulic fluid to the pump. To facilitate the connection of the components to the pipes, the servomotor with the pump was placed transversely to the direction of the hydraulic cylinder.

We have adjusted the mounting plate of our device so that it can be easily fixed to the laboratory workbench. If necessary, our device can be easily and quickly dismantled and moved to another location. Final layout of device with all components is presented in Figure 6.
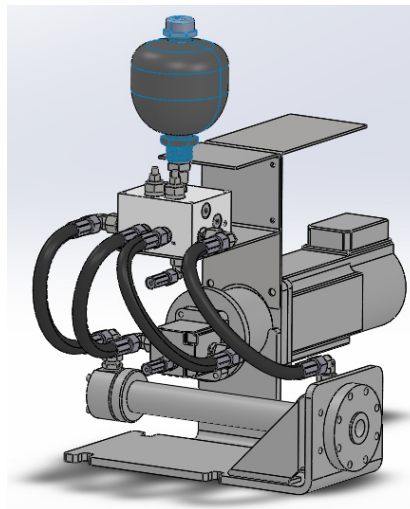
Figure 6: Final 3D model of the device with all components.

4   Performance and capabilities of direct driven servo hydraulic actuator

Based on the selected hydraulic cylinder, which has a piston diameter of 32 mm, a piston rod diameter of 22 mm and a working stroke of 315 mm, we calculated that the cylinder has 17.7 kN of working power and in the retracting direction 0.93 kN of power. The speed of moving outwards at full pump speed is 0.25 m/s and inwards 0.47 m/s.

4.1   Manual and closed-loop control

We first ran the system manually to check the correct operation and eliminate any errors. In doing so, we confirmed the assumption that the hydraulic cylinder moves outwards and inwards at different speeds. This results in different sizes of hydraulic cylinder chambers. This can be seen from Figure 7, as on the left the green curve rises with a smaller slope.
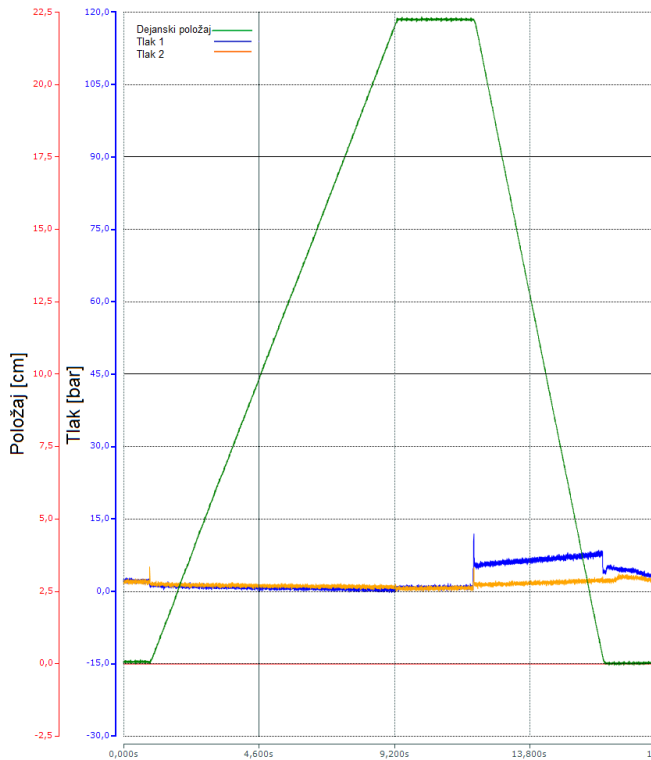
Figure 7: Results of manual system control.

When the system in manual mode worked properly without errors, we ran the system in automatic mode. The problem that occurred when starting in automatic mode was setting the PID controller. The problem arose due to the different speed of movement of the cylinder. We used the Ziegler-Nichols method to set the PID controller correctly. After setting the PID controller, the response of the system is extremely fast, as the hydraulic cylinder is controlled directly via the hydraulic pump, consequently via the servo motor.

The red line in Figure 8 represents the desired position and the green line the actual position of the hydraulic cylinder. The slope of the green line rise also depends on the set maximum permissible revolutions of the servo motor.
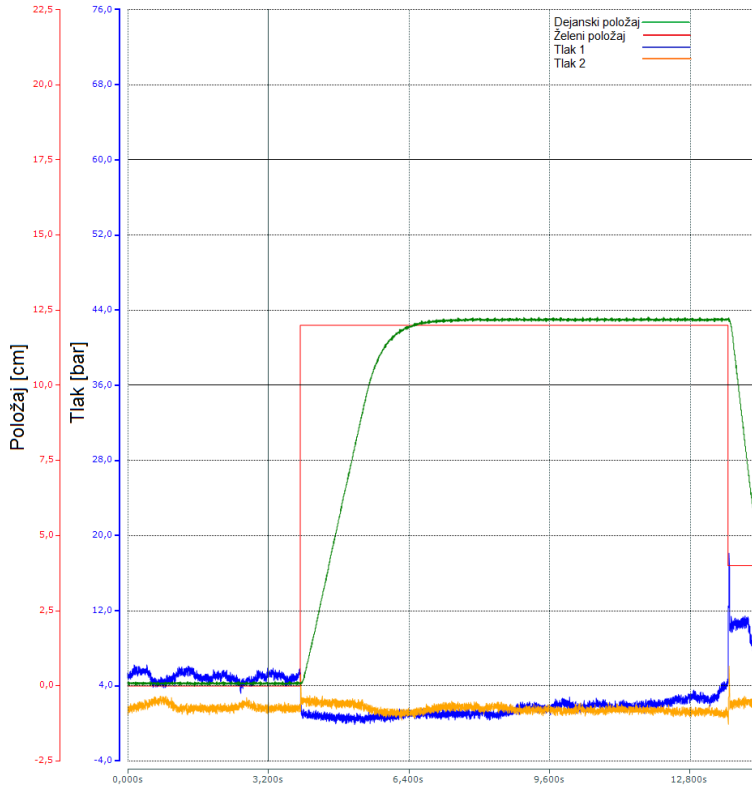
Figure 8: Results of position closed loop system control.

4 Conclusion

In the design and manufacture of the device, we limited ourselves to the size of the device and its usability for the purposes of a laboratory study.

When designing the device, it was necessary to think about how to vent the system later, to place the device in the laboratory so that it does not pose a danger to those present, and to consider all the necessary quantities that we had to calculate. We found our device to be powerful and rigid. The operation and behaviour of the device is smooth. There are no large pressure peaks in the system that would be observed as a nonlinear change in the position of the hydraulic cylinder.

References

[1]   Rydberg, K. E. (2016). Hydraulic Servo Systems – Dynamic Properties and Control. Linköping University. Linköping.

[2]   Cleasby, K. G., Plummer, A.R. (2008). A novel high efficiency electrohydrostatic flight simulator motion sysytem. *Fluid Power and Motion Control* (FPMC 2008).

[3]   Hewett, A. J. (1993). Hydraulic Circuit Flow Control. Vancouver, BC, Canada Patent 5329767, 21 January 1993.

[4]   Clewlow, R. R. (2016). Car-sharing and sustainable travel behaviour: Results from the San Francisco Bay Area. *Transport Policy, 51*, 158-164. doi:10.1016/j.tranpol.2016.01.013

University of Maribor Press

Challenges in modelling and simulating hydraulic servovalve

JOERG EDLER & SAMO GOLJAT

Abstract Modelling accurate response from hydraulic system in practice is difficult, especially establishing right mathematical model and getting all the parameters for certain hydraulic component. In this paper we mentioned two different different approaches for modelling hydraulic components, specifically Moog G761-series, made by company Moog. Approaches mentioned in this paper are using classical Matlab Simulink environment to show example of the first order model. Main focus is on using Matlab Simulink Simscape, which already includes some of the basic hydraulic components. We discussed problems and challenges when obtaining and simulating real components. We developed our own Simulink Simscape model for simulating Moog G761 servovalve. Simulation results were compared with the datasheet values from Catalog.

Keywords: • servovalve • modelling • Matlab • Simulink • Simscape •

CORRESPONDENCE ADDRESS: Jörg Edler, Graz University of Technology, Institute of Production Engineering, Graz, Austria, e-mail: Joerg.edler@tugraz.at. Samo Goljat, University of Maribor, Faculty of Mehanical Engineering, Maribor, Slovenia, e-mail: samo.goljat@um.si.

1   Introduction

Modelling of hydraulic system is an option, when it comes to simulating real physical components or system as a whole. It can be done either by setting up right mathematical equations for each system or subsystem. There are many hydraulic simulating software available, some known examples are: FluidSIM – Festo, Simulink (Matlab based), DSHplus simulation software, Visual Solutions, HydroCAD, Flowmaster 2, HyPneu, Hopsan, ACSL simulation software, Dynhax™ and many more. Specialised software for simulating hydraulic systems is easier to use, but there is still problem obtaining real process parameters, that must be set in simulation program. So simulating results should always be checked by conducting the experiment.

In this paper we focused on two approaches, first one being more "traditional" approach using Matlab Simulink, or more modern approach using libraries in Matlab Simulink Simscape environment, where some of the basic components are already developed and we can model more complex system/component behaviour by use of the basic Simscape library components. We focused on the Simscape model, because Li Lingjun [1] has already developed Classical Simulink model for hydraulic servovalve. Both approaches can provide similar results. While Simulink Simscape approach may be seen as more simple or user friendly, both approaches require degree of understanding the hydraulic component behaviour and some deepening in the field of establishing proper mathematical equations, especially in classical Matlab Simulink environment, where for each hydraulic component has its own or multiple equations are taken into consideration.

2   Servovalves

First appearance of electrohydraulic servovalve made appearance in the latter 1940s, developed specifically for aerospace, because fast response servo control was in need. At that time there wasn't much difference between electrohydraulic servo system and electrical servo, because electrohydraulic servo system lacked an element which could rapidly tranlate electrical signal into hydraulic flow. First series of servovales were actuated by small electric servomotor, which in comparison to magnet torque motors had large time constant, resulting in limited system performance [2].

W. C. Moog Jr. has developed in 1950 the two-stage servovalve using pilot stage without friction. Second-stage spool in a three way mode was driven by a flapper and nozzle variable orifice in conjuction with a fixed orifice. Such servovalve construction provided reduction in valve treshold, high dynamic response because of the lower mass of the first-stage parts. It was possible to use servovalves in high gain position. Hydraulic servovalves have developed and improvements were made both in reliability and life expectancy from the first introduction in 1951 [3]. One example is switching from steel ball to carbide ball on the feedback mechanism, which proved to not have any signs of wear after 1 billion cycles.

2.1   Behaviour and types of electrohydraulic servovalves

Similar to normal servovalves, also servovalves can come in different designs or stages. In single-stage servovalve consist of a torque motor which is directly attached to and positions a spool valve. The problem with single-stage servovalves is limited power capability, this limits the flow capacity of single-sate servovalve and can influence stability in certain applications [2].

Two-stage servovalves in comparison to single-stage servovalves have hydraulic preamplifier, which substantially multiplies the force output of the torque motor, leading to much more efficiency when overcoming flow forces, stiction forces and forces resulting from acceleration or vibration. Two-stage servovalves can be classified in three types, depending of feedback used which are spool position, load pressure and load flow feedback. Out of those, position feedback two-stage servovalves are the most common and even those are classified into three groups of construction, those are direct feedback, force feedback and spring centered spool. Direct position feedback is constructed that main spool follows the first stage valve in a one-to-one relation. In force feedback the position of main spool is converted into force by a feedback sping and this force is balanced at the torque motor armature against the torque due to input current. The third basic type uses stiff springs at the spool ends to center the spool against the pressure differential of the pilot stage, which is less frequently used [2].

2.2   Two-stage electrohydraulic servovalve from company Moog

As we mentioned single-stage two major faults which are limited flow capacity and stability problems depending on load dynamics. Focus of the paper went into structure and modeling of G761 servovalve made by company MOOG. Structure of Moog servovalve is seen on Figure 1. Servovalve is made of a polarized electrical torque motor and two stages of hydraulic power amplification. Two motor coils are surrounding the armature, one on each side of the flexure tube [3].

As seen on Figure 1, the flapper of the first stage is rigidly attached to the midpoint of the armature. Flapper then extends into flexure tube, which acts as seal between electromagnetic and hydraulic sections of the valve. The flapper passes two nozzles, which variable orifices are then used to control pressure in the end areas of the second stage spool. Input signal induces a magnetic charge in the armature and causes a deflection of the armature and flapper. With this the size of one nozzle orifice is increased and other one is decreased. This leads to differential pressure on each side of the spool, causing spool motion.

Servovalve uses cantilever feedback spring, which is fixed to the flapper and center of the spool. When spool is displaced, a linear force is induced on the feedback wire, which opposes the original input signal torque. Spool movement continues until the feedback wire force equals the input signal force [3] .
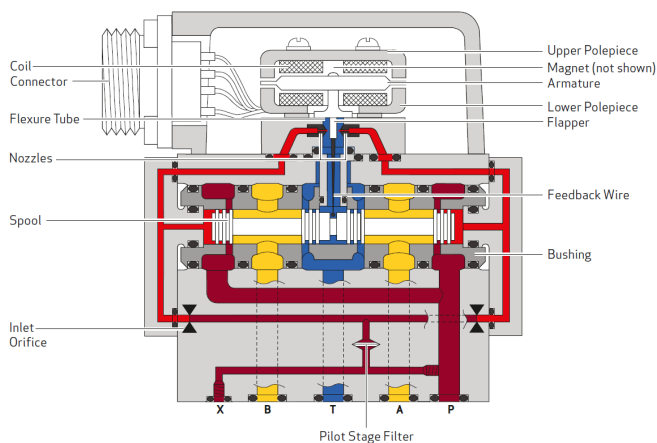
Figure 1: Structure of two stage Moog G761 servovalve [3]**.**

3   **Modelling hydraulic servovalve**

One of the problems when modelling hydraulic servovalve is nonlinearity, which has not been solved effectively yet [1]. Causes are throttle characteristics of electro-hydraulic elements, control element and problems with hydraulic power mechanism for example hyseresis, dead zone, limiting properties and more.

Servo valve is complex system to simulate, because several parameters can only be estimated within wider range or are completely unknown. According to previous research [1] it can be described as second order system.

$$\frac{Xv(s)}{I(s)} = \frac{K_{SC}}{\frac{s^2}{\omega_{sv}^2} + \frac{2\zeta_{sv}}{\omega_{sv}} + 1} \tag{1}$$

Where I is the input of current, Xv is the output of spool displacement of servovalve, ω_{sv} is natural frequency, ζ_{sv} is damping ratio, K_{SC} is the gain of servovalve.

In some cases, servo valve was defined as first order system:

$$\frac{Xv(s)}{I(s)} = \frac{K_{SC}}{\frac{s}{\omega_s} + 1} \tag{2}$$

If low frequency signal is used as reference signal, the dynamic characteristics of servo valve can be ignored and it can be treated as a proportional part:

$$x_v = K_{sc} \times I \tag{3}$$

According to research work [1], the first order model can describe dynamic characteristics of the G761 series servovalves from MOOG company completely. Open loop transfer function is:

$$\frac{Q_0(s)}{I(s)} = \frac{K_{sv}}{\frac{s}{\omega_{sv}} + 1} \tag{4}$$

K_{sv} presents flow-current gain of the servo valve: $K_{sv} = K_q K_{sc}$

3.1   Electro-hydraulic Servo Position Control

On Figure 2 example of simulating cylinder system with four-way valve, double-rod cylinder is shown.
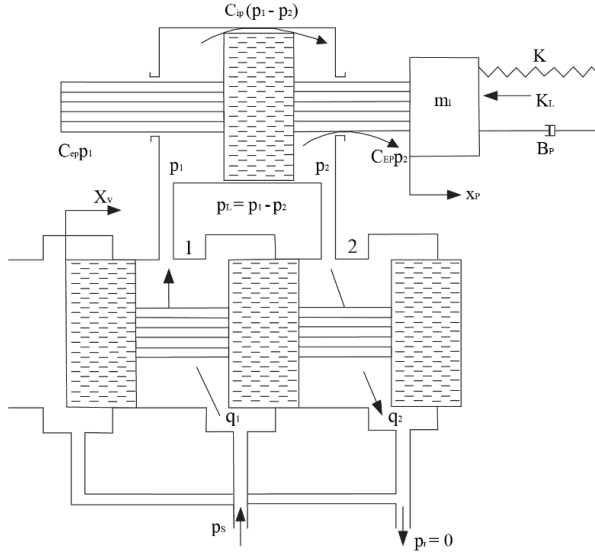
Figure 2: Schematic of valve-controlled cylinder system [1]**.**

Simplified equation was taken into consideration. When modelling several assumptions were made, i. e. supply pressure p_s is constant, return pressure p_r is zero, pressure loss in pipes and valves were ignored, the flow coefficient in each valve port is the same and four-way spool is ideally centered. Also pressure loss in pipes is ignored, it is assumed that system runs at constant temperature, bulk modulus, internal and external leakage is considered laminar flow. Considering pressure flow equation of the control valve, the continuity equation of fluid and pressure-load equation and with neglecting spring stiffness, simplified equation was formed:

$$\frac{X_p(s)}{Q(s)} = \frac{\frac{1}{A}}{s(\frac{s^2}{\omega_h^2}+\frac{2\zeta_h}{\omega_h}s+1)} \tag{4}$$

Where ω_h represents natural frequency and ζ_h damping ratio.

When cylinder with bearing strip is used, influence of friction must be considered. There are a lot of friction model developed, but in this paper simple friction model was used, where F_f presents friction force and B_f is friction coefficient.

$$F_f = B_f \frac{dx_p}{dt}$$

(5)

Since high quality MTS R-Series position sensor is used, which has position measurement uncertainty under 0.01 %. Also non-ideal dynamic for this type of position sensor is greatly above the bandwidth of the cylinder and servovalve. Sensor-amplifier system thus is considered ideal and its open loop transfer function reduces to

$$F(s) = 1$$

(6)

By combining derived transfer functions of the servovalve, the cylinder, the friction and the position sensor mathematical model of the electro-hydraulic servo position control system is formed [1].

$$\frac{X_p(s)}{I(s)} = \frac{\frac{K_{sv}}{A}}{s(\frac{s^2}{\omega_h^2}+\frac{2\zeta_h}{\omega_h}s+1)+(\frac{s}{\omega_{sv}}+1)}$$

(7)

3.2 Modelling in classical Simulink environment

Simulation example is seen on Figure 3. Electro-hydraulic servo position control system was simulated using transfer function (7). For that already measured hydraulic coefficientsw were used, where, for 40 kN cylinder with bearing strip from research [1] and available in laboratory, where ω_h= 2157.2 , ζ_h = 0.9766, ω_{sv}= 1005.3 and K_{sv}=0.0114.
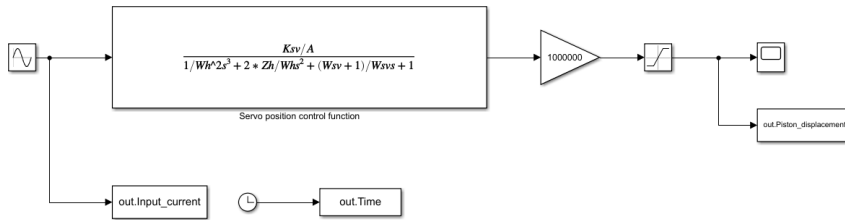
Figure 3: Matlab Simulink approach to simulate electro-hydraulic servovalve piston displacement dependent on input current.

Results are shown on Figure 4. Amplitude was set to 20 mA and frequency to 1 rad/sec. We can see that we do get slight delay of piston movement compared to input signal, which is also the case in real world applications because of response time of servovalves and time necessary for each piston chamber to fill up with hydraulic fluid.
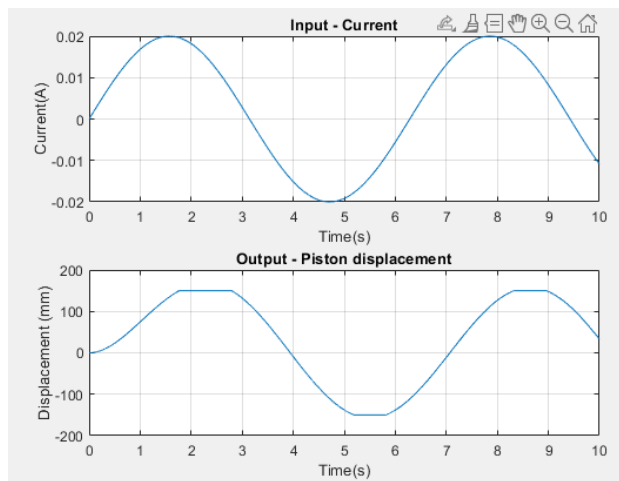
Figure 4: Example using classical Matlab Simulink approach to model servosystem.

3.3   Modelling in Matlab Simulink Simscape

Approach for modelling MOOG G761 hydraulic servovalve in Matlab Simulink Simscape is different from classical Matlab Simulink. Difference is that in Simulink Simscape there are already developed blocks from libraries to simulate mathematical equations. In both cases functioning of the hydraulic system must

be broken down to basic components, for example physical behaviour of flow between different orifices, where certain parater must be considered, to get simulation as close we can to real world scenario.

3.4   Obtaining necessary parameters of the servovalve

Getting real world behaviour of hydraulic component or system can be difficult because companies do not provide all the necessary parameters. On Figure 5 we developed our own MOOG G761 servovalve model, where we tried to cover as parameters as we could.

3.5   The first option is to use the available data in the servo valve datasheet.

From the Moog G761 and D761 datasheet [3], certain parameters were obtained, as seen in Table 1:

Table 1: Parameters obtained from Moog G761 and D761 datasheet

Information in the Datasheet	
Nominal flow at 35 bar/spool land	19 l/min
Null leakage flow at *	2.3 l/min
Pilot leakage flow at *	0.7 l/min
Pilot flow * (max) for 100 % step input	0.3 l/min
Spool drive area	0.34 cm²
*at 210 bar, 32 mm²/s, 40°C	

Second option is to obtain the information from other literature. Certain values and parameters were obtained from book "Servohydraulik" from authors e. g. H. Murrenhoff [4], which can be seen in Table 2:

Table2: Parameters obtained from the literature

Information in the book	
Torque motor stroke	0.25 mm
Flapper movement	± 0.035 mm
Torque motor force	40 Nmm

3.6   Simscape model of Moog G761 servovalve

For Simscape model certain behaviours were neglected. System is configured to run under ideal pressure of 210 bars. Also the forces between nozzle, flapper and oil volume in pilot stage, were neglected. The coil of the torque motor also wasn't considered because the input signal is [N·mm], so electricity part of the torque motor, was also neglected.
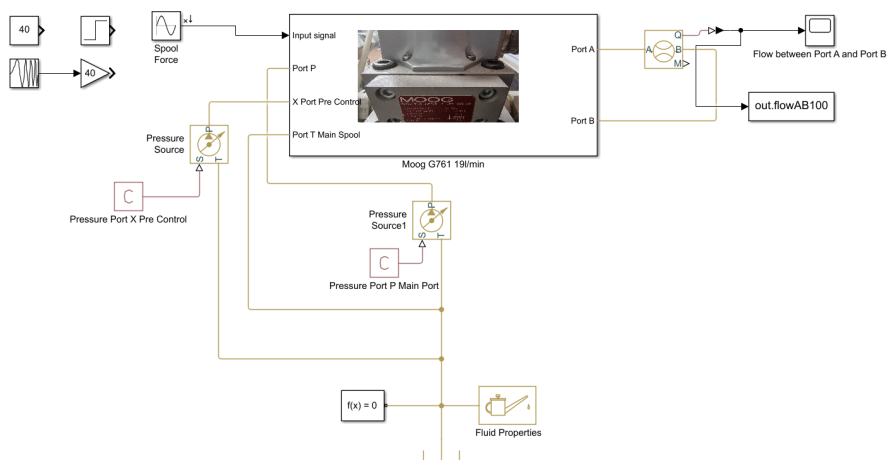
Figure 5: Simscape model of MOOG G761 servovalve.

Parameters can be defined either in the model in Simulink Simscape blocks itself or they can be set up in Matlab code and sent to Workspace. In this case parameters were insterted in Simscape blocks. On Figure 5 main system of the servovalve is shown, where pressure supply is connected to port P and X port of the servovalve. Input signal is in [N mm] and 40 means valve is fully opened in one direction.

Servovalve main system consists of the four subsystems as seen on Figure 6. These subsystems are for torque motor and flapper, hydraulic pre control, main spool mechanic and main spool hydraulic. As mentioned before, we replaced electric subsystem for torque motor with input of the physical signal in [N mm], which is from source [4]. Our system is configured to run simulation on 210 bars, with ISO VG 32 oil at temperature 40 °C.
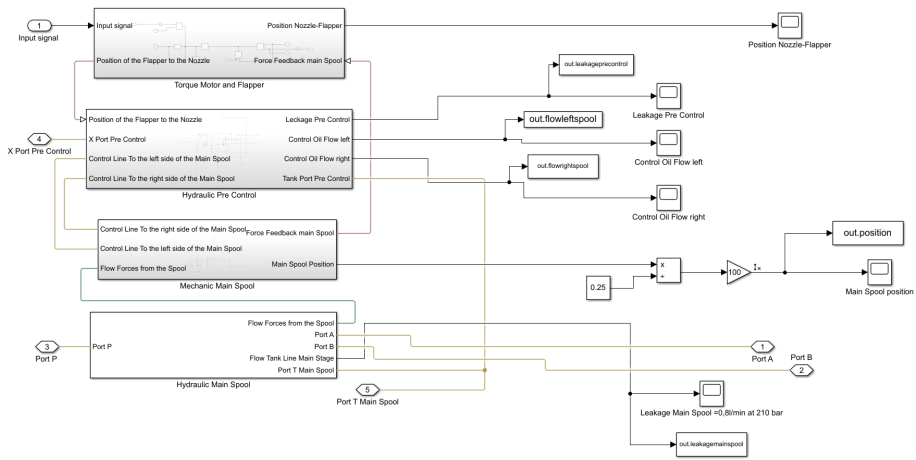
Figure 6: Subsystems of the MOOG G761 servovalve.

Figure 7 represents example of inserting necessary parameters into Simulink Simscape block. For example, leakage area was calculated with calculation for orifice (8).

$$Q = \alpha A \sqrt{\frac{2\Delta p}{\varrho}} \tag{8}$$
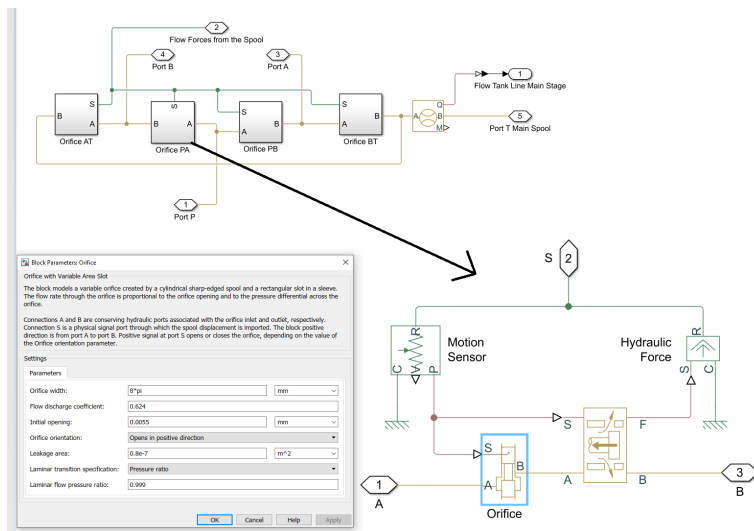
Figure 7: Orifice parameters inside of the orifice between port P and port A in the hydraulic subsystem fort he main spool.

4   Simulation results

Simulation of our Moog G761 were runned in Simscape model. In datasheet response time from 0 to 100 % stroke of the hydraulic spool was defined 5 ms for 19 l/min G761 Moog servovalve. Simulation results were compared to datasheet and the results are similar to those in the datasheet.
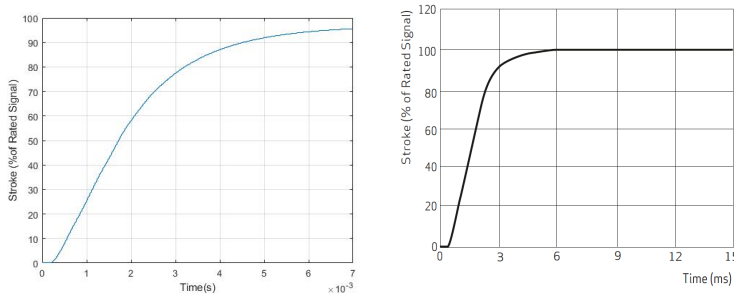
Figure 8: Simulated stroke (left), stroke value from the Moog G761 Datasheet (right) [3]**.**

Actual flow is dependent upon electrical command signal and valve pressure drop. Simulations were perfomed with 70 bar valve pressure drop and compared to datasheet value on Figure 9 and results look promising.
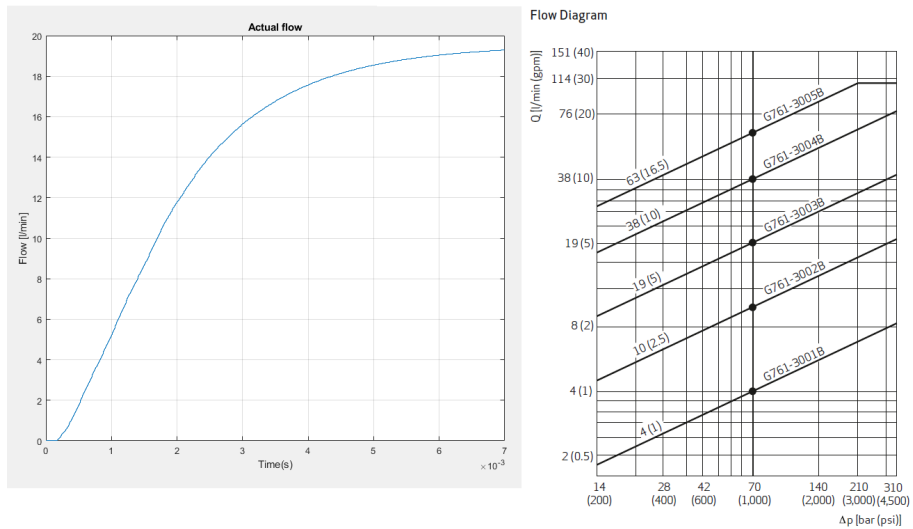
Figure 9: Simulated actual flow (right) and flow value from the Moog G761 datasheet

In Figure 10 pilot stage leakage flow was simulated and compared with data available in G761 datasheet [5], which is practical same servovalve, but older datasheet (D-series). Newer datasheet (G-series) does not provide these parameters. The structure of servoventil is same but G-series are newer models.
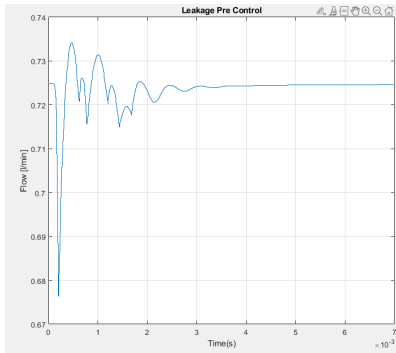
Figure 10: Pilot stage leakage simulation (left) and pilot stage leakage flow value given in datasheet (right).

If we compare data from Figure 11, specifically maximum pilot flow which is defined at 0.3 l/min, simulated results show us maximum pilot flow around 0.2 l/min.
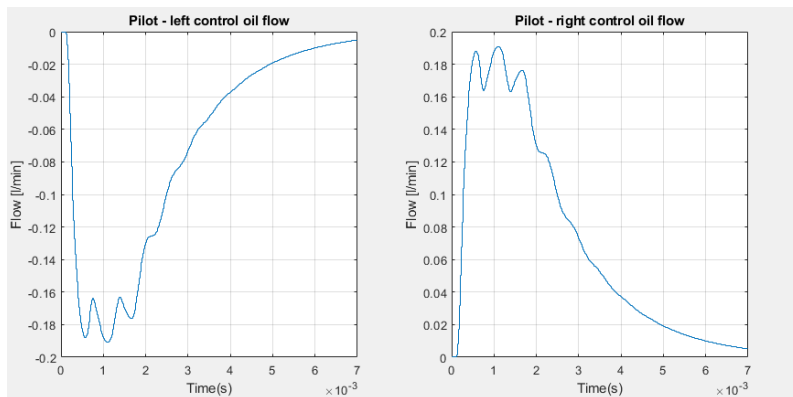
Figure 11: Simulating results of oil flow through pilot stage.

5   Conclusion

In paper Simulink Simscape model of Moog G761 servovalve with 19 l/min nominal flow was developed. The results were comparable with datasheet provided by company of the servovalve. Obtaining all necessary parameters for simulating hydraulic servovalve still remained the problem. Companies usually don't provide all the necessary data needed for hydraulic component simulation. Also it was noted, that in case of Moog G-761 datasheet newer datasheet contains less information than in older Moog d-series datasheet. So, the more information is provided in datasheet, better can the model be. This is the reason why servovalve is normally simulated only as one block, with first and second order model, compared to Simscape model developed in our paper. where some parameters are not given by the companies. In further research it would be necessary to compare simulated and datasheet values to the measured values, by conducting experiments on Moog G761 servovalve.

References

[1]   Li, L. (2015). Simulation and control of Servo Hydraulic Actuators for Test Applications. Ph.D. dissertation, Graz University of Technology, Graz. Accessed on: 18 July, 2021. [online].   Available: https://diglib.tugraz.at/download.php?id=576a7b6ccc7df&location=browse

[2]   Merritt, H. E. (1967). Hydraulic control systems. United States of America, John Wiley & Sons, Inc. ISBN 0-471-59617-5

[3]   Rev, K. (2016). Servo valves Pilot Operated Flow control Valve with analog interface G761/761   Series,   Size   04.   Moog   Inc.   (Pdf).   Available: https://www.moog.com/content/dam/moog/literature/ICD/Moog-ServoValves-G761_761Series-Catalog-en.pdf [16 July, 2021]

[4]   Murrenhoff, H. (2012). Servohydraulik. Germany, Shaker Verlag, ISBN 978-3-8440-0947-7, 2008

[5]   Moog Inc. Servovalves D761 Series ISO 10372 Size 04. Moog Inc. (Pdf). Available: https://www.moog.com/literature/ICD/d761seriesvalves.pdf

University of Maribor Press

Influence of differently viscous hydraulic fluid on the flow behaviour inside a hydraulic tank

IGNACIJO BILUŠ, LUKA LEŠNIK, LUKA KEVORKIJAN & DARKO LOVREC

Abstract The viscosity of a hydraulic fluid is certainly one of the most important material properties of a fluid, as it affects a whole range of phenomena in the hydraulic system and the operation of the entire system. Among other things, it affects the efficiency of the hydraulic device directly. Thus, the development of hydraulic fluids goes in the direction of fluids with lower viscosity, which, in turn, results in different flow behaviour and processes inside the hydraulic tank. The paper presents the results of a study of the flow conditions in a small hydraulic tank for cases of different fluid viscosities. The results were obtained based on a detailed simulation of conditions inside the tank. Apart from the impact of the changed flow conditions, the lower viscosity of the liquid also influences the elimination of solid contaminants and air.

Keywords: • hydraulic tank • mineral oil • viscosity • flow condition • simulation •

CORRESPONDENCE ADDRESS: Ignacijo Biluš, University of Maribor, Faculty of Mechanical Engineering, Smetanova 17, 2000 Maribor, Slovenia, e-mail: ignacijo.blus@um.si. Luka Lešnik, University of Maribor, Faculty of Mechanical Engineering, Smetanova 17, 2000 Maribor, Slovenia, e-mail: luka.lesnik@um.si. Luka Kevorkijan, University of Maribor, Faculty of Mechanical Engineering, Smetanova 17, 2000 Maribor, Slovenia, e-mail: luka.kevorkijan@um.si. Darko Lovrec, Prof., University of Maribor, Faculty of Mechanical Engineering, Smetanova 17, 2000 Maribor, Slovenia, e-mail: darko.lovrec@um.si.

1   Introduction

The hydraulic fluid is a key component of any hydraulic system. It transmits power, lubricates components, dissipates heat and thus cools the components, acts as a sealing agent and helps minimise the harmful effects of contamination like dirt and water. Hydraulic fluid has become increasingly important when it comes to overall system efficiency.

Requirements for today's hydraulic fluids arise from trends in the development of hydraulic components and systems, as well as from operating conditions, taking into account operating trends [1]:

- Higher operating pressures: Typical operating pressures for hydraulic equipment are up to 350 bar or 450 bar.
- Smaller and lighter components: Reduced fluid volume and, consequently, increased flow rates and more intensive circulation and, therefore, less residence time for cooling and elimination of contaminants.
- Higher fluid operating temperatures: In some cases 80 $^{\circ}$C, common for mobile hydraulics with more than 100 $^{\circ}$C peak temperature, or low ambient temperatures.
- A wider operating temperature range.
- Increasing energy efficiency of the plant, including structural components` design, implementation of energy-saving control concepts, and use of energy-efficient hydraulic fluids with excellent lubricating properties over the wide operating temperature range.

The fluid and components of the hydraulic system must always be considered as an interacting whole. Together they determine the system efficiency and lifetime. The critical elements of a hydraulic fluid are the fluid type and its viscosity. A hydraulic system that operates with an inappropriately selected fluid relative to the component will show weaknesses in:

- changed flow conditions,
- decreased efficiency,
- lack of lubrication,
- reduced components` lifetime,

I. Biluš, L. Lešnik, L. Kevorkijan & D. Lovrec: Influence of differently viscous hydraulic fluid on the flow behaviour inside a hydraulic tank

107

- corrosion, sludge and varnish,
- heat generation.

Most of the mentioned requirements and possible negative consequences thus refer to the properties of hydraulic fluids, especially those related to the viscosity of the fluid. The fluid must have the appropriate viscosity on the one hand, and additionally, this should be, as little as possible, dependent on the temperature on the other. The influence of the viscosity on the operation and performance of the hydraulic system is shown in Figure 1.
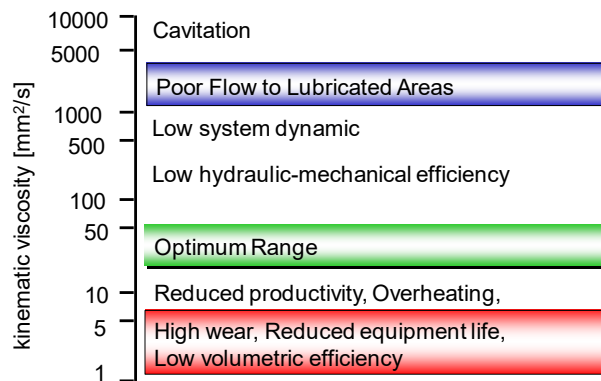
Figure 1: Importance of fluid viscosity within a hydraulic system [2]**.**

Although various fluid properties have an impact on different performance functions, the viscosity is a key material property of the hydraulic fluid that affects the performance and efficiency of the hydraulic components and the entire system. The fluid viscosity affects hydraulic systems in several ways, for example on:

- value of volumetric efficiency,
- value of mechanical efficiency
- (elasto)hydrodynamic and boundary lubrication,
- risk of cavitation,
- heat dissipation,
- Air release ability,
- filterability…

Given all the above, the viscosity of a hydraulic fluid is certainly that material property of the fluid that deserves priority attention. Also, due to the fact that selection of suiTable viscosity is related closely to the efficiency of operation of the individual hydraulic components and the overall system. In the present study, the numerical simulation of flow conditions inside a hydraulic tank was performed for three mineral based hydraulic oils with different viscosities. The results were compared and their influence on tank "performance" was analysed.

2   Viscosity and system efficiency

In hydraulic systems much of the energy input is lost in the pumps, fluid lines and actuators. As stated by the manufacturers and researchers of energy-saving hydraulic fluids, in a case of selected inappropriate viscosity and an inappropriately designed hydraulic system, only around 40 % of input energy is available to perform work – Figure 2 (e. g. [3], [4], [5]). In the end, this is reflected in higher electricity consumption, or higher fuel consumption in the case of mobile hydraulics.
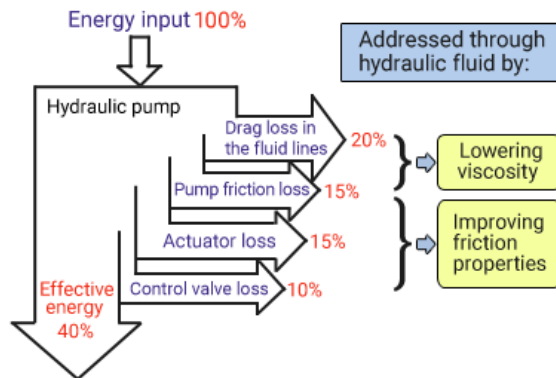
Figure 2: Shares of energy lost [3].

If the selected hydraulic oil viscosity is too low the oil film will be too thin, causing direct metal to metal contact, which leads to excessive wear on components. Low viscous hydraulic oils also increase the risk of internal leakages generating a lower volumetric efficiency of hydraulic pumps and motors. It also leads to overheating, high wear and shorter component life. If the oil viscosity is too high, the system will suffer from slow dynamics, poor flow to lubricated areas and reduced mechanical efficiency. This generates energy losses and

I. Biluš, L. Lešnik, L. Kevorkijan & D. Lovrec: *Influence of differently viscous hydraulic fluid on the flow behaviour inside a hydraulic tank*

109

unnecessary heat generation. Other negative effects of a high oil viscosity are cavitation, poor air release and inadequate lubrication, and, in the worst case, mechanical failure.

Losses inside hydraulic components (and accordingly efficiencies), can, therefore, be divided into two main groups:

- hydraulic-mechanical losses – energy loss due to fluid friction, as a resistance of the motion of the component parts in the fluid itself, non-stationary flow condition, which is reflected in lower available force on the actuator,
- volumetric losses – energy loss as the result of internal leakage within all component parts with gaps: Pumps, valves, hydromotors,which is reflected in lower actuator speed.

In order to maximise energy efficiencies in hydraulic systems, hydraulic-mechanical and volumetric losses must be balanced, so that the sum of these losses is minimised. Since the hydraulic-mechanical losses in sealing gaps are proportional to the fluid viscosity, and volumetric losses inversely proportional to viscosity, it is clear that an optimal viscosity must be selected.

Figure 3 shows, as an example, the effect of viscosity on the hydraulic pump efficiency. Apart from the above-mentioned risks in the operation of the device, both too low and too high viscosity are reflected in the efficiency, both volumetric, hydraulic-mechanical, and, consequently, the overall efficiency.
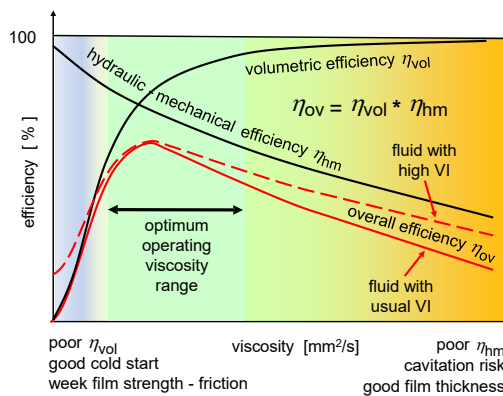
Figure 3: Effects of viscosity on efficiencies [2].

The resulting requirements must be fulfilled by the lubricant, in general: The ability of a lubricant to maintain optimum viscosity under a wide operating temperature range can be achieved with a shear sTable, low viscous fluid, with temperature independent viscosity (with high viscosity index VI – see Figure 3), and with a low friction coefficient at both the start and operating temperatures [2].

Higher viscosity index values result in more favourable viscosity behaviour than temperature - favourable Viscosity-Temperature (VT) behaviour, which means less change in viscosity with temperature. From the point of view of the pump, which is the first to start work at the start of the hydraulic system and is the most and permanently loaded during operation, the high value of the viscosity index means fewer problems, both during start-up and during continuous operation. This is especially important when it comes to stricter operating conditions, such as low temperatures on the one hand and higher operating temperatures on the other.

Due to all the aforementioned advantages of low-viscous hydraulic fluids, the direction of development of hydraulic fluids in recent years has been in the direction of fluids with lower viscosity and higher (high) viscosity index. In this way we can reduce drag in the lines, improve cold start-up performance, and improve frictional properties to reduce sliding resistance and increase machine efficiency. In a hydraulic system, pressure loss in the lines is linked closely to the kinematic viscosity of the hydraulic fluid.

In connection with the use of a lower viscosity fluid, however, another issue arises that has not yet received much attention. The lower viscosity of the hydraulic fluid certainly also affects the flow conditions inside the hydraulic tank. This also results in the effectivenes of air bubbles and solid contaminants` elimination.

3   Influence of viscosity on flow conditions in a hydraulic tank

Kinematic viscosity is the most important physical property of lubricating and hydraulic fluids – and it is a criterion for resistance to flowing of the liquid under active pressure. According to the definition, its value is given by the ratio between the active shear stress and shear velocity gradient. Fluid (kinematic) viscosity is

I. Biluš, L. Lešnik, L. Kevorkijan & D. Lovrec: Influence of differently viscous hydraulic fluid on the flow behaviour inside a hydraulic tank

111

defined by viscosity grade VG (with a deviation of the standard value of +/- 10 %) given at a standard temperature of 40 °C.

The most commonly used ISO viscosity grades in the case of hydraulic mineral oils are VG 15, VG 22, VG 32, VG 46 and VG 68. There are two other ISO viscosity grades, ISO VG 10 and VG 100, but they are rarely used in the field of Hydraulics, more in special cases. In principle, higher viscous fluid is used for higher loads, and lower viscous fluids in cases of lower ambient temperatures (cold start of the device), and in terms of using the fluid as an energy-efficient fluid. Grades VG 22 and VG 32 belong to the low-viscosity oils that are used today as energy-saving fluids.

For the purpose of the simulation studies of the flow conditions inside the hydraulic tank, it is first necessary to obtain accurate material data on the fluids used, in our case, the actual values of viscosity, and also the density of the predicted mineral oil, so we could later compare the simulation results with the experiment. The actual value of the viscosity (and viscosity index) of a specific product can be determined by measuring the viscosity (and calculating the viscosity index). Hydraulic mineral oils of the Hydrolubric VG type (manufactured by OLMA) were used to determine the value of the viscosity of mineral hydraulic oils (and the corresponding viscosity index). For the measurement, we used the standard oil viscosity grade according to ISO, where the oil was VG 46 in two different batches. The exact values of viscosity, as well as the density of the mineral oils used, measured in the manufacturer's laboratory, are given in Table 1. For measuring the kinematic viscosity, in our case, a Cannon-Fenske viscometer with the necessary peripheral equipment (tempered bath, stopwatch) was used, and the measurement performed according the ASTM D445 Standard.

Table 1: Measured values of viscosity and density of the discussed hydraulic oils

Viscosity Grade ISO	Kinematic Viscosity at 40 °C [mm²/s]	Viscosity Index [–]	Density at 20 °C [kg/m³]
VG 22 / B1	21.18	107	856.80
VG 32 / B1	34.91	114	862.30
VG 46 / B1	46.98	104	876.20
VG 46 / B2	47.07	119	879.40
VG 68 / B1	70.07	98	881.00
VG 100 / B1	94.01	96	888.30

Remark: B1 – Batch 1, B2 – Batch 2

As a hydraulic tank we used a 30-litre cast aluminium tank for simulation studies – Figure 4. The tank is suiTable for a net fluid volume of approx. 27 litres and for normal pump flows of approx. 6 l/min.
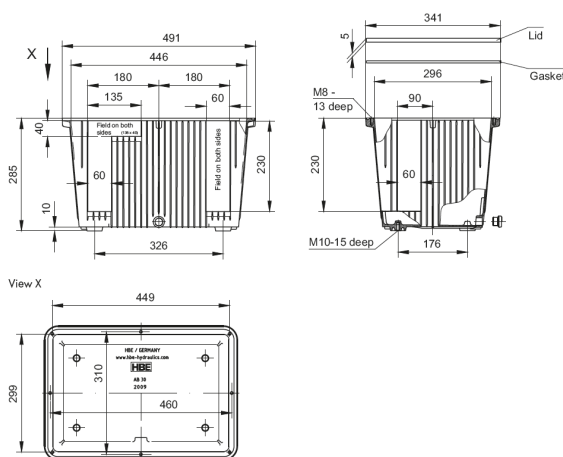
Figure 4: Considered 30-litre aluminium oil tank.

4   Modelling, Mesh, Boundary conditions

A Eulerian approach to describe fluid flow was used in this study. This approach is implemented and readily available in commercial CFD solvers, in this study ANSYS CFX 2020 R2. [6], [7], [8] In all simulations the flow was isothermal, with the fluid properties listed in Table 1, and steady-state mode was selected. The

I. Biluš, L. Lešnik, L. Kevorkijan & D. Lovrec: *Influence of differently viscous hydraulic fluid on the flow behaviour inside a hydraulic tank*

113

same operating regime with flowrate $Q_P = 6$ l/min was applied to the numerical simulation of the fluid. In Table 2 the Reynolds number (eq. 1) values in the hydraulic tank inlet and exit pipe are calculated, depending on the flow rate, and used fluid kinematic viscosity.

$$Re = \frac{u \, d}{v} \tag{1}$$

Where u is the fluid velocity in the pipe, d is the pipe diameter and v is the fluid kinematic viscosity.

Table 2: Fluid properties and Reynolds number value in the hydraulic tank pipes

Liquid (Oil)	Kinematic Viscosity [m²/s]	Reynolds number value in the inlet pipe	Reynolds number value in the exit pipe
ISO VG 22	0.00002118	275.5	216.5
ISO VG 46	0.00004698	124.2	97.6
ISO VG 68	0.00007007	83.3	65.4

It is evident from the Table that the Reynolds number value in both pipes for all analysed fluid viscosities is in a laminar flow regime. According to this, the fluid flow is described with the continuity equation:

$$\frac{\partial \rho}{\partial t} + \vec{\nabla} \cdot (\rho \vec{u}) = 0 \tag{2}$$

and Navier-Stokes equations:

$$\frac{\partial (\rho \vec{u})}{\partial t} + \rho (\vec{u} \cdot \vec{\nabla}) \vec{u} = -\vec{\nabla} p + \mu \nabla^2 \vec{u} + \rho \vec{g} \tag{3}$$

where ρ is fluid density, $\vec{u}$ is fluid velocity, p is pressure, μ is fluid dynamic viscosity and $\vec{g}$ is gravitational acceleration.

Following the laminar flow regime in the hydraulic tank pipes, the higher density mesh was applied for simulation. Details about the used mesh are presented in Table 4.

Table 3: Mesh metrics

Number of elements	Minimum element orthogonality	Maximum element aspect ratio
2,675,435	0.0499	6708

Mesh density near the hydraulic tank wall is depicted in Figure 5.
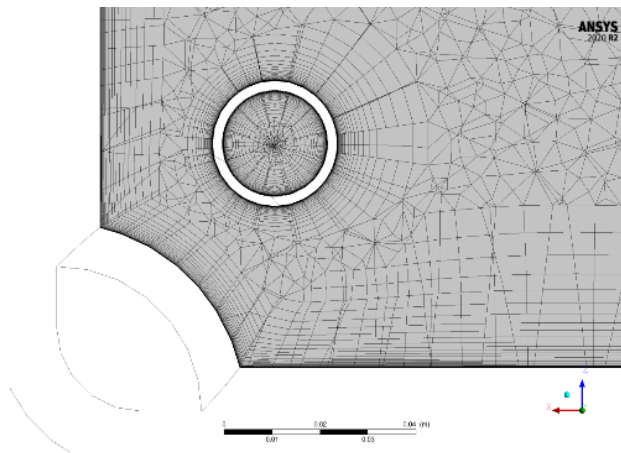
Figure 5: Numerical mesh.

5   Results

The comparison of numerical simulation results for hydraulic mineral based oils ISO VG 22, ISO VG 46 and ISO VG 68 is presented in Figures 6 to 8.

Figure 6 shows streamlines starting at the inlet pipe for all the analysed fluids. It is evident from a comparison of the results that increased viscosity results in a fluid regime that is calmer and more focused. From an integral point of view, we should expect more intensive mixing of fluid and, therefore, fast flow dynamics, with intensive flow to lubricated areas in the case of low viscosity fluid (ISO VG 22).

I. Biluš, L. Lešnik, L. Kevorkijan & D. Lovrec: Influence of differently viscous hydraulic fluid on the flow behaviour inside a hydraulic tank

115

ISO VG 22   ISO VG 46   ISO VG 68
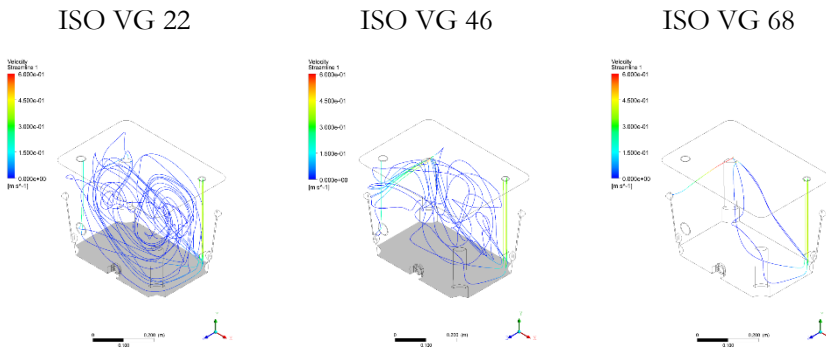
Figure 6: Streamlines in the hydraulic tank for three different viscous hydraulic oils.

Figure 7 shows a comparison of the velocity vector fields in the plane through the centre of the inlet and outlet pipes of the analysed hydraulic tank. Despite the two-dimensional presentation of velocity fields, it is evident that lower fluid viscosity results in smaller local flow structures (vortices), while higher viscosity points out the higher velocity gradients, which may cause lower hydraulic efficiency of the system.

ISO VG 22   ISO VG 46   ISO VG 68
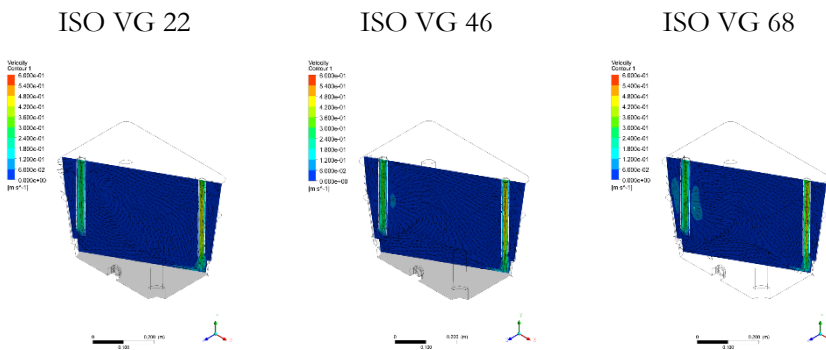
Figure 7: Velocity field in the plane for three different viscous hydraulic oils.

Figure 8 shows the comparison between the shear strain rate at the bottom of the analysed hydraulic tank for all the used fluids. A larger area of increased shear strain rate is evident, which may indicate an intensified fluid regime with poorer excretion of gas bubbles and poorer sedimentation of solid particles in the case of lower viscosity fluids. Higher shear strain gradients indicate more intensive energy dissipation in the case of ISO VG 68.

ISO VG 22   ISO VG 46   ISO VG 68
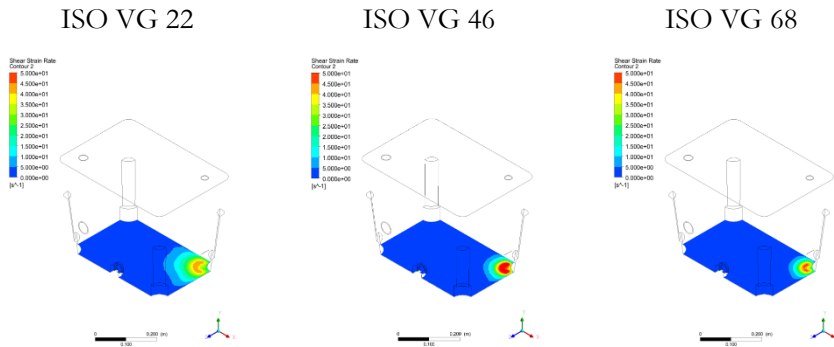
Figure 8: Shear strain rate at the tank bottom for three different viscous hydraulic oils.

6   Conclusion

The trend of development and use of hydraulic fluids goes in the direction of lower viscosity hydraulic fluids, but with higher values of the viscosity index. The main reason for this is to improve the efficiency of the hydraulic system. However, the lower viscosity of the fluid, in addition to what happens inside the active hydraulic components such as pumps and valves, also affects the flow conditions inside the hydraulic tank.

Due to the lower viscosity of the fluid, the flow inside the tank is expected to be livelier, which also affects the settling and distribution of solid contaminants, the excretion of air bubbles and the cooling of the liquid through the tank walls. This needs to be examined further and considered if lower viscosity hydraulic fluids are used.

References

[1]   Javalagi, S., Singireddy, S. (2012) Hydraulic fluid properties and its influence on system performance. Master's Thesis, LIU-IEI-TEK-A--12/01284—SE, Linkoeping University, Sweden

[2]   Lovrec, D., Tič, V. (2020). Ionic liquids as wide operating temperature range lubricant. *New technologies, development and application III : [International Conference New Technologies, Development and Application, Sarajevo, Bosnia and Herzegovina, on 25-27 June 2020]*, ISSN 2367-3370, Vol. 128). Cham: Springer. cop. 2020, vol. 128, pp. 348-359, doi: 10.1007/978-3-030-46817-0_40

[3]   Eneos   (2016).   Energy-Saving   Hydraulic   Fluids, https://www.eneos.co.jp/english/company/rd/intro/lubricants/shoene.html (6. 8. 2021)

I. Biluš, L. Lešnik, L. Kevorkijan & D. Lovrec: Influence of differently viscous hydraulic fluid on the flow behaviour inside a hydraulic tank

117

[4]   Rydberg, K. E. (2013) Hydraulic Fluid Properties and their Impact on Energy Efficiency, *13th Scandinavian International Conference on Fluid Power Proceedings*, Linkoeping, Sweden, ISBN: 978-91-7519-572-8; Article No. 44, 447-453

[5]   Rydberg, K. E. (2015). Energy Efficient Hydraulics – System solutions for loss minimization, *National Conference on Fluid Power*, Linköping University, Linköping, Sweden.

[6]   Škerget, L. (1994). Mehanika tekočin. Tehniška fakulteta v Mariboru, Univerza v Mariboru in Fakulteta za strojništvo v Ljubljani, Univerza v Ljubljani

[7]   Ansys, INC. (2021). ANSYS CFX Solver-Theory Guide, Release 2021 R1. ANSYS, Inc., 275 Technology Drive Canonsburg, PA 15317

[8]   Rodrigez, S. (2019). Applied Computational Fluid Dynamics and Turbulence Modelling, Practical Tools, Tips and Techniques, *Springer Nature Switzerland* AG

University of Maribor Press

Flow conditions inside a small hydraulic tank at excessive flow rates

DARKO LOVREC & IGNACIJO BILUŠ

Abstract The basic purpose of a hydraulic tank is to hold a volume of fluid, transfer heat from the system, allow solid contaminants to settle and facilitate the release of air and moisture from the fluid. To perform these important tasks more efficiently, the tank must be dimensioned properly. Above all, it must have an appropriate size. If the tank is too small the flow conditions inside the tank deteriorate, resulting in inadequate conditioning of the hydraulic fluid. Based on the simulation, the paper presents the difference in the change of flow conditions in the case of adequate and insufficient tank sizes. A small industrial hydraulic tank with a capacity of 30 litres filled with hydraulic mineral oil was used as the example of the study.

Keywords: • hydraulic tank • sizing • circulation number • flow condition • simulation •

CORRESPONDENCE ADDRESS: Darko Lovrec, University of Maribor, Faculty of Mechanical Engineering, Smetanova 17, 2000 Maribor, Slovenia, e-mail: darko.lovrec@um.si. Ignacijo Biluš, University of Maribor, Faculty of Mechanical Engineering, Smetanova 17, 2000 Maribor, Slovenia, e-mail: ignacijo.blus@um.si.

1   Introduction

The primary function of a tank in a hydraulic system is to store the fluid used by the system. Apart from e fluid storage, the tank provides a variety of other functions that are beneficial to the hydraulic system and its components, and most of them are related to the size of the tank.

As fluid flows through hydraulic system it warms up wherever friction is generated by the fluid flow or by moving the mechanical parts inside hydraulic components. As the fluid circulates back to the tank, the heat is dissipated into the surrounding atmosphere, because there are large areas of tank housing from which it can be released. A more powerful cooling system must be installed in the case of a tank that is too small, and, consequently, has too small tank surfaces.

The next important task, which is also related to the size of the hydraulic tank, is the extraction efficiency of air in form of air bubbles. Air can be introduced into hydraulic fluid in variety of ways: During the movement of the cylinder, via leaky pump suction pipe connections, due to improper design of the inside of the tank (e. g. from the return flow jet due to too short a return pipe), or due to large occasional stirring turbulence of the liquid in the tank occurring during a sudden increase in return flow. Whatever is the cause, air bubbles must be removed from the hydraulic fluid as quickly as possible. If sized properly, the tank serves as a place where the fluid can settle down for a period a time to allow the air to rise to the surface and dissipate before being pumped back into the system.

Also, in the elimination of solid particles – solid contaminants, the size of the tank plays an important role. They can enter the hydraulic tank from a contaminated environment, or are generated internally, inside the hydraulic system as a result of component wear. These particles enter the tank through the return flow. Larger particles, especially metallic ones, settle at the bottom, and usually do not get recirculated back into the system by the pump. However, it takes some time for these particles to settle. The higher the efficiency of particle extraction is the calmer is the flow of fluid in the hydraulic tank.

Slowing the fluid flow inside the tank has an effect, and the associated effects on the elimination of air bubbles and solid contaminants are related directly to the tank`s size. In the case of too small a tank volume, the flow conditions inside the tank are unfavourable, and worsen the processes of removing contaminants.

2   Sizing the tank and circulation ratio

Various recommendations can be found in the professional literature, different publications and posts regarding the appropriate tank size, both by tank manufacturers and users of hydraulic systems (e. g. [1], [2], [3], [4]).

So often we come across a recommendation that, in general, for most industrial applications, the minimum reservoir size should be approximately 2.5 or 3 times the pump(s) flow – a so-called rule of thumb. Additionally, consideration must be given to the return flow, which may be greater than the original pump flow.

The rule of thumb "three times the flow rate" should be considered in more detail, given the limitations on the installation space and the economics of using the hydraulic device. The first thing that needs to be determined when sizing a hydraulic tank is the size and oil requirements of all components, such as cylinder displacements, accumulator volumes, etc. Secondly, heat must be a factor, as this results in any unused power being converted to heat. Dissipating this heat can only be effective if a tank is sized with a sufficiently big surface area, which allows a temperature difference to exist between the oil and ambient environment to dissipate the heat.

From this point of view, the following recommendation could be made: "Bigger is better". Due to the larger tank volume the longer t dwell time the fluid must have to give up contaminants – solid particles, water and particularly air. But as there is not always the possibility to find a lot of space for placing the tank, we need to know and follow the minimal requirements for system calculation.

It is necessary to consider the following factors when designing a hydraulic tank:
 – Enough oil must be kept for system function,
 – An adequate surface area to dissipate heat,
 – Sufficient volume to minimise turbulence and allow air bubbles to escape and contaminates to settle,

- – Keeping the suction and return lines separated,
- – The use of baffle plates between the suction and return lines,
- – Access for maintenance and cleaning,
- – Room for installing system components.

When dimensioning and designing a tank we can also look at Standards and Recommendations e. g. NFPA/T3.16.2 and ISO 4413: 2010, as two essential documents when designing a new hydraulic power unit. Table 1 summarises all the available information regarding the appropriate tank size.

Table 1: Generally recommended tank size values

Minimum value	Recommendation
Industrial application – mineral oil	
2.5 times all pumps` flow	3 to 5 times all pumps` flow
Industrial application – HFC and HFD	
5 times all pumps` flow	8 times all pumps` flow
Mobile application – Open loop system	
1.5 to 2 times all pumps` flow	2.5 times all pumps` flow
Mobile application – Close loop pumps	
1 to 2 times all charge pumps` flow	1.5 to 2 times all pumps` flow

In the case of the use of HFC or HFD fluids, which generally have a higher density, the elimination of contaminants is less efficient. Therefore, the recommended tank volume is larger. In all cases, however, the obtained tank volume value must be increased by approx. 10 to 15 % (air cushion, fluid level fluctuations due to thermal expansion of the fluid and chambers of different sizes in hydraulic cylinders…).

The ratio between the tank volume V_T and the flow of the pump Q_P can be given in the form of circulation ratio C_r. Similarly, such a ratio may also be used in the case of other tanks, e. g. for bearing lubrication systems, and can be given in different ways, as V_T vs Q_P, or vice versa. [5], [6] As written in Table 1, the circulation ratio can be given as:

$$C_r = \frac{V_T}{Q_P} \qquad \text{[min]} \tag{1}$$

The circulation ratio indicates how often the entire fluid volume in the tank is recirculated or pumped per time interval, e. g. per minute. In harsher operating conditions, the fluid (e. g. oil) needs more time to recover (otherwise the entire filling will need to be replaced more frequently). This applies, for example, in the case of higher temperatures and low oil quantities with a low value of circulation ratio. According to the record in Table 1, a higher value of C_r is desired.

In the case of (too) small tanks, both in the fields of stationary and mobile hydraulics, the elimination of contaminants is worse. Depending on the flow of the pump, a too small selected tank volume leads to overheating and faster ageing of the hydraulic fluid, to a shorter service life of the installed hydraulic components due to faster wear and to many other side effects, such as e. g. increased elasticity of drives, greater oscillations and signal delay, diesel effect and cavitation, varnishing and sludge…

3   Small hydraulic tanks and excessive pump flow

The too small selected tank volume in relation to the pump flow is not always the result of an error in sizing and selecting the tank size. In certain cases, however, we want to have smaller tanks according to the flow of the pump. This is especially useful or desirable in the case of testing the durability of hydraulic fluids, e. g. mineral oils, because, in the test, we want to load the fluid more and degrade faster. These are so-called tribological tests with hydraulic pumps. Some typical parameters of such established tribological pump tests are given in Table 2.

Table 2: Circulation ratio values of different tribological pump tests

Test	Tank fluid volume [l]	Volumetric flow rate [l/min]	C_r [min]
Denison Vane Pump HF0 Test	189	265	0.71
Sundstrand Piston Pump – Series 22	45	95	0.47
Vickers test with a 35VQ-25 pump	196	144	1.36
Komatsu test	75	20 to 60	3.75 to 1.25
Integrated durability test device [7]	27	11	2.45

In all these mentioned tribological tests with hydraulic pumps, the values of the circulation ratio are much lower than those recommended for normal operating conditions e. g. when using mineral oil at the recommended tank size as 3 to 5 times the pump flow value (see Table 1).

The flow conditions in the tank are not visible to the naked eye, and are therefore not known exactly, as the tanks have a metal housing. It does not matter whether the too small volume of the tank is due to an error in choosing the appropriate size of the tank, or whether a smaller volume of the tank is chosen purposely than e. g. in the case of tribological tests with pumps.

In our case, the flow conditions in the undersized hydraulic tank were studied based on an industrial 30-litre aluminium cast tank used in the case of the integrated test device mentioned in Table 2. There was 25 l of mineral oil in the tank. The appearance of the considered tank is shown in Figure 1.

Figure 1: 30-litre cast aluminium oil tank.

4   Simulation of flow conditions inside a small tank

Insight into the flow conditions inside the tank and the influence of different designs and dimensions of the tank is provided by a computer simulation based on the appropriate numerical model of the hydraulic tank and the relevant parameters of the tank. The latter can be obtained based on comparative experimental research, or based on the experience of previous research. Simulation of flow conditions and phenomena inside a hydraulic tank have been the subject of several studies [8], [9], [10], [11], [12], [13].

A Eulerian approach to describe fluid flow is used in this study. This approach is implemented and readily available in commercial CFD solvers, and the ANSYS CFX 2020 R2 was used in this study. In all simulations the flow was isothermal, with the fluid properties for ISO VG 46 listed in Table 3 and steady-state mode selected. Three different flow rates were prescribed to simulate normal, increased and excessive flow rate in the system. Both inlet and outlet boundary conditions were prescribed as average inlet and outlet velocity, and all other surfaces of the tank were taken as no-slip walls, as shown in Figure 2.

Table 3: ISO VG 46 mineral oil properties used in the simulations

Viscosity Grade ISO	Kinematic Viscosity at 40 °C [mm²/s]	Viscosity Index [−]	Density at 20 °C [kg/m³]
VG 46	46.98	104	876.20

The reference pressure within the computational domain was set to 1 atm, an advection numeric scheme was chosen to be upwind, and Root Mean Square (RMS) convergence criterion was set to 10⁻⁴ for all equations.
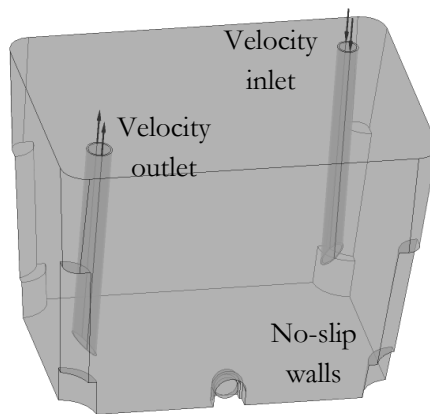
Figure 2: Boundary conditions.

In Table 4 the test cases are presented with the circulation ratio (eq. 1) and Reynolds number values (eq. 2). The Reynolds number is calculated as:

$$Re = \frac{u \, d}{v} \tag{2}$$

where u is the fluid velocity in the exit pipe, d is the pipe diameter and ν is the fluid kinematic viscosity.

It is evident from the Table 4, that Reynolds number value in exit pipes for all analyzed fluid flowrates is in laminar flow regime.

Table 4: Test cases and boundary conditions used in the simulations

Test case	Volume of fluid in the tank [l]	Volumetric flow rate [l/min]	Cr [min]	Reynolds number value in the exit pipe
Recommended flow rate	27	6	4.5	275.5
Increased flow rate	27	30	0.9	1377
Excessive flow rate	27	60	0.45	2755

According to this, fluid flow is described with the continuity equation:

$$\frac{\partial \rho}{\partial t} + \vec{\boldsymbol{\nabla}} \cdot (\rho \vec{\boldsymbol{u}}) = 0 \tag{3}$$

and Navier-Stokes equations:

$$\frac{\partial (\rho \vec{\boldsymbol{u}})}{\partial t} + \rho\big(\vec{\boldsymbol{u}} \cdot \vec{\boldsymbol{\nabla}}\big)\vec{\boldsymbol{u}} = -\vec{\boldsymbol{\nabla}}p + \mu\nabla^2\vec{\boldsymbol{u}} + \rho\vec{\boldsymbol{g}} \tag{4}$$

where ρ is fluid density, $\vec{\boldsymbol{u}}$ is fluid velocity, p is pressure, μ is fluid dynamic viscosity and $\vec{\boldsymbol{g}}$ is gravitational acceleration.
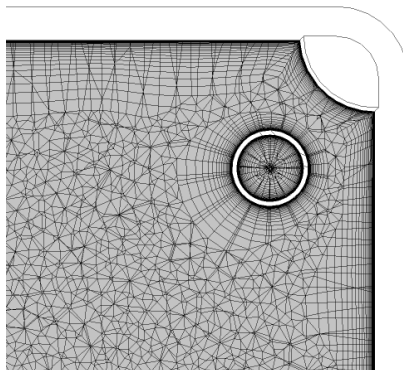
Figure 3: Mesh detail.

Following the laminar flow regime in the hydraulic tank pipes, a tetrahedral mesh was used for simulation with 2,675,435 elements, minimal orthogonality of 0.0499 and an aspect ratio of 6708. The mesh detail is shown in Figure 3.

5 Results

Figure 4 shows streamlines in the hydraulic tank for three analysed flow cases. It is evident that an increase of flow rate extends the path (trajectory) of the fluid element. Despite the laminar flow regime, it is evident that increased and excessive flow rates cause more vorticity.

Recommended Qp = 6 l/min	
Increased Qp = 30 l/min	
Excessive Qp = 60 l/min	
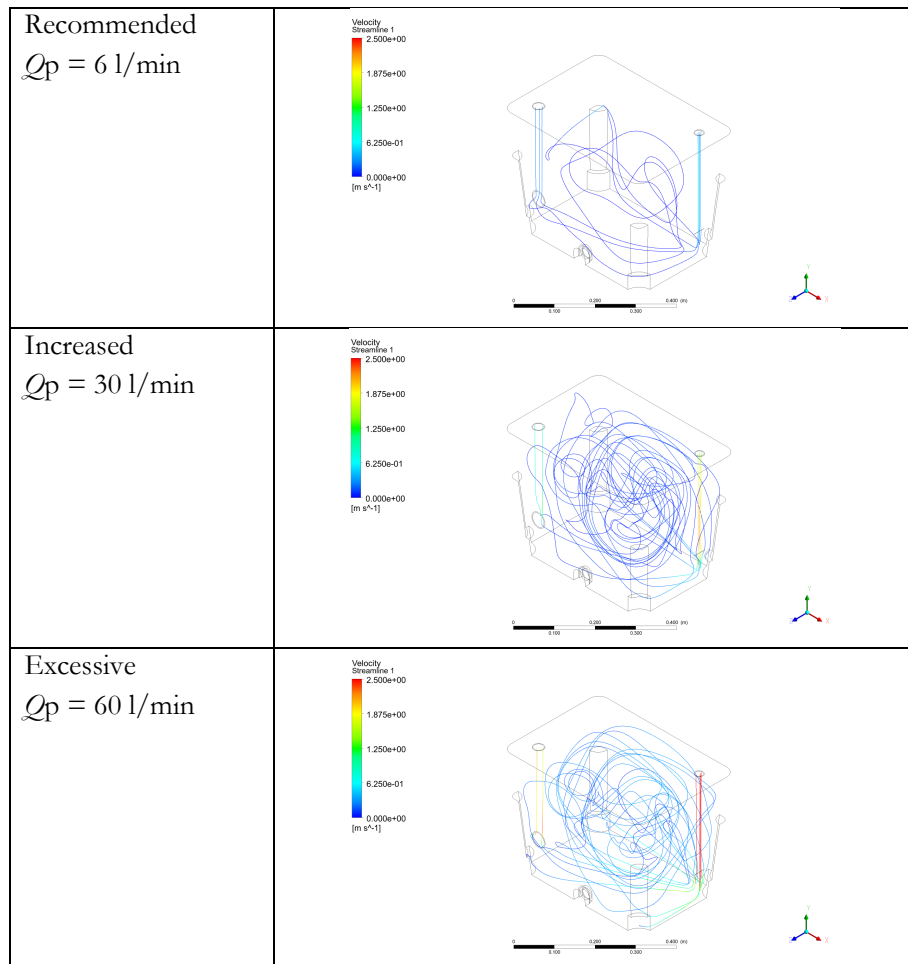
Figure 4: Streamlines in the hydraulic tank for the analysed flow cases.

Figure 5 shows the velocity vector field for all the analysed flow cases. It is evident that the vector field remains similar, which is a logical consequence of a laminar flow regime. The velocity magnitude and gradients are higher when flow rate is increased or excessive.

Recommended Qp = 6 l/min	
Increased Qp = 30 l/min	
Excessive Qp = 60 l/min	
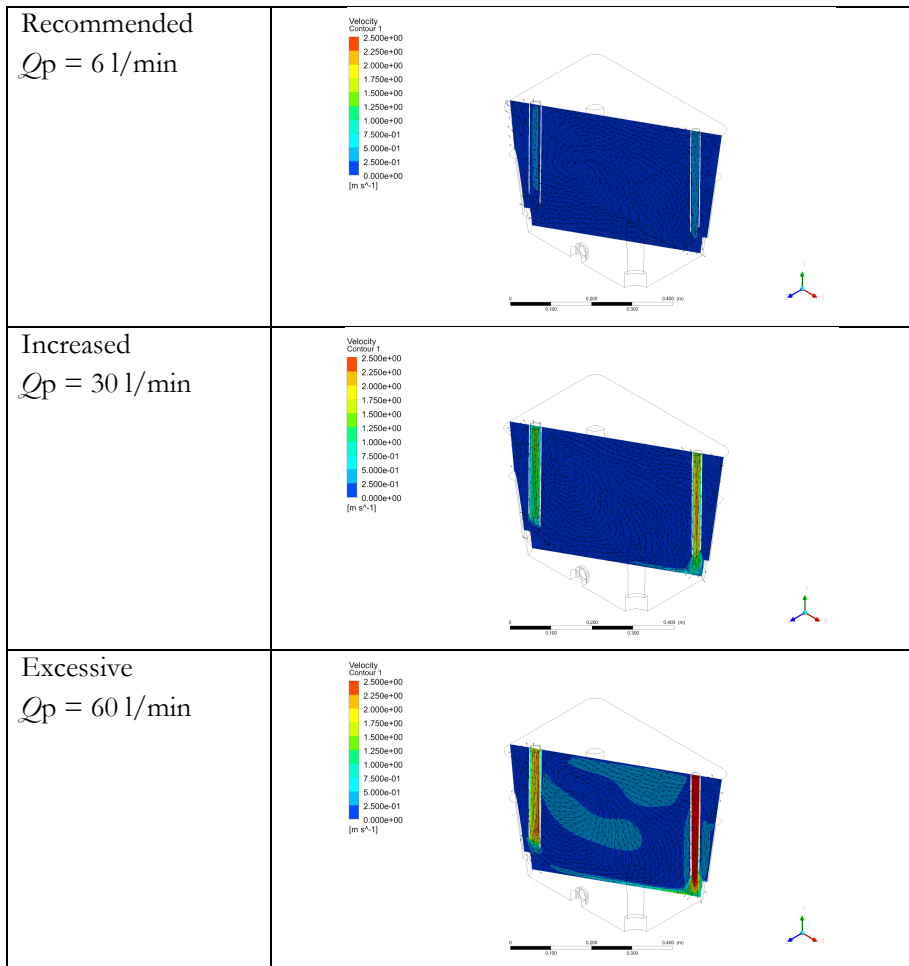
Figure 5: Velocity field for the analysed flow cases.

Figure 6 shows the shear strain rate at the tank bottom. Following the velocity field, it is evident that an increase of flow rate in the hydraulic tank leads to higher shear strain rate on the walls. According to this, increased flow rates result in poorer excretion of gas bubbles and poorer sedimentation of solid particles. This effect seems to have similar consequences as viscosity decrease of the fluid.

Recommended Qp = 6 l/min	
Increased Qp = 30 l/min	
Excessive Qp = 60 l/min	
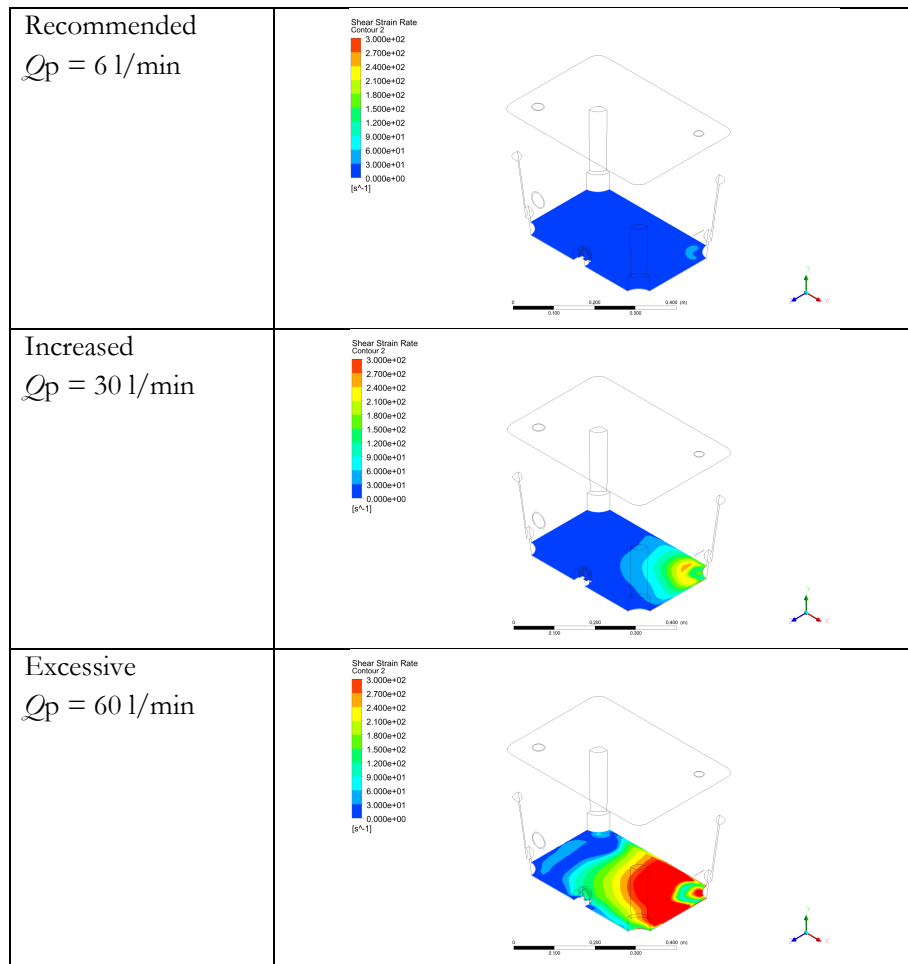
Figure 6: Shear strain rate at the tank bottom for the analysed flow cases.

5 Conclusions

The presented study, based on an appropriate model and simulation, deals with the flow conditions inside a hydraulic tank. As an example, a smaller 30-litre aluminium tank was used, and mineral hydraulic oil as the most used fluid.

At the forefront of the discussion is the impact of the relationship between tank size and pump flow. Three typical cases were considered. In the first case, the size of the tank was determined according to a recommendation that usually ensures optimal flow conditions. In the second and third cases, the influence of increased and excessive pump flow in the same large tank is shown. The latter may be due to an error - inappropriate selection of tank size according to the pump flow, or due to a purposefully selected smaller tank, as in the case of tribological tests with pumps. Similar conditions can also occur in the case of speed-controlled hydraulic pumps. The obtained insight into the current conditions inside the tank enables a more precise selection of the appropriate tank size or the use of a suitable tank design.

References

[1] Casey, B. (2016). How to size a hydraulic tank, *Hydraulics and Pneumatics*, pp.4. https://www.hydraulicspneumatics.com/print/content/21884901. (6. 8. 2021)

[2] Gannon, M. (2015). Hydraulic reservoir design considerations. *FluidPower World*, paper, https://www.fluidpowerworld.com/understanding-hydraulic-reservoir-designs/.(6.   8. 2021)

[3] Windsor   Manufacturing.   (2016).   Sizing   Hydraulic   Reservoir. https://windsormfg.com/sizing-hydraulic-reservoir/. (6. 8. 2021)

[4] N.N. (2012). Fundamentals of Hydraulic Reservoirs. *Hydraulics and Pneumatics*. pp. 7. https://www.hydraulicspneumatics.com/technologies/reservoirs-accessories/article/21882642/fundamentals-of-hydraulic-reservoirs. (6. 8. 2021)

[5] FAG Schaeffler. (2016). Large Size Bearings. p. 1139. Schaeffler Technologies AG & Co.

[6] ISO 4413:2010. (2010). Hydraulic fluid power — General rules and safety requirements for systems and their components.

[7] Lovrec, D., Tič, V. (2021). A new approach for long-term testing of new hydraulic fluids.. *New technologies, development and application IV,* Sarajevo, Bosnia and Herzegovina, ISSN 2367-3370, Vol. 233), Springer Natur. cop. 2021, Vol. 233, 788-801, doi: 10.1007/978-3-030-75275-0_87.

[8] Tič, V., Lovrec, D. (2012). Design of modern hydraulic tank using fluid flow simulation. *International journal of simulation modelling*, ISSN 1726-4529, Vol. 11, Iss. 2, 77-88, doi: 10.2507/IJSIMM11(2)2.202.

[9]   Tič, V., Lovrec, D. (2013). Air-release and solid particles sedimentation process within a hydraulic reservoir. *Tehnički vjesnik Technical Gazette,* ISSN 1330-3651, 2013, Vol. 20, No. 3, 407-412. http://hrcak.srce.hr/index.php?show=clanak&id_clanak_jezik=153000.

[10]   Močilan, M., Žmindák, M., Pecháč, P., Weis, P. (2017). CFD Simulation of Hydraulic Tank, *Procedia Engineering*, Vol. 192, 609-614, https://doi.org/10.1016/j.proeng.2017.06.105.

[11]   Vollmer, T., Frerichs, L. (2016), Development of hydraulic tanks by multi-phase CFD simulation, *10th International Fluid Power Conference*, Dresden 2016, 619-630.

[12]   Muttenthaler L., Manhartsgruber, B., (2019). Prediction of Particle Resuspension and Particle Accumulation in Hydraulic Reservoirs Using Three-Phase CFD Simulations, *ASME/BATH Symposium on Fluid Power and Motion Control*, doi: 10.1115/FPMC2019-1617.

[13]   Muttenthaler L., Manhartsgruber, B. (2020). Euler–Lagrange CFD simulation and experiments on accumulation and resuspension of particles in hydraulic reservoirs, *Journal of the Brazilian Society of Mechanical Sciences and Engineering.* 42(4), doi:10.1007/s40430-020-02292-8.

Results of identification and optimization of the parameters of axial piston pump

RADOVAN PETROVIĆ, NENAD TODIĆ, SLOBODAN SAVIĆ &
MAJA ANDJELKOVIĆ

Abstract In the development of applicative software for mathematical modelling, identification, and optimization of parameters of axial piston pumps, special attention is paid to the real need of the engineers' practice. We used the original graphical 2D and 3D software for the application in real-time with a simultaneous presentation and processing in 24 windows of high resolution. Here it is mentioned that during optimization and identification of axial piston pump's parameters, we automatically form and present several hundreds of the complex 2D diagrams, which enables to intervene at any point in the study of hydrodynamic processes by the change of input data, where the following flow of identification and optimization is changed.

Keywords: • axial piston pump • mathematical modelling• simulation • identification and optimization • experiment •

CORRESPONDENCE ADDRESS: Radovan Petrović, University "Union-Nikola Tesla" of Belgrade, Faculty of Information Technology and Engineering, Staro sajmište 29, 11070 Novi Beograd, Serbia, e-mail: radovan4700@yahoo.com. Nenad Todić, University of Kragujevac, Faculty of Engineering, Sestre Janjić 6, 34000 Kragujevac, Serbia, e-mail: ntodic@gmail.com. Slobodan Savić, University ofKragujevac, Faculty of Engineering, Sestre Janjić 6, 34000 Kragujevac, Serbia, e-mail: ssavic@kg.ac.rs. Maja Andjelković, University "Union-Nikola Tesla" of Belgrade, Faculty of Information Technology and Engineering, Staro sajmište 29, 11070 Novi Beograd, Serbia, e-mail: maja.andjelkovic@fpsp.edu.rs.

1   Introduction

Developed program for mathematical modelling, identification and optimization of axial piston pumps, enables for the further studies of hydrodynamic processes the development of entire families of the pumps with the analysis of advantages and disadvantages of the axial piston pumps with fixed and variable flow.

2   The applied ultra-rapid measuring system ADS 2000-CADEX

Total number of the data measured in this case was (4+1) x4096 = 20480 per a revolution (cycle), i. e. 204800 for 10 successive cycles. Number of 4096 samples wasn't selected randomly, but it was given on purpose due to the application of the Fast Fourier Transform (FFT) of the measured signals. Measurements were performed for seven operating modes with parameters given in Table 1.

Table 1: The applied operating modes in experimental testing of the pump

Number	Example	Cylinder pressure p_c [bar]	Number of revolutions n [min^{-1}]
1.	R03	180	1000
2.	R04	50	800
3.	R05	160	800
4.	R06	180	800
5.	R07	200	800
6.	R08	200	1000
7.	R09	200	875.6

The structural scheme of the applied ultra-rapid measuring system ADS 2000-CADEX is depicted in Figure 1.

R. Petrović, N. Todić, S. Savić & M. Andjelković: *Results of Identification and Optimization of the Parameters of Axial Piston Pump*

135
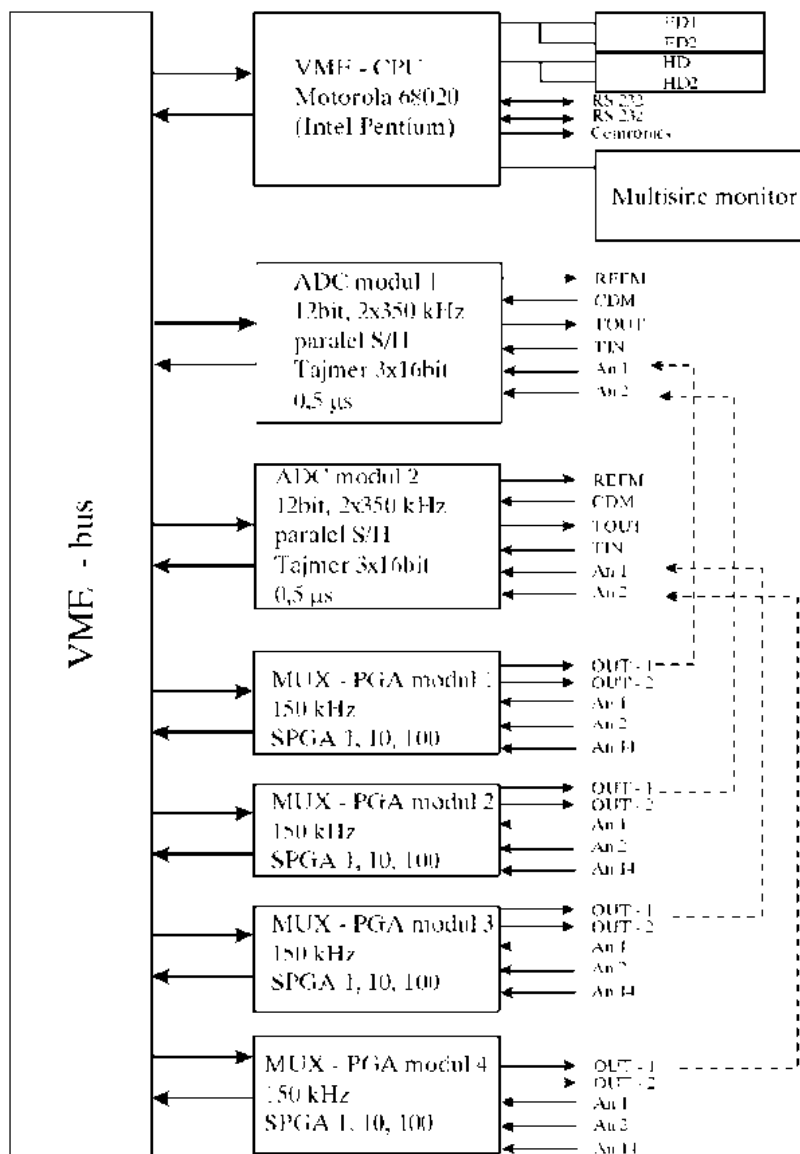
Figure 1: Structural scheme of the applied ultra-rapid measuring system ADS 2000-CADEX.

Figure 2 (a to f) shows the measured pressures for the individual, i. e. ten successive cycles of the examined axial piston pump. The results refer to the experiment labelled by the number 7 and the example R09 at the operating mode $p = 200$ bar and $n = 875.6$ min^{-1}.
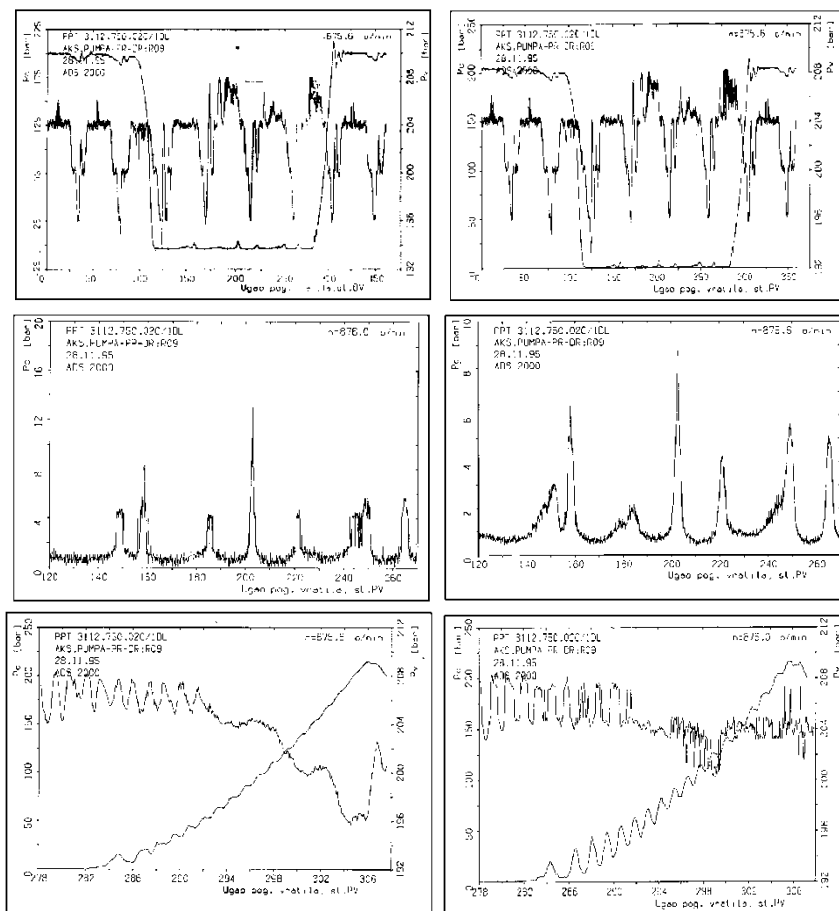
Figure 2: (a to f) Diagrams of the pressures measured in the operating mode
n = 875. 6 min^{-1} and p_n = 200 bar.

Figure 2 (a and b) presents the pressure flow in the cylinder (p_c), measured for one, i. e. mid of the 10 successive cycles in the function of the angle φ of the drive shaft. From the diagram we can observe the pressure gradients in the phase of the compression and expansion, as well as the appearance of the "peaks" during the suction. The same Figures show the pressure flow in the discharge chamber (p_p) for one, i. e. mid of the 10 successive cycles in the function of the angle of the drive shaft.

Pressure pulsations in discharge chamber depend on the number of cylinders, which is obvious in this case, because it is about a pump with eight cylinders.

R. Petrović, N. Todić, S. Savić & M. Andjelković: Results of Identification and Optimization of the Parameters of Axial Piston Pump

137

The appearance of the "peaks" in the suction phase for one, i. e. the mid of 10 successive cycles at the angle interval of the drive shaft of 120-270° is presented in Figure 2 (c and d).

Figure 2 (e and f) shows that pressure flow in the cylinder (p_c), measured for one, i. e. mid from 10 successive cycles in the angle interval of the drive shaft of 278 – 307°, with the aim to analyse the gradient of the pressure increase in the compression phase with more details. The same diagrams in the same interval also show the pulsations of the pressure in the discharge chamber.

3   Statistical and Fast Fourier Transform (FFT) analyses of the axial piston pump operating process parameters.

Quantities of the vibration amplitudes of the pump's housing measured for the mid of the ten successive cycles are presented in Figure 3. The applied decibel scale enables easier comparison of the absolute level of the amplitudes of the measured quantities per a recommended reference level.

Vibrations level is defined by the relation of the amplitudes in the following manner:

$$N, in\ decibels = 20\ log_{10} \frac{A}{A_{ref}} \tag{1}$$

where:
N – is the number of decibels,
A – measured level of amplitudes,
$A_{ref} = 10^{Kref}$ – recommended reference level.

Reference level is marked by the exponent K_{ref} on the appropriate diagrams.
From the presented diagrams of the harmonic analysis of pressures in the discharge chamber, a dominant order for maximum pressure amplitudes was observed, which contains a module that equals the number of cylinders (2).

$$\sigma = z \cdot n \tag{2}$$

Where:
z is the number of cylinders,
n= 1,2,3...is the number of cycles.
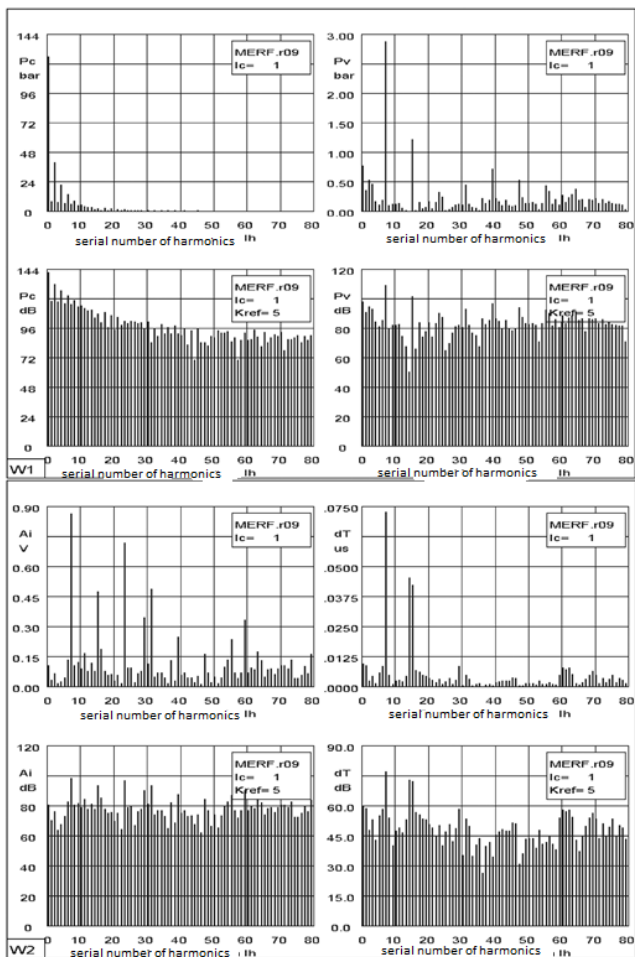
Figure 3: Results of the harmonic analysis of the measured pressures, vibrations and time intervals for one cycle in case of n = 875.6 min^{-1} and p = 200 bar with graphical presentation of 80 harmonics.

Figure 3 also shows us the appearance of the peaks of amplitudes in case of the harmonics. General conclusions about the results of measurement and analysis are principally valid for all the examined operating modes of the axial piston pump.

R. Petrović, N. Todić, S. Savić & M. Andjelković: Results of Identification and Optimization of the Parameters of Axial Piston Pump

139

4   Conclusion

Within the performed experimental studies, the measurement of pressure was performed in the cylinder, discharge space and discharge pipeline, as well as the vibration amplitude of the pump's housing, depending on the angle of the drive shaft. All the pressures and vibrations are measured parallel at each cca 0,09° of the drive shaft of the pump (exactly 4096 times per one revolution of the shaft). As an incremental angle encoder, the optical encoder with 1024 impulses per a revolution was used. The impulses of the angle encoder were doubled with the help of an interface for angle encoders in an ultra-rapid measuring system ADS 2000-CADEX, so that we obtain 4096 impulses per a revolution of the shaft.

In order to observe the repeatability of the successive cycles in the unaltered operating mode, 10 successive cycles were measured. At the same time, the time interval from angle to angle was measured in order to determine the equality of angular velocity of the drive shaft and the control of the operation of incremental angle encoder. All the analogue signals (of the pressure, vibrations) are parallel converted into cyphers with the help of four ultra-rapid converters that work simultaneously (parallel).

References

[1]   Petrovic, R. (1999). Matematičko modeliranje i identifikacija parametara višecilindričnih klipno-aksijalnih pumpi. *Mašinski fakultet Univerziteta u Beogradu*, Beograd.

[2]   Ivantysyn, J., Ivantysynova, M. (2001). Hydrostatic Pumps and Motors. Principles, Design, Performance, Modelling, Analysis, Control and Testing. *Akademia Books International*. New Delhi.

[3]   Jankov R. (1984). Matematičko modeliranje strujno - termodinamičkih procesa i pogonskih karakteristika dizel - motora, kvazistacionarni modeli. *Naučna knjiga*, Beograd.

[4]   Jankov R., Tomić M., Štavljanin M. (1986). Istraživanje kibernetičkih metoda projektovanja i razvoja sistema ubrizgavanja dizel motora. *Mašinski fakultet Beograd*. Beograd.

[5]   Petrović R. (2009). Mathematical Modeling and Experimental Verification of Operating Parameters of Vane Pump With Double Effect. *STROJNIŠKI VESTNIK – Journal of Mechanical Engineering*, Vol.55, No1, p.26-32

[6]   Petrović R. (2009). Mathematical Modeling and Experimental Research of Characteristic Parameters of Hydrodynamic Processes in an axial piston Pump. *STROJNIŠKI VESTNIK" – Journal of Mechanical Engineering*, Vol.55, No4, p.224-229

[7]   Savković, M., Gašić, M., Arsić, M., Petrović, R. (2010). Analysis of the axle Fracture of the bucket wheel excavator. *Engineering Failure Analysis*. doi:10.1016/j.engfailanal.2010.09.031,

[8]   Petrović R., Todić N. (2008). Modeling and experimental research of characteristic parameters hydrodinamic processes of axial piston pumps with constant pressure and variable flow. *The 20 th International Conference on Hydraulics and Pneumatics*. Prague

[9]   Petrović R., Pezdirnik J., Todić N. (2009). Results of measuring the parameters of operating process in an axial piston pump and its statistic and FFT analysis. *Medunarodna konferencija FLUIDNA TEHNIKA 2009*. Maribor

[10]   Plummer, A.R.   (2007). Control techniques for structural testing: a review Proc. Instn. Mech. Engrs, Part I. *Journal of Systems and Control Engineering*. Vol.221, No2, p.139-169.

[11]   Petrović R., Ivanović P., Todić N. (2008). Experimental research of characteristic parameters of hydrodinamic processes in a piston axial pump, *Tractors and power machines*. Vol. 13, No. 1, p. 35 – 42

[12]   Petrović R., Đuričić Lj., Pezdirnik J., Banaszek A. (2011). Identification of Characteristic Parameters of Advanced Seawater Hydraulic Axial Piston Pump. *The 52nd National Conference on Fluid Power (NCFP) were presented during the International Exposition for Power Transmission (IFPE 2011)*. Las Vegas

[13]   Petrović R., Mihailović G., Đuričić Lj. (2011). Experimental Research and Analysis of Working and Constructive Parameters of Hydro Pumps with Const. Pressure and Var. Flow. *3rd International Workshop on Aircraft System Technologies AST 2011*.Hamburg

[14]   Petrović R., Pezdirnik J., Banaszek A. (2011). Mathematical Modeling and Experimental Research of novel seawater hydraulic axial piston pump. *The Twelfth Scandinavian International Conference on Fluid Power*.Tampere

[15]   Todic, N., Vulovic, S., Petrovic, R., Vujovic, I., Savic, S. (2018) Sustainable development of agriculture techniques using water hydraulic components. *The journal Tractors and power machines*. Vol.23, No.(1/2), p.71-77

University of Maribor Press

Challenges of numerical modelling and simulation of flow inside the hydraulic tank

LUKA KEVORKIJAN & IGNACIJO BILUŠ

Abstract The basic purpose of the hydraulic tank is to hold a volume of fluid, transfer heat from the system, allow solid contaminants to settle and facilitate the release of air and moisture from the fluid. To perform these important tasks more efficiently, the tank must be properly dimensioned and it must operate in correct flow rate range. At high flow rates it can be subjected to effects of turbulence, leading to poorer performance of the tank. To predict turbulent effects correctly a numerical simulation, based on RANS approach is prepared and run. Difference between $k - \varepsilon$ model and $k - \omega$ Shear Stress Transport (SST) is investigated and results are presented. Impact of choice of turbulence model is discussed.

Keywords: • hydraulic tank • turbulence modelling • wall y^+ • RANS • simulation •

CORRESPONDENCE ADDRESS: Luka Kevorkijan, University of Maribor, Faculty of Mechanical Engineering, Smetanova 17, 2000 Maribor, Slovenia, e-mail: luka.kevorkijan@um.si. Ignacijo Biluš, University of Maribor, Faculty of Mechanical Engineering, Smetanova 17, 2000 Maribor, Slovenia, e-mail: ignacijo.bilus@um.si.

1   Introduction

One of the functions of a hydraulic tank is to remove air bubbles and particulate contaminants that have been introduced into hydraulic fluid due to various reasons, among them leaks in the pipe connections and wear of hydraulic system components. Depending on flow conditions (turbulent intensity) particles settle and air bubbles rise with varying degree of efficiency, less disturbed and turbulent flow allows for a higher efficiency of removal of contaminants.

In anticipation of occurrence of unfavourable flow conditions it can be beneficial to have detailed information about the flow inside the hydraulic tank before the final design is decided. For this purpose a computational fluid dynamics (CFD) study can be performed on an early design proposal (or to analyse existing tank). However, as complexity of analysed flow increases so does the complexity of modelling the flow.

With respect to flow rate (or velocity) through the tank, two distinct types of flow occur, laminar and turbulent. Turbulent flow introduces additional complexity in description of the flow and different approaches exist to obtain numerical solution of turbulent flow. From practical standpoint RANS approach provides a good balance between computational effort, modelling complexity and accuracy of predicting turbulence in the flow. Within the RANS approach different models based on Boussinesq hypothesis exist. These are classified by number of additional equations to model turbulent viscosity, such as one equation Spalart-Allmaras model and several two equation models among them k-epsilon (k-ε), k-omega (k-ω) and Menter's Shear Stress Transport (SST) model [1], [2].

In this work we applied the k-epsilon (k-ε) model and Menter's Shear Stress Transport (SST) model and compared the resulting flow.

2   Numerical modelling

An Eulerian approach to describe fluid flow is used in this study. This approach is implemented and readily available in commercial CFD solvers, in this study ANSYS CFX 2020 R2 was used [2]. In all simulations the flow was isothermal with fluid properties listed in Table 1 and steady-state mode was selected.

Table 1: Liquid properties used in simulations

Liquid (Oil)	Density [kg/m³]	Dynamic viscosity [kg/m s]	Kinematic viscosity [m²/s]
ISO VG 22	856.8	0.018147024	0.00002118

Fluid flow is described with continuity equation:

$$\frac{\partial \rho}{\partial t} + \vec{\nabla} \cdot (\rho \vec{u}) = 0 \qquad (1)$$

and Navier-Stokes equations:

$$\frac{\partial (\rho \vec{u})}{\partial t} + \rho(\vec{u} \cdot \vec{\nabla})\vec{u} = -\vec{\nabla}p + \mu \nabla^2 \vec{u} + \rho \vec{g} \qquad (2)$$

where ρ is fluid density, $\vec{u}$ is fluid velocity, p is pressure, μ is fluid dynamic viscosity and $\vec{g}$ is gravitational acceleration.

To model turbulent flow equations (1) and (2) are Reynolds-averaged and the resulting equations are Reynolds-Averaged Navier-Stokes equations (RANS). Any time dependent flow variable $\phi(t)$ is split:

$$\phi(t) = \overline{\phi}(t) + \phi'(t) \qquad (3)$$

So that $\overline{\phi}(t)$ represents a mean value and $\phi'(t)$ represents time-dependent fluctuation with respect to this mean value. Mean value is obtained by applying sliding time-averaging window:

$$\overline{\phi}(t) = \frac{1}{2\Delta t} \int_{t-\Delta t}^{t+\Delta t} \phi(t)dt \qquad (4)$$

where the time-averaging window is written as an interval $[t - \Delta t, t + \Delta t]$.

After applying the Reynolds averaging procedure, continuity equation is rewritten as:

$$\frac{\partial \rho}{\partial t} + \vec{\boldsymbol{\nabla}} \cdot \left(\rho \overline{\vec{\boldsymbol{u}}} \right) = 0 \tag{5}$$

And Navier-Stokes equations (RANS) are rewritten as:

$$\frac{\partial \left(\rho \overline{\vec{\boldsymbol{u}}} \right)}{\partial t} + \rho \left(\overline{\vec{\boldsymbol{u}}} \cdot \vec{\boldsymbol{\nabla}} \right) \overline{\vec{\boldsymbol{u}}} = -\vec{\boldsymbol{\nabla}} \overline{p} + \mu \nabla^2 \overline{\vec{\boldsymbol{u}}} - \vec{\boldsymbol{\nabla}} \cdot \left(\rho \overline{\vec{\boldsymbol{u'}} \vec{\boldsymbol{u'}}} \right) + \rho \vec{\boldsymbol{g}} \tag{6}$$

where $\overline{\vec{\boldsymbol{u}}}$ is now a mean flow velocity, $\overline{p}$ a mean pressure and $\vec{\boldsymbol{u'}}$ is fluctuation of fluid flow velocity with respect to its mean value. An additional term in equation (6) arises as a result of averaging procedure, named Reynolds stress. In this work this term is modelled based on the Boussinesq hypothesis:

$$\rho \overline{\vec{\boldsymbol{u'}} \vec{\boldsymbol{u'}}} = \mu_t \left[\left(\vec{\boldsymbol{\nabla}} \overline{\vec{\boldsymbol{u}}} + \vec{\boldsymbol{\nabla}} \overline{\vec{\boldsymbol{u}}}^T \right) - \frac{2}{3} \left(\vec{\boldsymbol{\nabla}} \cdot \overline{\vec{\boldsymbol{u}}} \right) \overline{\overline{\boldsymbol{I}}} \right] \tag{7}$$

where a turbulent viscosity μ_t is introduced and $\overline{\overline{\boldsymbol{I}}}$ is the identity matrix.

Turbulent viscosity is expressed with turbulent kinetic (k) energy and rate of dissipation of turbulent kinetic energy (ε) within the $k - \varepsilon$ turbulent model formulation:

$$\mu_t = C_\mu \rho \frac{k^2}{\varepsilon} \tag{8}$$

To model turbulent viscosity two additional transport equations for two turbulent variables are introduced. Turbulent kinetic energy is defined as:

$$k = \frac{1}{2} \left(\overline{u_x' u_x'} + \overline{u_y' u_y'} + \overline{u_z' u_z'} \right) \tag{9}$$

For two equation turbulence models isotropy of turbulence is assumed $\overline{u_x' u_x'} = \overline{u_y' u_y'} = \overline{u_z' u_z'}$ and transport equation for turbulent kinetic energy is written

$$\frac{\partial (\rho k)}{\partial t} + \vec{\boldsymbol{\nabla}} \cdot (\rho k \overline{\vec{\boldsymbol{u}}}) = \vec{\boldsymbol{\nabla}} \cdot \left[\left(\mu + \frac{\mu_t}{\sigma_k} \right) \vec{\boldsymbol{\nabla}} k \right] + P_k - \rho \varepsilon \tag{10}$$

For k-ε model the second transport equation is written for transport of the rate of dissipation of turbulent kinetic energy (ε)

$$\frac{\partial(\rho\varepsilon)}{\partial t} + \vec{\boldsymbol{\nabla}} \cdot (\rho\varepsilon\vec{\boldsymbol{u}}) = \vec{\boldsymbol{\nabla}} \cdot \left[\left(\mu + \frac{\mu_t}{\sigma_\varepsilon}\right)\vec{\boldsymbol{\nabla}}\varepsilon\right] + \frac{\varepsilon}{k}(C_{\varepsilon 1}P_k - C_{\varepsilon 2}\rho\varepsilon) \qquad (11)$$

In equations (8) and (9) P_k is production of turbulent kinetic energy, additional terms are sometimes added to account for buoyancy and other effects. Model parameters are listed in Table 2.

Table 2: k-ε turbulent model parameters

$C_{\varepsilon 1}$	$C_{\varepsilon 2}$	σ_k	σ_ε	σ_μ
1.44	1.92	1.0	1.3	0.09

Another two equation turbulence model is k-ω Shear Stress Transport (SST) model. Turbulent viscosity is then expressed as:

$$\mu_t = \frac{\rho k}{\omega}\frac{1}{max\left[\frac{1}{\alpha^*},\frac{SF_2}{a_1\omega}\right]} \qquad (12)$$

where $\omega = \varepsilon/k$ is specific rate of dissipation of turbulent kinetic energy, α^* is low Reynolds number damping coefficient set to 1 in a high Reynolds number flow, a_1 is a model constant, S is the strain rate magnitude and F_2 is the second blending function. Strain rate magnitude is defined as:

$$S = \sqrt{2\overline{\overline{\boldsymbol{SS}}}} \qquad (13)$$

where $\overline{\overline{\boldsymbol{S}}}$ is the strain rate tensor:

$$\overline{\overline{\boldsymbol{S}}} = \frac{1}{2}\left(\vec{\boldsymbol{\nabla}}\vec{\boldsymbol{u}} + \vec{\boldsymbol{\nabla}}\vec{\boldsymbol{u}}^T\right) \qquad (14)$$

Second blending function is defined as

$$F_2 = tanh\left[\left[max\left(\frac{2\sqrt{k}}{\beta^*\omega y},\frac{500\nu}{y^2\omega}\right)\right]^2\right] \qquad (15)$$

where β^* is a model constant, y is distance to the wall and ν is kinematic viscosity of fluid. Transport equations for turbulent kinetic energy (k) and for specific rate of dissipation of turbulent kinetic energy (ω) are:

$$\frac{\partial(\rho k)}{\partial t} + \vec{\nabla} \cdot (\rho k \vec{u}) = \vec{\nabla} \cdot \left[\left(\mu + \frac{\mu_t}{\sigma_k}\right)\vec{\nabla}k\right] + P_k - \rho\beta^* k\omega \tag{16}$$

$$\frac{\partial(\rho\omega)}{\partial t} + \vec{\nabla} \cdot (\rho\omega\vec{u}) =$$
$$\vec{\nabla} \cdot \left[\left(\mu + \frac{\mu_t}{\sigma_\omega}\right)\vec{\nabla}\omega\right] + \rho\frac{\gamma}{\mu_t} - \beta\rho\omega^2 + 2(1-F_1)\frac{\rho\sigma_{\omega,2}}{\omega}\left(\vec{\nabla}k\right)\cdot\left(\vec{\nabla}\omega\right) \tag{17}$$

where P_k is production of turbulent kinetic energy, β is a model parameter, F_1 is the first blending function and $\sigma_{\omega,2}$ is a model constant. σ_k, σ_ω are model parameters further defined as:

$$\sigma_k = \frac{1}{F_1/\sigma_{k,1} + (1-F_2)/\sigma_{k,2}} \tag{18}$$

$$\sigma_\omega = \frac{1}{F_1/\sigma_{\omega,1} + (1-F_2)/\sigma_{\omega,2}} \tag{19}$$

where $\sigma_{k,1}$, $\sigma_{k,2}$ and $\sigma_{\omega,1}$ are model constants.

The first blending function is defined as:

$$F_1 = tanh\left[\left[min\left[max\left(\frac{\sqrt{k}}{\beta^*\omega y}, \frac{500\nu}{y^2\omega}\right), \frac{4\sigma_{\omega 2}k}{CD_{k\omega}y^2}\right]\right]^4\right] \tag{20}$$

where $CD_{k\omega}$ is defined as

$$CD_{k\omega} = max\left(2\rho\sigma_{\omega 2}\frac{1}{\omega}\left(\vec{\nabla}k\right)\cdot\left(\vec{\nabla}\omega\right), 10^{-10}\right) \tag{21}$$

Model constants are listed in Table 3.

Table 3: k-w Shear Stress Transport (SST) model constants

α^*	a_1	β^*	$\sigma_{k,1}$	$\sigma_{k,2}$	$\sigma_{\omega,1}$	$\sigma_{\omega,2}$
1	0.31	0.09	1.176	1.0	2.0	1.168

3 Geometry and computational mesh

In this study the analysed geometry was a hydraulic tank WN-LC-63-1RO with 30 litre capacity, shown in Figure 1.

Two turbulent models under consideration have different requirements for near wall mesh cell size (density). With standard k-ω model a standard log-law wall function approach is employed, therefore the recommended dimensionless wall distance is: [2], [3]

$$30 < y^+ < 300 \tag{22}$$

Dimensionless wall distance (y^+) is defined as:

$$y^+ = \frac{y}{\nu}\sqrt{\frac{\tau_w}{\rho}} \tag{23}$$

where y is normal distance from cell centroid to the nearest wall, ν is the kinematic viscosity of fluid, τ_w is the wall shear stress and ρ is fluid density.

For k-ω SST the condition for y^+ is more relaxed, however the benefit of this turbulent model is for sufficiently small values of $y^+ < 5$ (sufficient mesh density near the wall) viscous sublayer can be resolved [2], [3]. This is beneficial for situations with adverse pressure gradients and separation of flow, where standard k-ε fails to correctly predict the flow.

Because of different required mesh densities near the wall, two meshes were created, one for each turbulent model. Details about both meshes are presented in Table 4 and difference in mesh density near the wall is visible in Figure 2.
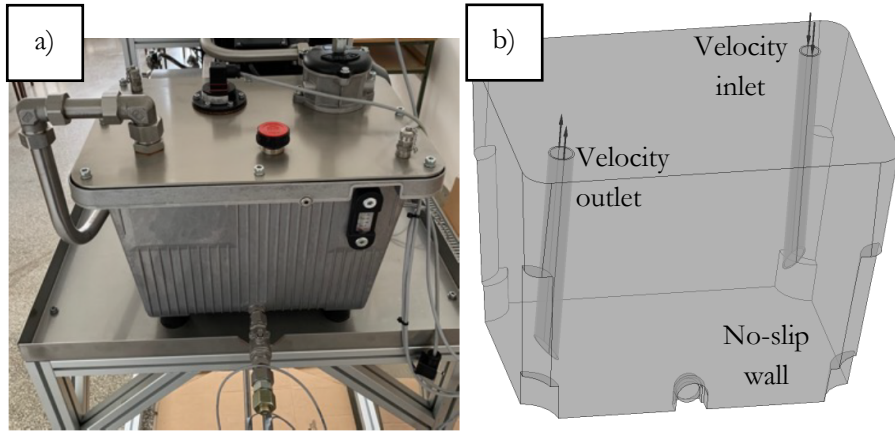
Figure 1: Considered hydraulic tank
a) appearance of the tank [3], b) computer generated 3D geometric model.

Table 4: Mesh metrics

Mesh name	Number of elements	Minimum element orthogonality	Maximum element aspect ratio	Minimum value of y^+	Maximum value of y^+
M1	366 862	0.0533	22.96	0	54.86
M2	2 675 435	0.0499	6708	0	0.4312
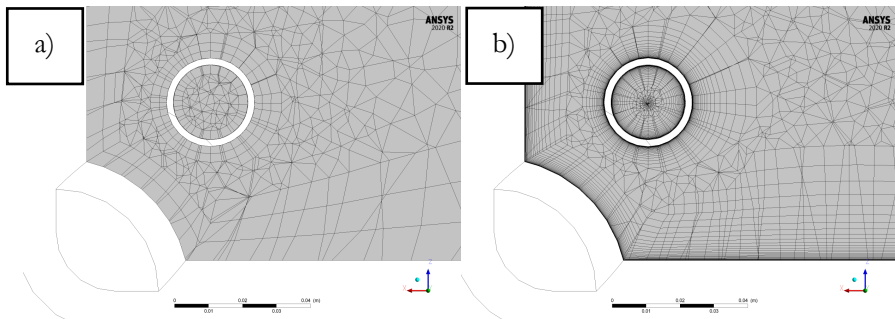
Figure 2: Geometry cut with a plane parallel to the bottom of the tank, visible corner with cut intake pipe;
a) mesh M1, b) mesh M2.

4   Boundary conditions and simulation setup

To ensure that turbulent flow is present inside the tank, flow rate through the tank was set such, that high enough Reynolds number in both the intake pipe and outtake pipe was achieved, as seen in Table 5. Both inlet and outlet boundary condition were prescribed as average inlet and outlet velocity, all other surfaces of the tank were taken as no-slip walls, as shown on Figure 2 b).

Table 5: Intake and outtake boundary conditions

Flow Rate [l/min]	Re_{intake}	$Re_{outtake}$	Average intake velocity [m/s]	Average outtake velocity [m/s]
60	2755	2164	2.675	1.651

Reference pressure within computational domain was set to 1 atm, turbulence intensity was set to 1 % as initial condition and as inlet boundary condition. Both advection and turbulent numeric scheme was chosen to be high resolution and Root Mean Square (RMS) convergence criterion was set to 10^{-4} for all equations. For velocity-pressure coupling Fourth Order Rhie Chow option was selected.

5   Results and conclusions

Both turbulent models resulted in flow with similar main features, such as vortices in the centre of the tank and close to the outtake pipe. This is shown visible in Figure 3 and Figure 4, where streamlines and velocity vector field are shown.
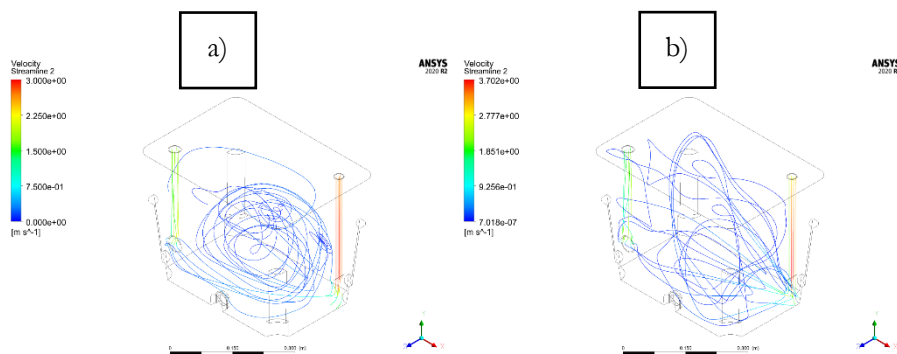
Figure 3: Streamlines, coloured by fluid velocity;
a) k-ε model, b) k-ω SST model
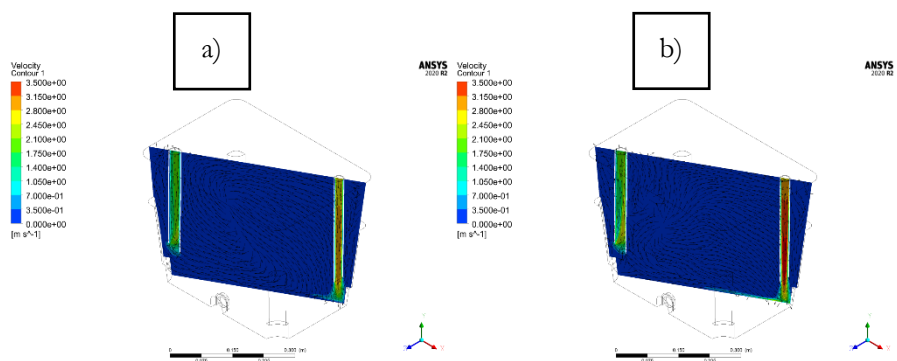
Figure 4: Velocity contour with normalized velocity vector field;
a) k-ε model, b) k-ω SST model.

Significant differences are seen in comparison of predicted wall shear strain rate, shown in Figure 5. Both models predict the highest values of shear strain rate on the bottom wall in the corner underneath the oil tank intake pipe, however $k-\varepsilon$ model predicts lower values compared to k-ω SST model. Although general features of the fluid flow were recognized to be similar for both turbulent models, a more detailed presentation is shown in Figure 6, where velocity magnitude is plotted along the height of the tank in the centre of the tank. From these velocity profiles it is apparent that k-ω SST model predicts different velocity profile compared to k-ε model, particularly higher velocity gradient on the bottom and top wall is observed in the case of k-ω SST model.

It should be noted that the difference in velocity profile could arise as a consequence of vastly different mesh densities in the bulk of the flow as well as near the wall, resulting in corresponding difference in flow solution resolution.
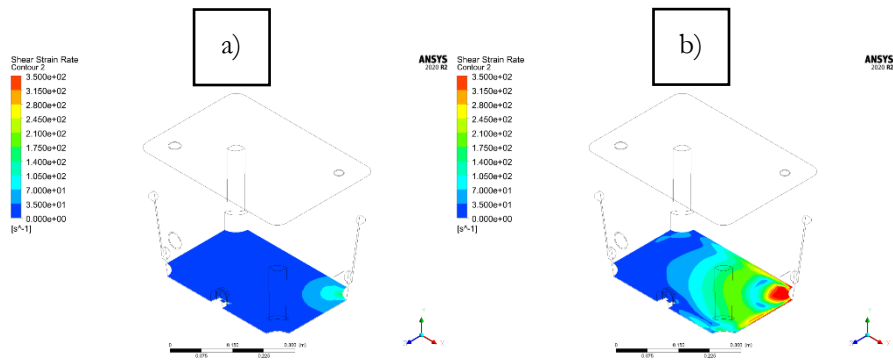
Figure 5: Shear strain rate on the bottom wall of the tank;
a) *k-ε* model, b) *k-ω* SST model.
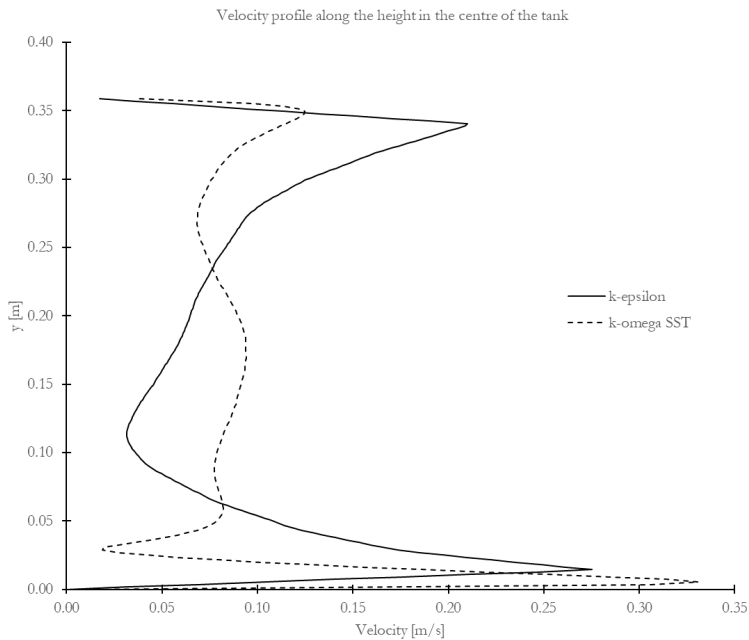
Figure 9: Vertical velocity profiles in the centre of the tank for both turbulent models under consideration.

6   Discussion

Both turbulence models gave similar flow field prediction. In the case of k-ω SST model higher shear strain rates were calculated, which would indicate more intensive energy dissipation. It would follow then that due to higher flow disturbance bubbles and particles would take longer to rise or to settle.

To validate the results and determine, which model is more appropriate comparison to experiment should be made. An interesting research avenue would be also to include thermal effects on predicted flow, particularly in combination with temperature dependent oil viscosity.

At the end it should be noted that for different flow rates or oil viscosity, the flow regime could become laminar, rendering turbulence modelling unnecessary.

References

[1]   Škerget, L. (1994). Mehanika tekočin. Tehniška fakulteta v Mariboru, Univerza v Mariboru in Fakulteta za strojništvo v Ljubljani, Univerza v Ljubljani.
[2]   ANSYS CFX Solver-Theory Guide (2020). ANSYS, Inc., 275 Technology Drive Canonsburg,PA 15317.
[3]   Cesar, J. (2020). Numerical Analysis of Flow in the Small Hydraulic Tank WN-LC-63-1RO. Bachelor thesis, Faculty of Mechanical Engineering, University of Maribor.
[4]   Lovrec, D. (2018). Fizikalno ozadje delovanja hidravličnih sistemov, Univerza v Mariboru, Fakulteta za strojništvo.

University of Maribor Press

Identification of root cause based on simulation approach

ANŽE ČELIK, MATJAŽ RUPNIK & MARKO ŽUST

Abstract The paper shows and explains customer claim regarding improper functionality of hydraulic brake valve integrated into harvester machine. Further, the paper also presents simulation-based approach to understand and solve the issue. In the first step, fully detailed one-dimensional (1D) lumped model has been made in order to reproduce customer issue. Here, it is essentially to mention that (simplified) customer environment/machine was also part of detailed 1D numerical model – customer engagement in root-cause analysis is important. Thanks to detailed simulation model, deep understanding of the key parameters that affect the machine malfunction was possible in the second step. Model allows performing sensitivity study on key parameters with high fidelity. Lastly, based on detected key parameters, harvester brake valve has been updated/redesigned and sent to customer for final validation. Customer satisfaction along with short and effective response time of Poclain development team convert challenge situation to success.

Keywords: • harvester • brake valve • numerical analysis • accumulator charging sequence • cut-in • 6. cut-out •

CORRESPONDENCE ADDRESS: Anže Čelik, Poclain Hydraulics d.o.o., Industrijska ulica 2, 4226 Žiri, Slovenia, anze.celik@poclain.com. Matjaž Rupnik, Poclain Hydraulics d.o.o., Industrijska ulica 2, 4226 Žiri, Slovenia, matjaz.rupnik@poclain.com. Marko Žust, Poclain Hydraulics d.o.o., Industrijska ulica 2, 4226 Žiri, Slovenia, marko.zust@poclain.com.

1   Introduction

Harvesters are self-propelled cutting machines (1). They are able to both fell and process stems. Wheeled or tracked (2), they feature a cutting head (3) that fells, delimbs and bucks trees to specific lengths. Harvesters also have a front or rear cab (4), which is either fixed or rotating. Attached booms may be telescoping (5). [8] A forest harvester is typically employed together with a forwarder that hauls the logs to a roadside landing [3]. Harvester machine works mainly with hydrostatic braking (6). See Figure 1 for details.
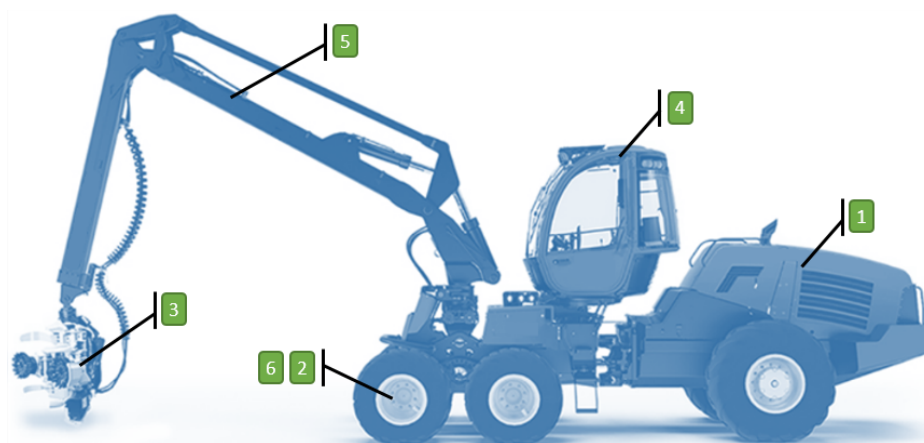
Figure 1: Typical harvester machine.

1.1   On hydraulic braking system

Machines that using such a braking system are usually equipped with spring applied hydraulically released (SAHR) brake, which is activated via parking/emergency brake valve. Hydraulic applied spring release (HASR) brake is activated when operator presses brake pedal. Service brake (HASR) can be also activated by master cylinder.

Typical hydraulic brake system consists of components, shown on Figure 2.
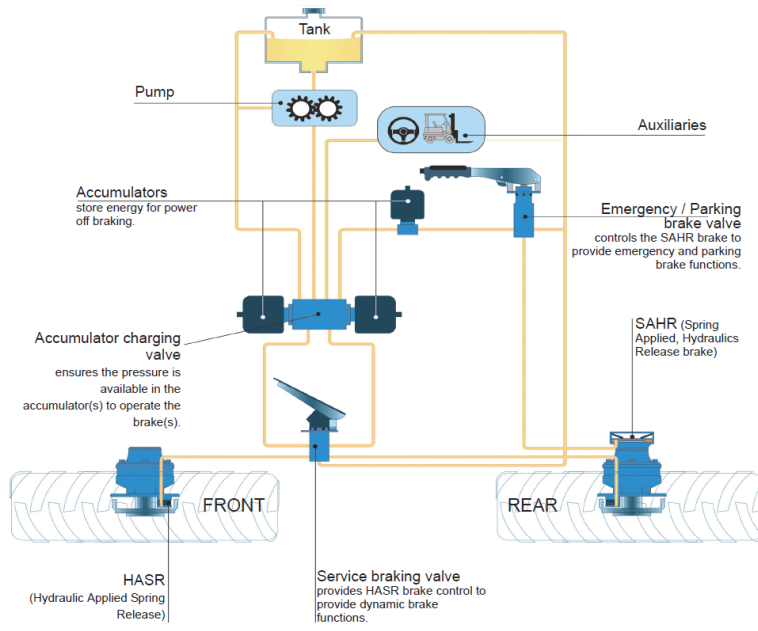
Figure 2: Hydraulic brake system.

1.1.1 Accumulator charging valve

Accumulator charging valve (ACV) charges the accumulators in a braking circuit (i.e. single or dual circuit) and maintains their pressure while supplying an auxiliary circuit (Figure 3). It consists of different parts: divider spool (1), cut-in/out spool (2), poppet isolating valve (3) or ball isolating valve (4).
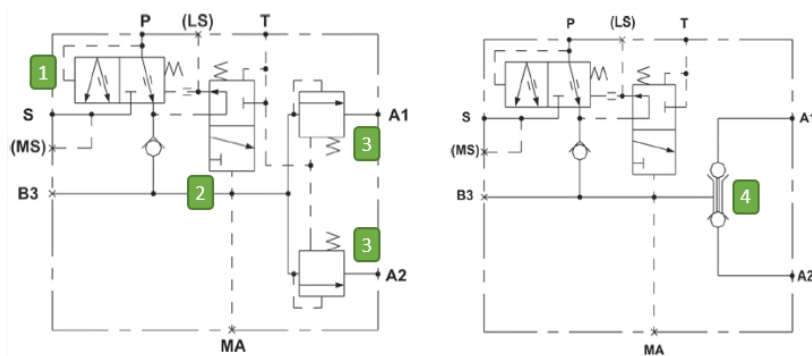
Figure 3: Hydraulic circuits of VB-200: with PRV (left) and IBV (right).

1.1.2   Meaning of underlap

In hydraulics, the parameter underlap (in its general meaning) is used to adjust the initial position of the spool. Figure 4 shows a positive and a negative underlap at zero displacement. Applying the positive value (in Amesim terminology called underlap), there will be a leakage in the central position. With the negative value of underlap (called overlap), there will be a dead-band effect.
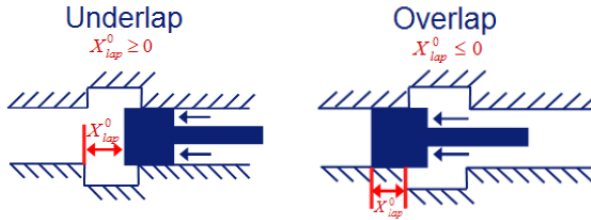
Figure 4: Graphical representation of underlap.

1.1.3   Service brake valve

Service brake valve (Figure 5) is a mechanically controlled, three-way, graduated release double pressure reducing valve. Single (i.e. VB3-010) or double (i.e. VB3-020) service brake valve provides precisely controlled output pressures (at F1 and/or F2) proportional to the pedal stroke and therefore to the force applied to the pedal. This provides the feeling of braking. In a braking circuit, VB3-010/020 is usually associated with VB-100/200 accumulator charging valve.
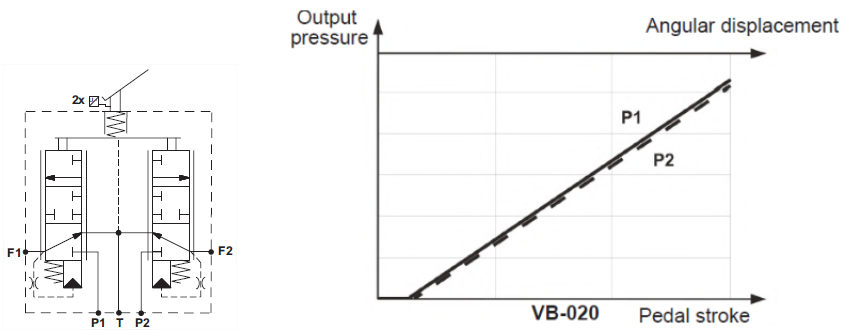
Figure 5: Hydraulic circuit of VB3-020 (left) and characteristic curve (right).

1.2 On harvester braking system

In general, harvester braking valve consists of accumulator charging valve (e.g. VB-200) as well as of service brake valve (VB-020), combined into single (i.e. compact) solution VB-220 (Figure 6). The modular approach of brake valve components enables several different design solutions.
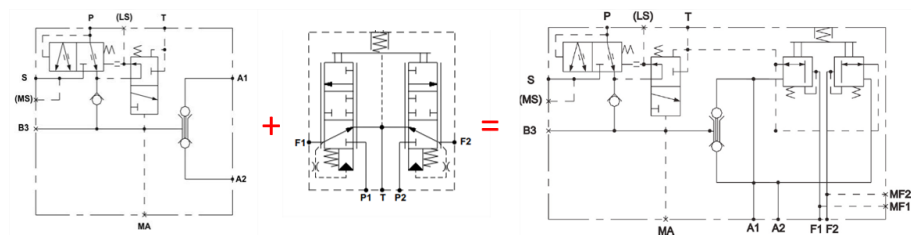
Figure 6: General schematic of VB-220 brake valve.

Actually, according to customer requirements, standard ACV valve (VB-200) and service brake valve (VB3-020) have been modified (Figure 7). Consequently, working principles of modified VB3-220 is a bit different compare to the catalogue one. One of the main difference is that harvester brake system has load-sensing pump (8) and port X is supplied by pressure upstream the divider spool (1). This could be seen on Figure 7.
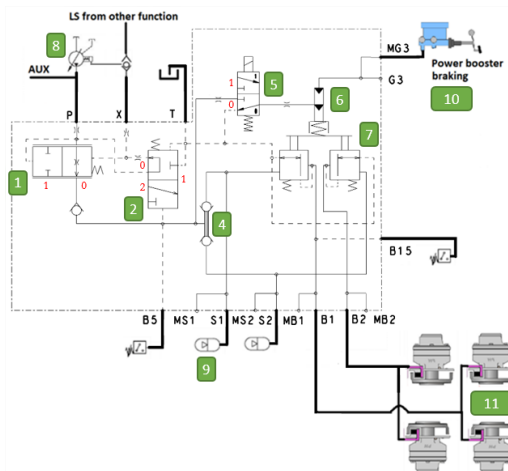
Figure 7: Harvester brake valve

Modified service brake valve (7) is piloted in two ways: either hydraulically (contrary to the standard version, which is mechanically piloted) by the special pilot valve (6), supplied by the accumulator pressure via directional control valve (5) in position 1; either hydraulically thanks to a boosted brake valve (10).

In case, that directional control valve (5) is set in position 1, maximal braking pressure is applied to HASR brake (11). Contrary, boosted brake (10) allows to gradually increasing braking pressure – proportionally to pedal stroke and therefore proportionally to the force applied to pedal.

1.2.1   Basic functionality of cut-in/out spool

Referring to Figure 7, accumulator charging sequence is performed if cut-in/out spool (2) is in initial position 0 and consequently divider spool (1) is in its initial position 0 as well. LS pump (8), which is controlled via supply on port X, charges the system. When maximal charging pressure is achieved, cut-in/out spool (2) shifts to position 2, which allows to release back pressure on divider spool (1) to T port. The divider spool (1) is then piloted to position 1. Along with cut-in/out spool (2) movement to position 2, link from port P towards port X is disconnected. This state is called "cut-out".

As soon as accumulator pressure decreases below critical value, cut-in/out spool (2) shifts back to its initial position 0 and so the divider spool (1); then, the whole charging procedure is repeated. This state is called "cut-in".
Isolating ball valve (4) assures that damaged braking circuit is isolated and therefore braking of harvester is still possible thanks to the pressure in second accumulator.

2   The scope of investigation

Based on customer feedback, the harvester valve worked according to specifications. However, there are some (random) situations that accumulator charging is not performed or last abnormal time (dozens of seconds).

Typical situation when such a valve malfunction appears is shown on Figure 8. Observing the P curve, issue appears just after 32 s and last up to 76 s (i.e. pressure on P channel increases slowly, which is not accepTable). Then, charging

sequence continues normally (i.e. sudden increase of pressure on P line). It needs to be noted that customer could not define conditions when this malfunction appears. Deep investigation needs to be performed in order to find the root cause of valve malfunctioning.
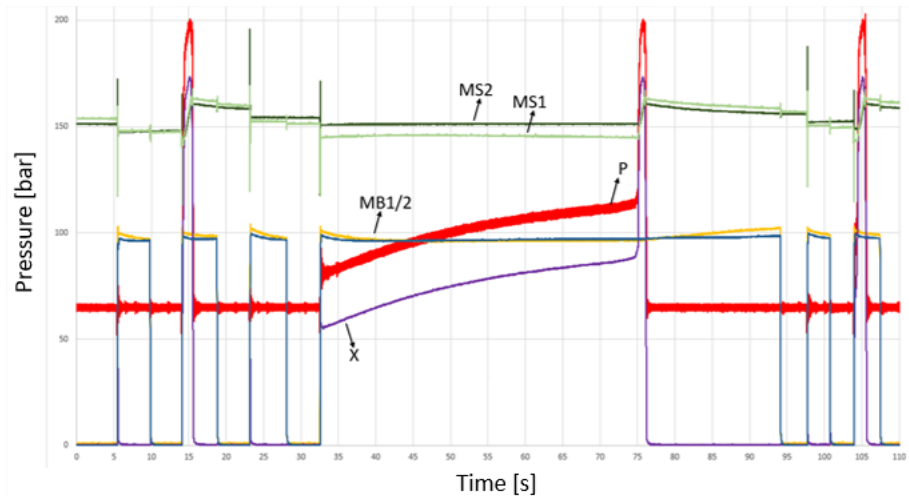
Figure 8: Measurements on customer machine.

The meaning of legend on Figure 8 is as follows: MS1 – accumulator 1, MS2 – accumulator 2, MB1 – brake 1, MB2 – brake 2, X – LS signal, P- pump. Channels refers to pressure [bar].

3   Numerical approach

Numerical evaluation has been performed by the commercial simulation tool Simcenter Amesim (2019.1). The primary goal of simulations is to (better, deeply) understand the model itself; then, it is essentially to reproduce customer issue; further, the focus has been made to discover key (design) parameters that impact the valve behavior - in particular the accumulator charging sequence. Numerical approach serves also as a first (and main) step towards further improvements of brake system which in the end could lead to customer satisfaction.

3.1   1D Amesim model

In the first step, detailed 1D lumped model has been created and shrank to a supercomponent (Figure 9) in order to allow easier manipulation and more user-friendliness for design team.
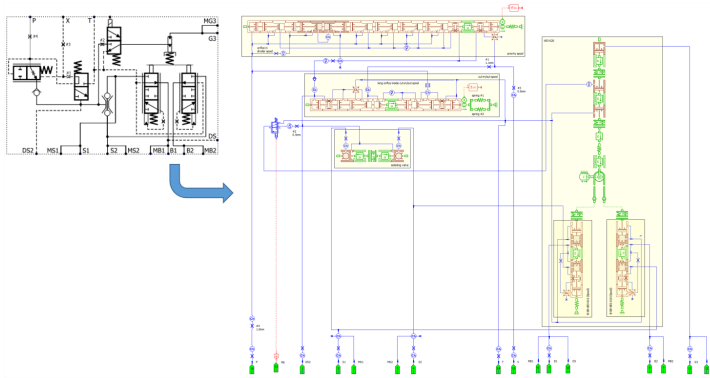
Figure 9: Detailed Amesim model of the VB3-220.

Besides the detailed modeling of problem in hand, it is very important to put the 1D simulation model into realistic environment – this means to prescribe the proper boundary conditions. Figure 10 shows the integration of detailed numerical model into simplified customer-like environment (similar to Figure 7).
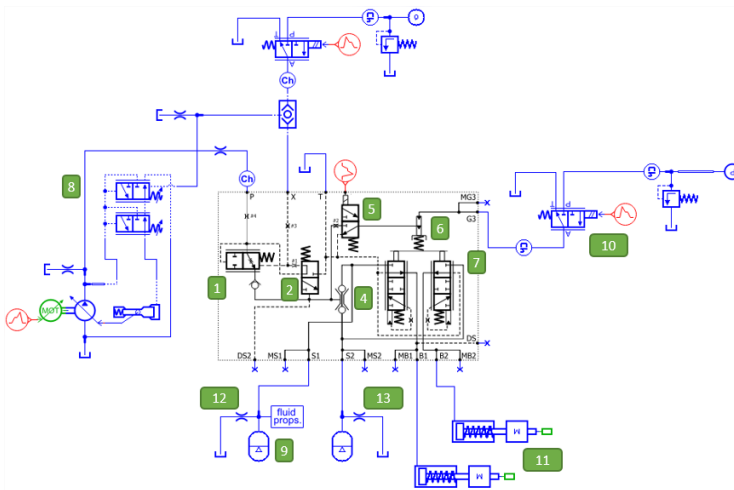
Figure 10: Simplified customer-like environment.

The environment refers to pressure and flow sources (e. g. load-sensing pump, piloting pressure and accumulators), consumers (e. g. brake cylinders) and other auxiliary components (e. g. shuttle valve and orifices).

On this step, it is essentially to have tight relation with customer in order to: understand his environment, get realistic parameters of components and other details needed for simulation purposes. Without customer involvement, it is very difficult to reproduce/evaluate customer machine behavior solely based on component-level simulation.

The initial numerical model is (usually) parameterized according to the nominal parameters. In this particular case, the initial model works according to customer specifications – no issue detected.

3.1.1 Basic model understanding and consistency

Basic consistency of numerical model has been checked in order to verify that the model was built correctly and that parameters were prescribed appropriately. Here, several different scenarios have been tested. Only few of them are explained below.

One of the most fundamental characteristic is flow rate toward accumulators (Figure 11). It can be seen that (in this particular case) maximal flow is approx. 7 l/min (on P port) and drop down to zero when accumulators are full.
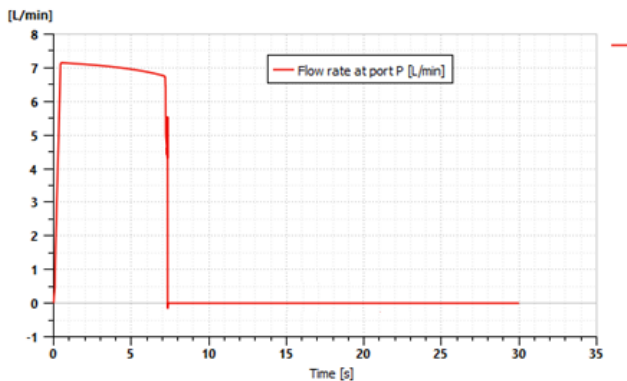
Figure 11: Flow rate on P.

Another important characteristic is pressure on accumulators (Figure 12). Initially there is a pre-charge pressure on accumulators (approx. 55 bar). Then, gradual increase of pressure could be seen up to 160 bar (from zero to approx. 7th second). Maximal charging pressure is defined by spring(s) of cut-in/out spool.
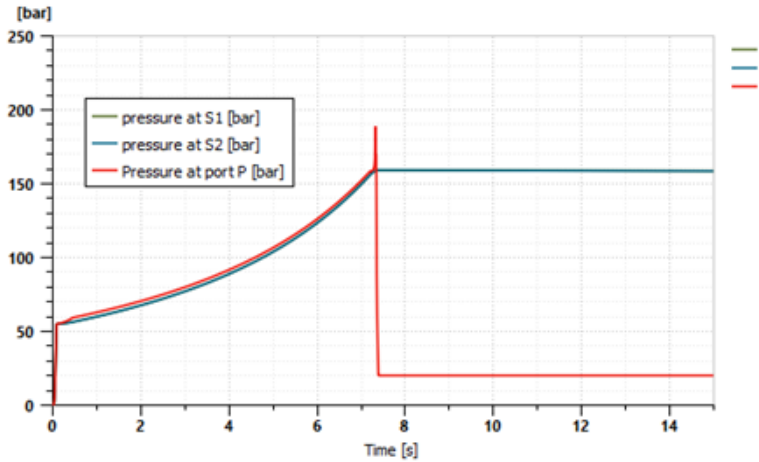
Figure 12: Pressure curves.

3.1.2   Accumulator charging sequence

Accumulator charging and discharging sequences are depicted on Figure 13.
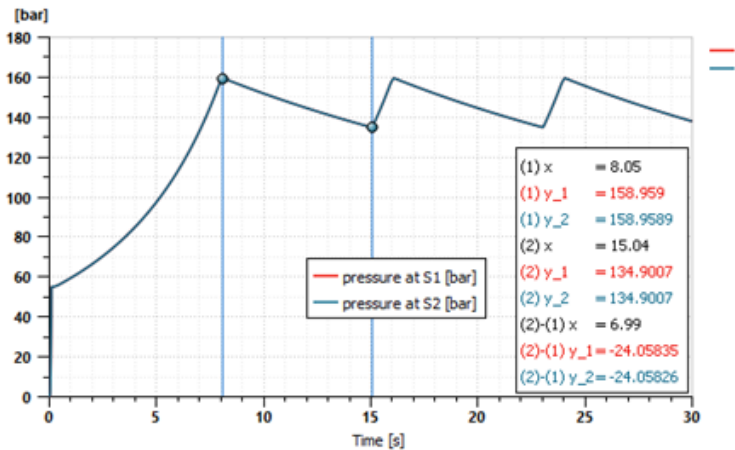
Figure 13: Accumulator filling sequences.

In order to speed up the discharging sequences, orifices (12) and (13) on Figure 10 are set to small value – which enables to simulate leakage flow out of accumulators. In reality, discharging appears due to the leakage on VB3-010/020 as well as on pressure relief valve or isolating ball valve (Figure 3) and last much longer time (from minutes to hours).

3.2 Sensitivity analyses of key parameters

Further, deeper investigation has been performed in order to detect main influential parameters on accumulator charging issue (i. e. for cut-in and cut-out states).

Note that for the purposes of decreasing computational effort, several simplifications have been introduced into the detailed model, without the cost of accuracy (e. g. complex sub-systems have been replaced by equivalent orifices/volumes or taken as simplified representation – mass, spring, damper – from software hydraulic library).

Based on extensive sensitivity study, it has been found out that main influential parameters are cut-in/out spool underlap (i. e. on metering edge from P to X and metering edge from X to T), as seen on Figure 14 and cut-in/out spool leakage (due to radial gap and spool eccentricity).
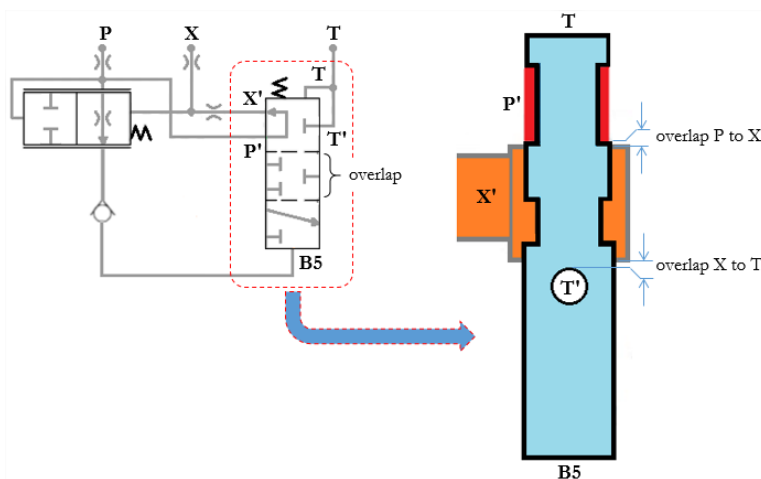
Figure 14: Cut-in/out spool symbol – explained.

By specific set of influential parameters, it was possible to reproduce accumulator charging issue (Figure 15). The cut-in and cut-out issues are clearly observable. While cut-in/out spool with given underlap and given diameter is relatively easy to produce and control, it is not true for spool eccentricity. It depends on several parameters (on spool and housing) and predicting its effect by the simulation tool (or analytical calculation) is the only feasible approach.

Along with this study, some other improvements have been proposed in order to make system more stable as well as to reduce overall pressure loss in the harvester brake valve.
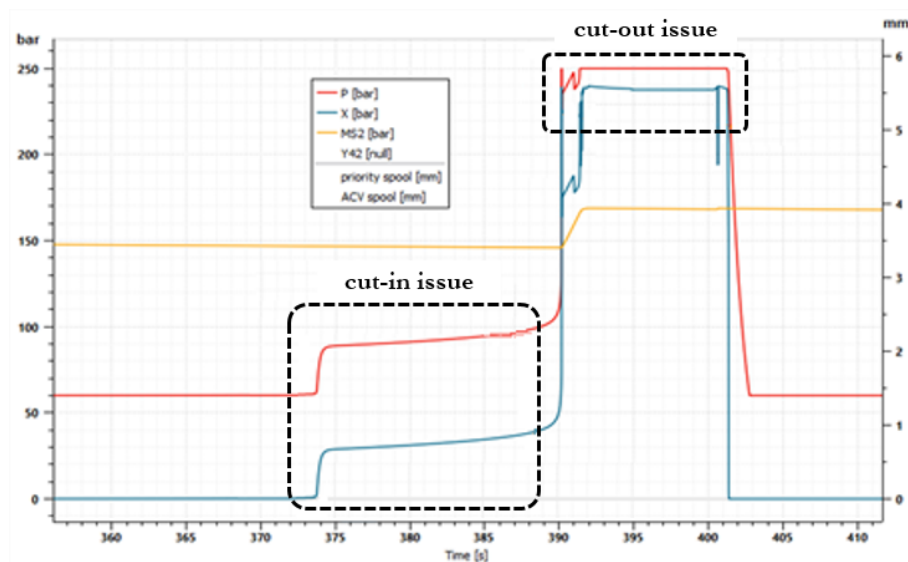
Figure 15: Reproducing customer issue.

4   Experimental approach

The harvester brake valve (VB3-220) has been developed, manufactured and tested internally by Poclain. No valve malfunction has been detected so far (Figure 16).
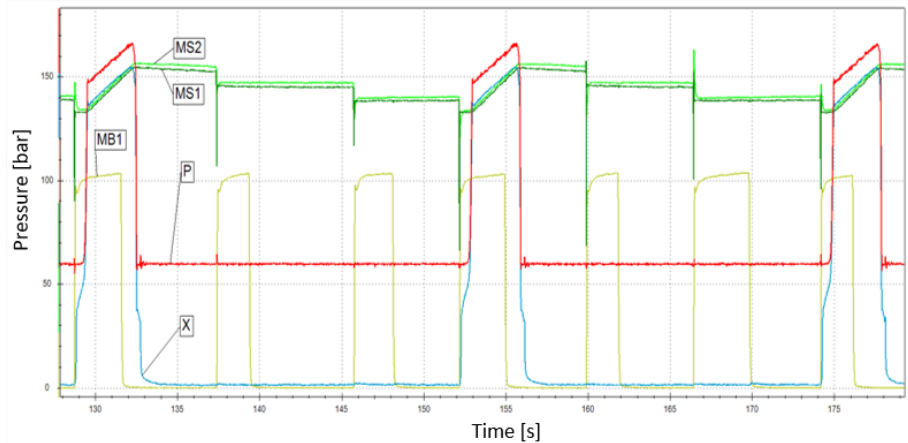
Figure 16: Initial measurements from the laboratory.

Then, the valve has been sent to customer for final evaluation and validation. As already explained, customer claimed that there were some situations that accumulator charging sequence did not work properly. The harvester valve has been recalled to Poclain test lab in order to try to reproduce the issue and to define conditions for the valve malfunction.

4.1   Root cause analysis

Although extensive experimental investigations have been performed, it was not possible to reproduce the issue in the lab. This was somehow expected, because the customer system (i.e. harvester machine) is much different compare to the simplified system in the lab (e.g. different pump, different piping – material stiffness/length/diameter, different braking cylinders etc.).

For that sake, numerical approach was the only solution to find the root cause. As explained in chapter 3, numerical model has been tested under different boundary conditions, different design parameters of valve components etc. Fully relying on the numerical model (which indeed reproduce customer issue) and simulation-based solution, new cut-in/out spools with different overlaps have been machined and then tested in the lab (Figure 17).
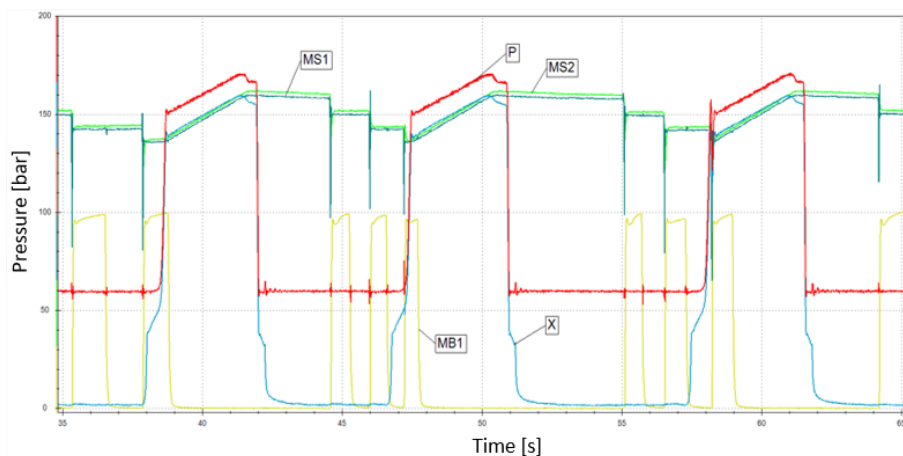
Figure 17: Additional measurements from the laboratory.

Despite that numerical analysis was able to reproduce customer issue and further proposed new spool design, additional in-lab tests of the harvester valve did not show (almost) any difference compare to initial measurements (comparing Figure 16 and Figure 17, some minor differences could be observed only on P curve). Note that shorter charging cycle on Figure 17 is due to shorter/more frequent actuation of working brake (pos. 5 on Figure 7).

For that sake, the only solution to confirm acceptance of new spool was to send the valve directly to customer. He performed several additional tests but the charging issue did not appears anymore (charging pressure raise up quickly). He treats valve as accepTable.

The meaning of legend on Figure 17 and Figure 18 is as follows: P – pump, MS1 – accumulator 1, MS2 – accumulator 2, MB1 – brake 1, X – LS signal. Channels refers to pressure [bar].
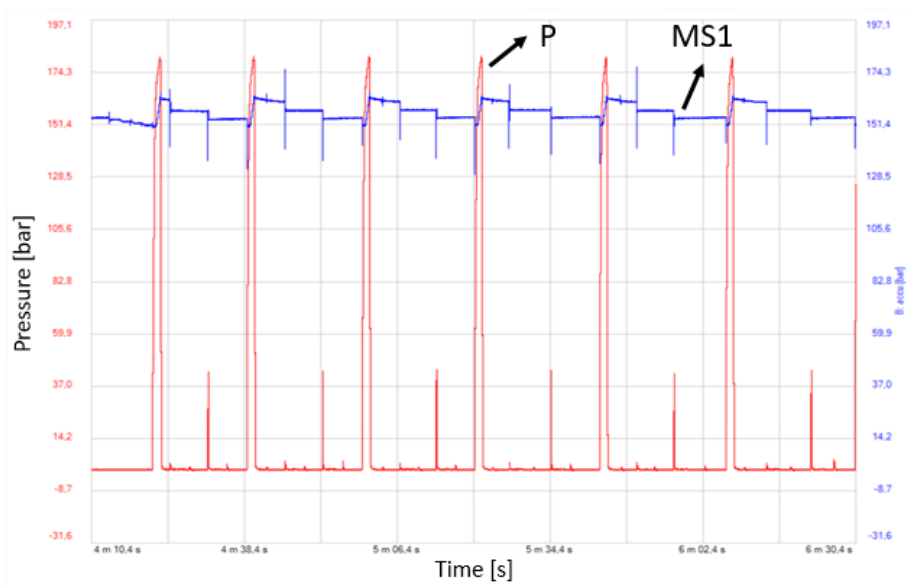
Figure 18: Additional measurements on customer machine.

5   Conclusion

The main goal of investigation is to find a root cause for harvester valve malfunction and to deploy better design solution. This was possible thanks to numerical approach (I .e. high fidelity numerical model) and customer proactivity.

In the numerical approach, in the first step, detailed 1D lumped model has been created. Preliminary simulations confirmed that model is fully functional and can be used for further investigations. The latter show that cut-in/out spool underlap and cut-in/out spool leakage are the main influential parameters that affect charging issue. Thanks to additional sensitivity analyses, it was possible to define suiTable set of those parameters that should prevent valve malfunction.

The numerical approach was followed by an experimental approach .Due to the system complexity and limitation of laboratory equipment (not possible to setup customer-like environment), charging issue was not reproduced neither it was possible to evaluate and validate new design proposals. Thanks to tests performed directly on harvester machine, new spool have been successfully tested and solution confirmed by the customer himself.

References

[1]   Poclain Hydraulics training center (various internal literature)
[2]   Simcenter Amesim Help, rev. 2019.1
[3]   https://www.poclain-hydraulics.com/en/Overview/forestry; last visited on 25.8.2021
[4]   https://www.poclain-hydraulics.com/en/products/valves/service-brake/vb3-020. (visited on 25.8.2021)
[5]   https://www.poclain-hydraulics.com/en/products/valves/accumulator-charging-valves/vb-200-4. (visited on 25.8.2021)
[6]   https://www.poclain-hydraulics.com/en/products/valves/service-brake-accumulator-charging-valves/vb-220-4. (visited on 25.8.2021)
[7]   https://en.wikipedia.org/wiki/Harvester_(forestry). (visited on 24.8.2021)
[8]   https://www.forestryequipmentguide.com/article/43277-overview-of-forestry-equipment. (visited on 24.8.2021)

University of Maribor Press

Research of the influence of the operating parameters of a mobile lift on the oscillatory processes occurring during the work operations

IGOR KYRYCHENKO, OLEKSANDR REZNIKOV, DMYTRO KLETS,
ANTON KHOLODOV, PAVLO YEHOROV &
OLEKSANDRA OLIEINIKOVA

Abstract The article provides an analysis of the results of an experimental study of oscillatory processes occurring in mobile lifts with working platforms (MLWP) during the working operations. According to the developed research methodology, the results of measurements of acceleration along the horizontal and vertical axes of the machine at the point of articulation of the boom and at the point of attachment of the working platform to the boom were obtained and analysed. The analysis of the obtained oscillograms indicates that the greatest oscillations occur at the point of attachment of the working platform to the boom along the vertical axis. Accordingly, a detailed analysis of the influence of the operating parameters of the mobile lift on the oscillatory processes occurring during the operation of the machine at the point of attachment of the working platform to the boom along the vertical axis was carried out.

Keywords: • mobile lift • operating parameters • process • hoist • vibration •

CORRESPONDENCE ADDRESS: Kharkiv National Automobile and Highway University, Faculty of mechanical engineering, Yaroslava Mudrogo St, 25, Kharkiv, 61002, Ukraine, e-mail Igor Kyrychenko igk160450@gmail.com, Oleksandr Reznikov ssr.sdm@gmail.com, Dmytro Klets, d.m.klets@gmail.com, Anton Kholodov antonkholodov23@gmail.com, Pavlo Yehorov antonkholodov23@gmail.com, Oleksandra Olieinikova olexandrachaplygina@gmail.com.

1   Introduction

The mobile lift market is developing dynamically, new types of lifts with excellent designs and better performance are emerging. An overview of popular mobile lifts in the Ukrainian and world markets shows that the most common are boom machines with a lifting capacity of up to 200 kg and a lifting height of up to 20 m [1]. It should be noted that during the operation of such lifts, oscillatory modes are observed during the operation of the machine and after the locking of the working platform. This phenomenon is unaccepTable from the point of view of labor protection for the operator of a mobile lift, in addition, this fact is undesirable, since vibrations of the working platform lead to fatigue cracks in the metal structure of the lift boom. That is why this issue requires additional theoretical understanding and experimental research.

2   Analysis of recent research and publications

In [8], considerable attention is paid to the technology of experimental research of technical systems, the results of an experimental study of the parameters of the motion of an auto-hydraulic lift with a rotary joint are given in [9]. However, insufficient attention is paid to the experimental study of oscillatory processes occurring in the MPP in modern works. This is due to the high cost and complexity of testing.

A large number of studies considering the load simulation modes of mobility lifts with working platforms [6], [7], the theoretical development of the working platform motion control systems hydraulic lift [2], [3], besides a large number of works devoted to the study of the processes occurring in the volume hydraulic drive machines [4-5]. However, a comprehensive study regarding the appearance of oscillatory modes during operation and stopping of the machine is currently lacking.

3   The purpose of the research

The purpose of the research is the experimental study of the influence of the operating parameters of a mobile lift, such as the mass of the load and the angles of inclination of the upper and lower sections of the boom, on the oscillatory processes occurring during operation.

To achieve this goal, the following tasks have been identified:

- to carry out a comparative analysis of the results of the experimental study;
- to determine the degree of influence of the MLWP operating parameters on the oscillatory processes occurring during the work operations;
- based on the obtained data, draw conclusions and make recommendations.

4   Presentation of the main material

According to the developed experimental technique [10], the measurement results were recorded in digital form on an electronic carrier. Then they were presented in the form of oscillograms, on which the accelerations were recorded at the point of attachment of the working platform to the boom and at the point of articulation of the MLWP boom along the x and y axes (Figure 1).

Figure 1: Points of installation of two-dimensional accelerometers.

Figure 2 shows the characteristic oscillograms of the oscillatory processes observed in the hoist during the working operations.
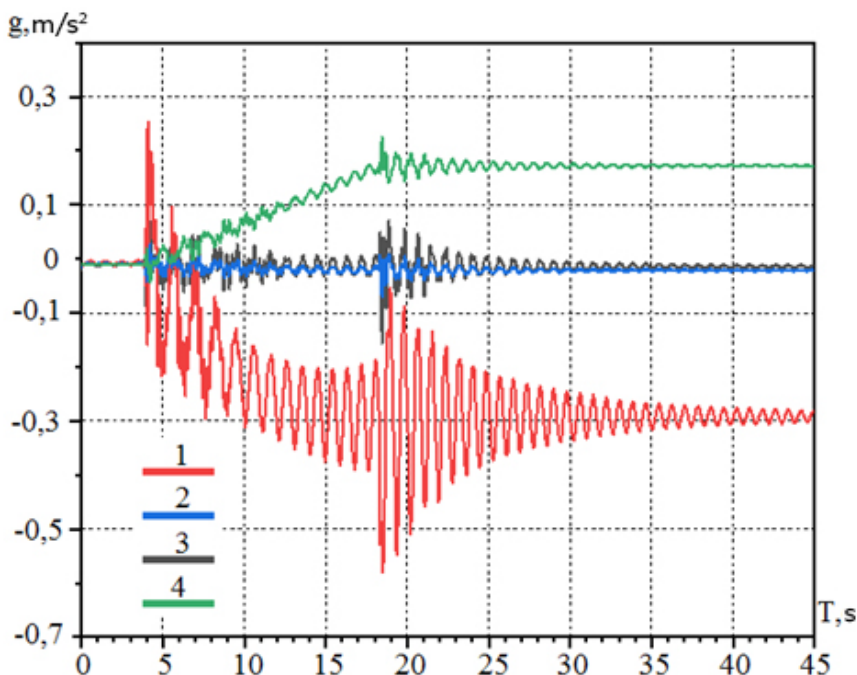
Figure 2: Typical oscillograms of oscillatory processes observed in the hoist during the working operations: 1- acceleration at the attachment point of the working platform to the boom along the Y axis; 2 - acceleration at the point of articulation of the MPC boom along the x axis; 3 - acceleration at the point of articulation of the MLWP boom along the Y axis; 4 - acceleration at the point of attachment of the working platform to the boom along the x axis.

Analysis of the obtained oscillograms of oscillatory processes observed in the hoist during working operations indicates that the greatest oscillations occur at the point of attachment of the working platform to the boom along the B axis. It should be noted that the acceleration at other points of the MLWP boom, in which the experimental data were recorded, is significantly less in amplitude of oscillations. It is advisable to consider the process of changing the accelerations at the attachment point of the working platform to the boom along the B axis in more detail. It is advisable to divide this process into the process of lowering (lifting) the working platform and the process of oscillating the working platform after stopping (Figure 3).
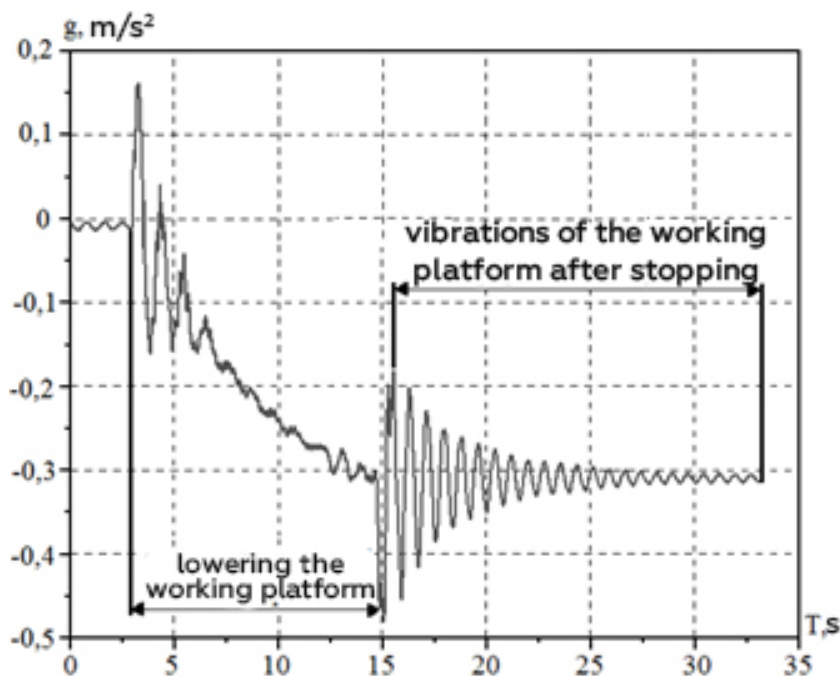
Figure 3: The process of changing accelerations at the attachment point of the working platform to the boom along the Y axis.

To determine the influence of the parameters that changed during the experimental study, on the oscillatory processes during the operation of the lift, let us consider the oscillograms of the change in accelerations at the point of attachment of the working platform to the boom along the B axis.

Figure 4 shows typical oscillograms of acceleration changes for the process of lifting and lowering the working platform. Analysis of the data obtained shows that the amplitude of oscillations of accelerations when lowering the working platform is 35 % greater than when lifting. This fact indicates that the lowering process of the working platform has high dynamic indicator.
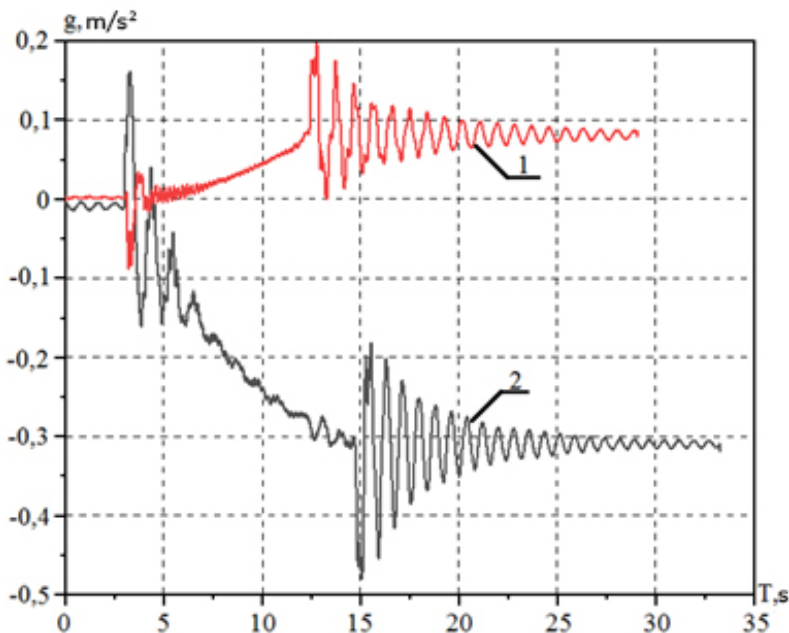
Figure 4: Change of accelerations for the process of lifting and lowering the working platform at the attachment point to the boom along the Y axis: 1- acceleration at the attachment point of the working platform to the boom during lifting; 2 - acceleration at the attachment point of the working platform to the boom when lowering.

After analysing the dynamic indicators of the processes of lifting and lowering, the influence of the mass in the working platform (Figure 5) and the tilt angles of the upper (Figure 6) and lower (Figure 7) boom sections on acceleration at the point of attachment of the working platform to the boom along the Y axis was analysed at lowering.

The result of the analysis of performance indicators for oscillatory processes indicates that with an increase in the working mass from 35 kg (analogous to lifting / lowering the working tool) to 105 kg (lifting / lowering the operator and the working tool), the amplitude of oscillations of the acceleration of the working platform increases by 38 % (Figure 5). At the same time, an increase in the decay time of oscillations after stopping the working platform by 13 seconds (52 %) should be noted.
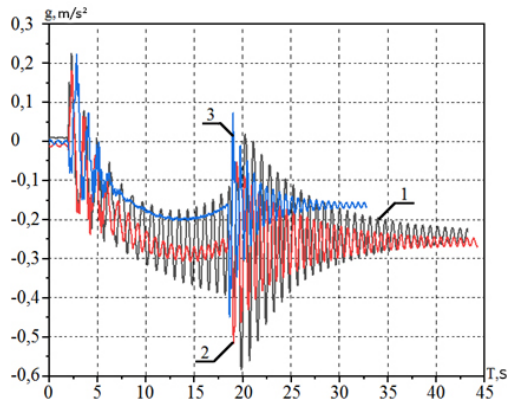
Figure 5: Changes in acceleration when lowering the working platform at the point of attachment to the boom along the Y axis: 1- operating weight 105 kg 2 - operating weight 70 kg 3 - operating weight 35 kg.

Changing the angle of inclination of the upper section of the boom from 45 ° to 15 ° (Fig. 6) with a working weight of 105 kg. leads to an increase in the amplitude of acceleration oscillations at the point of attachment of the working platform to the boom along the Y axis by 20 % and an increase in the decay time of the oscillation process after stopping the working platform by 7 seconds (31 %).
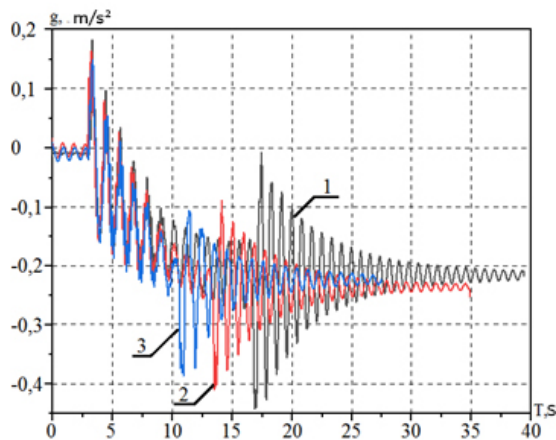
Figure 6: Change in acceleration when lowering the working platform at the point of attachment to the boom along the Y-axis: 1- tilt angle of the upper boom section 15°; 2 - the angle of inclination of the upper section of the boom is 30°; 3 - angle of inclination of the upper section of the boom 45°.

When the angle of inclination of the lower boom section is changed from 15° to 45° (Fig. 7) with a load weight of 105 kg. there is an increase in the amplitude of acceleration oscillations at the point of attachment of the working platform to the boom along the Y axis by 47 %, and the damping time of the oscillation process after stopping the working platform increases by 8 seconds (27 %).
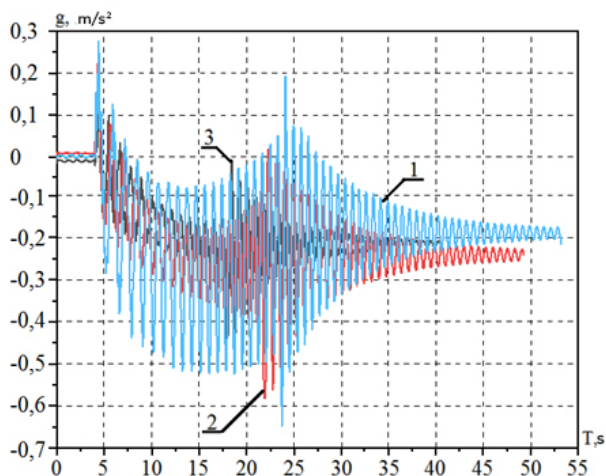
Figure 7: Change in acceleration when lowering the working platform at the point of attachment to the boom along the Y-axis: 1 - tilt angle of the lower boom section 45° 2 - tilt angle of the lower boom section 30°; 3 - the angle of inclination of the lower section of the boom is 15°.

In the process of lifting the lower section of the boom to an angle of inclination of 45° with a load weight of 105 kg (Fig. 7, oscillogram No. 3), unusual fluctuations in the acceleration of the working platform, which have a significant amplitude, are observed. This operating mode can be considered emergency and not recommended for MLWP operators.

The analysis of the oscillatory processes indicates that the greatest amplitude of acceleration oscillations at all modes of the MLWP load is observed at the moment of locking the working platform.

5   Conclusion

According to the specified purpose and objectives of the study, the following conclusions can be drawn:

1. Comparative analysis of the results of the experimental study indicates that the operating parameters of the mobile lift significantly affect the indicators of oscillatory processes, such as the amplitude, period and damping time of oscillations occurring in the machine during operation.

2. The amplitude of oscillations of accelerations when lowering the working platform is 35 % greater than when lifting, with an increase in the working mass from 35 kg to 105 kg, the amplitude of oscillations of the accelerations of the working platform increases by 38 %, the change in the angle of inclination of the upper section of the boom is from 45° to 15° leads to an increase in the amplitude of oscillations by 20%, when the angle of inclination of the lower section of the boom changes from 15° to 45°, the amplitude of oscillations increases by 47 %.

3. During the operation of the lower section, with the maximum working mass of the load, equivalent to the mass of the working and working tools, an emergency mode of operation is observed, which is not desirable.

References

[1]   Anali`z ri`vnya tekhni`chnogo rozvitku mobi`l`nikh pi`djomniki`v i`z robochimi platformami / [I`.G. Kirichenko, O.O. Ryezni`kov. Yu.V. Rukavishni`kov ta i`n.] // Vi`snik KhNADU. – 2021. – Vip. 92. – S. 149-153

[2]   Barkov A.Yu. Rezhimy` nagruzheniya stroitel`ny`kh gruzopassazhirskikh pod`emnikov. Interstrojmekh-2001 / A.Yu. Barkov, M.A. Stepanov // Trudy` Mezhdunarodnoj nauchno-tekhnicheskoj konferenczii. – Sankt-Peterburg : Izdatel`stvo SPbGTU, 2001g. – S. 14-18

[3]   Barkov A.Yu. Analiz rezhimov nagruzheniya privodov stroitel`ny`kh pod`emnikov. Interstrojmekh-2002 / A.Yu. Barkov, M.A. Stepanov // Materialy` Mezhdunarodnoj nauchno-tekhnicheskoj konferenczii., Mogilev : Izdatel`stvo MGTU, 2002g. – S.391-394.

[4]   Tekhnologi`ya naukovikh dosli`dzhen` i` tekhni`chnoyi tvorchosti` / [E.V. Gavrilov, M.F. Dmitrichenko, V.K. Dolya ta i`n.] // Sistemologi`ya na transporti` : kniga 2. – K. : Znannya Ukrayini, 2005. – 315 s

[5]   Gurko O. G. Dosli`dzhennya parametri`v rukhu avtogi`dropi`di`jmacha z obertal`nimi zchlenuvannyami / O. G. Gurko, Yu. O. Dolya // Novi` materi`ali i` tekhnologi`yi v metalurgi`yi ta mashinobuduvanni`. – 2016. – #2. – S. 121-127

[6]   Matematicheskoe modelirovanie proczessov v sisteme gidroprivoda lesny`kh manipulyatorov / [P.I. Popikov, P.I. Titov, A.A. Sidorov i dr.] // Nauchny`j zhurnal KubGAU. – 2011. – # 69(5) – S. 1-11

[7]   Ob`yomny`j gidroprivod v mobil`ny`kh pod`yomnikakh s rabochimi platformami : monografiya / [I.G. Kirichenko, G.A. Avrunin, V.B. Samorodov i dr.]. – Khar`kov : KhNADU, 2018. – 295 s

[8]   Shherbakov V.S. Avtomatizacziya modelirovaniya optimal`noj traektorii dvizheniya rabochego organa stroitel`nogo manipulyatora : monografiya / V.S. Shherbakov, I.A. Rebrova, M.S. Kory`tov. – Omsk : SibADI, 2009. – 106 s

[9]   Gurko A. G. Razrabotka sistemy` upravleniya dvizheniem avtogidropod`emnika / A. G. Gurko, I. G. Kirichenko // Budi`vnicztvo. Materi`aloznavstvo. Mashinobuduvannya. Seri`ya : Pi`djomno-transportni`, budi`vel`ni` i` dorozhni` mashini i` obladnannya. – 2014. – S. 210-220

Design and control of mechatronic systems with pneumatic and hydraulic drive

ŽELJKO ŠITUM, JURAJ BENIĆ, KLARA PEJIĆ, MARKO MIROSLAV BAČA,
IVAN RADIĆ & DOMINIK SEMREN

Abstract This paper presents four handmade laboratory systems with pneumatic and hydraulic drive. The article first presents an example of a pneumatic motor speed control using a proportional directional control valve. Then the paper presents the design and control of a test device with pneumatic drive for determining the dynamic strength of materials, on which the fracture mechanics of materials due to the action of dynamic stress can be experimentally demonstrated and the resistance of materials to cyclic stress can be analyzed. The article then describes the design, construction and control of a pneumatically driven system for sorting products marked with a bar code using a vision system. The final section of the article describes an experimental setup for precise position control of a hydraulic cylinder using 2/2 cartridge valves, which can clearly demonstrate the application possibilities of these valves in industrial plants and mobile systems.

Keywords: • speed control • dynamic strength of materials • product sorting • cartridge valves • position control •

CORRESPONDENCE ADDRESS: Željko Šitum, University of Zagreb, Faculty of Mechanical Engineering and Naval Architecture, Ivana Lučića 5, 10000 Zagreb, Croatia, e-mail: zeljko.situm@fsb.hr. Juraj Benić, University of Zagreb, Faculty of Mechanical Engineering and Naval Architecture, Ivana Lučića 5, 10000 Zagreb, Croatia, e-mail: jbenic@fsb.hr. Klara Pejić, Marko Miroslav Bača, Ivan Radić & Dominik Semren, students at the University of Zagreb, Faculty of Mechanical Engineering and Naval Architecture, Ivana Lučića 5, 10000 Zagreb, Croatia, email: kp204938@stud.fsb.hr; mb213853@stud.fsb.hr; ir210937@stud.fsb.hr; ds199138@stud.fsb.hr.

1   Introduction

We are witnessing rapid technological growth, advances in digital technology, and concepts such as the Internet of Things, Industry 4.0, vision systems, 5G networks or artificial intelligence are becoming the subject of scientific research and practical applications in various fields [1]. However, for now the mentioned advanced technologies are rarely associated with fluid power systems. There are even opinions that in today's digital era, pneumatics and hydraulics as "traditional" techniques do not have the potential to adapt to new solutions based on information technologies. The question is: can pneumatic and hydraulic systems preserve their current wide applicability also in the future, in relation to the radical demands of digital technologies and energy efficiency? Many designers and constructors of technical solutions consider pneumatic and hydraulic components as energy inefficient systems, and manufacturers of industrial equipment in the field of fluid power technology focus on ensuring the basic tasks of the system by trying to eliminate the shortcomings of these systems. The directions of development of modern fluid power systems are towards greater involvement of microprocessors, sensors and communication components. Mechatronic engineering, which includes mechanical, electrical and information technologies, represents a way to modernize traditional fields such as hydraulic and pneumatic systems and enables the digital transformation of these established disciplines as well as new areas of application [2]. The realization of high performance systems in modern industrial applications requires a symbiosis of mechanical systems with technologies such as microelectronics, sensorics, and sophisticated control methods in order to achieve optimal system behaviour. In many applications, pneumatic drives can be a cheaper alternative to electric and hydraulic systems, especially for light loads [3]. Unfortunately, position, speed or force control of pneumatic and hydraulic actuators are often quite complex due to existing nonlinear effects in fluid power systems, variations of load and process parameters during operation etc. Thus, increased attention is being paid to the development of better working elements of the system, as well as to the improvement of control strategies. By introducing the electronic data transfer and signal processing, the application of advanced control techniques to fluid power drives and the application of these systems in industrial and mobile plants based on the principles of modern digital technology is enabled. Thus, the range of potential applications of pneumatic and hydraulic systems is extended to the field of flexible modules that are networked in complex production systems,

Ž. Šitum, J. Benić, K. Pejić, M. M. Bača, I. Radić & D. Semren: Design and control of
mechatronic systems with pneumatic and hydraulic drive

181

robotic systems, modern systems for the production of renewable energy sources, etc. [4]. This paper presents several self-made experimental systems actuated by pneumatic and hydraulic drives, which have been designed and manufactured as test models within the fields of fluid power systems, mechatronics and feedback control education, based on the application of modern digital technologies.

2 Pneumatic servo system

Rotational motion in many drive systems is most often achieved by using different types of electric motors. However, pneumatic motors also have many positive features that could give them an advantage over electric motors in certain applications [5]. The favorable characteristics of pneumatic actuators such as high specific power, insensitivity to overload and drive failure, safety in explosive environments, high rotational speeds, the possibility of self-cooling, etc. may give preference to the use of pneumatic motors over commonly used electric motors [6]. However, they also have certain disadvantages such as their lower efficiency compared to electric motors, the problem of compressed air supply, the need for an air tank, the existence of noise during operation, etc. Despite certain shortcomings, there are many opportunities to further examine the possibility of using pneumatic actuators in automated industrial plants and mobile systems instead of the use of electrical actuators.

In order to test the advanced methods for speed control of the pneumatic motor in different operating modes, an experimental setup of the pneumatic servo drive was made, which is shown in Figure 1. The pneumatic servo system contains the drive, measuring and control part. The drive part includes the pneumatic vane motor (GAST 2 AM-ARV-92), the proportional valve (FESTO MPYE-5-1/8-HF-010-B), the magnetic coupling (FL-6-S) and two claw couplings. An incremental encoder with 600 ppr is used to measure the rotational speed of the pneumatic motor. The control part of the system consists of a PWM driver (HEYO-24V916PWM) for the magnetic coupling, a control card (NI USB-6001) and a power supply (SPD2460). The components are mounted on holders and connected to an aluminum profiled plate. The electromagnetic clutch has two axes and is located between the pneumatic motor and the incremental encoder, and is connected to them by two claw couplings. The driver (PWM controller) for controlling the magnetic coupling and the signal acquisition card are also attached to the base plate. The

proportional valve is used to control the air flow to the vane pneumatic motor (four-bladed reversible model). The acquisition card receives the measuring signals from the encoder and sends the control signals to the proportional valve. A laptop PC is used as a control device, while the control algorithm and visualization process was realized in the LabView program.
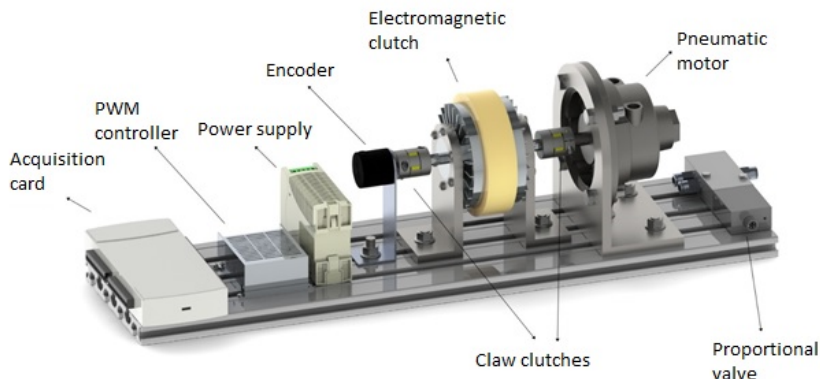
Figure 1: Conceptual design of a pneumatic servo system.

The driver for controlling the magnetic coupling and the proportional valve require a 24 V power supply, while the acquisition card needs a 5 V power supply which it receives from the computer. The encoder is connected to the acquisition card. The electromagnetic powder clutch/brake has a stator part and a rotor part. When electricity is supplied to the clutch, the magnetic field inside the coil begins to fluctuate depending on the ratio of the current intensity. The magnetic field fluctuations affect the viscosity of the magnetic powder between the rotor and the stator which produces friction and braking occurs. When the current is disconnected, centrifugal force presses the powder against the stator. This subsequently releases the rotor, which can be rotated freely again. The pneumatic motor slows down as the load increases. At the same time the torque increases to the point where it corresponds to the load. When the load is reduced, the engine accelerates, and the torque is now reduced to match the load. When the load is increased or decreased, the speed can be regulated by decreasing or increasing the air pressure. The initial engine torque is less than the torque during engine operation. Although this allows the engine to start smoothly without high initial pressure. To start the engine under heavy loads it is necessary to have additional pressure in the air line.

Ž. Šitum, J. Benić, K. Pejić, M. M. Bača, I. Radić & D. Semren: Design and control of mechatronic systems with pneumatic and hydraulic drive

183

To demonstrate the operation of the system, it is necessary to connect the valve to the compressor and the acquisition card to the laptop PC. After the air is released, the motor shaft together with one shaft of the magnetic coupling begins to rotate. By adjusting the PWM driver current to the magnetic coupling the other shaft also begins to rotate. In this way we check whether the set-up is correctly arranged and then the system control can be achieved. The constructed pneumatic servo system is shown in Figure 2.
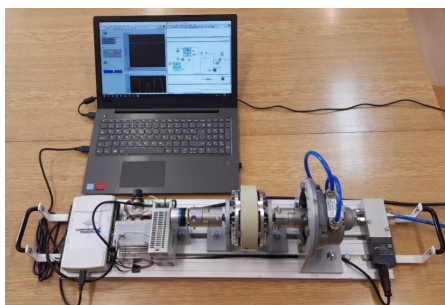
Figure 2: Pneumatic servo system.

2.1 Position and speed control of the pneumatic motor

A standard PID controller was used to control the position and speed of the pneumatic motor, and the control algorithm was performed in the LabView program, shown in Figure 3.
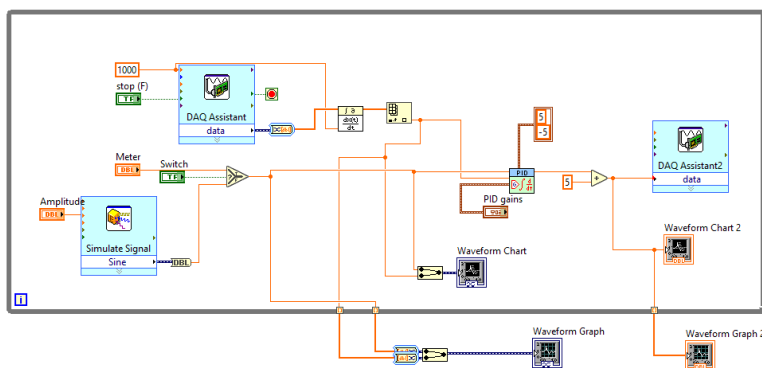
Figure 3: Control algorithm in the graphical program LabVIEW.

Experiments were made for angular position control and speed control of air engines. A PD controller was used for angular position control and a PI controller was used for speed control. In both cases, the sine and step functions are applied as reference signals, but it is also possible to define reference inputs using random points selected on the interaction interface. The parameters of the controller for different operating modes were determined experimentally, and the obtained results are shown in Figure 4.

a) Position control for step and sinusoidal reference signal

b) Speed control for step and sinusoidal reference signal
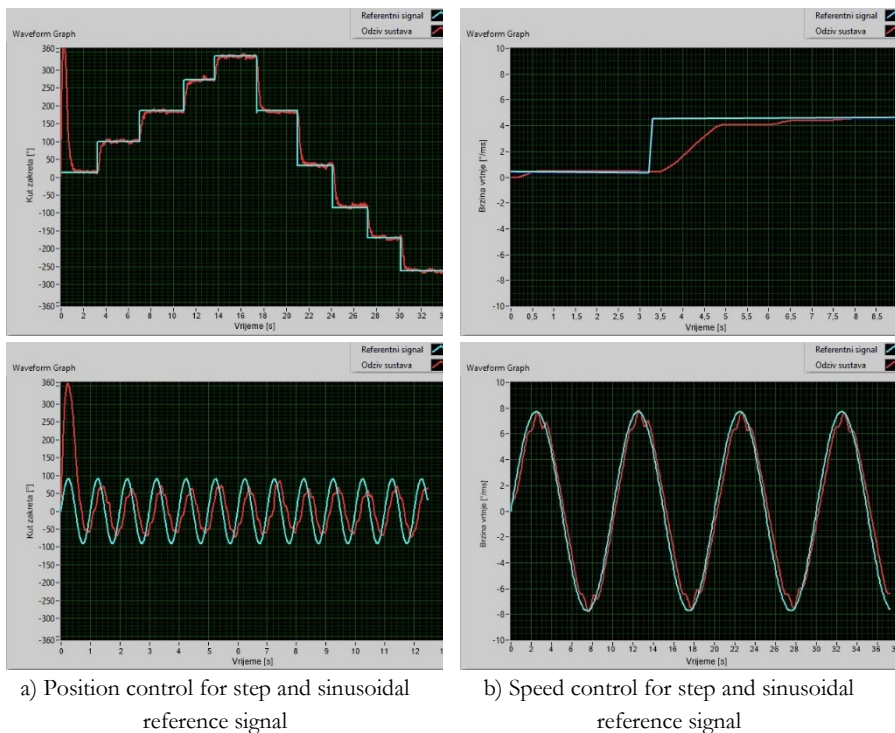
Figure 4: Experimental results for position and speed control.

For angular position control of the motor, a relatively fast system response and good trajectory tracking for the step reference signal can be observed, and slightly lower accuracy for sinusoidal functions. For speed control the response is more accurate and slightly slower for both step and sine reference signal.

Ž. Šitum, J. Benić, K. Pejić, M. M. Bača, I. Radić & D. Semren: Design and control of mechatronic systems with pneumatic and hydraulic drive

185

3   Pneumatic device for testing dynamic strength of materials

In materials science, tests of mechanical properties of different materials under conditions of long-term dynamic action of variable stress have special significance because the results of these tests determine the dimensional calculation of mechanical structures [7]. Understanding the fatigue mechanism is important for considering various technical conditions and this knowledge is essential for the analysis of fatigue properties of an engineering structure [8].

The realization of our own laboratory and educational test device, which serves for experimental demonstration of the fracture mechanics of materials caused by dynamic stress, analysis of the resistance of materials to cyclic stress and the development of cracks due to material fatigue is a valuable achievement in deepening knowledge of materials. An important feature of this test device is the use of pneumatic components to achieve the required dynamic forces and a user interface with a touch screen to set the parameters of the material testing process, while reference and measured force values are displayed on the screen in real time. The construction of the test device is made from standard aluminium profiles due to the high modularity and wide choice of shapes that allow the connection of various profiles using angle joints. The upper horizontal beam is used as a support for the pneumatic cylinder. It is movable along the vertical axis and ensures the required position of the pneumatic actuator. The conceptual design of a pneumatic device for testing dynamic strength of materials is shown in Figure 5.
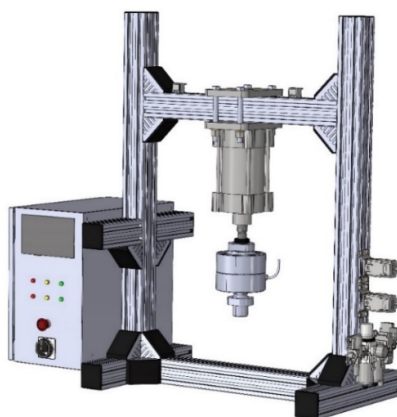
Figure 5: Conceptual design of a device for dynamic testing of materials.

Pneumatic part of the system. In order to achieve low piston speeds with low pressure in the cylinder chambers, a smooth, slow-moving cylinder of the new generation, type SMC C96YDB125-100, was chosen. A proportional pressure regulator is used to control the pressure in the cylinder chamber. The selected model ITV2050-312N3 on the pneumatic side contains 3 connections. The first input is connected to the line from the compressor, the second output from the regulator is connected to the cylinder, and the third output is the line for connecting a silencer. The pressure valve is supplied with a standard industrial voltage of 24V, and the control voltage signal is in the range from 0 to 10 V. When the control signal is applied, the pressure output from the regulator can take a value from 0.005 to 0.9 MPa. A standard FRL group is installed at the inlet of the pneumatic system, which contains a direct operated 3/2 solenoid valve for supplying compressed air into the system.

Electrical part of the system. The control device of the system is a CONTROLLINO MAXI controller, and it was chosen because of the large number of input and output pins, the device contains analogue outputs and has the ability to receive signals from sensors. The digital outputs are galvanically isolated and have a high output voltage of 24V so they can operate at standard industrial voltages. All input-output connectors have ESD protection, which indicates that Controllino device is an industrial computer that combines the advantages of open source and programming methods with standard PLCs. A force sensor is used to measure the applied force on the cylinder piston. The main requirement for the sensor is the ability to measure the force in a compressive and tensile range with high accuracy. The selected sensor type HBM U10 enables precise measurements of accuracy class 00 according to ISO 376, and has a measuring range from 50 N to 10kN. The main features of this sensor are overload protection, TEDS (Transducer Electronic Data Sheet) and long life. For proper operation of the force sensor, a 1-channel amplifier of the same accuracy class, type HBM-BM 40, was also selected. All amplifier settings such as signal filtering options and sampling time can be set via a web browser.

Ž. Šitum, J. Benić, K. Pejić, M. M. Bača, I. Radić & D. Semren: Design and control of mechatronic systems with pneumatic and hydraulic drive

187
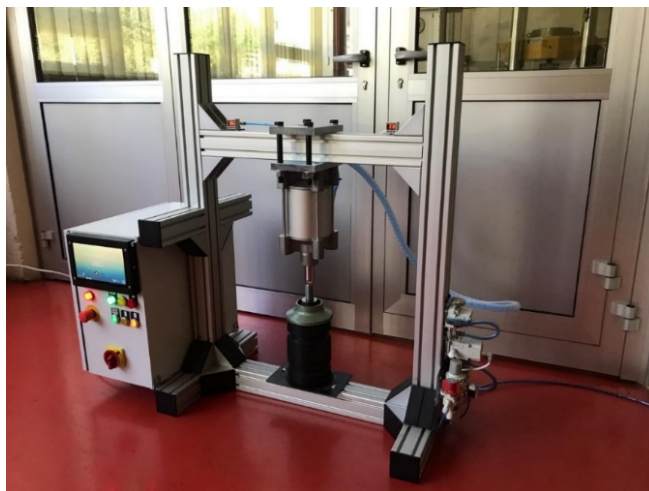
Figure 6: Pneumatic device for testing dynamic strength of materials.

The 9 inches LCD screen is selected for communication between the system and the operator. The screen size is suiTable for simply entering the required parameters of the test process and to display graphs of measured values from the sensor. The HMI system type SK-90DT from 4DSystems enables easy communication and data transfer with the control unit. The programming process is done in the Workshop software from 4Dsystems, while the program uses a combination of a graphical interface and the C programming language. The constructed pneumatic device for testing the dynamic strength of materials is shown in Figure 6.

4   Pneumatic system for products sorting

Transporting products on the conveyor belt and sorting them according to different characteristics is a very common task in automated production lines. The technology of marking and identifying various objects has long been used, and one widespread way of marking products intended for automatic detection is barcode, which can be read using a reader with a photo diode and a decoder, but with the involvement of a human operator. Using a camera to capture items on the conveyor belt and sort according to specific product features, the sorting process could be automated. Therefore, the practical implementation of an educational model using a vision system for sorting products marked with a barcode can be useful in teaching automatic control and vision systems [9].

Through years of research and development, computer vision systems have become more efficient in terms of image perception, detection, and processing [10]. Today they are used in many branches of industry, trade, medicine, and transport. Furthermore, vision systems are increasingly used in security systems, face recognition, fingerprint, and other applications. A barcode is a way of marking a product through a series of dark and light lines. This code is easy and simple to read using a camera or laser, so it is widely utilized in product recognition. Most often the bar code is added to the products after the production process is completed and after the product leaves the production line. Consequently, each product has its own unique code that is easy to read and follow up over a lifetime.

The designed conveyor belt has a drive drum powered by an electric motor, and a driven drum at the other end of the conveyor belt. The gravity tank contains the products with barcode to be sorted. The products are arranged vertically, and at the bottom of the tank a pneumatic cylinder (SMC CJ2B10-60) pushes objects one after another onto the conveyor belt. After one operation is performed, the cylinder rod is retracted, the next product falls into the position of the previously pushed object and the procedure is repeated. The operation of the vision system is based on a camera that reads a 2D barcode. The collected data is sent to the Raspberry Pi2 module Due to compatibility with the control unit, an 8-megapixel Raspberry Pi V2.1 camera from the same manufacturer is used, because the motherboard of the control unit contains the original connector for this camera. In the terminal software of the Raspberry Pi it is necessary to install the SimpleCV module which allows barcode reading and image processing. Another module that must be installed is Zbar which processes barcodes. If the camera is properly installed and if its operation is enabled in the Raspberry Pi software terminal, the bar code is read when the object comes into the camera's detection field. After the camera detects the barcode, that code is saved and compared in the program with the code values from the database. During the testing of the operation of the conveyor belt, the moment of activation of an individual cylinder was determined after the barcode was detected on a certain type of product. This setup can sort three types of products, so two cylinders (SMC CD85F25-160-B) are used to push the product off the belt into separate containers, and a third type of product falls into the container at the end of the belt. Three monostable 4/2 solenoid valves (SMC VQD1121) are used to control the movement of the cylinders. The air pressure at the system inlet is adjusted using the pressure regulator (SMC-AR20-F02H-N).

Ž. Šitum, J. Benić, K. Pejić, M. M. Bača, I. Radić & D. Semren: Design and control of mechatronic systems with pneumatic and hydraulic drive

189

Figure 7: Pneumatic conveyor belt for products sorting.

A support pole is attached to the conveyor belt, which carries the camera and the control unit. The computer power supply is used to operate the conveyor, control unit and relay, while the valves are connected to a separate 24 V power supply. The Python programming language is used to program the control unit. Figure 7. shows the developed pneumatic conveyor belt system for sorting products using a vision system.

5   Position control of a hydraulic cylinder using cartridge valves

Cartridge valves can be used to obtain various functions in the hydraulic circuit which are usually achieved by using traditional valves to control the pressure or flow of the working fluid [11]. By using cartridge valves it is possible to realize cheaper hydraulic systems, which are more compact and require less installation space, they have a shorter switching time than classic solenoid valves, less fluid leakage, less sensitivity to oil contamination, require less assembly time and enable construction of compact hydraulic systems because they are installed in a drilled aluminium block or manifold. In order to use these valves properly, a good understanding of their operation is required. Therefore, the design of a hydraulic servo system that uses cartridge or logic 2/2 valves to achieve precise positioning of the hydraulic cylinder could clearly demonstrate the possibilities of application of these valves in mobile systems and industrial plants. Cartridge valves are usually built into drilled manifold but they can also be available in

individual bodies and currently they play an important role in many fluid power systems across a broad spectrum of industries. Valve cartridges can be thought of as bodyless-valves without an integral housing, until they are inserted into a suiTable housing. There are two types of cartridge valves: screw-in catridges and slip-in catridges. Directional screw-in cartridge 2/2 valves were used to make a functional hydraulic circuit on a realized experimental setup. The use of cartridge valves is common in mobile machines where built-in valves are an integral part of the working hydraulic circuits. In the process of designing machines, there is often a requirement for the compactness of hydraulic systems, so hydraulic integrated circuits (HIC blocks) are performed. By using different types of cartridge valves such as directional control valves, pressure and flow control valves, load holding valves or sequential valves, complex HIC blocks can be realized that enable multi-actuator operation.

Figure 8 shows a functional diagram of a developed system for controlling the position of a hydraulic cylinder using cartridge valves. By activating the 2/2 valve (position 1.12) and the flow control valve set in the bypass (position 1.7), the flow towards the control valves can be changed. The system is unloaded by activating the 2/2 valve (position 1.10) in the second bypass line.

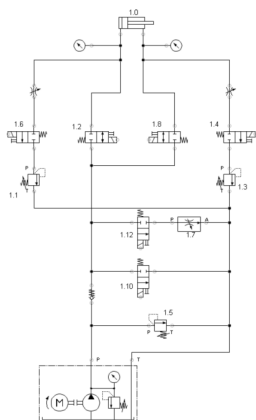**Figure 8: Functional diagram of hydraulic cylinder controlled with cartridge valves.**

Figure 9: Experimental setup of a hydraulic cylinder controlled with cartridge valves.

The Controllino Maxi controller was used as a control device. It combines the flexibility and advantage of an open source program like the Arduino with the security and reliability of a PLC as a standard industry component. The

Ž. Šitum, J. Benić, K. Pejić, M. M. Bača, I. Radić & D. Semren: Design and control of mechatronic systems with pneumatic and hydraulic drive

191

Controllino device enables USB communication, the use of analogue and digital inputs or outputs to activate the cartridge valves, and can receive signals from the encoder. The encoder and the program code constantly monitor the current position of the cylinder piston also during manual control so that the program has information about the position of the cylinder at the time when the user activates the switch for automatic mode. When the automatic mode is started, the program already has the value of the piston position obtained from the encoder. This current position will in almost all cases be different from the setpoint value, so a control error is calculated and then it is determined which cartridge valves must be activated to achieve the desired position. The program then determines whether the difference is positive or negative, two cartridge valves with a higher nominal flow (positions 1.2 and 1.8) are activated and the movement of the cylinder piston starts. When the piston comes close to the set position (according to the program, this is the range between 13 and 25 pulses), a logic valve (position 1.12) is activated which slows down the movement of the cylinder piston. Furthermore, when the piston comes very close to the desired position (the range between 1 and 13 pulses), cartridge valves (position 1.4 and 1.6) with lower nominal flow are activated (and at the same time valves with higher flow are deactivated). This ensures a low cylinder piston speed and thus the cylinder reaches the desired position with high precision. The control program does not stop after only one positioning, because at the end of the program a new desired position is set which the cylinder should reach. In this way, the program code will be executed as long as the switch is deactivated, the automatic mode will be stopped and the user can continue working in manual mode. However, as mentioned earlier, after the automatic mode is interrupted, the generated pulses from the encoder are still collected in case the user decides to return to the automatic mode.

The experimental setup made to demonstrate the position control of the hydraulic cylinder using cartridge valves is shown in Figure 9. The developed experimental system is an interesting educational setup where the capabilities of cartridge valves in hydraulic cylinder positioning tasks can be demonstrated. Also, various terms in the field of electrohydraulics and programming process can be explained. The system also has great potential for further development and upgrades.

6   Conclusion

The paper has presented four experimental systems powered by pneumatic or hydraulic drive. These systems have been designed in the Laboratory for Automation and Robotics at the Faculty of Mechanical Engineering and Naval Architecture, University of Zagreb as projects within student undergraduate and graduate theses. The systems can be used as test models within the field of fluid power drives and automatic control education of mechanical engineering students. The complete educational experience involving theoretical and practical applications of different control techniques applied to different implementations of fluid power systems provide a realistic insight into the actual behavior of the system.

The article was first introduced an example of a pneumatic motor speed and position control using a proportional directional control valve. This project is largely based on experiences from past activities in our Laboratory, which has resulted in several successfully implemented experimental systems in the field of mechatronic systems actuated by pneumatic actuators [12, 13]. Then the paper has described the design and control of a test device with pneumatic drive for determining the dynamic strength of materials, on which the fracture mechanics of materials due to the action of dynamic stress can be experimentally demonstrated and the resistance of materials to cyclic stress can be analyzed. Then the article has presented the design, construction and control of a pneumatically driven system for sorting products marked with a bar code using a vision system. Finally, the article has presented an experimental setup for precise position control of a hydraulic cylinder using 2/2 cartridge valves, which can clearly demonstrate the application possibilities of these valves in industrial plants and mobile systems.

By using these experimental systems students have the opportunity to learn about mechanical systems construction and control of practical systems built from real industrial components.

Ž. Šitum, J. Benić, K. Pejić, M. M. Bača, I. Radić & D. Semren: Design and control of mechatronic systems with pneumatic and hydraulic drive

193

References

[1]   Xu, H., Yu, W , Griffith, D., Golmie, N. (2018). A Survey on Industrial Internet of Things: A Cyber-Physical Systems Perspective. IEEE Access, Special Section on Towards Service-Centric Internet of Things (IoT): From Modeling to Practice

[2]   *Scheidl, R., Linjama, M., Schmidt, S. (2012). Discussion: Is the future of fluid power digital? Proceedings of the Institution of Mechanical Engineers, Part I: Journal of Systems and Control Engineering,* 226 (6) 721–723.

[3]   Sandoval, D., Latino, F. (1997). Servopneumatic Systems Stress Simplicity Economy for Motion Solutions. *Control Engineering Online*, Magazine Articles.

[4]   Vukovic, M., Murrenhoff, H. (2015). The next generation of fluid power systems. Procedia Engineering 106, 2–7

[5]   Pandian, S. R., Takemura, F., Hayakawa, Y. Kawamura, S. (1999). Control Performance of an Air Motor – Can Air Motors Replace Electric Motors?, International Conference on Robotics & Automation, Detroit Michigan, 518-524

[6]   Beater, P. (2007). Pneumatic Drives: System Design, Modelling and Control. Berlin: Springer-Verlag, ISBN 978-3-540-69470-0

[7]   Gela, T. (2006). Mechanical Design Handbook, Chapter 6: Properties of Engineering Materials. , McGraw-Hill Book Company

[8]   Murugan, S. (2020). Mechanical Properties of Materials: Definition, Testing and Application. Int. J. of Modern Studies in Mechanical Engineering (IJMSME) 6, 2, 28-38

[9]   Palmer, R. (1995). The Bar Code Book: A Comprehensive Guide To Reading, Printing, Specifying, Evaluating, And Using Bar Code and Other Machine-Readable Symbols. Helmers Publishing

[10]   Szeliski R. (2010). Computer Vision: Algorithms and Applications, Springer.

[11]   *Weeks, J. (2020). Understanding Logic Valves in Hydraulic Systems. Machinery Lubrication* https://www.machinerylubrication.com/Read/31788/*hydraulic-logic-valves*

[12]   Šitum, Ž. (2017). Fluid power drives in robotic systems. Invited Lecture. *International Conference Fluid Power 2017*, Maribor, Slovenija, 11-23

[13]   Šitum, Ž., Benić, J., Grbić, Š., Vlahović, F., Jelenić, D., Kosor, T., Mechatronic systems with pneumatic drive, *International Conference Fluid Power 2017*, Maribor, Slovenija, 281-293.

University of Maribor Press

Force control on direct driven servo hydraulic actuator

ALEKS PETROVIČ, MIHAEL JANEŽIČ & VITO TIČ

Abstract Direct Driven Servo Hydraulic Actuator also known as Pump Direct Driven Cylinder (PDDC) represents a decentralized modern concept of energy efficient cylinder control without damping loses of direction valves. Such systems have many advantages over conventional hydraulic systems and combine benefits of hydraulic and electric drives. PDDC system developed in Laboratory for Oil Hydraulics at University of Maribor consists of hydro motor, which is used as a reversible pump that is directly driven by servomotor and is designed for experimental testing with differential hydraulic cylinder. In this paper, the aforementioned system runs experimental setup for force control of hydraulic cylinder, with load produced by pneumatic bellow.

Keywords: • PDDC • PID • trajectory • step • HMI •

CORRESPONDENCE ADDRESS: Aleks Petrovič, University of Maribor, Faculty of Mechanical Engineering, Smetanova ulica 17, 2000 Maribor, Slovenia, e-mail: aleks.petrovic@student.um.si. Mihael Janežič, University of Maribor, Faculty of Mechanical Engineering, Smetanova ulica 17, 2000 Maribor, Slovenia, e-mail: mihael.janezic@student.um.si. Vito Tič, University of Maribor, Faculty of Mechanical Engineering, Smetanova ulica 17, 2000 Maribor, Slovenia, e-mail: vito.tic@um.si.

1   Introduction

In comparison to conventional systems, PDDC systems don't use direction valves. Direction is controlled by rotation of servomotor connected to reversible pump. PDDC system are very compact, mobile, universal and powerful which bring many advantages such as:

- productivity,
- overload safety,
- robustness (longer maintenance intervals),
- easier maintenance,
- accuracy and dynamic of servomotor,
- small use of hydraulic oil (because of system compactness),
- ability to connect to other systems (industry 4.0).

Such systems are usually used to bend, press, move, lift and position objects [11].

For this paper, an experiment using different ways of force trajectory type was designed. PDDC system is force controlled using step, three-phase and sinus trajectory. For maintaining force value, trajectories are used as an input value of PID regulator. Parameters of various trajectories and PID regulator parameters are initialized using Windows forms C# application developed in Visual Studio. User can easily change all of parameters of specific control for better control of the desired trajectory.

2   Experimental setup

Experimental system consist of Rexroth Indramat permanent magnet servomotor MKD071B that is speed and torque controlled by Indramat DKC03 servo motor driver. For this particular application, motor torque is set to 24 Nm with speed limited to $+/-$ 3000 min^{-1}. It's connected to directly driven hydraulic pump using bell housing with coupler, which is connected to custom made hydraulic block with screw in check valves, filters, hydraulic accumulator and adjusTable pressure relief valves set to 210 bar for both sides of differential cylinders chambers, shown in Figure 1. Each cylinder chamber pressure is measured with Hawe DT2-4 pressure sensor. Additional pressure sensor is also mounted on hydraulic block to monitor pressure in tank/accumulator line. Complete hydraulic scheme is shown in Figure 3.

Differential hydraulic cylinder (d=22 mm, D=32 mm, cylinder stroke = 200 mm) made by Bosch Rexroth is used as hydraulic actuator. Given above max. pressure and size of cylinder, it can push up to 16 kN of force and pull up to 8,5 kN. Closed loop system control is based on Beckhoff industrial soft PLC mounted in electrical cabinet shown in Figure 2.

Figure 1: PDDC.

PLC Beckhoff

Indramat DKC03
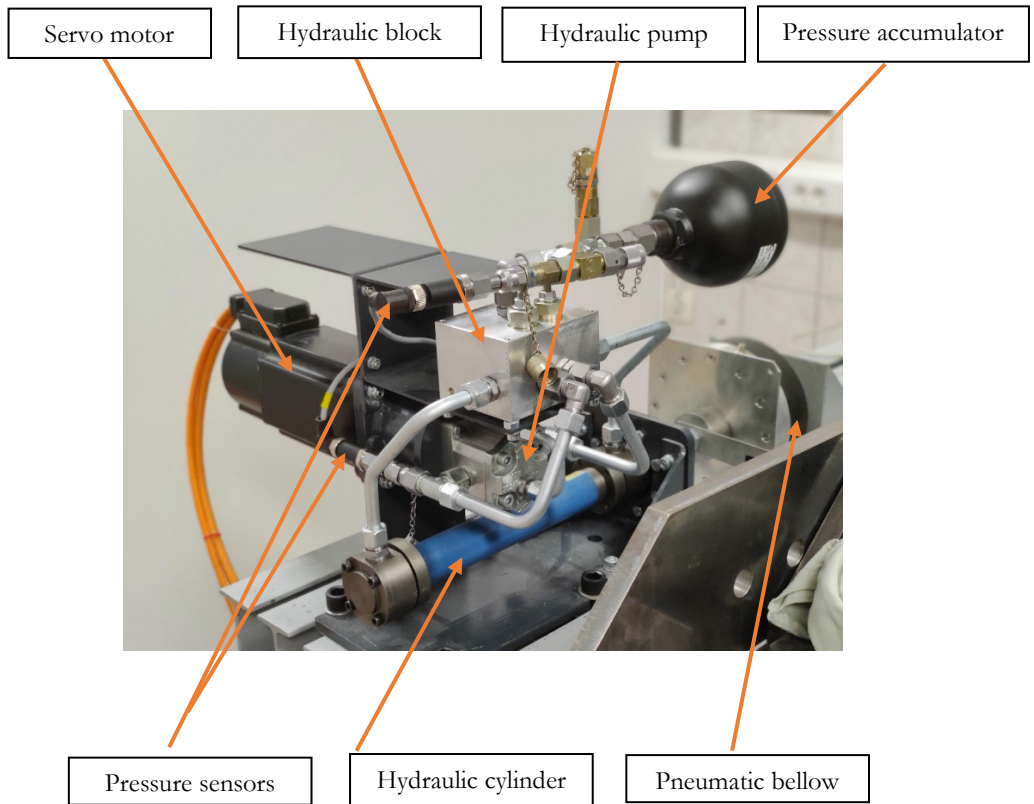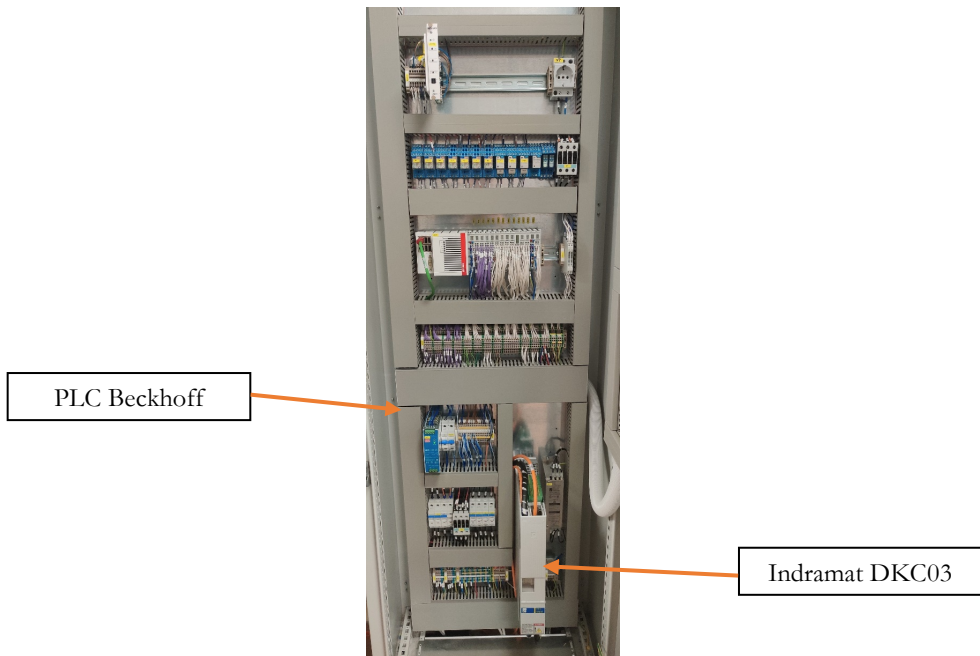
Figure 2: Electrical cabinet.
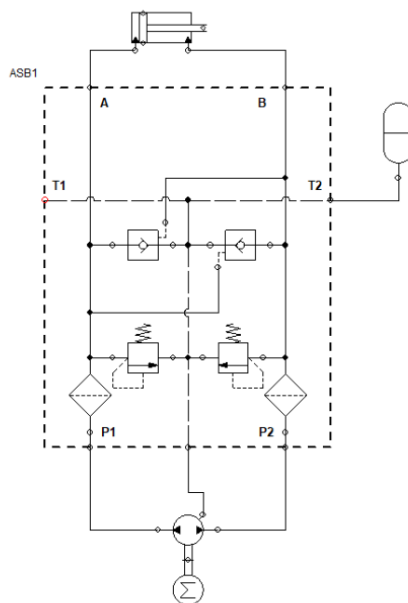
Figure 3: Hydraulic scheme [1].

2.1 Beckhoff soft PLC

PLC used in system is CX5140 that is made by company Beckhoff. This PLC was chosen because of its modularity whit I/O cards (current configuration is shown in Figure 4), that are DIN rail compatible so they can be easily changed. Its technical data can be found in Table 1 [2].

PLC – PC connection is done with Ethernet connection via RJ45 port. PLC – PC connection is used for programming, troubleshooting and real time monitoring. Final program and HMI interface are uploaded to PLC and run locally on soft PLC that simultaneously run real-time PLC program and developed Windows Forms application on Windows 7 Embedded.

Table 1: PLC technical data

Tehnical data	CX5140
Procesor	Intel Atom® E3845, 1.91 GHz
Number of cores	4
Flash memory	Slot for Cfast card and microSD cards
Main memory	4 GB DDR3 RAM
Interfaces	2x RJ45 10-1000Mbit/s 1x DVI-I, 4 x USB 2.0
Diagnostic LED	1 x power, 1 x TC status, 1 x flash access, 2 x bus status
Operating system	Windows Embedded Compact 7 (supports only one CPU core),
	Windows Embedded Standard 7 P, Windows 10 IoT Enterprise 2016 LTSB,
	Windows 10 IoT Enterprise 2019 LTSC, TwinCAT/BSD
Control software	TwinCAT 2 runtime, TwinCAT 3 runtime (XAR)
I/O connection	E-bus or K-bus, automatic recognition
Power supply	24 V DC
Current supply E-bus/K-bus	2A
Max. power consumption	16 W
Max. power consumption (with loading UPS)	23 W
Dimensions (W x H x D)	142 mm x 100 mm x 92 mm
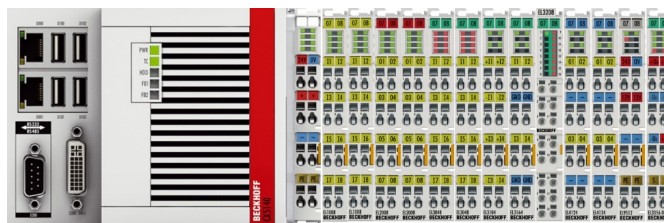
Figure 4: PLC with I/O cards [4].

2.1.1   I/O Devices

There are multiple cards in system that are not used for current experiment. They will be used in future experiments. List of all cards and their current configuration are listed in Table 2.

Beckhoff EL1008 [5] card is used as an electrical cabinet switch state input and Indramat digital output state check. For relay activating and controlling of digital inputs on Indramat servo-motor controller, EL2008 [6] was used. Analog values received from HAWE DT pressure sensors and Omron ZX-1 CMOS sensor are read using EL3048 [7] card. EL3014 [8] card is used to read analog outputs from Indramat servo-motor controller. Analog inputs of Rexroth Indramat servo-motor controller are controlled using El4134 [9] card.

Table 2: List of I/O cards

Card (current order)	caracteristics
EL1008	8-channel digital input, 24 V DC
EL1008	8-channel digital input, 24 V DC
EL2008	8-channel digital output, 24 V DC, 0.5 A
EL2008	8-channel digital output, 24 V DC, 0.5 A
EL3048	8-channel analog input, current, 0…20 mA, 12 bit, single-ended
EL3048	8-channel analog input, current, 0…20 mA, 12 bit, single-ended
EL3104	4-channel analog input, voltage, ±10 V, 16 bit, differential
EL3164	4-channel analog input, voltage, 0…10 V, 16 bit, single-ended
EL3208	8-channel analog input, temperature, RTD (Pt100), 16 bit
EL4124	4-channel analog output, current, 4…20 mA, 16 bit
EL4134	4-channel analog output, voltage, ±10 V, 16 bit
EL9512	Power supply terminal 12 V DC
EL3356	1-channel analog input, measuring bridge, full bridge, 16 bit

2.2   OMRON ZX1-LD600A81

For measuring piston rod movement, OMRON laser displacement sensor with CMOS sensor is used. It allows us to measure up to 0.08 mm of movement in standard mode with 50 ms response time. With some accuracy loss, sensor is also capable of high speed capturing with 1.5 ms response time. In our application sensor does not play any role in regulation of the system. Sensor is mounted in custom-made 3D printed enclosure visible in Figure 5.
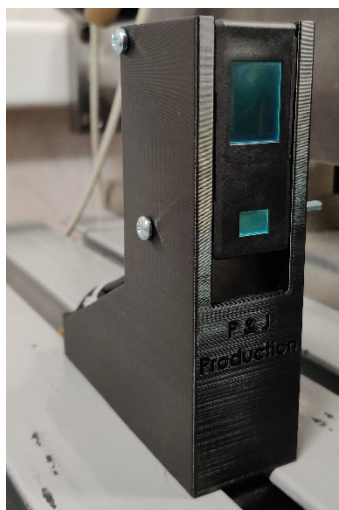
Figure 5: Omron laser.

3   Software solutions

PLC program was designed in TwinCAT 3 development environment. Different program languages such as FBD, SFC and ST were used. For human machine interface (HMI), we have developed user interface using Windows Forms C# for controlling and monitoring different parameters of PLC program.

As mentioned in introduction, PID controller is used to control trajectory of the system by following three different types of generated trajectory (step, three-phase trajectory and sinus).

3.1   PLC Program

PLC program developed in Twincat3 is running locally on Beckhoff soft PLC controller. Main program is written in Structured Text language (ST), and uses Case statements for selecting subprograms (Figure 6), which determine working mode of PDDC system.

```
1    Read ();
2
3    CASE Gv1.stanje OF
4    0:
5        Count();
6    1:
7        Manual();
8    2:
9        EHAClosedLoopPosition ();
10   3:
11       SERVO_CL();
12   4:
13       HAWE();
14   5:
15       EHA_Force_PID();
16
17   END_CASE
18
19   CycleTest_calc();
20   Write ();
```

Figure 6: Main program.

Mode subprograms are also written in Structured Text language with Case statements that determine the behaviour of the system using subprogram. For example in Figure 7, program is in Force control mode and in system start up procedure.

```
1    CASE gv1.EHA_MODE OF
2        1:
3        EHAstart();
4        2:
5        EHAstop();
6        3:
7        EHA_FORCE();
8    END_CASE
```

Figure 7: Mode subprograms.

For start-up and stopping procedure of Rexroth Indramat servo driver, subprograms EHA_Start and EHA_Stop are used. Both subprograms are used multiple times in PLC program. Subprogram for stopping procedure is visible in Figure 8. Program logic is shown in Figure 9.

```
start1:= gv1.timerEHAStop;


gv1.DriveEnable :=FALSE;
gv1.INDR_PS_BR:= FALSE;
gv1.E_stop:= FALSE;
gv1.DriveHalt:= FALSE;

Timer1(IN:= start1, PT:= T#1000MS);
IF Timer1.Q THEN
    gv1.INDRAMAT_POWER_ON := FALSE;
    gv1.timerEHAStop :=FALSE;
    gv1.EHA:= 0;
    gv1.HAWE_SET_MODE:= 5;
    gv1.EHA_MODE := 0;


END_IF
```

Figure 8: Stopping procedure subprogram.
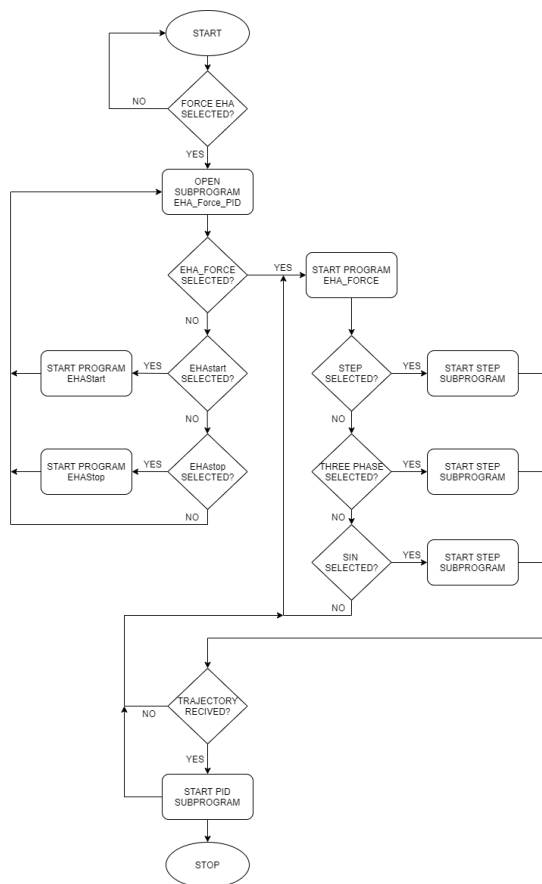
Figure 9: Program logic.

3.2   Step response

Subprogram *forceSTEP_EHA*, written in ST, is used to generate trajectory for step response.

It reads user input value and directly applies it to the input of PID controller as desired value (Figure 10).

```
gvl.trajectory_OUT_eha := gvl.STargetPosForceEHA;
```

Figure 10: Step trajectory subprogram

3.3   Trajectory

Trajectory control is one of the most widely used control of movement in industry. To generate trajectory, we have used three phase trajectory generator that can be found in Twincat 3 libraries. This subprogram was written in FBD language (Figure 11). Generator is controlled by binary values that determine its state. Generator parameters are defined in initialization subprogram and are combined in array structure called *stParams* that consist of start position, target position, start velocity, desired velocity, start acceleration/deceleration, desired acceleration/deceleration, control cycle time and task cycle time (Figure 12). Generated structure is inserted in one of the inputs of the three-phase generator.

```
                           force_3p_eha
                   FB_CTRL_3PHASE_SETPOINT_GENERATOR
    gvl.sstartForceEHA —— bStart          fSetPos ———————————— gvl.trajectory_OUT_eha
     gvl.sstopForceEHA —— bStop          fSetVelo — gvl.VelocityForceOutEHA
    gvl.sresetForceEHA —— bReset          fSetAcc — gvl.AccelerationForceOutEHA
                  100 —— fOverride          bDone — gvl.bdone
   Force_3p_Params_eha ——⊣ stParams
```
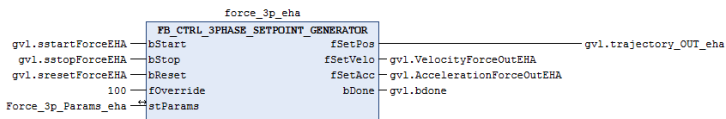
Figure 11: Three phase set point generator.

```
// 3p

Force_3p_Params_eha.fStartPos := gvl.EHAForceValue;
Force_3p_Params_eha.fTargetPos := gvl.STargetPosForceEHA;
Force_3p_Params_eha.fStartVelo := 0;
Force_3p_Params_eha.fVelocity :=gvl.SVelocityForceEHA;
Force_3p_Params_eha.fTargetVelo := 0;
Force_3p_Params_eha.fAcceleration := gvl.SAccelerationForceEHA;
Force_3p_Params_eha.fDeceleration := gvl.SDecelerationForceEHA;
Force_3p_Params_eha.tCtrlCycleTime := T#1MS;
Force_3p_Params_eha.tTaskCycleTime := T#1MS;

eModeFORCEgen := gvl.EHA_SIN_Emode;
eModeFORCE := gvl.EHA_PID_Emode;
```

Figure 12: StParams structure

3.4 SIN

For quick constant changes of trajectory, sinus generator from Twincat 3 library was used (Figure 13). It generates sin wave using amplitude and offset parameters that are defined in array structure called *stParams* shown in Figure 14. Working mode of generator is defined in *eMode* (passive, active). *E state* parameters show current state of the generator.
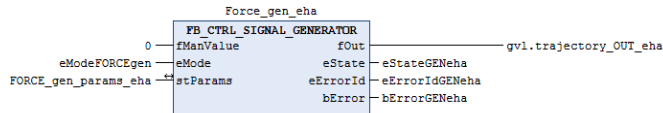
Figure 13: Sinus signal generator.

```
//sin
FORCE_gen_params_eha.fAmplitude := gvl.FORCEAmplitudeEHA;
FORCE_gen_params_eha.fOffset := gvl.FORCEOffsetEHA;
FORCE_gen_params_eha.tCtrlCycleTime := T#1MS;
FORCE_gen_params_eha.tTaskCycleTime := T#1MS;
FORCE_gen_params_eha.eSignalType   := 1;
// E_CTRL_SIGNAL_TYPE;
FORCE_gen_params_eha.tCylceDuration := gvl.FORCEFreqEHA;
FORCE_gen_params_eha.tStart         := T#00MS;
```

Figure 14: Sinus StParams structure.

3.5 PID

Trajectory generated from step, 3 phase trajectory or sinus are written in global variable called *trajectory_OUT_eha* which is used as input for PID controller (Figure 15). PID controller used is taken from Twincat 3 library. It compares actual (*gvl.EHAForceValue*) and desired value (*gvl.trajectory_OUT_eha*). Parameters for PID controller are written in array structure *stParams* and set in initialization subprogram. MUL block is used to convert motor direction. Limit is set to limit motor speed. Actual force of hydraulic cylinder is calculated from acquired pressure from both sides of cylinder chambers (by subtracting forces in each cylinder chamber in *Read* subprogram) [12].
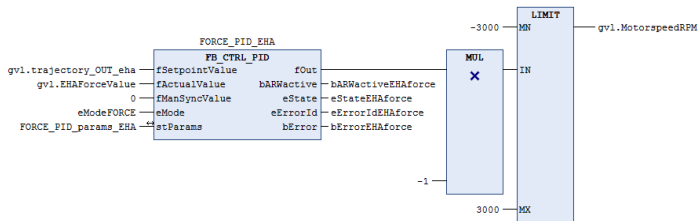
Figure 15: PID controller

4   HMI

For easier control and data monitoring HMI was created in Windows Forms C# application using Visual studio. It connects to PLC with ADS communication protocol.

Main goal when designing HMI was to make it simple and easy to use. From HMI user can initialize Start/Stop procedure, select work mode (Step, Sinus, 3-phase trajectory) and type of regulator (P, PI, PD, PID). User can also define the parameters for work mode, trajectory and closed-loop control parameters.

Scope is used to monitor and display actual and desired force value of piston. It also shows position of hydraulic cylinder from Omron distance laser.
HMI can also be used in case of emergency. Emergency stop button turns of system and stops servomotor instantly. System can be started again using Clear Error button, which clears errors on Rexroth Indramat and enables the system. System state can be monitored by true/false indicators shown in Figure 16.

TwinCAT 3 ADS notifications protocol is used for event driven reading of variables. Library waits for designated variables to change state and sends them to HMI using separate thread of UI thread. In HMI, communication thread is opened, variables are then transferred to UI thread. When transfer is completed, communication thread is closed and variables are assigned to their local variables. Those local variables can then be displayed without UI lag.

Library can work with up to 500 variables without causing delays in responsiveness of UI.
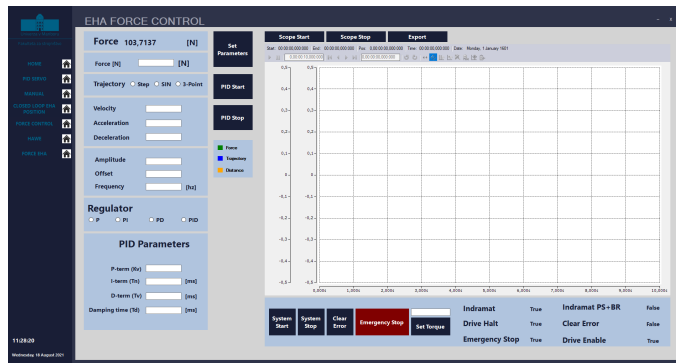
Figure 16: HMI

5 Experimental results

System responses are monitored in Visual studio using Twincat 3 Scope. Experiment was executed on three various type of trajectory (step, three-phase and sinus). The responses are commented in paragraphs below.

5.1 Step trajectory response

First experiment was done using step trajectory. As visible in Figure 17 response of the system with PID regulator follows desired trajectory with small amount of phase shift and error in amplitude. At holding constant force, we can notice jerking of force caused by jerking of PID controlled servomotor.

Figure 17: Step response.

5.2   Three phase trajectory response

Second type of trajectory used in experiment was three-phase trajectory. Figure 18 shows a small amount of overshoot visible in lowering of force and jerking of PID controlled servomotor when trajectory levels out and force is constant.

Figure 18: Three phase response

5.3   Sinus trajectory response

Sinus trajectory was the last trajectory tested in experiment. System follows desired force very well, shows only a small amount of overshooting, and phase delay (Figure 19). Jerking of force on peaks off sine wave is caused by changing of the servo motor rotation direction.

Figure 19: Sinus response

6　　　Conclusion

Experimental results have shown that PID controller has tracking error and slower dynamics. Satisfying results are achieved only in slower trajectories. As soon as trajectories are changed quickly, more significant overshoot is seen and system lags behind trajectory, which results in phase shift in square and sine waves. Parameters of PID controller were selected with trial and error method.

For better responses, non-linear control algorithms should be considered. Better accuracy of force control could also be achieved using load cell, which would eliminate reading errors of calculated forces of cylinder.

Experimental setup represents a good foundation for further experiments on different PID controllers for PDDC systems.

References

[1] Tine, J. (2020), Zasnova in izdelava direktno vodenega elektro-hidravličnega aktuatorja : magistrsko delo [online]. University of Maribor, Faculty of Mechanical Engineering. (Accessed 24 August 2021)
Retrieved from: https://dk.um.si/IzpisGradiva.php?lang=eng&id=77183

[2] Beckhoff Automation. [Accessed 24 August 2021]. Retrieved from: https://www.beckhoff.com/en-en/company/

[3] Beckhoff Information System [Accessed 24 August 2021]. Retrieved from: https://infosys.beckhoff.com/english.php?content=../content/1033/tcplccontrol/html/tcplcctrl_statement_if.htm&id=2531424188494754278

[4] Beckhoff Automation EtherCAT terminal [Accessed 24 August 2021] Retrieved from: https://www.beckhoff.com/sl-si/products/i-o/ethercat-terminals/

[5] Beckhoff Automation EL1008 EtherCAT terminal [Accessed 24 August 2021] Retrieved from: https://www.beckhoff.com/sl-si/products/i-o/ethercat-terminals/el1xxx-digital-input/el1008.html

[6] Beckhoff Automation EL2008 EtherCAT terminal [Accessed 24 August 2021] Retrieved from: https://www.beckhoff.com/sl-si/products/i-o/ethercat-terminals/el2xxx-digital-output/el2008.html

[7] Beckhoff Automation EL3048 EtherCAT terminal [Accessed 24 August 2021] Retrieved from: https://www.beckhoff.com/sl-si/products/i-o/ethercat-terminals/el3xxx-analog-input/el3048.html

[8] Beckhoff Automation EL3104 EtherCAT terminal [Accessed 24 August 2021] Retrieved from: https://www.beckhoff.com/sl-si/products/i-o/ethercat-terminals/el3xxx-analog-input/el3104.html

[9] Beckhoff Automation EL4134 EtherCAT terminal [Accessed 24 August 2021] Retrieved from: https://www.beckhoff.com/sl-si/products/i-o/ethercat-terminals/el4xxx-analog-output/el4134.html

[10]   Omron   Industrial   Automation   [Accessed 24 August 2021]   Retrieved   from: https://industrial.omron.eu/en/products/ZX1-LD600A81-2M

[11]   Lovrec Darko, Uvod v hidravlično pogonsko-krmilno tehniko. Univerzitetna založba, November 2018

[12]   Kiker Edo, Regulacijska tehnika.Univerza v Mariboru, 5. 9. 2000

University of Maribor Press

Ionic liquids – the path to the first industrial application

DARKO LOVREC

Abstract When using hydraulic fluids, users rarely ask themselves how the development of the hydraulic fluid they use in their hydraulic device has gone. Perhaps only curious users want to know the approximate composition of the newer, better hydraulic fluid, compared to the fluid of the previous generation. Rarely, however, do they know the developmental pathway of the new fluid. Even in the case of minor changes in the chemical composition of the fluid, e. g. a newer package of additives for mineral oils, or other base oil, requires lengthy fluid testing. First, in the manufacturer's laboratories, and then in the industrial environment. In the case of a completely new type of hydraulic fluid, the development path is much longer. The paper presents the behind-the-scenes development of a completely new type of hydraulic fluid - ionic liquid, from learning about the liquid itself all the way to industrial application.

keywords: • hydraulic fluids • ionic liquids • selecting • testing • application •

1   Introduction

The development of hydraulic fluid is a long-lasting process. Before the fluid is suiTable for use in an industrial environment, a lot of targeted testing is needed, first in a laboratory environment, and then in an industrial environment, after which the process is usually repeated based on users` feedbacks. If the hydraulic fluid has to meet specific operating requirements, the path is even more difficult. In the case of a completely new type of hydraulic fluid, the development is even more difficult, associated with high costs, lengthy and extensive testing and incomparably more unknowns than in the case of "adaptation" of an already known fluid.

We encountered this problem in the development of a completely new type of hydraulic fluid - Ionic Liquid (IL), which would be suiTable for use in hydraulic devices. Not only that, but such IL, which would have the properties provided by different types of hydraulic fluids: Nonflammable, environmentally friendly, with good lubricating properties, low temperature dependence, low vapour pressure and others. In addition, when changing the fluid, the user would not need to pay special attention to the compatibility of the fluid with the materials used in the hydraulic components.

The paper provides an insight into our own experience in the development of Ionic Liquids which would be suiTable for use in modern hydraulic systems. The entire development path, which has lasted for more than a decade, is presented, divided into individual phasese or stages of development. These phases are: learning about the matter and assessing their suitability, finding suitable project partners, selecting suitable candidates, laboratory tests of individual properties, endurance testing on a dedicated test device and, finally, an industrial application.

2   Stage 1: Learning about the material - Ionic Liquids

Ionic Liquids are usually, and very simply, called liquid salts. The application of high temperature molten salts in ancient China dates back to the 2nd century B.C., and is even evident during the Shang Dynasty (16th to 11th centuries B.C.). These molten salts, based on alkali nitrates and chromates, were used for the surface modification of bronze weapons, in order to make them harder and corrosion protected. Ionic Liquids are defined as molten salts with a melting temperature

of 100 °C or lower [1], [2] in the liquid state, a large number of them even being liquid at room temperature, and then being called "room temperature molten salts". Compared to conventional molten salts they show some characteristical differences, as presented in Table 1.

Table 1: Comparison of "molten salts" and "Ionic Liquids" [1]

"Molten Salts"	"Ionic Liquids"
High melting points: ~200 °C to ~1500 °C	Melting point ≤100 °C down to approx. -60 °C
Aggressive chemical reactivity, high corrosion	Mild chemical reactivity, low corrosion
Considerable vapour pressure	Virtually no vapour pressure
Inorganic cations and anions	Organic cations
Strongly coordinating ions	Weakly coordinating ions

In 1888 *Gabriel* and *Weiner* published details of the organic salt ethanolammonium nitrate ($HOC_2H_4NH_3^+NO_3^-$) with a melting point of 52 to 55 °C [3]. In 1914, the field of true room temperature Ionic Liquids started off with the fateful discovery of ethylammonium nitrate ($EtNH_3^+NO_3^-$), having a melting point of only 12 °C. Ionic Liquids have evolved rapidly to the present day, with the structure and properties of IL adapted to the field of application. Ionic Liquids typically consist of an organic cation and an inorganic or organic anion (R denoting an alkyl or aromatic rest, optionally functionalised).

Ionic Liquids with a melting point at ambient temperature, which is suiTable for use as a liquid lubricant and as a hydraulic fluid, consist of extensive and asymmetric organic cations such as 1-alkyl-3-methylimidazolium, 1-alkyl-pyridinium, 1-methyl-1-alkylpyrrolidinium or ammonium ions. Many anions are in use, from simple halides that lower high melting points, to inorganic anions such as tetrafluoroborates and hexafluorophosphates, and to large organic anions such as bis (trifluorosulfonyl) amides, triflates or tosylates [4]. An example is shown in Figure 1. For non-chemists, Ionic Liquids are complex chemical structures and their names are also complex too. Therefore, often when we talk about the type and structure of Ionic Liquid, we use an abbreviation, such as, e. g., for the often-mentioned Ionic Liquid EMIM EtSO4 >: 1-Ethyl-3-methylimidazolium ethyl sulfate.
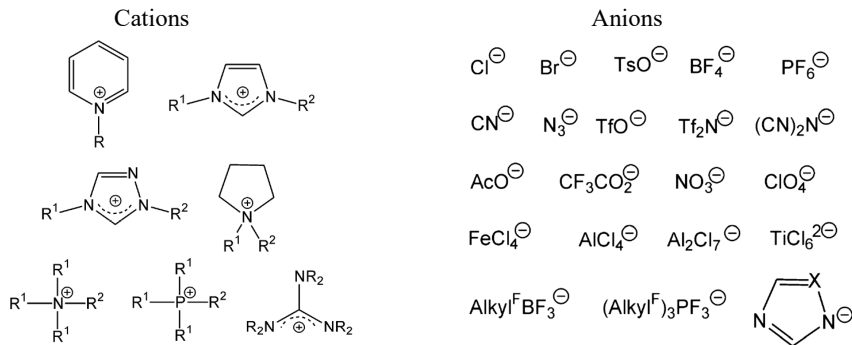
Cations   Anions

$Cl^{\ominus}$ $Br^{\ominus}$ $TsO^{\ominus}$ $BF_4^{\ominus}$ $PF_6^{\ominus}$

$CN^{\ominus}$ $N_3^{\ominus}$ $TfO^{\ominus}$ $Tf_2N^{\ominus}$ $(CN)_2N^{\ominus}$

$AcO^{\ominus}$ $CF_3CO_2^{\ominus}$ $NO_3^{\ominus}$ $ClO_4^{\ominus}$

$FeCl_4^{\ominus}$ $AlCl_4^{\ominus}$ $Al_2Cl_7^{\ominus}$ $TiCl_6^{2\ominus}$

$Alkyl^F BF_3^{\ominus}$ $(Alkyl^F)_3 PF_3^{\ominus}$

Figure 1: Various cations and anions in Ionic Liquids [3].

Since the 1990'ies thousands of review papers and dozens of books have been published describing the amazing physical and chemical properties of Ionic Liquids, (see the references given in [1]). The most outstanding properties of Ionic Liquids reported in different publications are the following:

- Excellent lubrication properties,
- Very low melting points (100 °C down to – 60 °C)
- Virtually no vapour pressure (no pollution via the gas phase),
- No boiling point,
- Non flammable (below the thermal decomposition point),
- Excellent thermal long term stability up to 300 °C and more,
- Very large liquidus range up to 400 °C,
- Unusual solvation properties (e. g. amphiphilicity),
- Frequently and improved catalytic performance,
- Small friction coefficients, good lubrication properties,
- Electrical conductivity (typically 100 to 10000 μS/cm at 20 °C),
- Bacteriozide to bacteriostatic properties, no biofouling,
- Tunable by structure variation of cations, anions and by changing their combination: Millions - virtually unlimited – structures, etc.

All of these highlighted excellent properties of a particular type of ionic fluid were reason enough to stimulate our interest in the possible use of ionic fluid as a hydraulic fluid. A fluid that would have all of the aforementioned excellent listed properties, would solve a huge number of problems arising from the use of the current hydraulic fluids.

3   Stage 2: Goal setting – project HOPE

Enthusiastic and encouraged, based on the information gathered, we started looking for partners for a project in which we could fully select, test and also use suiTable fluids in hydraulic systems. Given this, a partner would certainly need to be a very experienced manufacturer of Ionic Liquids, a company that had experience in the production and testing of conventional hydraulic fluids and was adequately equipped for these tasks, and also a company that would be willing to approach the development in terms of hydraulic components, and, of course, a Research Institution that would conduct and direct the research, perform certain special tests, connect all partners in the project and, based on the research results, look for suiTable applications for the practical use of Ionic Liquids.

The partners in this project came from three different countries: Austria, Germany and Slovenia: The HAWE company – a manufacturer of hydraulic components and systems, the OLMA company – the leading Slovenian manufacturer of lubricants, the Proionic company from Graz/Austria, one of the leading global manufacturers of ILs, and the University of Maribor, where we carried out the majority of the research and connected all the partners, in cooperation with the Technical University of Graz/Austria and other partners from the industry e. g. Bogadi, a specialist in the production of seals, Mettop, a specialist in the production of machines and devices for the steel industry.

The main goal of project HOPE was to check the suitabilities of the existing ILs for usage within hydraulic systems, and/or to synthesise such ILs, which would have better physical and chemical properties – should be (almost) an ideal hydraulic fluid, which we were already looking for from the first hydraulic presses onwards.

The following main objectives were set in the implementation of the project:
- From a wide range of ILs suiTable for technical usage, to find an appropriate IL for use in modern hydraulic systems,
- Determinations of their physical-chemical properties,
- Performing a comparison with today's more commonly used hydraulic fluids: Mineral oil, fire resistant fluids, and biologically rapidly degradable fluid,

- To provide recommendations for the usages of ILs with the best properties within various industrial applications,
- To check the suitability of existing laboratory methods for determining the properties of ILs.

4   Stage 3: Preselection – checking the properties

As already mentioned, ILs consist of an organic cation and an inorganic or organic anion. However, when combined with certain specified cation anions, you will obtain another liquid salt – which, if it does not work by trial and error but intentionally, can be synthesised into a completely new material with entirely new properties. In our case, we are looking for "liquid salts", which would have the characteristics of a perfect hydraulic fluid.

An important feature of Ionic Liquids is the possibility of adapting these physical-chemical properties through changing the natures of the anions and cations. The number of possible combinations is extremely high, which is why the best Ionic Liquid is supposed to be adapted for different usage: 1.10^{18}. For this reason, the first objective of the project was, from the almost unlimited possibilities of combinations of ions and cations, with a screening process, to extract those combinations which would be suiTable for use as a hydraulic fluid.

Selecting the "best ILs` suiTable candidates" for use as hydraulic fluids, the work with ILs, is however, not as uniformly definite as with other conventional lubricants. It is because of their unique properties that Ionic Liquids frequently impose the use of special laboratory equipment.

The majority of laboratory measurements were carried out within the chemical laboratory of the lubricant manufacturer, which has the appropriate equipment, using a wide assortiment of analytical methods, out of which many were also applicable for ILs, for example, measurements of viscosity, density, corrosion, Karl Fischer titration, UV/VIS spectroscopy, FTIR spectroscopy, Thermo-Gravimetric Analysis, measurements of lubricating and foaming properties, etc. Some methods, such as the measurement of breakdown voltage, filtration capacity, Stribeck's curve, and Contact Angle were applied in other proper laboratories.

Test procedures for determining the individual parameters, sample amounts and the equipment used, relate mainly to the usual lubricants, in accordance with the relevant Standard. In addition, the tests of Ionic Liquids (as lubricants), were based on those processes intended particularly for the testing of mineral oil (liquid lubricants), and, as such, served as a starting-point. In our case, we first performed the following standard tests:

- Flash and fire points by the Cleveland Open Cup tester; ASTM D 92,
- Flash-point by the Pensky-Martens Closed Cup Tester; ASTM D 93,
- Determination of density by a densimeter; ISO 12185,
- Kinematic viscosity at 40 °C and 100 °C; ASTM D 445,
- Determination of viscosity index; ASTM D 2270,
- Determination of corrosion within a humid chamber; ISO 6270-2,
- Determination of corrosiveness to copper; ASTM D130,
- Determination of demulsifying properties; ASTM D 1401,
- Determination of foaming in lubricating oils; ASTM D 892,
- Determination of the welding point and wear diameter; IP 239-85,
- Determination of the pour-point; ASTM D 97.

The methods listed so far are used as the standard methods for the determination of physical-chemical properties, particularly of different lubricating oils, and were used as a starting-point for testing the Ionic Liquids' properties.

In addition to the mentioned and used standard tests, special purposeful measurements of physical-chemical properties were also used for testing the Ionic Liquids, as well as comparing fluids:

- Filterability; ISO 13357, and compatibility with filter materials,
- Compatibility with paint coats and with sealing material,
- Compatibility with metals used within hydraulic components,
- Measurement of Stribeck's curve,
- Measurement of compressibility and sound propagation,
- Electric breakdown voltage-IEC 156, IEC 60156,
- Contact Angle and wettability,
- Corrosiveness in open air…

Table 2 shows only a small section of the Data Table obtained during the selection process, and for only some of the tested ILs. Determining the suitability of IL was based first on corrosivity testing, then on lubricating properties. Only those ILs that showed good corrosion protection and good lubricating properties were tested further for other properties [5] to [14].

Table 2: Comparisons between some physical-chemical properties of tested ILs

Property	Viscosity 40°C	Viscosity index	Welding point	Wear diameter	Corrosion
Unit	[mm^2/s]	[/]	[kg]	[mm]	[cycles]
Sample					
Hydrolubric VG 46	47.07	119	130/140	0.58	0 (3 h)
EMIM-EtSO$_4$	39.44	168	140/180	1,0	0 (15 min)
EMIM-TFSI	71.89	132	1100/1200	0.68	0 (1.5 h)
10PI 453-1	/	/	/	/	0 (5 h)
10PI 453-2	/	/	/	/	0 (1 h)
10PI 453-3	/	/	/	/	0 (1 h)
10PI 453-4	/	/	/	/	0 (30 min)
10PI462 (EMIM-TFS2)	/	/	360/380	0.83	0 (30 min)
10PI465	/	/	>480	1.07	0 (30 min)
16PI028-5 (TOMA-DBP)	/	/	/	/	0 (30 min)
10PI028-3 (TOMA-HFB)	/	/	/	/	0 (45 min)
16PI062-2 (TOMA-DBP)	59.14	/	160/170	/	0 (4 h)
16PI062-1 (TOMA-HFB)	61.46	/	110/120	/	0 (5 min)
18PI094	49.28	109	120/130	1.04	0 (15 min)
19PI042	193.30	116	300/320	0.63	0 (15 min)
TOMA-DBP+10 % TOM-P	60.29	133	130/140	0.82	0 (2.5 h)
EMIM-SCN+42,3 % TOMP	/	/	>200	/	0 (15 min)
17PI064	102.90	105	180/190	0.49	1
18PI163	47.36	155	150/160	0.38	0 (3.5 h)
17PI045	46.59	155	140/150	0.35	0-1 (>7.5 h)

The process of selecting a suitable IL has shown that certain ILs do indeed have excellent individual material properties, as reported in publications. For their use as a hydraulic fluid, the individual excellent properties of different fluids should apply to the same fluid. However, in most cases, due to one good but another bad property, the specific IL is not suiTable for use within hydraulic systems.

5 Stage 4: Endurance tests

After the selection process only with those ILs which showed most of the good properties important for use as a hydraulic fluid, it made sense to proceed the testing with real hydraulic equipment and under real operating conditions.

Endurance tests are the next stage of testing the suitability of an Ionic Liquid. For these purposes, so-called tribological tests are usually used with hydraulic pumps (Vickers-Eaton test, Rexroth test, Denison test, Sundstrand test, Komatsu test, etc.) [15]. Unfortunately, these tests focus only on the pump, and not on other, equally important and active components within the hydraulic system. In addition, most of these tests use pumps with large flow rates and, consequently, a large amount of test quantities needed and, consequently, large test devices. The latter can lead to major test stand damage in the case of an unsuiTable tested fluid. In addition, it makes sense to test the characteristics and performance of the new fluid in comparison with a known, commonly used hydraulic fluid, e. g. with mineral hydraulic oil [16], [17].

For the purpose of testing new hydraulic fluids, e. g. Ionic Liquids, a new test device concept has been designed and constructed, appropriate for the combined testing of as many hydraulic components as possible, in the market quality. The testing is carried out under demanding, but still normal operating conditions, and with lower energy consumption. The mentioned tribological endurance pump-tests are limited only to a hydraulic pump. Therefore, it is reasonable to design a different concept of testing for a comprehensive insight. The starting points for the new test device design:

- To determine the suitability of the new fluid under real operating conditions,
- Using a variety of hydraulic components of industrial quality, commonly used within hydraulic systems,
- Take into account the aspect of energy consumption,
- Take into account the scale of the test device,

- Take into account the duration of the test,
- Take into account the cost of testing,
- The possibility of on-line monitoring of all important data,
- At certain intervals, to check the changes in the characteristics of the tested components,
- To use the standard test procedures, where possible,
- The possibility of cost-optimal repetition of the test…

In accordance with the listed requirements, a test device was designed for the integrated testing of the impact of a new hydraulic fluid on all components of the hydraulic system– Figure 2.
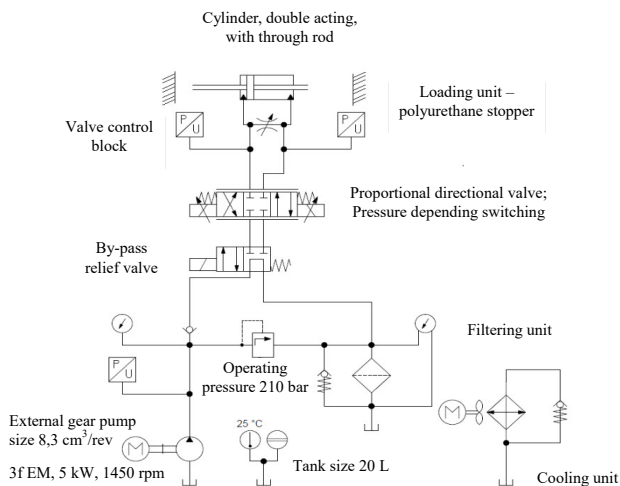

Figure 2: Layout of test device for integral endurance testing of fluid-component interaction [15]**.**

When designing devices for testing of hydraulic fluids along with hydraulic components, there are a few things to consider: Selection of appropriate components, power consumption of the device and type of loading profile. For the testing of an absolutely new fluid, another aspect should be taken into account: Cost effective design.

The test device allows insight into the pump wear, investigation of wear on the vital parts of different valve types (directional spool valve, poppet valve), the impact of the new liquid on a variety of materials used within other hydraulic system components (filter material, paint coat …), as well as the on-line and off-

line monitoring of the degradation process of the components – Figure 3. Some of these changes are monitored on-line and others off-line after the tests are completed, in total more than 50 different parameters.
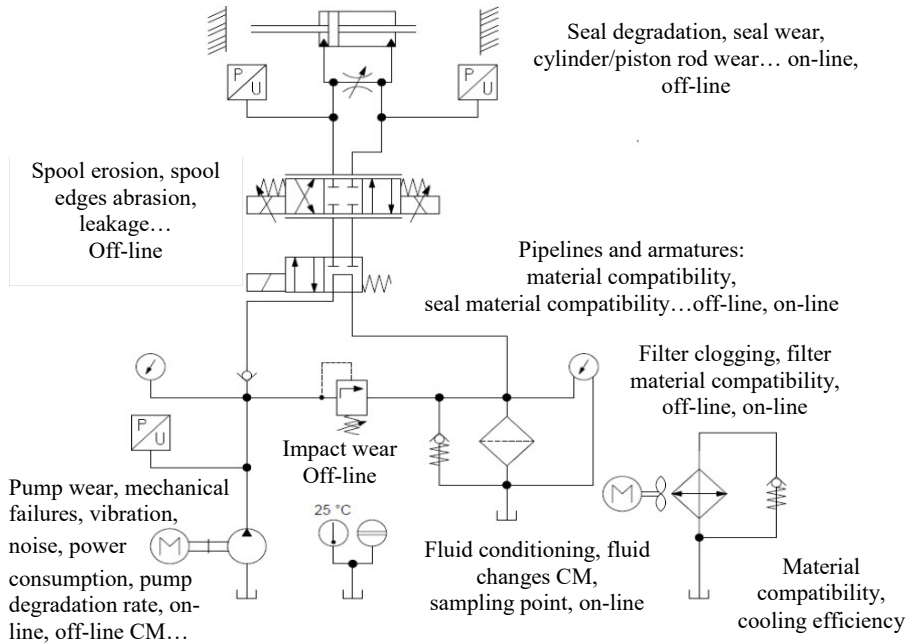

Figure 3: Points of interest and observed parameters [15]**.**

In this way, we got a more comprehensive insight into the effect of the tested new fluid type on the behaviour of the entire hydraulic system during operation, and the effect of the fluid on the degradation of an individual component exposed to real operating conditions (more information available in [15]).

Only after successfully completed endurance tribological tests, which provided a comprehensive insight into the impact of ionic fluid on all components of the hydraulic system, the tested fluid can be used for real industrial application.

6   Stage 5: Industrial application

Ionic Liquids have been used in industrial applications for some time. The first use case dates back to 1936, when IL was used to dissolve and alter cellulose chemically. At present, ILs are used industrially as solvent, catalysts, electrolytes, performance additive, cooling fluid, operating fluid, reagents within different technological processes. [1] However, as a hydraulic fluid, ILs have so far not found their use in the industrial environment (according to available official publications).

The first example of a simple hydraulic lifting device operating on an Ionic Liquid was presented at the international conference Fluid Power 2015. A demonstration device constructed with the industrial hydraulic components used is shown in Figure 4.
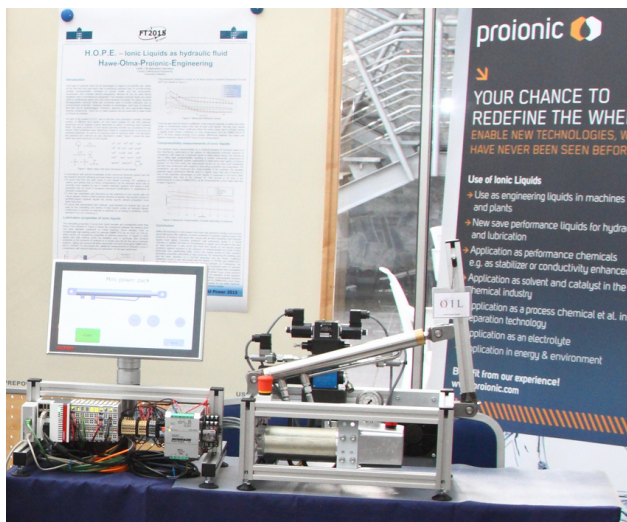

Figure 4: Smal lifting device operating on Ionic Liquid

The first major industrial application of a hydraulic system using an Ionic Liquid is the so-called tuyere press, which is used in the metallurgical industry. It is a special application, where no other type of hydraulic fluid can be used. A version was required with the lowest possible weight of the unit with adjusTable cylinder speeds and the possibility of integrating additional functions. The main condition, however, was to ensure the fire-safe design of the unit. It is a modern version of the electro-hydraulic axle, where the hydraulic cylinder is controlled

directly by a speed-regulated hydraulic pump with a built-in safety control unit mounted on a linear unit. The advantage of the design is the small amount of Ionic Liquid and a closed system isolated from the specific environment. The appearance of the unit is shown in Figure 5.

Figure 5: The final appearance of the axis during the testing phase.

7   Conclusion

In this paper, the process of developing a new type of potential hydraulic fluid, from the first idea to the first industrial application, is presented on the example of an ionic fluid. The path of development is very long, and usually requires the involvement of experts from various fields, and takes place over at least five stages: From setting target properties, through screening suitable candidates, extensive and varied laboratory tests, and only through long-term laboratory tests of fluid endurance under real operating conditions and components, we arrive at the first application. Based on the feedbacks received, however, certain steps (if necessary) need to be repeated.

References

[1]   Kalb, R. (2015). Ionic liquids – A New Generation of High-Tech Engineering Liquids, A Review. International conference Fluid Power 2015, Maribor. University of Maribor. Proceedings. ISBN 978-961-248-491-0, 49-77.

[2]   Laus, G., Bentivoglio, G., Schottenberger, H., Kahlenberg, V., Kopacka, H., Röder, T., Sixta, H. (2005). Ionic liquids: Current developments, potential and drawbacks for industrial applications, Lenzinger Berichte. 84. 71-85.

[3]   Gabriel, S., Weiner, J. (1988). Über einige Abkömmlinge des Propylamins. Berichte der deutschen chemischen Gesellschaft, Vol. 21. No. 2. 2669-2679.

[4]   Kambič, M., Lovrec, D. (2011). Hidravlične tekočine prihodnosti: na poti iskanja idealne hidravlične tekočine. Mednarodna konferenca Fluidna tehnika 2011, Maribor. Univerza v Mariboru. 149-162.

[5]   Lovrec, D. (2017). Corrosion protection properties of ionic liquids. ISCAME 2017. 5th International Scientific Conference on Advances in Mechanical Engineering, 017 Debrecen. Hungary. Debrecen: Faculty of Engineering. 306-311.

[6]   Lovrec, D. (2017). Ionic liquid as a novel, high performance hydraulic fluid - selection process. ISCAME 2017, 5th International Scientific Conference on Advances in Mechanical Engineering, Debrecen. Hungary. Debrecen: Faculty of Engineering, 300-305.

[7]   Kambič, M., Kalb, R., Lovrec, D. (2015). Lubrication properties of ionic liquids suiTable for use within hydraulic systems. Proceedings of International Conference Fluid Power 2015, University of Maribor. 79-93.

[8]   Lovrec, D., Tič, V. (2019). Excellent lubricating properties of ionic liquid - myth or truth. Serbiatrib '19 - 16th International Conference on Tribology, Kragujevac. Serbia. ISSN 2620-2832, Vol. 1. No. 1. University of Kragujevac. Faculty of engineering. 555-562.

[9]   Kambič, M., Kalb, R., Tašner, T., Lovrec, D. (2014). High Bulk Modulus of Ionic Liquid and Effects on Performance of Hydraulic System, The scientific world journal, ISSN 1537-744X. Vol. 2014. Art. No. 504762. 1-10, doi: 10.1155/2014/504762.

[10]   Tič, V., Manhartsgruber, B., Gubeljak, N., Lovrec, D. (2018). Low compressibility of ionic liquids and its effects on pulsation within hydraulic system. 11th International Fluid Power Conference, Vol. 1. Aachen. Germany. 486-493.

[11]   Lovrec, D. (2017). Filterability of ionic liquid used as a hydraulic fluid. The 5th Virtual Multidisciplinary Conference QUAESTI. Zilina, Slovak Republic. ISSN 2453-7144. Vol. 5. Iss. 1. EDIS - Publishing Institution of the University of Zilina. 160-164.

[12]   Lovrec, D., Tič, V. (2020). Ionic liquids as wide operating temperature range lubricant. New technologies, development and application III, Sarajevo, Bosnia and Herzegovina. ISSN 2367-3370. Vol. 128). Cham: Springer. cop. 2020. Vol. 128. 348-359.

[13]   Kambič, M., Kalb, R., Tič, V., Lovrec, D. (2018). Compatibility of ionic liquids with hydraulic system components. Advances in production engineering & management, ISSN 1854-6250. Vol. 13. No. 4. 492-503. doi: 10.14743/apem2018.4.306.

[14]   Kambič, M., Lovrec, D. (2017). Problems of testing new hydraulic fluids. Internal conference Fluid Power 2017. Conference proceedings. 1st ed. Maribor. University of Maribor Press. 281-293.

[15]   Lovrec, D., Tič, V. (2021). A new approach for long-term testing of new hydraulic fluids. New technologies, development and application IV, International Conference New Technologies, Development and Application. Sarajevo. Bosnia and Herzegovina. ISSN 2367-3370. Vol. 233. Cham: Springer Natur. cop. 2021. 788-801.

[16]   Lovrec, D. (2018), Ionic liquids vs. conventional hydraulic oils a comparison of properties and challenges. TMT 2018 - 21st International Research/Expert Conference "Trends in the Development of Machinery and Associated Technology", Karlovy Vary. Czech Republic. ISSN 1840-4944. Year 21. No. 1.: University of Zenica. 73-76.

[17]   Lovrec, D., Kalb, R., Tič, V. (2020). Basic aspects when using ionic liquids as a hydraulic fluid. 12th International Fluid Power Conference - 12. IFK, Dresden. Vol. 1. Technische Universität Dresden. 273-282.

University of Maribor Press

Electrically tuneable viscosity of Ionic Liquids

VITO TIČ

Abstract Viscosity is an essential property of lubricant, as it affects its capacity to form the lubricating film or to reduce friction and wear. One of highly desirable effect in tribology is to be able to control the viscosity of the lubricant externally in real-time without changing the lubricant. One of the possibilities is to apply an electric field to the lubricant. Since ionic liquids are solvent-free electrolytes, their properties can be usually altered by applying voltage. This preliminary research results reveal that viscosity of tested ionic liquid can be tuned by means of applying DC voltage.

Keywords: • ionic liquid • viscosity • friction • electric field • hydraulic fluid •

_____
CORRESPONDENCE ADDRESS: Vito Tič, University of Maribor, Faculty of Mechanical Engineering, Smetanova ulica 17, 2000 Maribor, Slovenia, e-mail: vito.tic@um.si.

1   Introduction

The simplified definition of "ionic liquids" says that ionic liquids (ILs) are liquid or molten salts. The ionic liquid consists fully of ions. Cations (usually organic) and anions (usually inorganic) present in ionic liquids are so formulated that the resulting salts hardly crystallize. Therefore, the ionic liquid is liquid in a wide temperature range [1]. An important feature of ionic liquids is the possibility of adaption of these physical-chemical properties through changing the nature of the anion and cation. The number of possible combinations is extremely high, that is why the best ionic liquid is supposed to be adapted for any case of use.

Another important feature of ionic liquids is the fact, that the ionic liquids are solvent-free electrolytes, so their properties can be usually altered by applying voltage. Several studies [2-5], which reveal that tribological properties of ionic liquids can be electrically tuned, were inspiration to us to conduct a preliminary research on possibility of electrically adjusting viscosity of tested ionic liquid. Namely, previous researches conducted at University of Maribor showed that selected IL for testing is a very promising candidate for new state-of-the-art lubricant and hydraulic fluid.

2   Ionic Liquids as lubricants

The ionic liquid lubricating properties have been tested many times in many ways. It has been proved that in most cases they are better than the conventional lubricants' properties. That can be explained with the fact that ionic liquid have a unique bipolar structure allowing them easy adsorption to sliding surfaces of mechanical parts in contact. Consequently, an effective boundary film reducing friction and wear is formed. That applies, particularly, to lower contact pressures and large surface areas.

Because of many good properties the ionic liquids are ideal candidates for new lubricants usable in harsh operating conditions, where conventional oils and greases or solid lubricants fail. A few studies in this sphere have already been carried out.

The cation and anion selection in ionic liquid and forming of ion side chains impose the basic ionic liquid properties, resulting in creation of adapted lubricants and lubricant additives [6]. For the first time, the ionic liquid as very

promising highly capable lubricants were mentioned in 2001 [7], lately, they have aroused high interest in the sphere of tribology.

3 Viscosity of ionic liquids

As there are a great number of possible ionic liquids, there are also so many different viscosities; usually, they are in the range from 0.035 to 0.500 Pas [8]. Similarly as in mineral oils the temperature in numerous ionic liquids has a strong impact on viscosity. In researches, so far, it has been proved that contaminants, particularly water (even small quantity from ambient air), have a great influence on the measured viscosities.

Viscosity of ionic liquids can be measured by one of the three viscometer types: with falling ball, capillary or rotational. So far we have measured kinematic viscosity of selected and tested IL, which is 18.6 mm²/s at 40 °C and 5.1 mm²/s at 100 °C with a viscosity index of 229, making it a perfect candidate for a low friction and low viscosity energy saving lubricant.

In order to be able to apply electrical voltage to the ionic liquid during the test, the rotational viscometer was chosen for this experimental setup. Rotational viscometer is such a type where a solid shaped body named cylinder or spindle is rotated immersing in the fluid whose viscosity is to be measured. A typical rotational viscometers work on the principle that the torque required to turn an object in a fluid is a function of the viscosity of that fluid. From the measurements of rotational speed of the solid body and the required torque, the viscosity is calculated.

4 Measurement setup

The dynamic viscosity of tested IL at room temperature (approx. 20 °C) was measured using Fungilab Smart rotational viscometer with cube (ф 19 mm) and sphere (ф 17,5 mm x 32 mm) setup. To test the possibility of adjusting viscosity by means of applying electrical field to the ionic liquid, a DC voltage ranging from 4 V to 7 V was applied between the cube and the rotating sphere, as shown in Figure 1. While applying the electrical field to the tested IL, the dynamic viscosity was constantly measured and recorded. Additionally, also the electrical voltage and electrical current were measured and recorded.
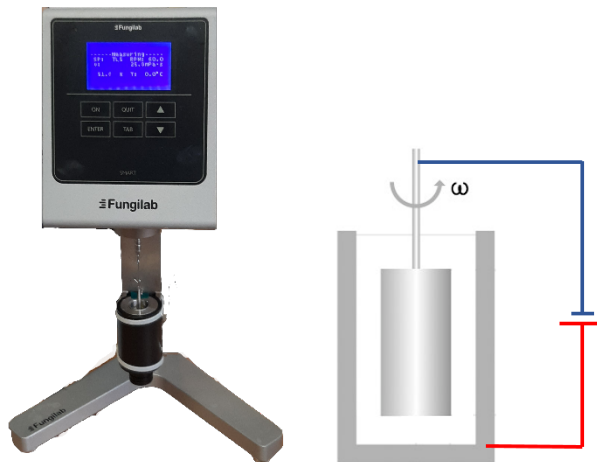
**Figure 1: Fungilab Smart rotational viscometer (left)
and scheme of applied voltage to tested liqud (right).**

5   Results

Since tested IL is electrically conductive (as well as most ILs), an electrical current passes through the liquid when voltage is applied, as results show in Table 1. Given the gap of 0.75 mm between the rotated sphere and cup we needed to apply at least 5 V of DC voltage between the sphere and the cup in order to alter the viscosity of tested IL.

After applying more voltage (7 V) the first tests have revealed that the dynamic viscosity of IL at room temperature can be raised from starting 30 mPas to 200 mPas and even higher, resulting in more than 600 % increase in dynamic viscosity. Of course, some equipment and test limitations occurred when trying to dynamically, in real-time, measure viscosity over such broad band.

After performing first tests to confirm that the dynamic viscosity of tested IL can be heavily influenced by applying and electrical field, we made several measurements (presented in Table 1) by applying different DC voltages from 4 V to 7 V. It can be seen that the current passing through the liquid is not linear to applied voltage.

Table 1: Measurement results

Voltage [V]	Average Current [A]	Viscosity without applied electric field [mPas]	Viscosity with applied electric field [mPas]
4	0.01	30	30
5	0.03	30	35
5.5	0.3	30	> 100 (out of range)
6	0.6	30	> 100 (out of range)
7	1.2	30	> 100 (out of range)

The results confirm that electrical field applied to tested IL affects its bipolar structure and thus its tribological properties since electric excitation changes the position and alignment of cations and anions.

The rate of viscosity change for two measurements at 5.5 V and 6.5 V is presented in Figure 2. Since this setup of rotational viscometer allowed us only measurements up to 100 mPas, in the first measurement 5.5 V was applied to IL between 0 and 20 seconds, and 6.5 V was applied to IL between 0 and 10 seconds in second measurement. The results reveal that higher voltage raises viscosity more quickly in comparison to lower voltage. It can also be seen, that viscosity is also altered for some period of time even after the voltage is disconnected.
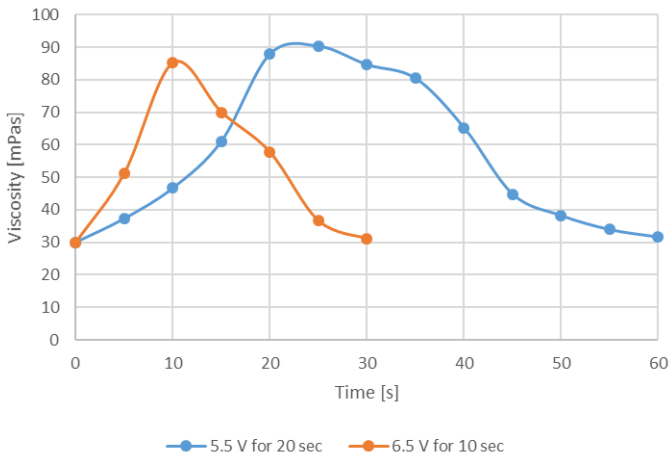
Figure 2: Ionic liquid viscosity change when applying DC voltage.

During the test we have noticed some changes to the ionic liquid. When applying more voltage and heavily rising the viscosity, the tested IL begun to foam at the surface. Also, when we have performed several measurements and raised the viscosity several times, the liquid changed its colour and became much darker. And at the end, we could not repeat the first test (7 V) to rise the viscosity up to 600 %. Thus, we assume that not only the colour, but also the structure and properties of tested IL have permanently changed.

6   Conclusion

The paper presents preliminary research findings about the possibility of electrically adjusting viscosity of tested IL (producer ProIonic GmbH) as a very promising candidate for new state-of-the-art lubricant and hydraulic fluid. Although results confirm that the viscosity can be raised by applying voltage to tested IL, the preliminary research left us with more questions then has given us answers. Definitely, more detailed research with better equipment is suggested in the future to investigate the effects of applying different electric fields to IL, such as AC, DC or PWM with different frequencies and amplitues.

References

[1]   Laus, G., Bentivoglio, G., Schottenberger, H., Kahlenberg, V., Kopacka, H., Röder, T., Sixta, H. (2005). Ionic liquids: Current developments, potential and drawbacks for industrial applications. *Lenzinger Berichte*, *84*, 71-85.

[2]   Michalec, M., Svoboda, P., Krupka, I. et al. (2020). Investigation of the tribological performance of ionic liquids in non-conformal EHL contacts under electric field activation. *Friction, 8*, 982–994. https://doi.org/10.1007/s40544-019-0342-y

[3]   Fajardo, O., Bresme, F., Kornyshev, A. et al. (2015). Electrotunable Lubricity with Ionic Liquid Nanoscale Films. *Sci Rep 5, 7698*. https://doi.org/10.1038/srep07698

[4]   Li, H., Wood, R. J., Rutland, M. W., Atkin, R. (2014). An ionic liquid lubricant enables superlubricity to be "switched on" in situ using an electrical potential. *Chem. Commun., 50-33*. 4368-4370. https://doi.org/10.1039/C4CC00979G

[5]   Gatti, F., Amann, T., Kailer, A. et al. (2020). Towards programmable friction: control of lubrication with ionic liquid mixtures by automated electrical regulation. *Sci Rep 10, 17634*. https://doi.org/10.1038/s41598-020-74709-2

[6]   Pensado, A.S., Comunas, M.J.P., Fernandez J. (2008). The pressure-viscosity coefficient of several ionic liquids, *Tribology Letters, 31-2*, 107-118.

[7]   Feng, Z., Yongmin, L., Weimin, L. (2009). Ionic liquid lubricants: designed chemistry for engineering applications. *Chemical Society Reviews, 9-38*, 2590-2599.

[8]   Joglekar, H. G., Rahman, I., Kulkarni, B.D. (2007). The path ahead for ionic liquids. *Chemical Engineering Technology, 30-7*, 819-828.

University of Maribor Press

Premium quality hydraulic oils

MILAN KAMBIČ

Abstract The base of the final product is the base oil. The final product is ready for use and is a mixture of base oil (or several base oils) and additives. Additives improve the properties of the base oil. Base oils can be mineral or synthetic based. Base oils or base stocks are created from separating and cleaning up crude oil. They are one of several liquid components that are created from crude oil. The crude oil refining process will be briefly described. The American Petroleum Institute implemented a system for describing various base oil types. The result was the development and introduction of base oils group numbers. The API numbers of various base oil groups and the main differences between them will be explained. At the end, premium quality hydraulic oil and its main characteristics will be presented.

Keywords: • base oils • refining • API group numbers • hydraulic oil • additives •

_____

CORRESPONDENCE ADDRESS: Milan Kambič, Olma d.o.o., Poljska pot 2, 1000 Ljubljana, Slovenia, e-mail: milan.kambic@olma.si.

1   Introduction

The hydraulic fluid is a very important component that is often casually considered. Most often, satisfying the requirements of only the pump seems to be the primary consideration for fluid selection [1]. Although the costs of hydraulic pump failures are generally one of the costlier occurrences within hydraulic systems, erratic operation of valves and actuators due to inadequate oil performance characteristics such as oil degradation (oxidation) that causes deposits to form in critical clearance areas, often leads to costly production losses [1], [2]. With the close clearances, different metallurgies, various elastomers, and high pressures and temperatures, service life and performance of all the system components depend on proper selection and maintenance of the hydraulic fluids.

Hydraulic fluids perform many functions in addition to transmitting pressure and energy. These include minimizing friction and wear, sealing close-clearance parts from leakage, removing heat, minimizing system deposits, flushing away wear particles and contamination, and protecting surfaces from rust and corrosion. The important characteristics of a hydraulic fluid vary by the components used and the severity of service [2]. A number of the physical characteristics and performance qualities of hydraulic fluids commonly required by most hydraulic systems are:

- viscosity,
- viscosity index (VI),
- wear protection capability,
- oxidation stability,
- antifoam and air separation characteristics,
- demulsibility (water-separating characteristics),
- rust protection,
- compatibility.

Oil qualities required by hydraulic systems depend on appliance. From the very beginning of the use of hydraulic fluids, man strives to improve their properties. As a result, in the good two centuries of their use, the number of different fluids used in hydraulic devices today has increased considerably. Each of them has advantages in a particular area of application. For example, water is non-combustible, mineral oil is the most universally useful, biodegradable oils are less

harmful to the environment, hydraulic oils for use in the food industry can come into contact with food etc. However, no liquid is so universal that it can meet sometimes very different or even contradictory requirements in individual applications. Development engineers are therefore still investing a tremendous amount of effort, time and resources in finding a hydraulic fluid that would be close to the ideal hydraulic fluid. Among other things, it should be non-flammable, non-toxic, have excellent lubricating properties, temperature-independent physicochemical properties [3], [4], [5].

The article will present a premium quality hydraulic fluid based on mineral oil. Therefore, the process of production of mineral base oils will be briefly described below.

2 Mineral base oils

The base of the final product is the base oil. The final product is ready for use and is a mixture of base oil (or several base oils) and additives. Additives improve the properties of the base oil. Base oils can be mineral or synthetic based [6].

2.1 Production of mineral base oils

The basic function of a refinery is to separate the crude oil into its useful components and remove the components of unwanted materials. Base oils or base stocks, as they are sometimes called, are created from separating and cleaning up crude oil. They are one of several liquid components that are created from crude oil. Gasoline is the lightest or smallest hydrocarbon component, followed by kerosene, or jet fuel, diesel fuel, base oils, waxes and asphalt or bitumen, which is the heaviest, thickest material. Base oils are prepared from crude oils through the use of the following series of processes which, to same degree, must be applied to all crude oils for refining processes. Base oils are typically created in four different viscosity grades within the refinery distillation process. This allow for the creation of the various ISO and API viscosity grades [6], [7].
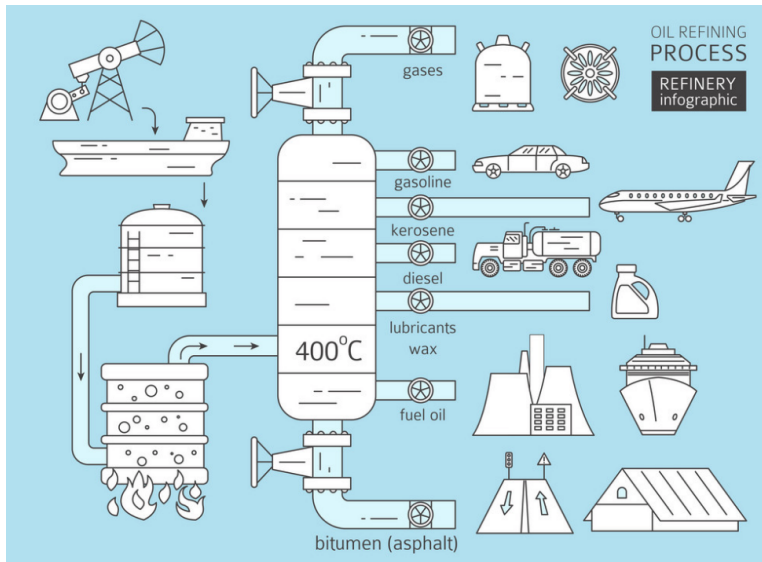
Figure 1: Schematic representation of the crude oil distillation process [8]**.**

Those processes are:

- Atmospheric distillation-is used initially to separate fuel, such as gasoline and diesel, from the remainder of the crude petroleum. Distillation is a separation process. The products of distillation are referred as distillates.
- Vacuum distillation-is performed to distill and therefore separate some heavier fractions that would not distill at atmospheric pressure without damaging them. It is used to obtain the initial base oil viscosity and flash point characteristics. This process provides the four various viscosity fractions (or distillates) from which the finished products are made.
- Refining-is performed to remove unwanted chemical structures (rings, etc.) from the base oil to reduce the tendency of the base oil to age in service and also to improve the viscosity/temperature characteristics.

    Three basic refining processes are used by oil companies:

    a) Sulphuric acid/clay refining (old, out-dated technology);
    b) Solvent extraction;
    c) Catalytic hydrogenation or hydrotreating[1].

---

[1] Hydrofinishing, hydrogenation or "hydrotreating", and high pressure hydrogenation or hydrocracking are three forms of increasing severity of using hydrogen gas to purify or clean crude oil to create base oils.

- De asphalting-is a step in the process to removes the heavy asphalt residue from the useful distillate fractions.
- De-waxing-is a step that is performed to reduce wax content of the base oil in order to improve the low temperature properties of the oil.
- Blending-is the final process in producing a finished lubrication oil. It involves the blending of different base oils to obtain the necessary viscosity, as well as the addition of specified additives to ensure that the finished oil has the right properties to provide to provide the intended lubricating ability.

2.2   API Group numbers

Almost every lubricant used in plants today started off as just a base oil. The American Petroleum Institute (API) has categorized base oils into five categories (API 1509, Appendix E). The first three groups are refined from petroleum crude oil.

Group IV base oils are full synthetic (polyalphaolefin) oils. Group V is for all other base oils not included in Groups I through IV. Before all the additives are added to the mixture, lubricating oils begin as one or more of these five API groups [9].

Group I base oils are the traditional older base oils created by a solvent-refining technology used to remove the weaker chemical structures or bad actors (ring structures, structures with double bonds) from the crude oil. Solvent refining was the primary technology used refineries built between 1940 and 1980. Group I base oils typically range from amber to golden brown in colour due to the sulphur, nitrogen and ring structures remaining in the oil. They typically have viscosity index (VI) from 90 to 105. Group I base oils are the most common type used for industrial oils, although increasingly more Group II base oils are being used [6].

The Table 1 indicates general trends in certain properties and the chemical makeup of some of tGroup I, II, II and IV base oils.

Table 1: General base oil properties [6]

	Naphthenic (Severely hydrotreated)	Group I	Group II	Group III	Group IV
Viscosity index	30-60	95	105	130	130
Pour point (%)	-45	-15	-15	-15	<-60
Volatility (%)	/	25	15	5-10	10
Aniline point (°C)	75	100	115	130	130
% Saturates (Paraffins)	65	80	99	99	100
% Polars & Aromatics	35	20	0,5	0,2	0
Nitrogen (ppm)	/	Up to 60	<5	<1	0
Sulphur (ppm)	0,05	Up to 7.000	10	<5	0

Group II base oils are created by using a hydrotreating process to replace the traditional solvent-refining process. Hydrogen gas is used to remove undesirable components from crude oil. This results in a clear and colourless base oil with very low sulphur, nitrogen or ring structures. The VI is typically above 100. In recent years, the price has become very similar to Group I base oils. Group II base oils are still considered to be mineral oils. They are commonly used in automotive engine oil formulations. Group II "Plus" is a term used for Group II base oils that have a slightly higher VI of approximately 115, although this may not be an officially recognized term by the API.

Group III base oils are again created by using a hydrogen gas process to clean up the crude oil, but this time the process is more severe and is operated at higher temperatures and pressures than used for Group II base oils. The resulting base oil is clear and colour less but also has a VI above 120. In addition, it is more

resistant to oxidation than Group I oils. The cost of Group III base oils is higher than Group I and II. Group III baser oils are considered mineral oils by many technical people because they are derived directly from refining of crude oil. However, they are considered as synthetic base oils by other people for marketing purposes due to belief that the harsher hydrogen process has created new chemical oil structures that were not present before the process. It has synthesized (created) these new hydrocarbon structures.

Group IV base oils are polyalphaolefin (PAO) synthetic base oils that have existed for more than 50 years. They are pure chemicals created in a chemical plant as opposed to being created by distillation and refining of crude oil (as the previous groups were). PAOs fall into the category of synthetic hydrocarbons (SHCs). They have a VI of greater than 120 and are significantly more expensive than group III base oils due to the high degree of processing needed to manufacture them.

Group V base oils comprise all base oils not included in Groups I, II, III and IV. Therefore, naphthenic base oils, various synthetic esters, polyalkilene glycols (PAGs), phosphate esters and others fall into this group.

3   Development of premium quality hydraulic oil Hydrolubric HC VG 46

The motive for the development of premium hydraulic oil is the fact that in recent years the share of hydraulic oils based on base oils of groups II and III has been increasing.

Among other things, we observed a trend in the use of such oils in plastic injection moulding machines. Hydrolubric VG 46 oil (in some cases also Hydrolubric VG 68) has been used successfully for this purpose for a long time. Hydrolubric VG 46 exceeds the oil requirements of one of the well-known manufacturers of plastic injection moulding machines Krauss Maffei. Nevertheless, some lubricant providers have been offering even higher quality oils for use on these machines for the past two or three years. Some users have also chosen to use hydraulic oils based on group II or group III base oils, or have started testing such oils in their machines. This was the main reason why we decided to develop the premium quality hydraulic oil Hydrolubric HC VG 46,

which significantly exceeds the properties of Hydrolubric VG 46 oil in terms of some properties, such as oxidative stability.

HYDROLUBRIC HC VG 46 hydraulic oil consists of specially selected hydrocracked base oils, anti-corrosion, anti-aging, EP and AW additives, viscosity improvers and anti-foaming additives. It has excellent thermal and oxidative stability, filterability (even in the presence of a small amount of water), excellent hydrolytic stability, good air release ability and is not prone to foaming.

Some physical and chemical properties of Hydrolubric HC VG 46 are shown in Table 2.

Table 2: Physical and chemical properties of Hydrolubric HC VG 46

	Method	Unit	Limit value	Measured value
Appearance	visual	/	Clear liquid	Clear liquid
Colour	ASTM D1500		<4	L 0.5
Flash point (COC)	ASTM D92	°C	>185	>240
Density at 20 °C	ISO 12185	kg/m³	850.0-890.0	854.5
Pour point	ASTM D97	°C	<-15	<-33
Viscosity at 40 °C	ASTM D445	mm²/s	41.4-50.6	46.21
Viscosity at 100 °C	ASTM D445	mm²/s	>6.100	7.125
Viscosity index	ASTM D2270	/	>110	113
Total acid number	ASTM D664	mgKOH/g	0.40-0.60	0.41
Copper corrosion	ASTM D130			1b
Oxidation stability, RapidOxy Grease 2	ASTM D8206	min		1067
Deemulsity 40/0/40 (O/E/W)		min	30	<15
Foaming test	ASTM D892	ml/ml	150/0 75/0 150/0	0/0 0/0 0/0

Oxidative stability of Hydrolubric HC VG 46 was measured in comparison with some other Olma mineral-based hydraulic oils ISO VG 46. The RapidOxy 100 tester shown in Figure 2 was used. The results are shown in Table 3.

Figure 2: Oxidation Stability Tester: RapidOxy 100.

Table 3: Comparison of oxidation stability of some Olma hydraulic oils.

Product	Method	Unit	Measured value
Hydroloubric HC VG 46	ASTM D8206	min	1067
Hydrolubric VG 46	ASTM D8206	min	664
Hydrolubric HD 46	ASTM D8206	min	570
Hydrolubric HLP 46	ASTM D8206	min	529
Hydrolubric VGS 46	ASTM D8206	min	672
Hydrolubric HVLP 46	ASTM D8206	min	787
Hydrolubric VG 46 D	ASTM D8206	min	536

Hydrolubric HC VG 46 meets the following specifications:

- DIN 51524/3   HVLP;
- ISO 6743/4   HV;
- ISO 11158   HV;
- Denison   HF-2, HF-0
- Vickers   I-286-S, M-2950-S
- Cincinnati Milacron   P-68, P-69, P-70;
- AFNOR   NFE 48-690 (dry);
- AFNOR   NFE 48-691 (wet);
- AFNOR   NFE 48-603.

After conducting laboratory tests in the laboratory of the company Olma, which confirmed our expectations, we started practical testing in some plastic injection moulding machines Krauss Maffei in three companies. We performed the first analyses of oil samples from these machines. However, it will be necessary to wait a longer time for the conclusions, as we can expect that the service life of the oil under normal conditions of use will be several years.

4   Conclusion

Due to the increase in the share of hydraulic oils based on higher quality base oils, which we have seen on the market in recent years, we decided to develop a premium hydraulic oil Hydrolubric HC VG 46.

Laboratory measurements have confirmed the expectation that this oil will exceed the properties of conventional hydraulic oils. The oxidation stability of this oil is significantly higher than that of other conventional hydraulic oils.

We started practical testing in some plastic injection moulding machines Krauss Maffei in three companies. However, it will be necessary to wait a longer time for the conclusions, as we can expect that the service life of the oil under normal conditions of use will be several years.

References

[1]   Kambič, M., Lovrec, D. Lovrec (2017). Problems of testing new hydraulic fluids. *Fluid power 2017*, Maribor

[2]   Pirro, -M. D., Wessol, A. A. (2001). Lubrication fundamentals, 2nd ed., New York, Basel: Marcel Dekker, Inc

[3]   Kambič, M., Lovrec, D. (2011). Hidravlične tekočine prihodnosti. *Fluidna tehnika 2011*, Maribor

[4]   Kambič, M., Kalb, R. (2013). Comparison of ionic liquids with conventional mineral oils. *Fluid Power 2013*, Maribor

[5]   Kambič, M., Kalb, R., Lovrec, D. Lovrec. (2015). Lubrication properties of ionic liquids suiTable for use within hydraulic systems. *Fluid Power 2021*, Maribor

[6]   Scott, R., Fitch, J., Leugner, L. (2012) The practical handbook of machinery lubrication. Tulsa, Oklahoma: Noria Corporation

[7]   Kambič M., Mineralna bazna olja. *IRT3000*, Izv. 16, št. 114, 2021.

[8]   Noria corporation. Oil refinery process infographic crude oil vector image. [Online]. Available: https://www.vectorstock.com/royalty-free-vector/oil-refinery-process-infographic-crude-oil-vector-35612726. [Accesed 14. 5. 2021].

[9]   Base oil groups explained. *Machinery lubrication*, no. 10, September-October 2012.

University of Maribor Press

Advanced approach to the maintenance of hydraulic and turbine oils

MATTHEW G. HOBBS, JANEZ TOMAŽIN & PETER T. DUFRESNE

Abstract: In the growing power demands, turbine users want to feel confident that their equipment is reliable, efficient, and delivering peak performance every day. Proper care and maintenance of turbine oils is critical to avoiding disruptive and potentially costly downtime, and can help extend oil and component life. The ISO 55001 Asset Management and EN 17485 Maintenance within Physical Asset Management: "Framework for improving the value of the physical assets through their whole life cycle" provides an opportunity for companies to review and improve asset owner and service provider relationships, improve performance and utilisation of assets, reduce operational risk arising from the various stages of asset management and reduce the cost of insurance and ensure regulatory compliance. With such an approach and the use of the best available technology, turbine oil is becoming an asset. This article focuses on turbine oils quality, their degradation, additives and, varnish removal.

Keywords: • asset management • turbine oil •polyalkylene glycol • soluble varnish • removal •

CORRESPONDENCE ADDRESS: Ph. Matthew G. Hobbs, The University of Calgary, Canada, mhobbs@cleanoil.com. Janez Tomažin, Bachelor of Science, Dimas Pro d.o.o., Ljubljana, Slovenia, janez.tomazin@dimaspro.eu Peter T. Dufresne Jr., Economics, Wilfrid Laurier University, 75 University Ave W, Waterloo, Canada, PDufresne@cleanoil.com

1 Introduction

According to Standard ISO 55001, Asset Management is coordinated activity of an organization to realize value from assets. If an organization accepts the fact that turbine oil is an asset and treats it as such, it can also realize value from a variety of perspectives.

If the organisation also follows the guidelines of the European Standard EN 17485 Maintenance within Asset Management, it can realize the value at all stages of the turbine oil life cycle. The Figure 1 shows a combination of both mentioned standards and turbine oil in all phases of its life cycle.
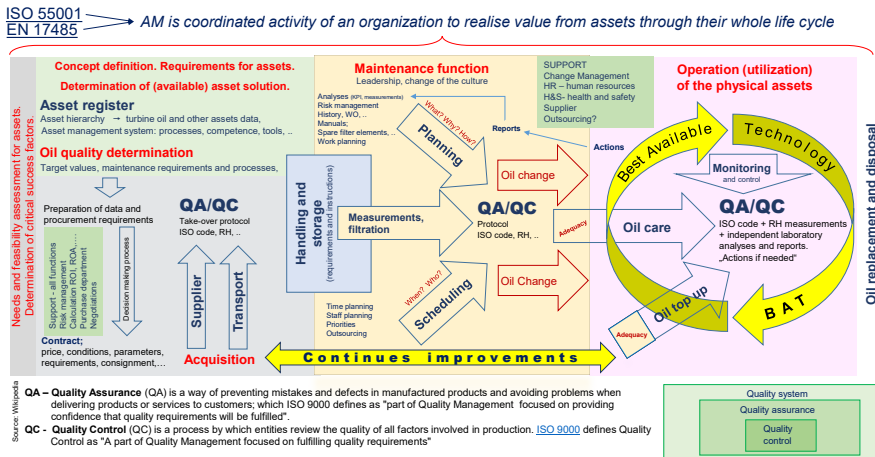
Figure 1: ISO 550001 and EN 17485 Standards and turbine oil care.

Turbine lubricants employ a variety of base fluids. Mineral oil-derived base stocks remain the most prevalent; however, synthetics are becoming increasingly common. These fluids are exposed to severe oxidative stress during service, leading to breakdown and varnishing (the primary cause of downtime in gas turbine applications). Recently, Polyalkylene Glycols – PAGs, have been positioned as varnish-free alternatives to more conventional mineral turbine oils. Our findings suggest that this claim is overstated. PAGs possess several advantages relative to conventional oils, however, well-formulated mineral oils proved almost as resistant to varnishing. Moreover, the risks associated with mineral oil varnishing can be effectively mitigated using established varnish-removal technologies.

2 Modern lubricants

Modern lubricants are formulated using a variety of base fluids and additives [1]. Many different base stocks are available. Those derived from crude oil (Groups I, II and III) are the most common as a result of their favourable lubrication properties and relatively low cost. Group IV and V fluids are made up of synthetic hydrocarbons and non-hydrocarbon synthetics, respectively. These synthetics generally feature improved performance and resistance to breakdown relative to their naturally-derived Group I – III analogues. These improved characteristics, however, typically come at a higher cost.

In gas turbine applications, the trend towards smaller, more powerful units and peaking in place of base load service has resulted in increased lubricant stress. Indeed, modern gas turbine peak temperatures may reach 150 – 280 °C [2]. During service, thermo-oxidative lubricant breakdown yields polar degradation products (acids and other varnish precursors) from non-polar base fluid hydrocarbons. With regards to polarity, "like dissolves like", therefore, polar degradation products often precipitate from non-polar hydrocarbon oils. As these breakdown products fall out of solution, organic varnish deposits form, leading to numerous problems including: filter plugging, restricted oil flow, poor heat transfer, valve sticking, fail-to-start conditions and costly unit trips [3]. Varnish is now the leading cause of unplanned downtime in the power generation industry.

PAGs are specialized Group V synthetics that have been positioned as more oxidative sTable, non-varnishing substitutes to conventional turbine lubricants [4]. PAGs are polyethers which feature oxygen amongst the carbon and hydrogen in their base oil molecular structure (Figure 2). As a result, they are more polar than hydrocarbon mineral oils. Like mineral oils, thermo-oxidative PAG stress yields polar breakdown products. PAG lubricants are, however, better able to dissolve these polar varnish precursors as a consequence of their own polarity. As a result, PAGs are often referred to as "non-varnishing" lubricants. While PAGs may indeed offer technical advantages over conventional turbine lubricants (lower coefficient of friction, greater viscosity index, faster air release), relatively inexpensive varnish removal technologies have been shown to effectively mitigate the risks associated with varnishing [5].
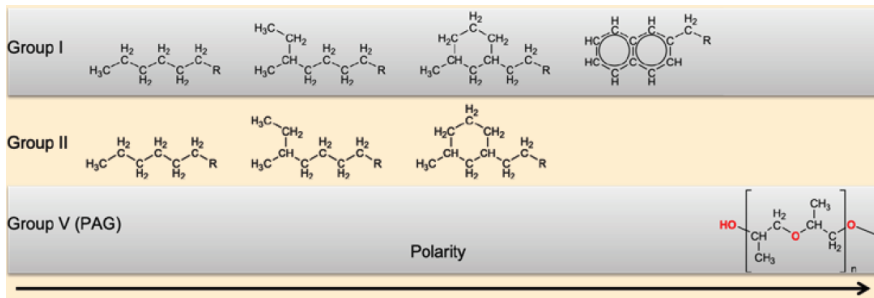
Figure 2: Typical Steam Turbine Bearing Arrangement.

To date, head-to-head comparisons of established hydrocarbon turbine lubricants and newer PAGs are lacking. PAGs undoubtedly represent an advancement in lubrication technology, however, their increased cost relative to the use of varnish-removal filters and well-formulated mineral oils has not yet been justified. Moreover, claims that PAG lubricants are non-deposit-forming require empirical confirmation.

3   Thermo-oxidative lubricant breakdown: Varnish formation in mineral oils versus PAGs

PAGs are often described as being more oxidatively sTable than mineral oils. In an effort to evaluate the oxidative stability of PAGs relative to more conventional oils, EPT subjected three commercially available virgin gas turbine lubricants to severe thermo-oxidative stress. The three turbine oils evaluated included a Group I oil (A), a Group II oil (B) and a Group V PAG (C). Dry air was passed through the stirred turbine oils while they were heated to 150 °C in the presence of an ASTM-standard copper strip [6]. The test temperature of 150 °C was selected to be representative of the peak temperatures experienced by gas turbine lubricants during service. Aliquots of the degrading lubricants were collected regularly to monitor their properties. The following tests were used to evaluate the condition of the lubricants:

- Varnish potential analysis by membrane patch colorimetry (MPC) [7].
- Potentiometric acid number analysis [8].
- RULER antioxidant additive analysis [9].

3.1   Group I turbine oils

As anticipated, the Group I turbine oil A was the least sTable of the three commercial turbine oils examined (Figure 3). Indeed, critical levels of organic varnish were detected in this fluid by MPC analysis after only 2 hours at 150 °C. While the varnish potential of this oil increased rapidly, its acid levels were quite sTable initially. Once the oil's amine antioxidant additive depleted, however, its acid number increased dramatically. This acid number increase occurred despite the continuing presence of phenol antioxidants. These results suggest that the amine additive plays a key role in mitigating acid build-up in this lubricant. The phenol additive appeared to be ineffective with regards to acid management and synergistic regeneration of the more vital amine additive. Clearly both additives were poorly suited to manage the build-up of the organic breakdown products which produce varnish as the fluid's MPC varnish potential became critical before any additive loss occurred.
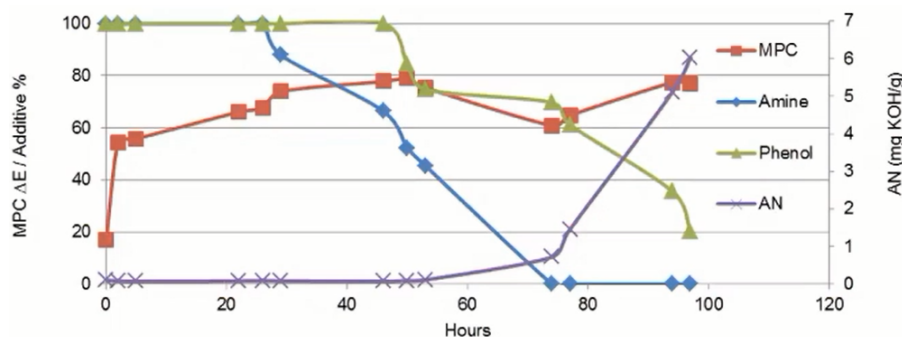
Figure 3: Properties of the Group I Commercial Turbine Oil (A) During Thermo-Oxidative Degradation.

3.2   Group II turbine oils

Unlike the Group I fluid examined earlier, the Group II turbine oil (B) proved to be quite robust (Figure 4). While the varnish potential of A reached critical levels in only 2 hours, 384 hours were required to breakdown B to a similar degree. Even after 1,224 hours at 150 °C, no significant change in the acid number of the Group II oil was noted. This is in stark contrast to the Group I lubricant whose acid number increased by more than 60 times following 97 hours

of thermo-oxidative stress. The antioxidants present in B also appeared to function as intended with phenols depleting prior to amine additives. An inverse correlation between the oil's antioxidant amine levels and its MPC varnish potential was observed; as amine depletion proceeded, the fluid's MPC values increased accordingly. All-together, these results suggest that lubricant B is comprised of an oxidative sTable base stock which benefits from effective antioxidant protection.
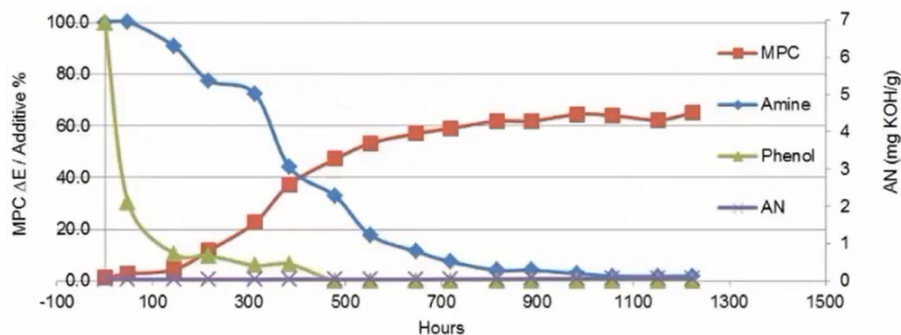
Figure 4: Properties of the Group II Commercial Turbine Oil (B) During Thermo-Oxidative Degradation.

3.3   Group V PAG turbine oils

Of the three turbine oils tested, PAG C was, as expected, the most resistant to the formation of varnish (Figure 5).
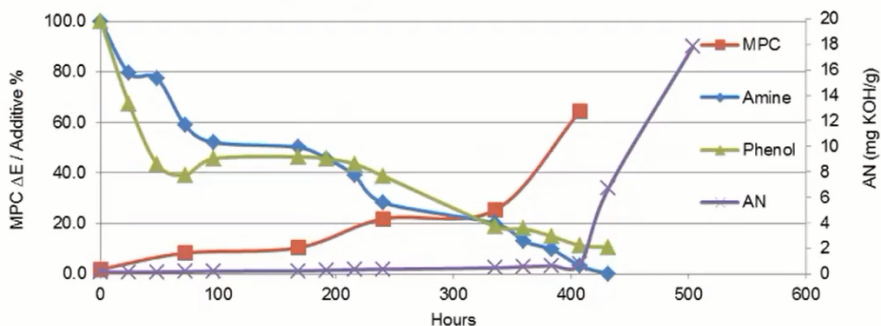
Figure 5: Properties of the Group V PAG Commercial Turbine Oil (C) During Thermo-Oxidative Degradation.

Be that as it may, the PAG lubricant did not outperform mineral oil B by a significant margin in this regard; while 384 hours at 150 °C were required for B to reach a critical MPC varnish potential, 408 hours under identical conditions were required for C to reach analogous varnish levels (Table 1).

Table 1: Degradation time required for turbine oil properties to reach critical values

TURBINE OIL	PROPERTY	MOST DEGRADED MEASUREMENT	DEGRADATION HOURS TO CRITICAL
Group I A	MPC ΔE	79.0	2
	AN (mg KOH/g)	6.02	74
	Antioxidant %	0 (Amine); 20 (Phenol)	74
Group II B	MPC ΔE	65.2	384
	AN (mg KOH/g)	0.06	> 1,224
	Antioxidant %	2 (Amine); 0 (Phenol)	552
Group V PAG C	MPC ΔE	64.5	408
	AN (mg KOH/g)	17.83	192
	Antioxidant %	0 (Amine); 11 (Phenol)	336

The observation of organic deposits on an MPC filter patch suggests that PAG lubricant breakdown can, indeed, lead to the formation of varnish on turbine surfaces; this is in contrast to the claims espoused by proponents of PAG use in gas turbine applications.

While PAG oil C and Group II lubricant B produced similar levels of varnish over a similar timeframe, the PAG fluid produced significantly more acid than B. Whereas critical acid levels never accumulated in B, critical acid levels were observed following 192 hours of PAG breakdown. Alarmingly, PAG breakdown accelerated exponentially beyond a certain point; within a 24 hour period, the acid number of C jumped from 0.79 mg KOH/g to 6.7 mg KOH/g. This jump appears to correspond with the exhaustion of the lubricant's amine antioxidant. Once the amine was exhausted, the PAG's acid number rapidly became extreme (17.83 mg KOH/g) and the lubricant became highly viscous. This level of acidic breakdown products was far beyond the highest observed for either the Group I or Group II mineral oils (6.02 and 0.06 mg KOH/g, respectively). Steady increases in the varnish potential of C accompanied the fluid's acid number

increases, suggesting that the deposits produced by PAGs are the result of breakdown mechanisms similar to those established for mineral oils. Despite the presence of critical acid levels after 192 hours, critical varnish potentials were not observed until 408 hours. This is a testament to the superior polarity/solvency of PAG lubricants. Indeed, C darkened significantly within 2 hours of heating, suggesting that breakdown products were already dissolved in the fluid at this time. By contrast, the Group II oil remained "clear and bright" after more than 1,000 hours at 150 °C.

4   Varnish removal

The prevalence and potential economic impact of varnishing in gas turbine applications is so significant that original equipment manufacturers (OEMs) recommend the use of varnish removal systems to mitigate risk [10]. These removal systems can be categorized as either particulate removal systems or soluble varnish removal (SVR) systems. Particle removal systems function on the basis of mechanical filtration, removing insoluble varnish but leaving its soluble precursors (breakdown products) behind. Since varnish can be dissolved in fluids at higher operating temperatures, these systems are most effective during shutdowns and are ill-suited to continuous use during operation. These systems cannot remove dissolved varnish feedstocks; they eliminate the effect (insoluble varnish) but not the cause (soluble varnish/breakdown products) of varnishing problems.

SVR systems are engineered to remove soluble contaminants and degradation products (including varnish and acids) from lubricants. Unlike particulate removal systems, SVR systems are effective at turbine operating temperatures, meaning that they can be employed continuously. This makes these systems ideally suited for lubricant restoration or maintenance. By removing soluble breakdown products, SVR systems effectively mitigate the risks associated with lubricant varnishing.

In an effort to demonstrate the potential benefit of SVR treatment, duplicate samples of the Group I mineral oil A were degraded at 90 °C. The duplicate samples were subjected to identical conditions with and without laboratory-scale SVR treatment. A was selected as its poor oxidative stability was expected to lead to observable varnish formation within a reasonable experimental timeframe.

The MPC varnish potential of the duplicate samples was monitored regularly as thermo-oxidative degradation proceeded (Figure 6).
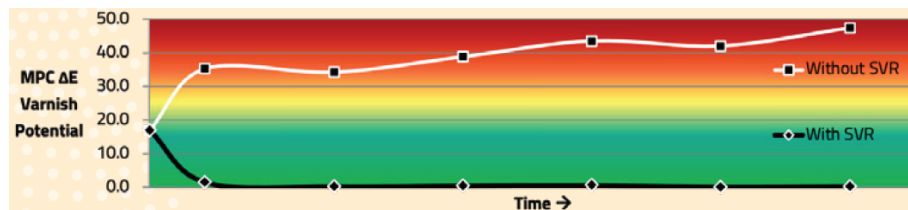
Figure 6: MPC Varnish Potential of Group I Oil A Samples Degraded With and Without SVR Treatment.

This side-by-side breakdown experiment yielded dramatic results. As anticipated, the varnish potential of the untreated fluid increased rapidly, reaching critical levels within 72 hours. Beyond this initially rapid MPC increase, breakdown products continued to accumulate at a relatively steady rate.

By contrast, the varnish potential of the SVR-treated oil actually decreased following the application of thermo-oxidative stress. By the time that the untreated sample's varnish potential had become critical, the SVR-treated oil featured a near-zero MPC ΔE. The initial MPC decrease noted occurred as a result of SVR removing the relatively low levels of breakdown products that were already present in the initial new oil sample. Impressively, as the degradation continued, SVR treatment maintained the lubricant's near-zero varnish potential for the duration of the experiment (1,272 hours). These results clearly demonstrate the advantages of continuous SVR filtration, which allows varnish and its precursors to be effectively removed as they form, preventing varnish problems all-together.

Although the more oxidative robust PAG oil C could not be broken down/ treated by SVR within a reasonable experimental timeframe, lab-scale SVR treatment of the virgin PAG lubricant confirmed that it is compatible with SVR filtration media (Table 2). These results suggest that, in addition to being beneficial with mineral oils, SVR treatment can be used to maintain PAG lubricants as well.

Table 2: Properties of virgin PAG turbine oil C prior to and following laboratory-scale SVR treatment

FLUID	AN (MG KOH/G)	AMINE (%)	PHENOL (%)
PAG C	0.14	100	100
SVR-Treated C	0.13	100	100
Change	- 7%	- 0%	- 0%

5   Summary

Modern turbine lubricants are formulated using a variety of base fluids and additives. Mineral oil-derived base stocks (Groups I, II and III) remain the most prevalent, however, hydrocarbon and non-hydrocarbon synthetics (Groups IV and V, respectively) are becoming increasingly common in gas turbine applications. These fluids are exposed to high levels of thermo-oxidative stress during service, leading to lubricant breakdown and varnishing which has been identified as the primary cause of downtime in the power generation industry. Among the Group V oils employed, PAGs have been positioned as varnish-free alternatives due to their inherent oxidative stability and superior base stock solvency.

In an effort to better understand the manner in which different turbine oils breakdown under thermo-oxidative stress, 3 commercially available virgin turbine lubricants were subjected to conditions representative of those present in an operating gas turbine.

As anticipated, the Group I mineral oil A exhibited the poorest oxidative stability. Indeed, this fluid broke down rapidly (< 2hours) under the test conditions. The more highly refined Group II mineral oil B, on the other hand, proved quite robust requiring nearly 200 times longer (384 hours) than its Group I analogue to degrade. Lastly, the PAG alternative C proved to be the most resistant to varnishing, requiring 408 hours to reach a critical varnish potential. Despite this finding, we must note that PAG C did not outperform mineral oil B by a significant margin in this regard. Indeed, while C slightly outperformed B from an MPC perspective, B dramatically outperformed C from an acid number standpoint. The ability of PAG C to hold such high acid levels is, no doubt, evidence of its superior base fluid solvency. The eventual observation of organic

deposits on an MPC filter patch, however, suggests that PAG C is not non-varnishing as claimed.

While the production of varnish from mineral oil breakdown is well-established, OEM-recommended technologies provide a convenient means of managing the risk of varnish-related failures in gas turbine applications.

Varnish-removal technologies can be divided into particulate-removal systems and soluble varnish removal (SVR) systems. The latter are more effective under turbine operating conditions since varnish tends to be dissolved in turbine oils at operating temperatures. In an effort to demonstrate the effectiveness of SVR treatment, duplicate samples of turbine oil A were degraded under identical conditions; one sample was continuously treated with SVR while the other was not. As before, the untreated sample broke down rapidly, reaching a critical varnish potential. The varnish potential of the SVR-treated sample, however, fell to near-zero levels and remained there over the duration of the experiment (1,272 hours). Lab-scale tests also suggest that SVR filtration is compatible with PAG turbine oils and that these fluids would benefit from SVR treatment in the same manner that mineral oils do.

While PAG turbine oils undoubtedly offer advantages relative to their more-established mineral oil analogs, their performance in these trials was not notably superior to well-formulated mineral oils with highly refined base stocks. Moreover, the evidence presented herein suggests that the description of PAG turbine oils as non-varnishing fluids is overstated. Like other lubricants, severe thermo-oxidative stress leads to the formation of organic deposits (varnish) in PAGs. The solvency of PAGs is, undoubtedly, superior to that of mineral turbine oils, however, soluble varnish removal provides an effective means of overcoming this limitation in the latter.

References

[1] Mortier, R. M., Fox, M. F., Orszulik, S. T. (2010). Chemistry and Technology of Lubricants. 3rd Edition. Springer Netherland. ISBN 978-1-4020-8661-8. 560.
[2] Noria Corporation (2013). Fundamentals of Machinery Lubrication. training material. 219.
[3] Atherton, B. (2007). Discovering the Root Cause of Varnish Formation, Machinery Lubrication. Noria Corporation. Tulsa, OK

[4]   Khemchandani, G. (2011) Non- Varnishing and Tribological Characteristics of Polyalkylene Glycol-Based Synthetic Turbine Fluid. *Lubrication Science*, 24/1, 11-21.

[5]   Dufresne, P., Hobbs, M. G. MacInnis, G. (2013). Lubricant Varnishing and Mitigation Strategies. *Combined Cycle Journal*. Q4. 34-40.

[6]   ASTM International. (2012). ASTM D130-12: Standard Test Method for Corrosiveness to Copper from Petroleum Products by Copper Strip Test. *Book of ASTM Standards*, West Conshohocken, PA.

[7]   ASTM International. (2012). ASTM D7843-12: Standard Test Method for Measurement of Lubricant Generated Insoluble Color Bodies in In-Service Turbine Oils using Membrane Patch Colorimetry. *Book of ASTM Standards*. West Conshohocken. PA.

[8]   ASTM International. (2011). ASTM D664-11a: Standard Test Method for Acid Number of Petroleum Products by Potentiometric Titration. *Book of ASTM Standards*, West Conshohocken. PA.

[9]   ASTM International (2014). ASTM D6971-09(2014): Standard Test Method for Measurement of Hindered Phenolic and Aromatic Amine Antioxidant Content in Non-zinc Turbine Oils by Linear Sweep Voltammetry. *Book of ASTM Standards*, West Conshohocken, PA.

[11]   GE Customer Technology Services (2005). Lube Oil Varnishing. *General Electric Technical Information Letter*, TIL1528-3. General Electric.

University of Maribor Press

Development of portable filtration unit with self-diagnostics for industrial use

NEJC NOVAK, ROK JELOVČAN & FRANC MAJDIČ

Abstract It is well known that contamination of fluids shortens the life of hydraulic systems. Sometimes the necessary operating conditions (high pressures and high flow rates) make adequate filtration in the suction, working, or return lines through the filter difficult because it would interfere with the work process. A high cleanliness of the oil can be achieved with a so-called "bypass" filtration, which is part of the whole hydraulic device with its own circuit. Another way to ensure fluid cleanliness is to filter the hydraulic fluid with a portable filtration unit, which is the main topic of this paper. The fluid is pumped from the reservoir of the main hydraulic device, through the portable filtration unit and returned to the reservoir. In this way it is possible to clean the hydraulic oil without the need for costly and unnecessary "bypass" hydraulic components for filtration.

Keywords: • portable filtration unit • self-diagnostics • filters • wear particles • hydraulic oil •

CORRESPONDENCE ADDRESS: Nejc Novak, University of Ljubljana, Faculty of Mechanical Engineering, Aškerčeva cesta 6, 1000 Ljubljana, Slovenia, e-mail: nejc.novak@fs.uni-lj.si. Rok Jelovčan, University of Ljubljana, Faculty of Mechanical Engineering, Aškerčeva cesta 6, 1000 Ljubljana, Slovenia, e-mail: rok.jelovcan@fs.uni.lj.si Franc Majdič, University of Ljubljana, Faculty of Mechanical Engineering, Aškerčeva cesta 6, 1000 Ljubljana, Slovenia, e-mail: franc.majdic@fs.uni.lj.si.

1   Introduction

Hydraulic filtration is a physical separation process in which solid particles are separated from the fluid using a filter medium. The process improves the cleanliness of hydraulic oil and also reduces miniature damage (wear) to pumps, valves, motors and other hydraulic components that are more sensitive to high levels of fluid contamination. Researchers at the University of Valencia describe the importance of "oil analysis used for reducing maintenance costs, improving reliability and productivity and providing peace of mind in different industry areas" and invested in an analytical approach to relate wear rate and oil analysis results [1]. T. M. Hunt emphasizes the importance of wear particle analysis and detection of particles in fluids to improve system life [2]. A recent study shows the importance of in-line monitoring of hydraulic oil contamination to improve the performance of hydraulic excavators [3]. Another study considers diagnostics and prognostics as the two main aspects to efficiently maintaining a machine in "good shape". This is a so-called Condition Based Maintenance (CBM) [4]. K. F. Martin in his paper discusses necessity for planned maintenance, condition-based maintenance and condition monitoring [5]. Scientists at the University of Novi Sad investigated how to increase the efficiency of hydraulic systems through reliability theory and monitoring of the system's operating parameters [6].

It is obvious that monitoring of parameters is important throughout the life of the machine and the need for it is growing daily. But there are setbacks for machines with self-diagnostic systems, because they are more expansive.

In our laboratory we have developed a portable filtration unit with self-diagnostics for the filtration of larger quantities of oil in hydraulic machines, such as hydraulic presses. This allows us to filter hydraulic oil while monitoring the properties of the oil in the current system. The unit can then be easily relocated to another hydraulic system where we can filter and monitor the oil of another hydraulic system. This service reduces the cost of installing a filtering and monitoring system on any hydraulic system, we are about to filter. The main function of the portable filtration unit is to filter hydraulic oil with a flow rate of up to 100 l/min or simply to pump used oil from the reservoir into other canisters for recycling. Self-diagnostics are integrated into the unit and measure oil temperature, dielectric constant, viscosity, oil cleanliness and oil relative humidity.

2 Portable filtration unit and filtering process

The portable hydraulic unit has two basic functions. The first is to filter oil and the second is to pump the used oil from the reservoir into waste canisters for further recycling. There are five different sensors to monitor the condition of the hydraulic oil, which are displayed on the HMI and stored on the controller for later use.

Figure 1: Portable filtration unit.

Unit is driven by two electric motors with pumps responsible for pumping the oil and passing it through the filters and sensors. A Siemens controller is used for data acquisition, data processing and control of the unit (Figure 1).

2.1 Filtering procedure

The portable filtration unit has a suction line and a return line. The inlet of the suction line is located just above the bottom of the reservoir, so any larger particles will not be filtered, as they often remain on the bottom throughout the life of the machine (Figure 2). Some of the newest reservoirs have a port for bypass filtration located at the very bottom of the reservoir so that all particles are filtered. The return line is located below the surface of the fluid, so that minimal air is injected into the fluid.
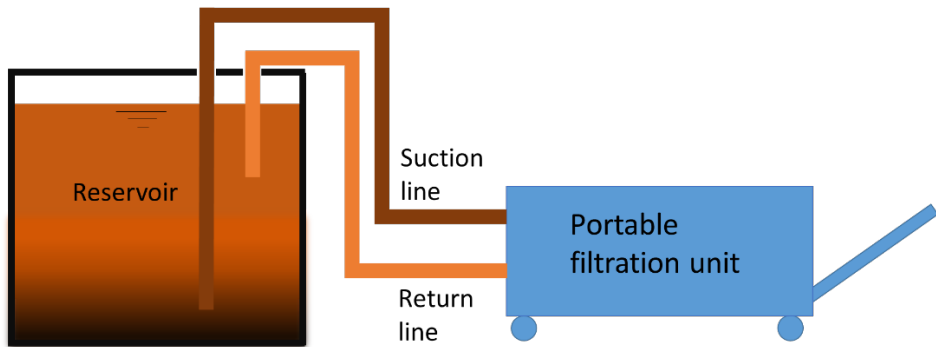
Figure 2: Schematic showcase of filtering hydraulic oil in reservoir.

The portable filtration unit has two magnetic filters at the beginning, which separate ferromagnetic particles (Figure 3). This is followed by two pre-filters and six fine filters that filter particles of all shapes and sizes. The two pre-filters remove larger particles and also extract water from the oil. Six fine filters remove fine particles. The filters were developed and manufactured in cooperation with TRM PRO d.o.o.
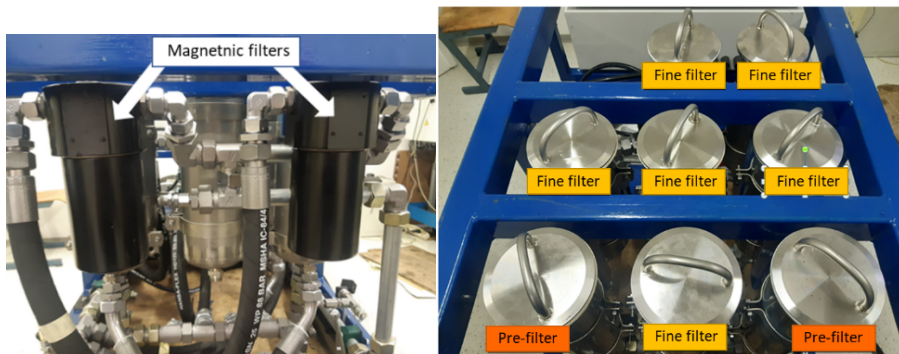
Figure 3: Magnetic filters (left) and pre-filters and fine filters (right).

2.2   Hydraulics

The main function of the unit is to filter hydraulic oil located in larger reservoirs through suction and return lines. Figure 4 shows quick couplings for the inlet and outlet of the oil. The unit has two pumps (main pump and auxiliary pump). The main pump is used to push the oil through the filters. Pressure sensors are located upstream and downstream of the filters to measure the pressure drop.

An electrically operated 4/2 valve is used to switch between the filter function and the function of pumping used oil into canisters for further recycling. The auxiliary pump is used to provide sufficient pressure and flow rate of the oil for the sensors to measure temperature, relative humidity, viscosity, dielectric constant and cleanliness.
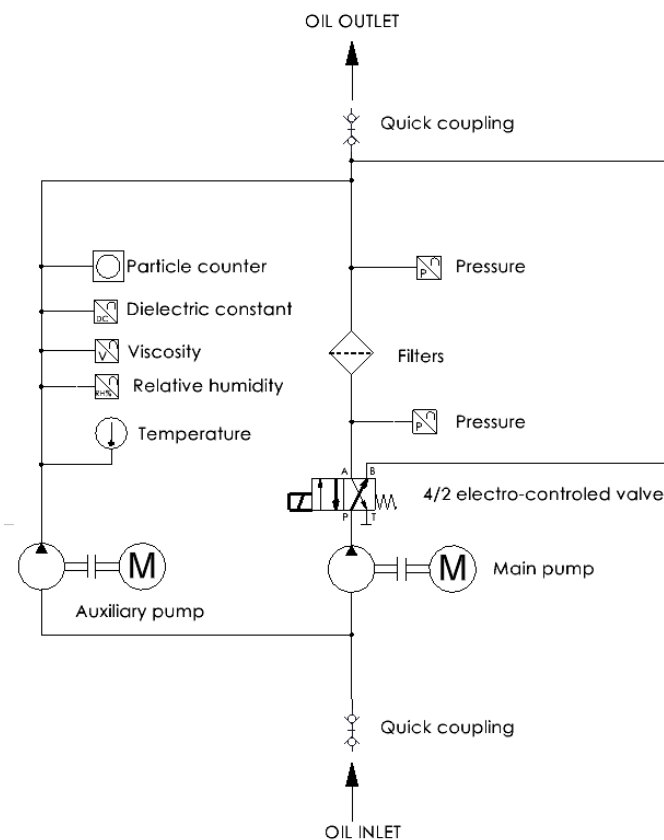
Figure 4: Simplified hydraulic block scheme.

2.3   Electrical-controlling part

In cooperation with Trecon d.o.o. we have developed an automated filtering procedure which is controlled by the SIMATIC S7-1200, CPU121C controller. SIMATIC-HMI KTP700 Basic Panel is used as a human-machine interface. The first function is that we can set the desired cleanliness and once it is reached, the unit stops. The second function is that we can set the allowable differential

pressure of the filters and once the limit is exceeded, the unit will stop. The third function is that we can set the desired time period for filtration and once it expires, the unit stops. It has also built-in self-diagnostics, which allows us to monitor the main fluid parameters (Figure 5), such as the elapsed time (pos. 1), the cleanliness of the fluid (pos. 2), the inlet pressure (inlet of the filters) (pos. 3), the outlet pressure (outlet of the filters) (pos. 3), the temperature (pos. 4), the relative humidity of the fluid (pos. 5), the dielectric constant (pos. 6) and the viscosity (pos. 7). It is possible to display the described parameters in time-dependent diagrams on the HMI display or to download the data to the USB stick as a .txt or .xlsx file.
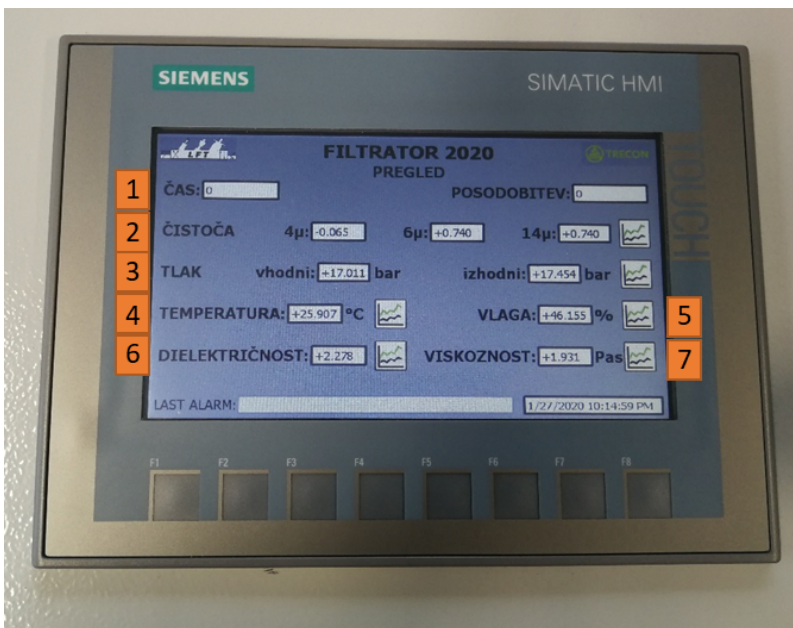
Figure 5: Display of key fluid parameters.

The unit has a built-in, electrically controlled 4/2 valve. When it is in the first position, the unit is filtering oil. When the valve is in the second position, the unit can pump used oil into canisters for further recycling. The duration of oil pumping before the unit stops can also be set here.

2.4 Robust design and transportation options

The portable filtration unit (Figure 6) is located in a Slovenian company. It has a robust design to withstand accidental collisions that could severely damage the unit. The unit stands on oil-resistant wheels and has a carrier bar to clamp to the trailer hitch for easy transportation with an electric vehicle. Another option for transport is with a forklift. The unit has two steel beams that attach to the bottom of the unit for this type of transport. The last option for transportation is with an overhead crane, as the unit has anchors at the corners of the metal structure. Figure 7 also shows a support for the hoses for the return and suction lines, which are connected to the unit via hydraulic couplings.

Figure 6: Portable filtration unit with self-diagnostics in industrial environment.

Figure 7: Carrier for hoses and hoses for suction and return line attached to the chain lift for easier transportation.

2.5 Measurements

In a Slovenian company we have in parallel measured the cleanliness of hydraulic oil, using a UCC20 bottle sampler according to SIST ISO 4406. Table 1 shows ISO code numbers or the number of particles per milliliter of fluid. Table 2 presents the corresponding cleanliness for different types of hydraulic systems.

Table 1: ISO 4406 code number meaning [7].

ISO code number	Number of particles per ml	
	More than	Up to and including
22	20 000	40 000
21	10 000	20 000
20	5 000	10 000
19	2 500	5 000
18	1 300	2 500
17	640	1 300
16	320	640
15	160	320
14	80	160
13	40	80
12	20	40
11	10	20
10	5	10
09	2.5	5
08	1.3	2.5
07	0.64	1.3

Table 2: Suggested accepTable contamination codes for various types of systems [7].

ISO code numbers	Type of system	Typical components	Sensitivity
23 / 21 / 17	Low pressure systems with large clearances	Ram pumps	Low
20 / 18 / 15	Typical cleanliness of new hydraulic oil straight from the manufacturer. Low pressure heavy industrial systems or applications where long-life is not critical	Flow control valves Cylinders	Average
19 / 17 / 14	General machinery and mobile systems Medium pressure, medium capacity	Gear pumps/motors	Important
18 / 16 / 13	World Wide Fuel Charter cleanliness standard for diesel fuel delivered from the filling station nozzle. High quality reliable systems General machine requirements	Injector valve and high pressure pumps/ motors Directional and pressure control valves	Critical
17 / 15 / 12	Highly sophisticated systems and hydrostatic transmissions	Proportional valves	Critical
16 / 14 / 11	Performance servo and high Pressure long-life systems e.g. Aircraft machine tools, etc.	Industrial servovalves	Critical
15 / 13 / 09	Silt sensitive control system with very high reliability Laboratory or aerospace	High performance servovalves	Super critical

NOTE: The three figures of the ISO code numbers represent ISO level contamination grades for particles of >4µm(c), >6µm(c) and >14µm(c) respectively.

Table 3 shows various measurements of cleanliness on hydraulic press 1, depending on where we took the sample. We vacuum the sample to remove air from the oil. Table 4 shows the results of hydraulic press 2, where all samples were also vaccumed before the measurements. Table 5 shows the results of the ON -LINE measurements of cleanliness.

Table 3: Cleanliness of oil on hydraulic press 1 according to ISO measured with UCC20 bottle sampler and vacuuming

Test number	Return line	Reservoir
1	20/17/12	20/16/11
2	21/19/15	21/20/16
3	20/17/12	20/16/11
4	20/17/13	20/16/10
5	20/17/12	20/16/11
6	20/17/13	20/16/11

Table 4: Cleanliness of oil on hydraulic press 2 according to ISO measured with UCC20 and vacuuming

Test number	Control line
1	21/19/15
2	21/19/15
3	21/19/15
4	21/19/15

Table 5: Cleanliness of oil on hydraulic press 1-ON-LINE measured with UCC20

Test number	ON-LINE-filter pressure port
1	20/13/08
2	20/13/09
3	20/12/07

3   Conclusion

We filtered the hydraulic press 1 with a capacity of 2000 l for 48 h. We measured the cleanliness of the press only after the 48 h filtration with the UCC20 bottle sampler (Table 3). The cleanliness was 20/17/13. Hydraulic press 2 had not yet been filtered and had a cleanliness of approximately 21/19/15 (Table 4). Table 1 shows that each increase in grade means that the number of particles doubles. Particles of size 4 μm(c) and above are present for 1 increment in grade more in hydraulic press 2 than in hydraulic press 1. Particles of size 6 μm(c) and above are present for 2 increments more in hydraulic press 2 than in hydraulic press 1, and the same is true for particles of size 14 μm(c) and above.

There are some disadvantages in dealing with cleanliness. Temperature, oil viscosity, relative humidity and air bubbles, sampling location and other factors affect the measurement of cleanliness. The factor of location is clearly seen in Table 4 where the same oil is measured in the return line and in the reservoir and it is surprisingly better in the reservoir than in the return line. Another example is the measurement with the Bottle Sampler (Table 3) and ON -LINE (Table 5). Again, there are different measurement locations and one cannot say with certainty whether the different results are due to the measurement method or the measurement location. The first grade is the same, but the other two are significantly lower. Further research is advisable to fully assess all factors affecting cleanliness.

References

[1]   Macián, V., Tormos, B., Olmeda P., Montoro L. (2003). Analytical approach to wear rate determination for internal combustion engine condition monitoring based on oil analysis, *Tribology International*, volume 36, pp. 771-776

[2]   T.M. Hunt. (1993). Handbook of wear debris analysis and particle detection in liquids. *Elsevier Applied Science*, London

[3]   F. Ng, J.A. Harding, J. Glass, Improving hydraulic excavator performance through in line hydraulic contamination monitoring. *Mech. Syst. and Signal Process. 83*, pp. 176-193

[4]   Jardine, A.K.S., Lin, D., Banjevic, D. (2006). A review on machinery diagnostics and prognostics implementing condition-based maintenance. *Mech. Syst. Signal. Process. 20*, pp. 1483-1510

[5]   K. F. Martin, A review by discussion of condition monitoring and fault-diagnosis in machine-tools, International Journal of Machine Tools and Manufacture, 34 (1994), pp. 527-551

[6]   Jocanović, M., Šević, D., Karanović, V., Beker, I., Dudić S. (2012) Increased efficiency of hydraulic systems through reliability theory and monitoring of system operating parameters. *Stroj. Vestnik-J. Mech. Eng., 58*, pp. 281-288

[7]   Tice D. E., Meeting ISO 4406 Cleanliness Standards with Diesel and Biodiesel Fuel, Parker blog (2016), website: http://blog.parker.com/meeting-iso-4406-cleanliness-standards-with-diesel-and-biodiesel-fuel

University of Maribor Press

Remediation of leakage of the hydraulic block presses MAC Master

DRAGAN GRGIĆ, MARIJAN BOGADI, MILOŠ LESJAK & ERNEST ANTOLIČ

Abstract The best way to prevent unplanned downtime of production machines is certainly adherence to the principles of preventive maintenance. In case of extremely difficult working conditions and the contaminated working environment of the machine, a major maintenance intervention is required. This involves not only the replacement of worn parts, but also design changes, the use of other materials or shapes, such as hydraulic cylinder seals. Such a major intervention often also presents a major logistical and organizational challenge. As such an example, the paper presents the reconstruction of an older special press for the production of molds for casting and is still of key importance for the production of the company. The challenge was to renovate a special hydraulic block with 63 hydraulic rollers mounted in a 9 x 7 matrix, which, in addition to the appropriate force for sand compaction in all molds, must also ensure flawless compression parallelism.

Keywords: • hydraulic mold press • leakage • renovation • cylinder matrix block • MAC Master •

CORRESPONDENCE ADDRESS: Dragan Grgić, NEVIJA d.o.o., Gregorčičeva ulica 29a, 2000 Maribor, Slovenija dragan.grgic@nevija.si. Marijan Bogadi, BOGADI Tesnila d.o.o., Karantanska ulica 21, 2000 Maribor, Slovenija, info@bogadi.si. Miloš Lesjak, BGS storitve, d.o.o., Valvasorjeva ulica 38, 2000 Maribor, Slovenija, info@bgs-storitve.si. Ernest Antolič, ENGAN Inženiring s.p., 2000 Maribor, Slovenija, engansp@gmail.com.

1. Introduction

The MAC Master press for the production of casting molds is of key importance for the production of the company LIVAR, Production and processing of castings, d.d. - PE Črnomelj. Despite 20 years of operation in very difficult operating conditions, the MAC Master press is thanks to careful maintenance still above average productive. The heart of the press is a hydraulic block with hydraulic rollers mounted in a 9 x 7 matrix. The rollers must ensure flawless parallel operation while ensuring adequate sand pressing force in all molds. The appearance of the special hydraulic block of the press is shown in Figure 1.
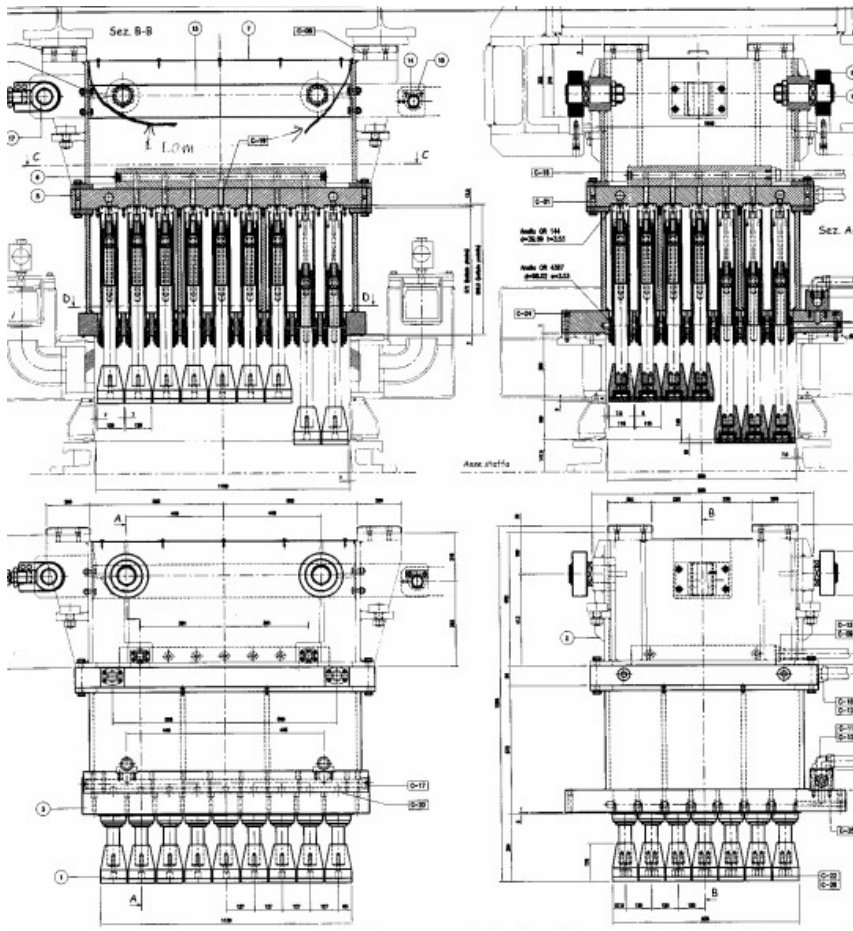
Figure 1: Hydraulic block with 63 rollers in 7 x 9 die.

Regarding the implementation of a possible remediation of the press and/or hydraulic block, there are two options:

a) Continuation of the continuous fight against leaks in the hydraulic block with 63 rollers, b) Replacement of the existing technology of the sand molds with a new one. The second option was the first to be disregarded due to the long delivery time (up to 2 years). On the other hand, there was a real possibility that the quality of the molds would become completely unsuiTable for the next phase of the production process. The limited remediation schedule (before the dismantling and defecation) was limited to a maximum of 2 weeks, and planned in the second half of December, which was an additional condition in the already demanding technical - maintenance mosaic.

The main cause of intensive wear of the hydraulic components of the block is operation in an environment with the presence of foundry sand, which accesses all the "pores" of the hydraulic components, which is practically impossible to prevent. The abrasiveness of the foundry sand causes rapid wear of the piston rods and seals of the hydraulic cylinders, which is reflected in the ever-increasing bearing capacity. This causes an uneven distribution of compressive force (simultaneously) operating 63 hydraulic cylinders located inside a two-part steel block - dimensions 1360 x 1020 x 700 mm. The presence of the foundry sand on all parts of the press is shown in Figure 2.

Figure 2: Presence of foundry sand on the press.

The mentioned presence of foundry sand and its intrusion into the interior of the hydraulic system was also reflected in the degree of purity of the hydraulic oil. The purity class of the hydraulic oil in the system, despite regular replacement of filter cartridges and occasional by-belt filtration, was 28/26/22 according to ISO 4406.

2.   Operational approach to hydraulic block rehabilitation

The dismantling of the entire hydraulic block (total weight 5.7 t) was a particular challenge due to the very limited space and obstacles around the press, as it was not possible to use any lift or forklift assistance. All disassembly had to be done manually, with the maintainers 'own physical strength (Figure 3). In addition to the problem of dismantling, an economic condition was set regarding the price and scope of renovation. When preparing the offer, it was necessary to take into account an estimation that quarter of the existing 63 hydraulic cylinders will have to be replaced with new piston rods. In fact, more than half of the existing piston rods had to be replaced with new ones.

Figure 3: Physically released hydraulic block of the press.

A further obstacle was also the modest technical documentation of the Italian-made press, as it did not contain a more detailed description of the hydraulic components. The only indication of the quality of the roller block design was the small engraving inside the hydraulic block. The logo of the manufacturer HUNGER, which was detected only after the separation of the cover and guide plate, indicated the fact that the block was manufactured by the company in the appropriate quality and thoughtful construction, and that it is a particularly demanding hydraulics. Due to the absence of documentation, it was necessary to dismantle the block according to the principle of hydraulic forensics - with real - time documentation and marking of individual parts - Figure 4.

Figure 4: Disassembly of the hydraulic block into component subassemblies.

The holes of all 63 special rollers had to be welded first and then mechanically processed. It was also necessary to process the grooves of the piston seals to a

uniform installation dimension (Figure 5). In this way, uniform sets of seals could be used, for all 63 pistons, regardless of their position in the matrix of the 7 x 9 block. A more durable material is used to make the seals: HPU (hydrolytic polyurethane) hardness 63 Shore D, filled with graphite, which provides sealing even in the event of minor damage to the seal. The main rings are made of PTFE.
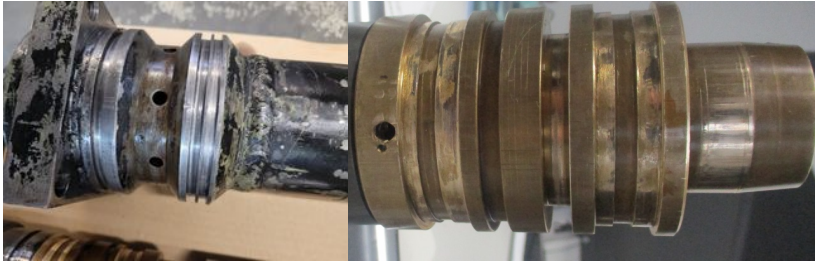
Figure 5: Cylinder hose with holes for hydraulic oil supply and cylinder piston.

A particular challenge has been the treatment of the roller's seats due to the frequency of the pressure load and the mechanical already slightly bent cover of the hydraulic block (Figure 6). The lower and upper matrix 7 x 9 must match in a tolerance of +/- 0.01 mm, otherwise the end roller would at best receive a hydraulic oil with a time gap, and at worst there would be a leakage   on the hydraulic block immediately.

Figure 6: Cover and guide plate form roller housings

Ensuring the simultaneous and uninterrupted supply of oil through the block to all 63 cylinders provides an equal distribution of pressure force on the surface of the plate 1360 x 1020 mm, is a condition for optimal compression of sand models into molds.

3.   Installation and operation test of the hydraulic block

Assembling individual cylinders and assembling a complex hydraulic block into a working whole, without prior sealing control, would be a rather risky act. Before transport from BOGADI Tesnila d.o.o. in LIVAR d.d. - PE Črnomelj, sealing control and simulation of simultaneous operation of all 63 hydraulic cylinders were performed.

Figure 7: Hydraulic block prepared for transport.

After installing the hydraulic block in the press, the by-pass filtration of the total amount of oil (8000 liters) to purity class 21/19/15 according to ISO 4406 was performed.

In the next phase of rehabilitation of the press, it will be necessary to rework and strengthen the method of mounting the main hydraulic cylinder and the supporting structure (Figure 8). Namely, the existing construction requires complete dismantling and thermal treatment after welding of the additional reinforcements, which was not possible in the time we had at our disposal.
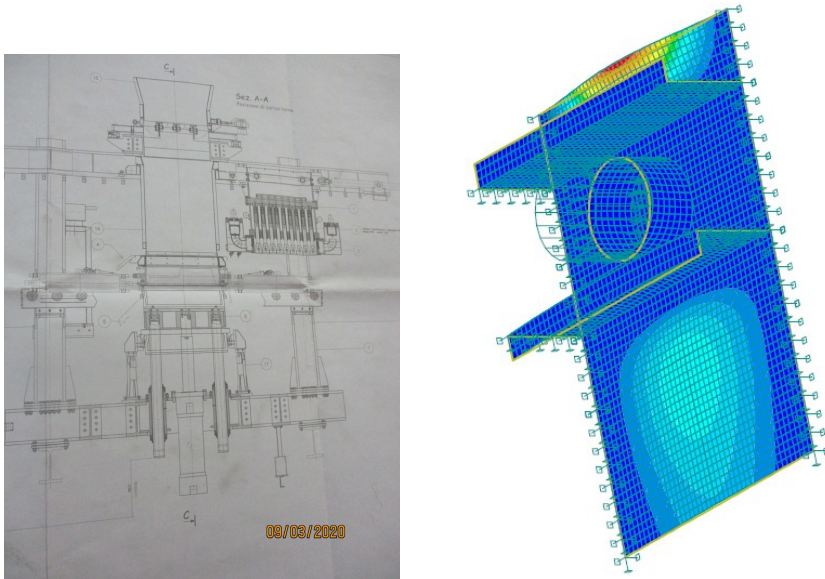
Figure 8: Press master hydraulic cylinder and stress simulation in the load-bearing structure of the clamp.

3.   Conclusion

The entire operation to repair the hydraulic block leakage was carried out in an extremely short time. After a few days of regular operation of the press, when the ambient temperature and hydraulic oil reached the maximum operating values, it was necessary - at two intervals, to reseal 5 of the total 63 hydraulic cylinders.

References

[1]   N.N.: Available Documentation for hydraulic presses MAC Master

University of Maribor Press

Challenges and pitfalls
of time constrained hydraulic projects

TADEJ TAŠNER & KRISTIAN LES

Abstract Almost all projects nowadays are fast paced as all industries are trying to shorten time to market and hydraulics is no exception. In order to compete in such environments all the processes in the company from engineering throughout production have to be streamlined, so they are able to effectively follow the ever-changing project requirements. Moreover, increasing lead-times and disrupted supply chains due to pandemic also influence the workflow, as components may not arrive in time. This article addresses all of the above-mentioned problems on a real world hydraulic project – a hydraulic drive of a forklift. It presents the evolution of hydraulic schematic, hydraulic manifold and control algorithms all the way from the first draft to the latest version.

Keywords: • hydraulics • production • manifold • forklift • time to market •

CORRESPONDENCE ADDRESS: Tadej Tašner, HAWE Hidravlični sistemi d.o.o., Ob Dragi 7, SI-3220 Štore, Slovenia. Kristian Les, HAWE Hidravlika d.o.o., Ob Dragi 7, SI-3220 Štore, Slovenia, e-mail: k.les@hawe.si.

1   Introduction

Nowadays, competitive pressures, dynamic information, and new technologies drive changes in markets. It is crucial that companies respond to these changes. It is often the first to field a new product that captures market share and profits.

Time to market defines the period from the conception of a new idea to the release of a product to the marketplace. Time to market varies widely by what is sold: product type, complexity, and industry. A typical time to market for a pharmaceutical is ten years, while a consumer social app could be conceptualized, researched, designed, prototyped, and launched in less than a year [1].

Table 1: Time to market by industry [1]

Industry	Time to Market Range (Years)
Energy	7-23
Aerospace & Defence	3-22
Healthcare & Pharma	9-19
Industrials	3-7
Automobile	3-5
Semiconductor	1-5 (2 year clock)
Consumer Goods	1-5
Mobile Phones	1-3 (3 year clock)
Technology	0.5-5

Hydraulic systems are normally subsystems of industrial and mobile applications, but often also fit into technology group, which has relatively short time to market, as seen in Table 1. In order to shorten time to market, our customers, who build our power packs into their products parallelize as much tasks as possible. Therefore, it is not possible to thoroughly test your product on the real application, which can sometimes lead to problems.

In order to handle such rapidly changing projects, internal processes of the company have to be very flexible. Firstly, there has to be free engineering capacity, that when a change request is received someone can start working on it immediately. The engineering work should be backed with software tools that enable fast redesigns. Fast transfer to production is possible by using mostly

internal standard components pool that are normally in stock. Moreover, there has to be as little internal bureaucracy as possible in order to be able to change all the required documents as quickly as possible and propagate all the changes through the ERP system to purchasing and production [2]. Finally yet importantly, you need flexible and competent (local) suppliers, which are able to follow you at such a fast pace [3]. All of the measures listed above base on the part of lean production methodology, which applies to individual or small series production [4].

This article describes the whole lifecycle of hydraulic project all the way from project specification to finished hydraulic system, which is commissioned into customer's end product – in our case a self-driving forklift.

2 Project Specification

Our power pack lifts the load on the driverless forklifts or forklift automated guided vehicles (AGVs).

Figure 1: Forklift AGV Amadeus Classic and free space for the power pack [5].

Customer specification consisted of the following main parts:
- available space for power pack,
- load properties (cylinder size, forklift load and forklift mast type),
- performance (lifting speed, lowering speed, zero leakage),
- power supply limitations,
- control interface,
- other operating conditions.

The biggest challenge was specified lowering speed resulting in more than 15 l/min cylinder flow also when the forklift is empty, as the load of the empty fork itself results in only 10 bar cylinder pressure. Same speed has to be reached also at 5 °C, while maintaining 1 mm position accuracy.

3   Proposed solution

Firstly, we proposed high efficiency brushless direct current (BLDC) drive with 4-quadrant operation gear pump capable of running at very low speeds. However, our customer informed us that they have bad experience with such system and such high-end drive was too expensive for them. Therefore, we had to switch back more than 20 years back to brushed DC motor in combination with a flow control valve.

We use a pressure filter before all the valves, one 3-way pressure compensated flow control valve for lifting and 2-way pressure compensated flow control valve for lowering. Unintentional lowering due to leakage is prevented with 2/2 way seated directional control valve with position monitoring. Load pressure is monitored using a pressure sensor. There is also a manual drain valve for lowering the load in case of emergency.

Customer has written his own control algorithm that runs on HAWE's CAN I/O 14+. CAN I/O is a small form factor CAN slave PLC with integrated inputs and outputs including proportional valve amplifiers [6].

4   Test procedure

We received a bare forklift mast for testing. For proof of concept pipe mount manifolds for each included component were connected using flexible hoses. Figure 2 shows the test setup. All the components have been tested with different load and speed combinations. The critical part was lowering speed, especially at low temperatures. Results of measured lowering speeds are therefore presented in the next paragraph.

Figure 2: Proof of concept test setup.

We have tested with VG 22 at 24 °C (44 cSt) oil to minimize valve losses and simulated VG 22 oil at 10 °C (96 cSt) using VG 46 oil at 24 °C (105 cSt). All results are displayed in Figure 3, where warm colors represent empty forklift mast with different oils and blue represents loaded forklift mast. It can be seen that we can reach linear (green) flow versus current relationship in our target flow range, that is between 0 and 15 l/min. Cylinder losses, pressure losses in the piping and losses in the flow control valve itself limit higher flow as shown on the right side of the graph (600 mA and up), where curves don't align any more. That means that not enough load pressure is available to reach the flow set by the flow control valve.
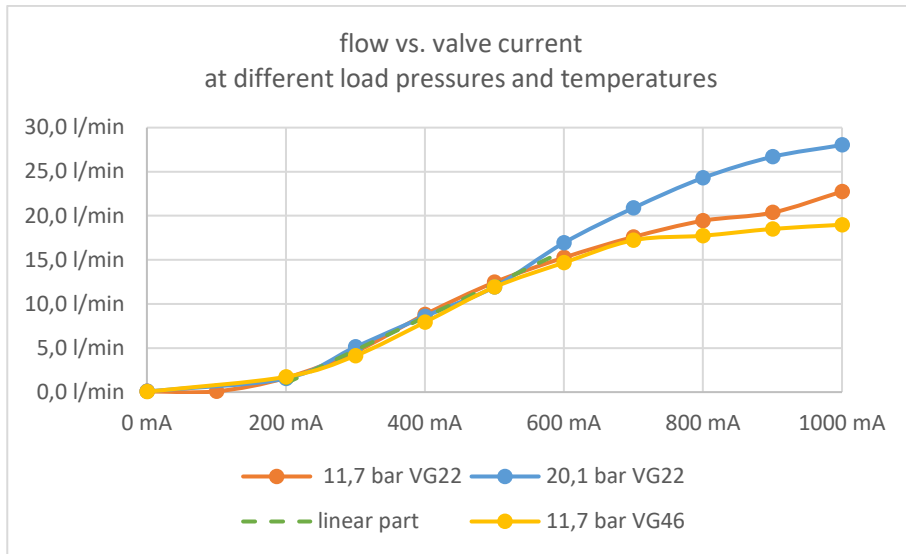
Figure 3: Initial test results for 2-way flow control valve used for lowering.

5   Commissioning results

After the tests, we designed first version of the manifold that we fit onto a standard compact power pack. Customer himself commissioned power packs at his facility. Soon after the first tests, we received a complaint that the unit is too loud. We thought that it was impossible, as it did not happen at our facility. After a more detailed investigation, we found out that the noise was coming from the oscillating lifting flow control valve at low flows 0-20 % and from 25-100 % loads. The reason why we did not experience the issue is the connection between the power pack and the forklift mast. We used a 4 m long flexible hose and they used a 1 m long rigid pipe.
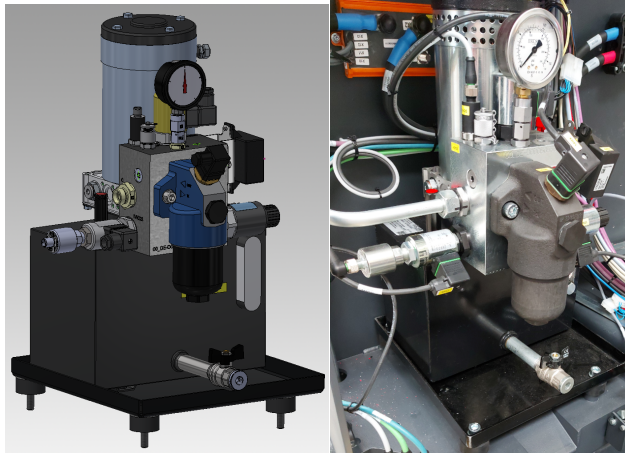
Figure 4: Initial test results for 2-way flow control valve used for lowering.

5.1   Fixing the problem

Because the noise was too loud for the machine to be sent to the end customer, we had to immediately find a solution for the problem. As one of the HAWE subsidiaries manufactures the 3-way valve, we included the design team of the valve for further investigation. They concluded that the valve is meant for systems with different dynamic behaviour mainly with lower inertia; therefore, the dampening in the valve was too small. In order to increase the dampening, the valve should undergo a major change, which would not be completed in time. The noise could be attenuated by using a different spring and metering orifice, but the dampening of the control piston of the valve itself could not be easily increased, so the noise could not be eliminated.

Therefore we proposed a new control concept to the customer. We eliminated the 3-way flow control valve for lifting and now lifting is controlled by letting excess flow with flow control valve for lowering into tank. Control algorithm now compensates pump flow variation with pressure, although the variation is quite significant due to brushed DC motors rpm decrease for increasing load . To be able to retrofit all the already shipped units, we prepared a plug for the 3-way flow control valve that plugs the tank line of the valve cavity.

6   Project and changes flow

The biggest challenge of the project was that there was no prototype order, as the customer's time to market is very short. The following bullets sum up the order and engineering flow of the project and Figure 5 shows the evolution of the manifold:

- quote and proof of concept made
- order for first series received
- engineering completed & manufacturing started (initial manifold)
- available space specification changed
- manifold redesigned (optimized manifold)
- further orders received & manufacturing started
- first series shipped & commissioned
- noise present → further tests → 3-way flow control valve eliminated
- manifold redesigned (one flow control valve)
- retrofit plug for all existing systems designed…
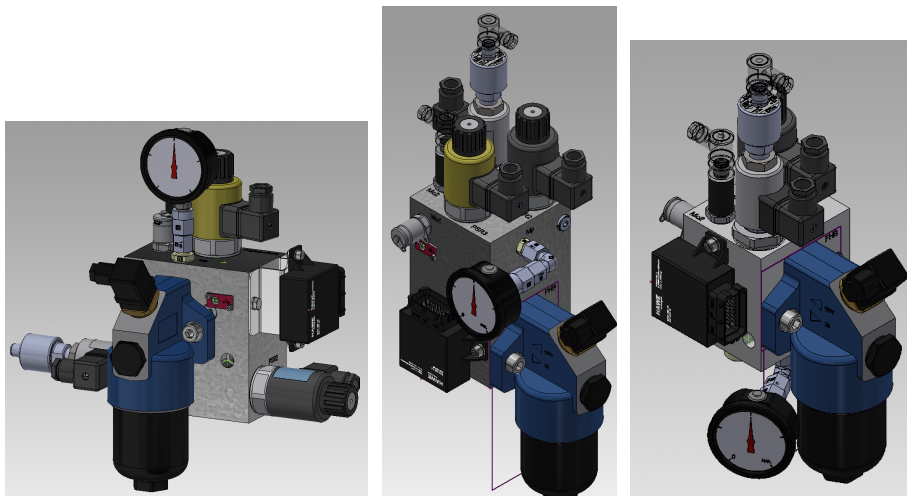
Figure 5: Manifold evolution – initial, optimized, one flow control valve.

State of the art digital design and production system enables us to quickly respond to the necessary changes. The Vault PDM system integrates fast version control for all of the design files, but it works especially well with Inventor, which paired with MD Tools add-in offers quick and intuitive manifold design. One

advantage of the correctly maintained 3D model library is ability to export bill of material of the power pack directly from Inventor. The bill of material is then semi-automatically synced with our ERP system, which automatically maintains stock levels for all of our standard components. Customer order creates a demand for all materials on the bill of material, which purchasing department buys based on current stock levels. However, tailored components such as manifolds cannot be purchased like ordinary components. Therefore, we have competitive local manifold suppliers that are able to handle small quantities in short times to keep up with our demand. Having local suppliers for such components is for us very important, as they can respond to potential problems on very short notice. With such workflow, we are able to handle projects such as these even during the pandemic, which increased lead times for many products.

7   Conclusion

This article presented how to achieve short time-to-market even for small series and individual production with minimal impact on product cost and effective employee utilization.

References

[1]   Carter, J. (2016). Time to Market: What it is, why it's important, and five ways to reduce it. https://www.tcgen.com/time-to-market

[2]   Hou, J., Su, C., Zhu, L., & Wang, W. (2008, August). Integration of the *CAD/PDM/ERP* system based on collaborative design. *2008 ISECS International Colloquium on Computing*, Communication, Control, and Management (Vol. 1, pp. 561-566). IEEE.

[3]   Kojun, H. (2010). Outsourcing versus in-house production: the case of product differentiation with cost uncertainty. *Seoul Journal of Economics*, 23

[4]   Mascitelli, R. (2007). The lean product development guidebook: everything your design team needs to improve efficiency and slash time-to-market. *Technology Perspectives*

[5]   DS Automotion. *Amadeus Classic Datasheet*. Available: https://www.dsautomotion.com/fileadmin/userdaten/downloadbereich/datenblaetter/en/DS-AUTOMOTION-AMADEUS-EN.pdf

[6]   HAWE (2021). *CAN-IO* valve controller – Product Documentation. https://downloads.hawe.com/7/8/D7845-IO_14-en.pdf

University of Maribor Press

The concept of automatic generation of hydraulic press cycle

DENIS JANKOVIČ, ROK NOVAK, MARKO ŠIMIC & NIKO HERAKOVIČ

Abstract The development of smart hydraulic press that allows rapid adaptation to high-volume variant production is a major challenge. Besides tool management, setting the control parameters, which can be considered as a correct press cycle, is an important part to achieve agile production. This paper presents a new approach to automatically generate a hydraulic press cycle where the important data of the production plan is known, such as the data or setting of the forming tool and the data of the product. In this case, RFID tracking system is used to read the tool/product data, which is input data for the mathematical algorithm for calculating the characteristic points of the hydraulic press cycle. The characteristic points are sent to the local PLC and stored as a matrix. The Beckhoff TwinCat platform is used for process control. Finally, a simple bending process is shown as a use case for concept verification.

Keywords: • hydraulic press • forming tool • RFID • automatic-generation • press cycle •

_____

CORRESPONDENCE ADDRESS: Denis Janković, University of Ljubljana, Faculty of mechanical engineering, Aškerčeva 6, 1000 Ljubljana, Slovenia, denis.jankovic@fs.uni-lj.si. Rok Novak, University of Ljubljana, Faculty of mechanical engineering, Aškerčeva 6, 1000 Ljubljana, Slovenia, rok.novak@outlook.com. Marko Šimic, University of Ljubljana, Faculty of mechanical engineering, Aškerčeva 6, 1000 Ljubljana, Slovenia, marko.simic@fs.uni-lj.si. Niko Herakovič, University of Ljubljana, Faculty of mechanical engineering, Aškerčeva 6, 1000 Ljubljana, Slovenia, niko.herakovic@fs.uni-lj.si.

1   Introduction

The progressive digitalization and interconnectivity of machines and equipment, improve production processes through automation and self-optimization. Intelligent and smart manufacturing systems in smart factories provide optimization of work plan, higher productivity, increase in Overall Equipment Efficiency (OEE) and reduction in manufacturing costs [1]. Hydraulic systems are not yet at the level of smart manufacturing systems, so expert systems with integrated smart sensors and actuators need to be developed to provide the necessary smart data flow. Standardized communication between subsystems and interoperability must be achieved to allow the expert system to make functional improvements and extensions [2]. Condition monitoring is required to fully understand the operational characteristics of the hydraulic system so that the stability of the hydraulic system and processes can be confirmed and automatic control optimization and predictive maintenance can be determined if necessary [3]. Complex hydraulic components such as hydraulic valves are already considered as a separate unit which has its own intelligent software and tools for data analysis and are able to draw the right conclusions about the component's operability [4]. Intelligent algorithms can introduce artificial intelligence (AI) into hydraulic systems and components to provide them with the ability to self-predict, self-adapt and make decisions instead of human operators [5]. Adaptive control systems for setting the control parameters considered as a correct hydraulic press cycle during the desired planned forming process can be designed based on mathematical [6, 7, 8] or numerical models [9]. Proper tool selection [10] and optimized tool change scheduling [11] result in higher OEE, higher productivity, reduced cycle times, and better dimensional tolerance of the product. However, demanding customer requirements increase product variability, which is associated with the constant modification and optimization of the production schedule. Therefore, it is necessary to increase the flexibility of the hydraulic press by using expert systems that allow adaptation to the changes.

2   The concept of smart hydraulic press

2.1   Expert system

According to the guidelines of I 4.0, the expert system of smart hydraulic press is proposed as its intelligence. The hydraulic press is treated as an individual intelligent system that can be integrated with the Manufacturing Execution System (MES) and Enterprise Resource Planning system (ERP) of the Smart factory. Figure 1 shows the concept of the hydraulic expert system with the inputs, outputs, Overall Equipment Efficiency sub-module (OEE) that consists of visualisation and statistical data analysis, acquisition of important process parameters and local intelligence.
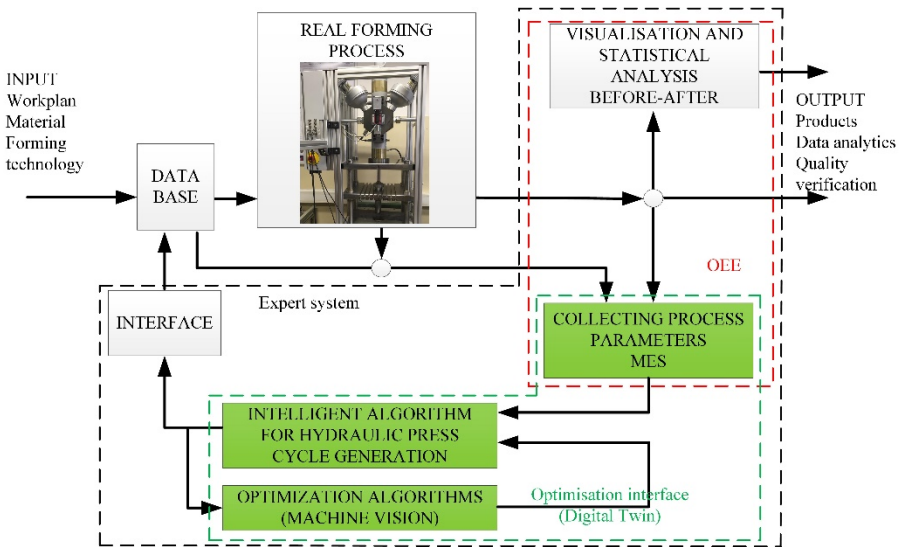
Figure 1: The concept of hydraulic expert system.

The main part of the paper presents the intelligent algorithm for the automatic generation of the hydraulic press cycle based on the data stored in the local database module (collecting process parameters MES). The important input data mainly includes the workplan, material properties and technology parameters. The workplan provides crucial parameters regarding the type and the number of

products to be manufactured. The material specifies the products in detail, i.e. the geometry properties (important in terms of handling, positioning and forming process). The technology provides crucial parameters of the machine and all other tools used to manufacture the products. The proposed expert system consists of six important steps: 1) reading and gathering all the input parameters from ERP and MES, 2) storing the parameters in local database module, 3) validation of the current state of the hydraulic press, tooling, material and confirmation the "ready for produce" status, 4) definition of the proper forming process, tooling, material (specimens), 5) automatic generation of the hydraulic press cycle, 6) execution of the forming process, process and product quality analysis and optimization of the press cycle to achieve quality of products.

In step 1, the information and input data from various sources is forwarded to a local database. At the global level of the smart factory ERP and MES systems provide production plan requirements such as product type (length, width, height), material properties, required forming operation (bending, deep drawing, coining etc.), required die tool, process parameters (bending angle, deep drawing height etc.). Tooling geometry properties are gathered based on digital models from research and development and construction department. Material properties are determined using tensile and flexural test [12]. The parameters of the hydraulic systems are measured with sensors as described in chapter 2.2. The expert system compares the real and the reference process parameters and sends a request for parameter adjustment via the interface.

In step 2, the collected data is sorted and filtered so that the subsystems involved in a hydraulic system can access and use the smart data for further operations.
In step 3, the expert hydraulic system uses the data collected from the sensors and actuators to self-validate the state of the hydraulic system, the currently installed die tool as well as its setting and the condition of the individual components of the hydraulic system. The hydraulic expert system predicts the necessary events/activities that guide the machine operator through the HMI interface, or, in the case of automation, robots that perform the handling operations. The expert system ensures that the forming process requirements are met.

In step 4, the specimen dimensional properties and type of material are selected. Based on the material properties, the forming cycle (ram speed) is adjusted as needed in the forming phase. If necessary, instructions are given for changing the die tool. Based on the collected data and expert system confirmation the product parameters are determined, which are the input data for the intelligent algorithm. In step 5, the intelligent algorithm determines the characteristic points of the forming process and considers the tool geometry errors that occur during the ram movement and are described in more detail in Chapter 3.

During the forming operation the product quality is monitored with the machine vision system (step 6). The type of forming process needs to be considered, as each forming operation has different impacts on the product quality. Springback effect is ever present in the case of sheet metal bending, where the sheet metal tries to revert back into its straight form, once it is bent [6], [8]. In the case of deep drawing the product quality can be measured with the process parameters such as forming force and blanking force to prevent fracture and wrinkling on products [9].

Optimization algorithms in step 6 monitor the product quality and process parameters and in case of bad product quality make decisions to improve the product quality.

2.2   IoT concept of hydraulic press

The proposed IoT of a hydraulic press represents an intelligent network of subsystems interconnected in a closed communication loop, as shown in Figure 2. Therefore, the presented IoT structure is divided into three subsystems: (1) database or local cloud, (2) expert system, and (3) control system. The designed IoT concept of hydraulic press enables rapid data exchange between devices so that the devices can perform operations without time delay. The responsiveness of the system is increased, which improves the efficiency of the production plan. When unpredicTable events occur, decision-making algorithms are used to improve system functionality at the edge device. Understanding the edge computing in the concept of smart factory, the hydraulic systems or its components have the potential to be implemented as an individual smart sub-system. The first subsystem of the IoT concept for hydraulic press is (1) the local cloud of processed data. Here, the historical data is available to all devices that

have permission to read the data. The proposed local cloud stores the data such as the workpiece storage state, tool warehouse state, die tool properties and other data relevant to the process monitoring. To determine the condition of the hydraulic system several sensors can be used:

- Position sensor to determine the cylinder displacement and hydraulic valve spool displacement.
- Strain gauges to determine frame deformation.
- Pressure sensors to monitor pressure in hydraulic cylinder.
- Force sensor to monitor the force generated, i.e., the forming force.
- Electrical current sensors in combination with electrical control voltage measurement to calculate the energy consumption.
- Tachometer to measure the speed of the electric motor.
- RFID systems to track input material and die tool changes settings.
- Inductive sensors or microswitches to monitor the die tool set-up.
- Machine vision systems to monitor the specimen position and quality of the products.

The purpose of (2) expert system is to perform the self-adjustment and optimization mechanism of hydraulic system based on current system status and provide a better-quality product with an improvement loop as described in depth in chapter 2.1.

The hydraulic press cycle and the control signal for servo valve is thereby corrected by closed-loop control analysing the difference between the reference signal and the error predicted by the expert system. The control system (3) reduces the error and correct the servo valve control signal to achieve better performance.
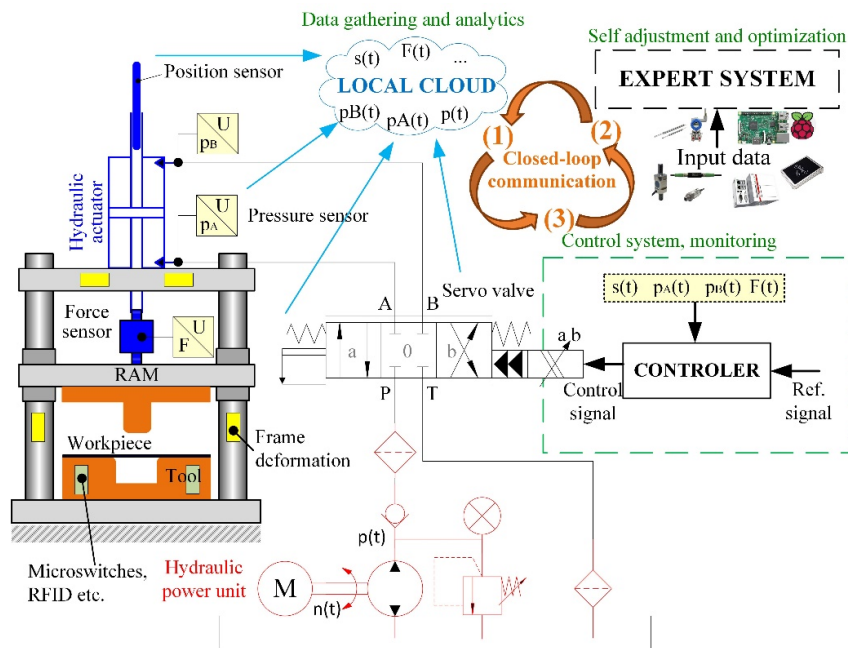
Figure 2: Scheme of hydraulic press divided into several functional IoT sub-systems.

3   Hydraulic press cycle generation – main structure of the intelligent algorithm

The structure of the proposed algorithm for automatic generation of the hydraulic press cycle consists of three basic elements, as shown in Figure 3. The first element presents the input data such as order requirements, hydraulic press characteristics, product shape and die tool geometry. Based on the variability of the product shape and the order requirements the self-recognizing part of the algorithm defines variables such as the bending angle and the required tool for the bending process. The purpose of the second element is to automatically generate the hydraulic press cycle considering the input data. The algorithm is the most important part and is represented in chapter 3.2 in detail. The output data of the proposed algorithm represents the hydraulic press cycle given by characteristic points of the forming cycle. The characteristic points are forwarded to the controller in the form of a reference signal to perform closed-loop position control.
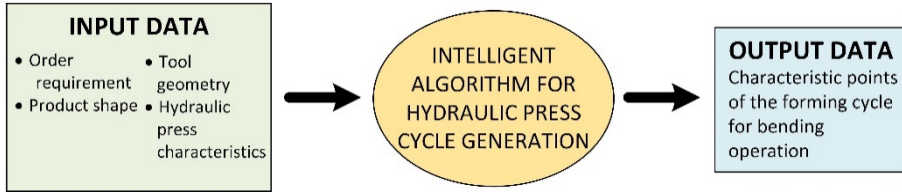
Figure 3: Structure of intelligent algorithm for hydraulic press cycle generation.

3.1   Intelligent algorithm for hydraulic press cycle generation

Various forming processes require different forming cycles that define a different number of characteristic points. For our case, we propose the hydraulic press cycle characterized by 7 typical points, as shown in Figure 4. Such a cycle is suiTable for bending process, deep drawing, etc. Each point is characterized by position of the cylinder/ram and the time (s, t).
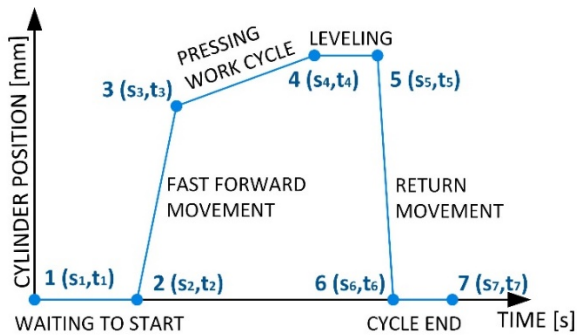
Figure 4: Hydraulic press cycle given by characteristic points.

Points (1) and (2) define the waiting phase of the forming cycle. The positions s_1 and s_2 are defined by considering the characteristics of the hydraulic press (stroke range) and the ram movement required for the handling process. The characteristics can be gathered from digital models of the press construction and the die tool and specimen properties. The time period between t_1 and t_2 is used to satisfy the forming conditions and to position the specimens correctly.

The fast forward movement of the ram towards the specimen is characterized by points (2) and (3). The maximal permissible cylinder velocity is determined by position s_3 and time t_3. Point (3) represents the starting point of the pressing work cycle and is chosen to allow a few mm of free movement before upper die tool touches the specimen. In our case we chose 3 mm of free movement for presented hydraulic press and bending process. The most important point of the hydraulic press cycle represents point 4 (s_4, t_4). The forming process demands appropriate ram speed to achieve proper deformation of the specimen, which is adjusTable by changing the time t_4. A more detailed calculation of the proper movement of the ram ($s_4 = x_{p,true}$) for the bending process is described in chapter 3.3. The time t_5 of levelling phase, between points (4) and (5), is optional and depends on the forming process requirements. The return movement is characterized by points (5) and (6) where $s_6 = s_2 = s_1$. Time t_6 is defined in similar way as for fast forward movement to achieve maximal permissible speed of hydraulic cylinder. During the time between points (6) and (7), the cycle ends and allows the setting of the waiting period t_7, while $s_7 = s_6 = s_2 = s_1$.

3.2   Determination of hydraulic press cycle (point 4)

The primary function of the intelligent algorithm is to determine the characteristic point 4 (s_4, t_4) just before a tool touches the specimen of the forming cycle shown in Figure 4. The secondary function of the algorithm is to determine the error during the sheet metal bending cycle caused by the movement of the sheet metal on the contact point of the tool. The main parameters describing the geometrical characteristics of the specimen and the die tool are shown in Figure 5. Here L represents the distance between the two supports of the lower die tool, R the lower die tool radius, r the upper die tool radius, and d the sheet metal thickness.
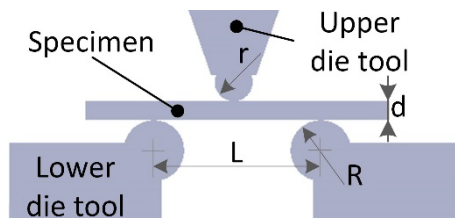
Figure 5: Dimensional properties of forming tool.

Figure 5 shows an initial contact point between a die tool and a specimen. The final movement of the ram is defined by the desired bending angle α (Figure 6). Equation (1) represents a simplified calculation of the forming depth x_p, without taking into consideration the error caused by the sliding motion of the specimen on the supports.

$$x_{p,simpl} = \frac{L}{2 \cdot tan\frac{\alpha}{2}} \qquad (1)$$

However two types of errors needs to be taken into consideration and added to the forming depth $x_{p,simpl}$ given in simplified equation (1). The first type of error occurs due to specimen slippage (from contact point 1 to contact point 2) on the lower die tool due to the assumed geometric properties of the lower die tool as shown in Figure 49. The contact point between specimen and the lower die tool is determined by the radius of the lower tool support R and the bending angle α.
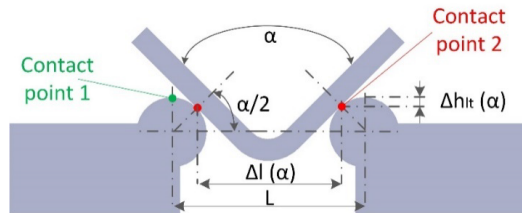
Figure 6: Error due to lower die tool.

Thus, the equation for the actual distance between contact points $\Delta l(\alpha)$ (between the specimen and the lower die tool) can be expressed by equation (2). Also, the actual height of the contact points $\Delta h_{lt}(\alpha)$ must be considered with equation (3) where bending angle α is considered.

$$\Delta l(\alpha) = L - 2R \cdot cos\frac{\alpha}{2} \qquad (2)$$

$$\Delta h_{lt}(\alpha) = \left(1 - sin\frac{\alpha}{2}\right) \cdot R \qquad (3)$$

The second type of error occurs due to the assumed geometric properties of the lower die tool $\Delta h_{lt}(\alpha)$. It is given as the difference between the height H and the radius of upper die tool r, as shown in Figure 7. The specimen thickness d is also considered in the height error $\Delta h_{lt}(\alpha)$.
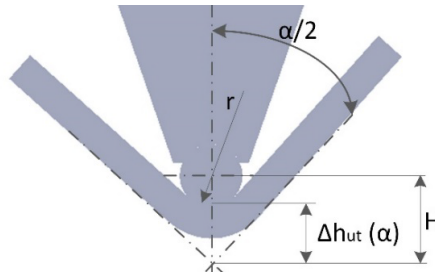
Figure 7: Error due to upper die tool.

The height H is derived according to Pythagorean Theorem and expressed by equation (4). Here in equation (4) the error that occurs due to geometric properties of the upper die tool h is expressed as the difference between the sum of error H and the radius of the tool r. As shown in equation (5) the error $\Delta h_{ut}(\alpha)$ is due to the radius of the upper die tool r and the variable bending angle α.

$$H = \frac{r+d}{\sin\frac{\alpha}{2}} \tag{4}$$

$$\Delta h_{ut}(\alpha) = H - r = \frac{r+d}{\sin\frac{\alpha}{2}} - r \tag{5}$$

Since both types of errors caused by the lower die tool $\Delta l(\alpha)$, $\Delta h_{lt}(\alpha)$ and the upper die tool $\Delta h_{ut}(\alpha)$ are not considered in the simplified equation (1), equation (6) represents a true forming depth, where the variability of the bending angle α (product requirement variability) and die tool geometry are considered.

$$x_{p,true} = \frac{l(\alpha)}{2 \cdot \tan\frac{\alpha}{2}} - \Delta h_{lt}(\alpha) + \Delta h_{ut}(\alpha) \tag{6}$$

4   Integration of algorithm in real hydraulic press

The interoperability between emerging connected devices and the speed of communication determines the efficiency of the expert system. Radio Frequency Technology (RFID) is used to read the word order via RFID tags. An intelligent algorithm processes the input data and generates a characteristic point for the bending operation. In the next step, the Graphical User Interface (GUI) is used to monitor and control the manufacturing process.

4.1   RFID material tracking and forming tool set-up recognition

The use of RFID in production systems is becoming increasingly popular for exchanging data between edge systems in a smart factory, such as a hydraulic system [13]. RFID technology can be used to collect important data about the forming die tool installed in the hydraulic press. Here, the identification code (ID) for each die tool stored in a warehouse and for each pallet containing samples is written on an RFID tag, as shown in Figure 8.
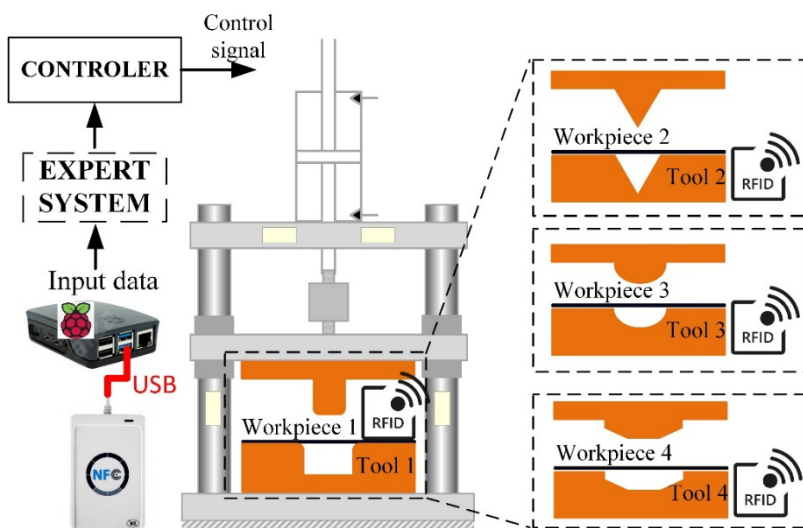
Figure 8: Concept of die tool and input material recognition.

The installation instructions are prepared by an expert system. In the proposed concept of hydraulic press, the microcontroller Raspberry Pie is used as an edge device for die tool tracking, material tracking and production plan determination using RFID tag. The RFID reader is connected to the microcontroller using USB communication protocol. The intelligent algorithm can perform automatic die tool recognition, die tool set-up recognition, and input material recognition (specimens) based on the currently manufactured product. The expert system with the algorithm also verifies the correctness of the input material, the selected or installed tool, the setup of the die tool, and the characteristics of the hydraulic press that allows the planed forming process to be performed. In the event of an error, the request is sent to the HMI interface to replace or correctly install the currently installed die tool or replace the input material.

4.2 Graphical user interface and hydraulic press cycle

The Graphical User Interface (GUI) shown in Figure 9 is designed to visualize the measured parameters of the hydraulic press and guide the operator until the production plan is completed. In case of unaccepTable errors during the production process, warnings are displayed on the GUI, such as excessive system pressure, incorrectly installed die tool, open safety door and product remaining in the die tool.
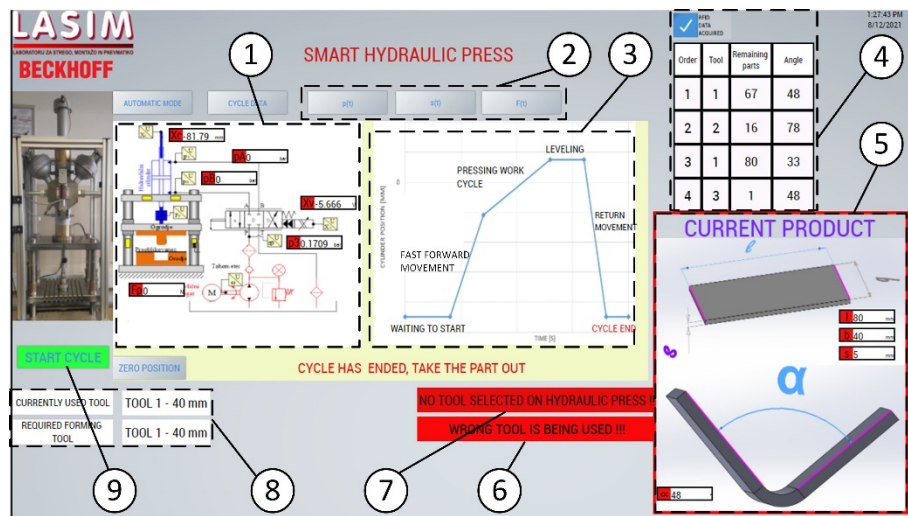
Figure 9: Graphical user interface for hydraulic press.

The developed GUI consists of the nine key elements that enable press cycle operate the press and manage the manufacturing process: 1) real-time monitoring of important parameters, 2) monitoring of pressure $p(t)$, ram stroke $s(t)$ and force $F(t)$, 3) monitoring of the forming cycle and determination of the current forming phase, 4) production plan and important planning data, 5) current product being manufactured and its characteristics, 6) warning signs in case the wrong die tool is used, 7) warning signs in case the tool is not properly set, 8) message to the operator when the forming process is finished, and 9) button to start the forming cycle.

The successful calculation of the hydraulic press cycle (the characteristic points) for the given product is shown in Figure 10. The characteristics points of hydraulic press cycle are defined based on local database information's (characteristics of hydraulic press, die tool and current product). The stroke of the ram (point 4, $x_{p,true}$) to achieve the proper forming angle of the product is calculated automatically according to the procedure presented in chapter 3.3, while the times are gathered from the local base satisfying the overall cycle time.
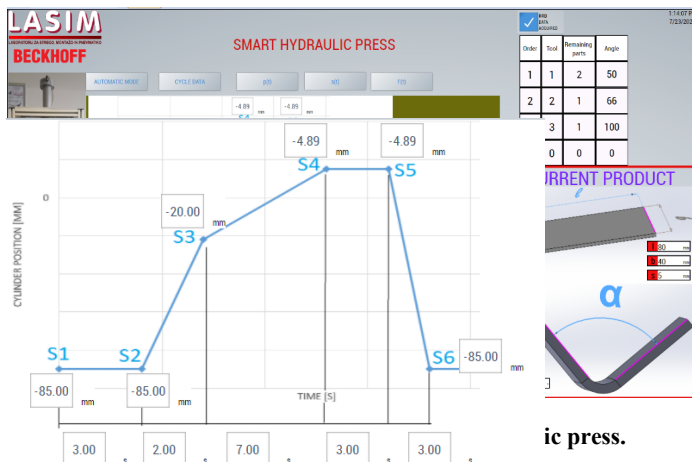
Figure 10: The characteristics points of hydraulic press cycle.

5   Conclusions

The paper focuses on the concept of smart hydraulic press suiTable for integration in smart factory. One of the proposed solutions consists of an expert system and an integrated intelligent algorithm for the automatic generation of the hydraulic press cycle. The other concept is an IoT solution that includes the

hydraulic press, the die tool, the input material, the local cloud database, the expert system, and the control system. RFID technology is used to detect the input material and the die tool. In our solution, the bending process is considered as a demonstration application for validating the intelligent algorithm for automatic generation of the hydraulic press cycle. The newly proposed approach and algorithm considers the characteristics of the hydraulic press such as the cylinder stroke range, the geometrical and dimensional parameters of the hydraulic press, the die tool and the specimen characteristics and dimensions. Based on these characteristics stored in the local database, the intelligent algorithm uses the data to automatically calculate the characteristic points of the hydraulic press cycle. The proposed solution represents the first step towards an intelligent and flexible hydraulic press capable of adopting to different production plans.

References

[1]   Wang B., Tao, Tai, F., Fang, X., Liu, C., Liu, Y., Freiheit, T. (2021). Smart Manufacturing and Intelligent Manufacturing: A Comparative Review. Engineering, vol. 7, no. 6, pp. 738–757, 2021, doi: 10.1016/j.eng.2020.07.017

[2]   Haack, S., Meißelbach, A. Industrial Hydraulics. (2018), Are we really on track concerning Industry 4.0 ?. *11th Int. Fluid Power Conf.* 11. IFK, March 19-21, Ger., 2018.

[3]   S. S. Chawathe. (2019) Condition monitoring of hydraulic systems by classifying sensor data streams. *IEEE 9th Annu. Comput. Commun. Work. Conf. CCWC 2019*, pp. 898–904, 2019, doi: 10.1109/CCWC.2019.8666564.

[4]   Xu, B., Shen J., Liu, S., Su, Q., Zhang, J. (2020) Research and Development of Electro-hydraulic Control Valves Oriented to Industry 4.0. A Review. Chinese J. Mech. Eng. English Ed., vol. 33, no. 1, doi: 10.1186/s10033-020-00446-2

[5]   Stadnicka, D., Litwin, P., Antonelli, D. (2019). Human factor in intelligent manufacturing systems - Knowledge acquisition and motivation. *Procedia CIRP*, vol. 79, pp. 718–723, 2019, doi: 10.1016/j.procir.2019.02.023.

[6]   Zhang, Z., Ma, R., Wang, C., Zhao J. (2019) Research on Springback Control in Stretch Bending Based on Iterative Compensation Method. Math. Probl. Eng., vol. 2019, doi: 10.1155/2019/2025717.

[7]   Ma R., Wang C., Zhai R., Zhao, J. (2019). An Iterative Compensation Algorithm for Springback Control in Plane Deformation and Its Application. *Chinese Journal of Mechanical Engineering (English Edition)*, vol. 32, no. 1. 2019, doi: 10.1186/s10033-019-0339-5.

[8]   Osman. M., Shazly. M., Mokadddem, A. El., Wifi, A. S. (2010) Springback prediction in V-die bending: modelling and experimentation. *J. Achiev. Mater. Manuf. Eng.*, vol. 38, no. 2, pp. 179–186

[9]   Meng, B., Wan, M., Wu, X., Yuan, S., Xu, X., Liu, J. (2014). Development of sheet metal active-pressurized hydrodynamic deep drawing system and its applications. *International Journal of Mechanical Sciences*, vol. 79. pp. 143–151, 2014, doi:10.1016/j.ijmecsci.2013.12. 005.

[10]   Kumar, S., Singh, R. (2005). An intelligent system for selection of die-set of metal stamping press tool. *J. Mater. Process. Technol.*, vol. 164–165, pp. 1395–1401, doi: 10.1016/j.jmatprotec.2005.02.066.

[11]   Opritescu, D., Hartmann, C., Riedl ,W., Ritter, M., Volk, W. (2019). Low-risk bypassing of machine failure scenarios in automotive industry press shops by releasing overall capacity of the production networks. *J. Manuf. Syst.*, vol. 52, no. June, pp. 121–130, 2019, doi: 10.1016/j.jmsy.2019.05.007.

[12]   Kim, H.,Gu, J. C., Zoller, L. Zoller. Control of the servo-press in stamping considering the variation of the incoming material properties. *IOP Conf. Ser. Mater. Sci. Eng.*, vol. 651, no. 1, 2019, doi: 10.1088/1757-899X/651/1/012062.

[13]   Centea, D., Singh, I., Boer, J., Boer. RFID in Manufacturing: An Implementation Case in the SEPT Learning Factory. *Procedia Manuf.*, vol. 51, no. 2019, pp. 543–548, 2020, doi: 10.1016/j.promfg.2020.10.076.

University of Maribor Press

Innovative solution of hybrid hydraulic fire wood splitting machine

DAVOR BIŠKUP, MIHAEL CIPEK, DANIJEL PAVKOVIĆ, JURAJ KARLUŠIĆ &
ŽELJKO ŠITUM

Abstract Hybrid powertrains have already proven themselves as viable solutions for reducing fuel consumption while maintaining the same operating performance of conventional ones, which is achieved by using an additional energy source in combination with energy recuperation. Many forestry machinery and tools which are intended for field use are hydraulics-based and powered by tractors or skidders. These tools may also be hybridized by incorporating a properly-sized hydraulic accumulator. This paper proposes an innovative solution of hydraulic fire wood splitting machine which uses a hydraulic accumulator in order to increase its efficiency. A simple model of conventional and hybridized machine is developed and presented in this paper. The model is then simulated over a defined operating cycle with realistic loads. Simulation results show that hybrid structure may improve the splitting performance with lower power requirements. Finally, the conventional and hybridized machine performances are compared and discussed.

Keywords: • forestry machinery • firewood splitting machine • hybridization • hydraulics • tractor attachment •

CORRESPONDENCE ADDRESS: Davor Biškup, University of Zagreb, Faculty of Mechanical Engineering and Naval Architecture, I. Lučića 5, HR-10000 Zagreb, Croatia, e-mail: davor.biskup@hotmail.com. Mihael Cipek, University of Zagreb, Faculty of Mechanical Engineering and Naval Architecture, I. Lučića 5, HR-10000 Zagreb, Croatia, e-mail: mihael.cipek@fsb.hr. Danijel Pavković, University of Zagreb, Faculty of Mechanical Engineering and Naval Architecture, I. Lučića 5, HR-10000 Zagreb, Croatia, e-mail: danijel.pavkovic@fsb.hr. Juraj Karlušić, University of Zagreb, Faculty of Mechanical Engineering and Naval Architecture, I. Lučića 5, HR-10000 Zagreb, Croatia, e-mail: juraj.karlusic@fsb.hr. Željko Šitum, University of Zagreb, Faculty of Mechanical Engineering and Naval Architecture, I. Lučića 5, HR-10000 Zagreb, Croatia, e-mail: zeljko.situm@fsb.hr

1   Introduction

Wood is an important natural resource and one of the few renewable energy sources. It predominates in everyday life, and it would be difficult to enumerate its many applications. For instance, almost all home furniture is made of wood [1]. However, one of the first things that is associated with wood is the solid fuel (biomass) used for firewood. Heating with biomass, especially wood, is one of the most sought-after types of heating in small-scale residential objects. Due to the higher costs of electricity and gas, this traditional type of fuel is also considered by people living in single-family homes (e.g. cottages), especially in the countryside. As we are witnessing climate changes taking place, primarily caused by harmful gases from combustion of non-renewable energy sources (oil and gas), increasing emphasis is being placed on residential heating impact on ecology. In that sense, wood is also accepted as the most widespread renewable source of energy in the form of biomass [2].

In recent years, great emphasis has also been placed on hybrid and electric powertrains in road vehicles, given the advantages this has regarding the reduction of fuel consumption and harmful gas emissions and, thus, on preserving the environment. Hybrid vehicles are a complex system which use two or more different on-board energy sources [3]. Lately, forestry vehicles have been also increasingly equipped with hybrid electric power-trains [4,5,6] in order to provide significant gains in fuel economy, and also to facilitate measurable reductions in greenhouse gases emissions.

This leads to many open questions, such as whether hydraulics-based forestry tools which are intended for field use and powered by tractors or skidders could also be hybridized by using a properly-sized hydraulic accumulator. This paper investigates one possible solution of hydraulic fire wood splitting machine which uses a hydraulic accumulator in order to increase its efficiency. A simple model of conventional and hybridized machine is developed and presented and then simulated over a defined operating cycle with realistic loads.

Davor Biškup, Mihael Cipek, Danijel Pavković, Juraj Karlušić & Željko Šitum: Innovative solution of hybrid hydraulic fire wood splitting machine

303

2   Firewood splitting machine models

A firewood splitting machine is a device used to produce logs that are suiTable for firewood, with recommended lengths typically between 20 and 100 cm, depending on the construction of the splitter. There is a wide variety of wood splitting machines on the market today, however, this paper deals only with the hydraulic one, powered by mechanical power from a tractor or a skidder.

2.1   Classical model

Within the classical system, force wood splitting is realized through a hydraulic cylinder driven by the flow of hydraulic oil, which is provided by a hydraulic pump. The hydraulic pump is driven by a tractor via a power take-off (PTO) shaft. Table 1 below lists the data for several vertical hydraulic tractor splitters and their specifications which are used as a basis for model development.

Table 1: Technical specifications of vertical hydraulic powered firewood splitting machines

	Krpan CV 18 K PRO [7]	Uniforest TITANIUM 18 [8]	Lancman STX 17 [9]	Robust R16 [10]	Zanon SVTK 16 [11]
F [kN]	170	160	170	160	160
P [kW]	25	21	22,7	25	22
x [mm]	972	1100	1100	1100	1000
t_2 [s]	3,1	4,2	3,33	4,57	-
t_3 [s]	6,3	6,5	8,33	-	-
t_1 [s]	3,2	4,2	5	5,71	-

The hydraulic wood splitting machine which will be primarily used for splitting pieces of wood one meter or less in length with a force of up to 160 kN (~ 16 tons) is selected for analysis in this paper. Due to possible errors when cutting the log to length, it is ensured that the log slightly longer than 100 cm fits under the splitter axe. Therefore, it was chosen that the height from the base to the top

of the axe is 105 cm (1050 mm). The selected splitting force of 16 t is the mean splitting force declared by the renowned manufacturers of splitters and forestry equipment, as indicated in Table 1. Based on the catalogue data [7-11], the reference splitting time at the high speed t_2 is 3 - 4 s, at the low speed t_3 is 6 - 8 s, and the return time of the axe to the initial position t_1 is 3 - 5 s. Looking at the travel speeds of 1000 mm, the high speed is 0.25-0.33 m/s, the low speed 0.14-0.17 m/s, and the return speed 0.2-0.33 m/s. According to the catalogue data [7-11], the oil flow in the system is 50-70 l/min and the pressure in the system is 200-250 bar. In order to avoid oil overheating issues, it would be convenient to have a relatively large volume of oil in the tank, i.e. between 25 and 35 L. The maximum PTO speed is 540 rpm. Figure 1 shows the hydraulic diagram of a splitter consisting of a hydraulic cylinder, a pump, a directional control valve, a filter, a non-return spring-loaded valve, a relief valve, and a fluid reservoir. Of course, in addition to all these components, hydraulic pipes and the fluid (oil) itself are also needed.
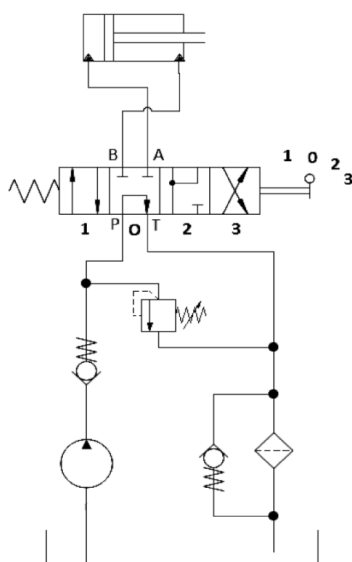
Figure 1: Hydraulics scheme of classical system.

The maximum force F of the cylinder that needs to be achieved to split the wood in this case is 160 kN. Wood splitters usually work at pressures between 200 and 250 bar, so the lower value of the working pressure p of 200 bar was chosen in this calculation as a kind of worst-case scenario. From the above data, the diameter d_{min} of the piston can be determined as follows:

Davor Biškup, Mihael Cipek, Danijel Pavković, Juraj Karlušić & Željko Šitum: Innovative solution of hybrid hydraulic fire wood splitting machine

305

$$d_{min} = \sqrt{\frac{4F}{\pi p}} \tag{1}$$

Based on the calculated minimum piston diameter of cylinder d_{min}, the first larger standard piston diameter is selected from a suiTable catalogue (Table 2, [12]). The usual double-acting hydraulic cylinder (i.e. the so-called "differential cylinder"), has two connections (for hydraulic hoses) that allow the cylinder to move linearly to one side or the other.

Table 2: Technical specifications of cylinder

Hydraulic cylinder (100/60-1050)	
p_{max}	250 bar
$F+$ (250 bar)	190 kN
$F-$ (250 bar)	120 kN
x_{max}	1050 mm
v_{max}	500 mm/s
d	100 mm

Note that, due to the different ratio of the surface area of the compressed oil at different sides of the piston, the piston also has different pulling and contracting forces. Moreover, due to the different volume of oil on both sides of the cylinder, the piston speed is different for different movement directions, i.e. the piston moves faster from one side to another compared to movement in the opposite direction. In particular, when the cylinder is "pulled out", the oil acts on the entire surface of the piston, in which case the cylinder command a greater force and moves at a lower speed. When the surface of the piston is smaller, the piston moves faster in that direction and therefore the cylinder overcomes less force. The ultimate goal is to have favourable time of lowering the axe between 6 and 8 s (see t_3 in Table 1). Although the cylinder is able to move even faster (achieving traverse time of just 2.1 s), this requires a much larger fluid flow (and a larger pump), which leads to higher component costs. On the other hand, the axe should not move too slowly in order to avoid unnecessary loss of time and decreased productivity. Therefore, the required fluid flow Q for movement can be calculated as:

$$Q = \frac{v d^2 \pi}{4 \eta_{vol}} \qquad (2)$$

where d is piston diameter and η_{vol} is volumetric efficiency of the system ($\eta_{vol} =$ 0.95 is chosen in this paper). An adequate pump volume V_p of 32 cm³ is determined to satisfy required fluid flow at the pump operating speed of 2000 rpm [12, 13]. Please note that there is also a quick-stroke cylinder position on the direction valve (see position 2 in Figure 1) that can be used for higher cylinder pull-out speeds, but only at lower loads.

2.2 Hybrid model

A hydraulic accumulator has been added to the classic hydraulic fire wood splitter system to increase its efficiency and productivity, and, consequently, the hybrid system now possesses two energy sources (mechanical and hydraulic) through hybridisation. The hydraulics scheme, showing the location of the hydraulic accumulator, is shown in Figure 2. In addition to the hydraulic accumulator, a manometer, a shut-off valve and a valve for relieving the pressure of the accumulator have also been added to the system.

Davor Biškup, Mihael Cipek, Danijel Pavković, Juraj Karlušić & Željko Šitum: Innovative solution of hybrid hydraulic fire wood splitting machine

307
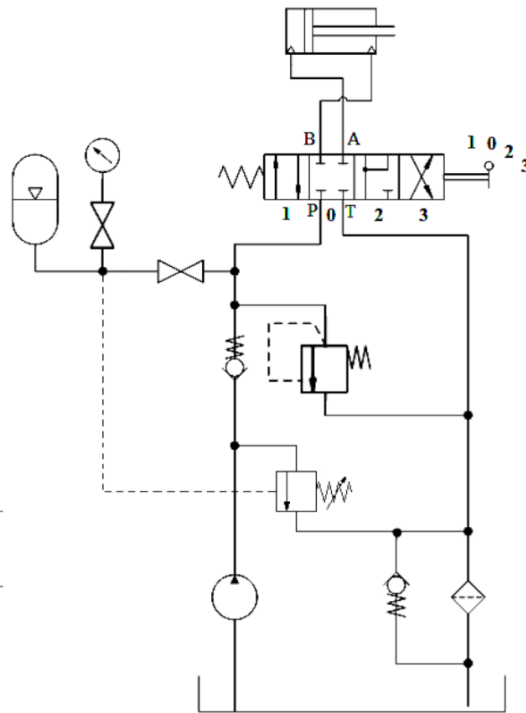
Figure 2: Hydraulics scheme of hybrid system.

Figure 3 shows the operating cycle of a cylinder that cyclically repeats the operating strokes. The durations of individual work cycles were measured in real life [13], and the arithmetic mean was taken from several measurements. One working cycle lasts a total of 29 s. It should be noted that in the analysis the first few working cycles during system warm-up and startup of the working machine (tractor) are not taken into account due to them having significantly longer durations compared to steady-state operating regimes.
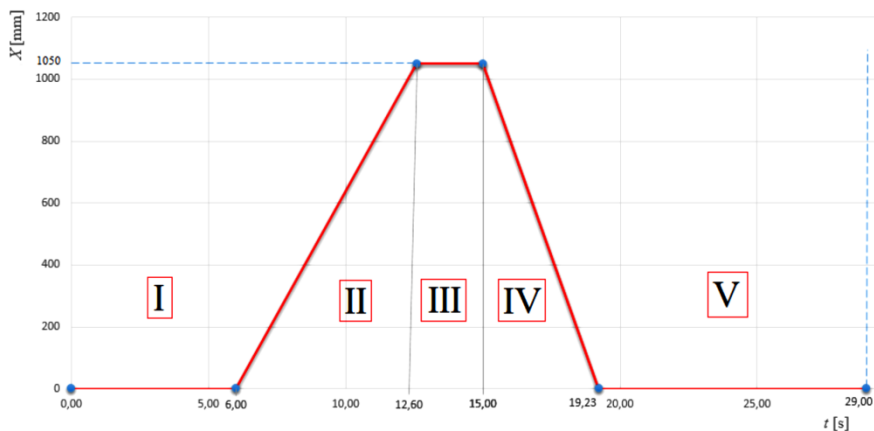
Figure 3: One duty cycle.

It can be seen that one operating cycle consists of 5 parts. The first (I) part is the preparation of wood, i.e. taking the log and placing it on the work surface. This takes 6 s and during this time both the cylinder and the axe are in their initial position ($x = 0$ mm). By holding the log on the splitter and pressing the lever downwards, the second (II) part begins, which represents the movement of the cylinder and the axe downwards, and the splitting of the wood begins. In this phase, the axe begins to enter the log which is already positioned on the splitter. With a log 100 cm long (the usual length), the stroke of the axe is 1050 mm, and this phase takes 6.6 s to complete. Afterwards, in the third (III) phase the lever is moved to the neutral position wherein the cylinder holds the final outward position for 2.4 s. During this phase it is sometimes necessary to manually separate the wood if it does not crack completely, but this does not frequently occur. Immediately after switching the lever upwards, the fourth (IV) phase is initiated, where the cylinder moves up to its initial position ($x = 0$ mm). The time required to return the cylinder is 4.23 s. Finally, in the fifth (V) phase logs are removed from the splitter, and are carried by a worker to their intended place

Davor Biškup, Mihael Cipek, Danijel Pavković, Juraj Karlušić & Željko Šitum: Innovative solution of hybrid hydraulic fire wood splitting machine

309

and arranged in a row. The whole process takes 14 s and the cylinder is at a standstill at the end of stage V (stands in the initial position), and the hydraulic pump is constant switched on, giving flow throughout. Figure 4 shows a flow diagram of the time that the pump must achieve to move the cylinder.
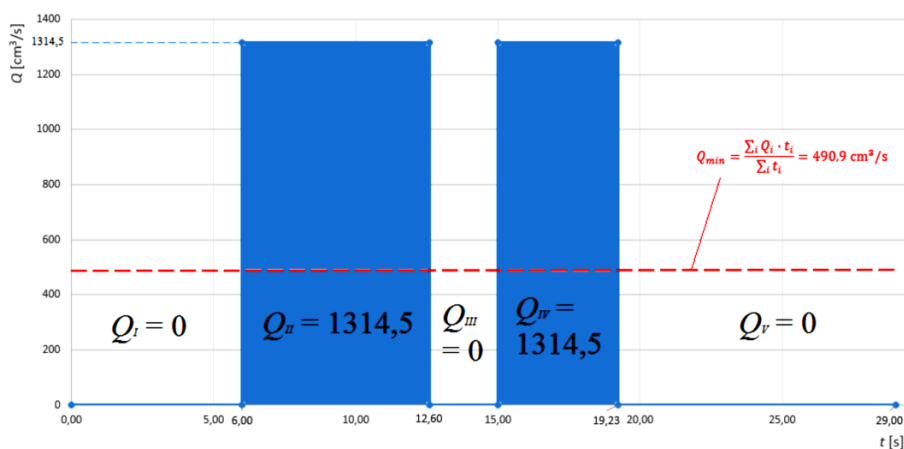
Figure 4: Required fluid flow for cylinder movement.

Figure 4 shows that parts I, III and V do not require fluid flow, i.e. the cylinder does not move in these phases, meaning that the hydraulic pump flow is not necessary. It is seen that the pump must operate only in phases II and IV. This is inefficient, as most of the time the pump provides a flow that is not actually needed by the system. When needed, the hydraulic oil flow is quite large, which means that a large hydraulic pump is needed for that purpose. The red dashed line in the diagram represents the pump flow Q_{min} which is determined as mean value for one duty cycle (490.9 cm³/s, or 29.45 l/min). If the required flow were distributed over the total time of one operating cycle, the required flow is almost three times lower compared to the peak flow. Therefore a smaller pump would be sufficient for that purpose.

Figure 5 shows a comparison of the volume provided by the average flow Q_{min} and the volume required for the entire operating cycle over time. The volume ΔV represents the part that needs to be compensated from the hydraulic accumulator. For dimensioning the hydraulic accumulator, the maximum ΔV is taken, which can be read from the diagram in Figure 5, and amounts to $\Delta V_{IV} = 886$ cm³. Data related to the hydraulic accumulator are as follows: charging

pressure $p_0 = 80$ bar, operating pressure in the system $p_1 = 200$ bar and maximum pressure $p_2 = 320$ bar. The volume of the hydraulic accumulator for the adiabatic process with the charge of the accumulator with nitrogen ($n = \varkappa = 1.4$) was defined according to the following expression:

$$V_a = \frac{\Delta V}{\left[\left(\frac{p_0}{p_1} \right)^{\frac{1}{n}} - \left(\frac{p_0}{p_2} \right)^{\frac{1}{n}} \right]} \tag{3}$$

Therefore, the required volume of the hydraulic accumulator is 5.98 L, which has been rounded up to 6 L for further analysis. Such hydraulic accumulators can be found on the market and meet the required specifications.
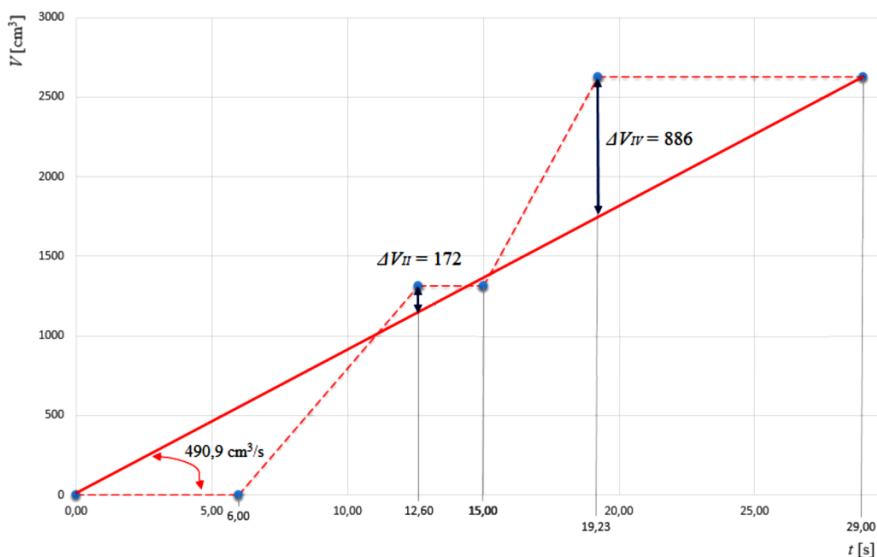
Figure 5: Required fluid flow for cylinder movement.

3   Simulation results

The previously analysed typical operating cycle of a classic hydraulic system for normal stroke scanario is simulated in FluidSIM environment. The results of this simulation scenario, including all five phases of piston operation (presented in Figure 3) are shown in Figure 6. The exact position of the cylinder in time can

Davor Biškup, Mihael Cipek, Danijel Pavković, Juraj Karlušić & Željko Šitum: Innovative solution of hybrid hydraulic fire wood splitting machine

311

be seen, which approximately corresponds to the previously drawn diagram in Figure 3. It can be clearly seen how long it takes for the cylinder to move out, returns inside, and how long it actually stands in place and moves. Below the position diagram is a diagram of the speed of movement of the cylinder.
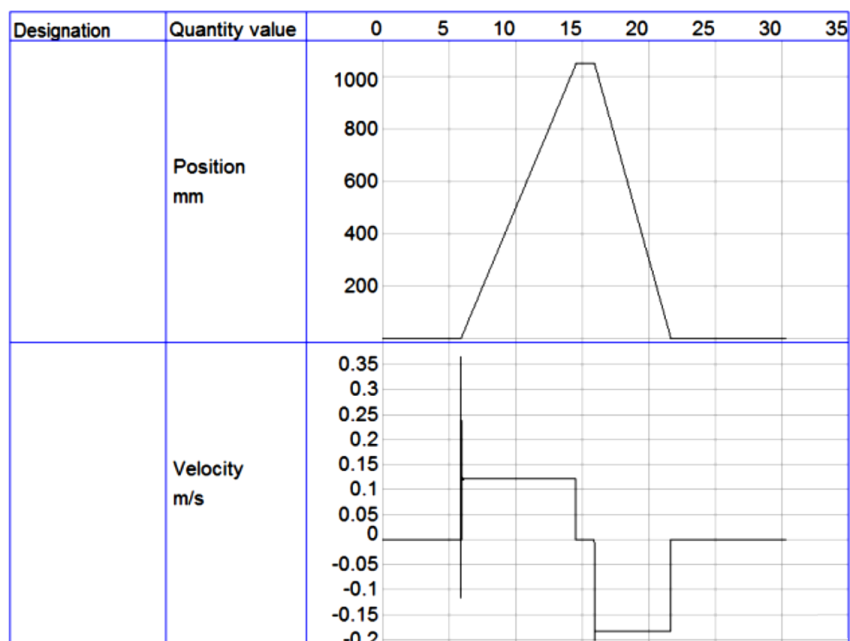
Figure 6: Simulation results of cylinder movement.

The simulation results of the splitter operation using the computer program FluidSIM are given further and are compared with calculations. The simulation results show how the designed hydraulic system works and confirm that both the classical and the hybridised system meet the predefined requirements. The final results are presented in a Table 3, comparing these two systems in terms of analytical calculations and simulations in the FluidSIM program. The differences between analytical calculations and simulation results are primarily due to the fact that simple mathematical models used for steady-state analysis do not take into account some real physical phenomena such as friction, elasticity and fluid compressibility, and piston motion dynamics. In this case the cylinder is set to overcome the friction between steel and wood, however, given the friction factor offered, the question is how well this factor corresponds to real values. In addition, not all required parameters within the components were known, so

some required values were assumed, which could greatly affect the final simulation results. Furthermore, some parameters have been simplified in the FluidSIM software tool also, and it is therefore not possible to enter the exact characteristics of the hydraulic components from the catalogue (e.g. proper filter characteristics). The quality of the obtained results largely depends on details of the developed scheme, but also on the selected components. Due to the idealization of the system and lack of information on all parameters, certain deviations in results can be expected from the actual application. However, in the particular case these discrepancies between the results obtained by the simulation model and the analytical calculations are pretty negligible.

Table 3: Comparison of classical and hybridised system [13]

	CALCULATION		SIMULATION	
	Classical system	**Hybridised system**	**Classical system**	**Hybridised system**
v [m/s]	0.122	0.159	0.12	0.15
t_2 [s]	8.6	6.6	8.8	6.9
t_3 [s]	3.09	2.39	3.1	2.44
t_1 [s]	5.51	4.23	5.8	4.4
V_p [cm³]	32	16	32	16
Q [l/min]	57.49	30.4	57.16	30.39
n [rpm]	2057	2052	2057	2052
P [kW]	20	10	-	-
V_a [l]	0	6	0	6

The design solution of the hybridized hydraulic splitter is shown in Figure 7 and more details on structural calculations can be found in reference [13].

Davor Biškup, Mihael Cipek, Danijel Pavković, Juraj Karlušić & Željko Šitum: Innovative solution of hybrid hydraulic fire wood splitting machine

313
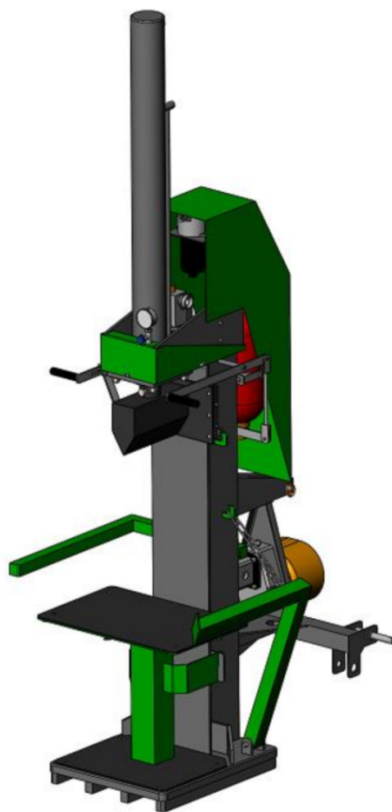
Figure 7: 3D CAD model of hybridised firewood splitting machine [13].

4   Conclusion

The paper proposes the concept of a hydraulic machine for splitting firewood that uses a hydraulic accumulator to increase its efficiency. The hydraulics were chosen due to their high power density, i.e. they enable the transmission of large forces with relatively small devices and elements and straightforward conversion of hydraulic energy into mechanical work. Moreover, based on the proposed splitter implementation, a very simple realization of linear motion of the axe is possible. The hydraulics are also characterized by favourable dynamics, i.e. low inertia of the moving parts, with extremely simple overload protection by means of a pressure relief valve. In addition, hydraulic oil as a liquid medium (fluid),

which ensures favourable lubrication and heat conduction (cooling). The addition of a hydraulic accumulator is a novelty in this group of machines.

The splitting time of the wood (log) itself is very short compared to the remainder of the working cycle, i.e. significant part of the work cycle time is spent on placing log on the splitter and removing the split wood. In the classical system, the speed of the cylinder depends on the flow of the pump, while in the hybrid system, using a hydraulic accumulator, the operating speed is higher due to the added flow and pressure from the accumulator. In addition, it is possible to use the main pump rated for lower fluid flow, and, thus, a lower input power is needed from the tractor to drive the system. In other words, the use of a hydraulic accumulator allows the system of equal force and higher splitting speed to be permanently driven by a smaller tractor (lower power drive).

It is expected that a hybrid splitter system using a hydraulic accumulator would only be slightly more expensive than the conventional system. However, the the cylinder speed is increased and the splitting times are shortened by using the hybridised system, whereas a pump of smaller volume is needed, which results in less required power. Therefore, lower fuel consumption of the tractor during operation can be expected if hybrid solution is used. Economic viability is more emphasised in lower-power tractors, which are cheaper than their higher-power counterparts.

However, despite all of its advantages, hydraulics also have some disadvantages. Among the most significant is that hydraulic elements are highly expensive. In addition, there is a slightly greater need for maintenance because due to impurities and wear of components, there is a possibility of increased friction and possible losses due to fluid leakage, which leads to a decrease in efficiency. The environmental component is also questionable due to increased noise, potential fluid leakage into the environment and fire hazards.

Acknowledgments

Davor Biškup, Mihael Cipek, Danijel Pavković, Juraj Karlušić & Željko Šitum: Innovative solution of hybrid hydraulic fire wood splitting machine

315

References

[1]   Sreevani, P. (2018). Wood as a renewable source of energy and future fuel. International Conference on Renewable Energy Research and Education (RERE-2018), doi:10.1063/1.5047972

[2]   https://www.hgk.hr/documents/hgkdrvojeprvokatalogweb5785f41bb12d8.pdf (Accessed: 19.07. 2021.)

[3]   Fuhs AE. (2009) Hybrid Vehicles and the Future of Personal Transportation. Taylor & Francis Group, LLC.

[4]   Fonseca, A., Aghazadeh, F., Hoop, C., Ikuma, L., Al-Qaisi, S. (2014). Effect of noise emitted by forestry equipment on workers' hearing capacity, International Journal of Industrial Ergonomics, 46.

[5]   Potočnik, I., Poje, A. (2017), Forestry Ergonomics and Occupational Safety in High Ranking Scientific Journals from 2005–2016, Croatian Journal of Forest Engineering, 38. 291-310.

[6]   Karlušić, J., Cipek, M., Pavković, D., Benić, J., Šitum, Ž., Pandur, Z., Šušnjar, M. (2020). Simulation Models of Skidder Conventional and Hybrid Drive. Forests, 11.

[7]   http://www.vitli-krpan.com/si/prodajni-program/cepilniki-drv/serija-cv/428-cv-18-k-pro (Accessed: 28.09.2020.)

[8]   https://uniforest.si/proizvodi/cepilniki_drv/57/titanium_18/ (Accessed: 28.09.2020.)

[9]   https://hr.lancman.si/product/cjepac-profesionalni/st17/ (Accessed: 28.09.2020.)

[10]   https://www.robust.si/prodajni-program/gozdarska-oprema/cepilniki/robust-r16/ (Accessed: 28.09.2020.)

[11]   https://www.messis.hr/cjepaci-i-strojevi-za-usitnjavanje/311-cjepaci-drva-traktorski-i-motorni-12-t-20-t (pristupljeno: 28. rujna 2020.)

[12]   http://www.rositeh.si/?gclid=EAIaIQobChMIpaewjdO-6wIVydmyCh18tQSBEAAYASAAEgJ6M_D_BwE (Accessed: 30.09.2020.)

[13]   Biškup, D. (2020). Projektiranje hidrauličnog cjepača za ogrjevno drvo, Design of hydraulic firewood splitting machine, MSc Thesis. https://urn.nsk.hr/urn:nbn:hr:235:130350

University of Maribor Press

IOT based Web application concept for monitoring and control of fluid power systems

JURAJ BENIĆ, ANĐELKO VICO, LUKA VUČETIĆ & ŽELJKO ŠITUM

Abstract This paper presents a novel concept of the WEB application for monitoring and control of fluid power systems. The proposed concept is based on the internet of things principles. WEB application is built on the Web2py framework which uses Python as the programming language. The client-side of the proposed application is based on the responsive open source AdminLTE dashboard. On the server-side Python is used for executing SQL queries sent to the database and for continuous data logging. The ModbusTCP protocol is used as the communication protocol between the server and systems. The application is tested on two experimental setups. The first one uses an industrial PLC and the second one is an Arduino PLC as a control device. Finally, experimental results are presented and a conclusion is given.

Keywords: • IoT • web application • Industry 4.0 • hydraulics • pneumatics •

CORRESPONDENCE ADDRESS: Juraj Benić, University of Zagreb, Faculty of Mechanical Engineering and Naval Architecture, Ivana Lučića 5, 10000 Zagreb, Croatia, e-mail: jbenic@fsb.hr. Anđelko Vico, University of Zagreb, Faculty of Mechanical Engineering and Naval Architecture, Ivana Lučića 5, 10000 Zagreb, Croatia, e-mail: andelkov@gmail.com. Luka Vučetić, Festo d.o.o, Nova cesta 181a, 10000 Zagreb, Croatia, e-mail: lukavctc@gmail.com. Željko Šitum, University of Zagreb, Faculty of Mechanical Engineering and Naval Architecture, Ivana Lučića 5, 10000 Zagreb, Croatia, e-mail: zsitum@fsb.hr.

J. Benić, A. Vico, L. Vučetić & Ž. Šitum: IOT based Web application concept for monitoring and control of fluid power systems

317

1   Introduction

The Internet of Things (IoT) is a new concept in the IT world that attracted the attention of many researchers over the last decade. For now, there is no unique definition of IoT, but it's considered as a global network that allows communication between human-to-human, human-to-things, and things-to-things anywhere in the world [1].

From the aspect of fluid power in [2], a short introduction to Industry 4.0 (I4.0) and IoT is given with basic strategies for improving flexible manufacturing. The concept of the I4.0 is described on a linear hydraulic actuator with all problems which need to be overcome for successful implementation of the I4.0. In [3] design of the direct-driven hydraulic system is proposed based on IoT technologies. The proposed design uses an ARM Cortex M3 microcontroller with an LCD touchscreen for system control. The IoT technologies allowed remote monitoring of measured data but remote system control wasn't implemented. A new concept of soft sensor networks which contributes towards industry digitalization is presented in [4] where soft sensors are based on physical models. The soft sensor can be easily used for predictive maintenance and by such lower the maintenance cost of equipment. In [5] web controlled pneumatic press is presented. It is connected to the internet over an ethernet shield on the Arduino Mega controller. The pneumatic press can be monitored and controlled online via a simple GUI or voice-controlled using neural networks. The proposed concept uses HTTP protocol to send data and socket communication to receive input given by the user. The main problem in this approach is that application is not scalable on another system and HTTP communication is slow in comparison to other protocols.

In this paper, a web application for monitoring and control of fluid power systems is presented. The proposed application is built on IoT principles and it's tested on two experimental setups. In Section 2 experimental setups are presented while in Section 3 working principle is given. The web application is described in Section 4. Conclusion and further work are given in Section 5.

2   Experimental setups

2.1   Hydraulic experimental setup

The hydraulic experimental setup used in this research is shown in Figure 1. The setup consists of a proportional electrohydraulic system and a direct driven hydraulic system with a double-acting cylinder placed in the gravitational field. For the control of the whole system, Mitsubishi electric PLC FX5U-32MT/ESS is used while HMI is used for the user interface. The PLC and HMI communicate mutually over the router while access to the server is only allowed to the PLC and Raspberry Pi 4. Video from the system si streamed over Raspberry Pi which uses a Logitech USB camera for capturing video. A detailed system description is given in [6].
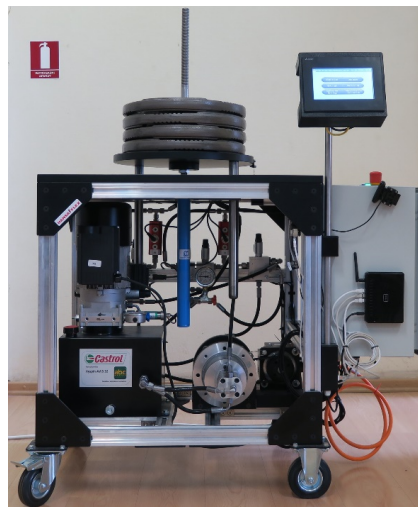
Figure 1: Hydraulic experimental setup.

2.2   Pneumatic experimental setup

The pneumatic experimental setup used for IoT application is shown in Figure 2. The proposed setup consists of seven double-acting pneumatic cylinders, two semi-rotary drives with a swivel angle of 180°, and two vacuum suctions. Festo compact valve terminal VTUG with eleven 5/2 monosTable and two 3/2 bisTable directional control valves is used for motion control. As a control device, Controllino Maxi Automation is used which is an industrial PLC based

J. Benić, A. Vico, L. Vučetić & Ž. Šitum: IOT based Web application concept for monitoring and control of fluid power systems

319

on Arduino Mega controller. Raspberry Pi 3 with Logitech USB camera is used for video streaming. Both PLC and Raspberry Pi are connected via a router to a web server.
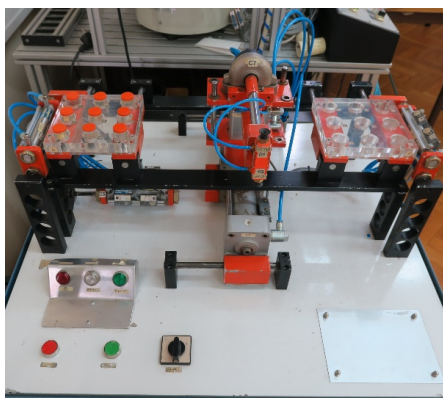
Figure 2: Pneumatic experimental setup.

3 Proposed concept

Schematics representation of the proposed concept is shown in Figure 3 and it's divided into three main blocks. Block 1 represents an individual system inside the production plant. Every system has its router which allows local communication between a PLC and HMI. The ModbusTCP protocol is used for communication between the server and a PLC while HMI doesn't communicate with the server. The Raspberry Pi streams the video from a USB camera via a router on port 8081. The server and a database are represented with block 2. For the webserver, Apache is used while for the relation database MariaDB server is used. Web2py framework is installed on the server and it allows the design of dynamical web pages. The users are represented with block 3. They can use any device with internet access and a web browser for accessing the web application. Depending on different user privileges some of the users can only see monitored data while others can send data back to the system.
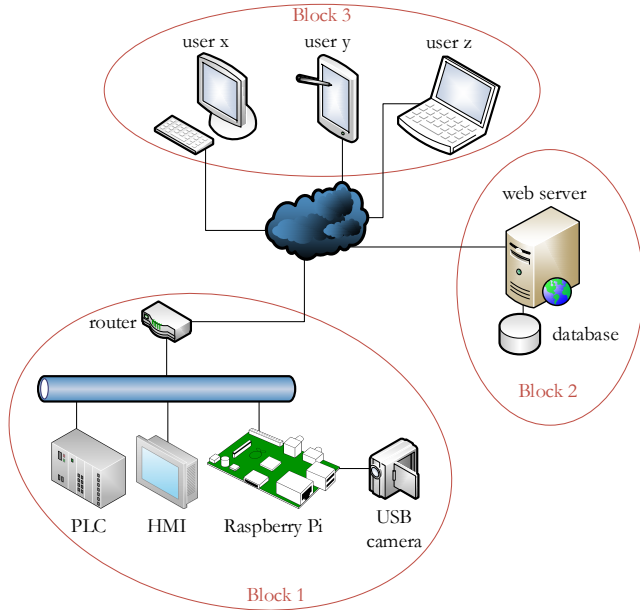
Figure 3: Schematics representation of the proposed concept.

4   IoT based web application

The proposed web application is built on the Web2py framework. Python 2.7 is used on the server-side for accessing the database and for achieving ModbusTCP communication between a server and a PLC. The client-side is based on the newest web technologies. The user interface is built on a free open source AdminLTE dashboard which includes Bootstrap 4.

After successful login in the web application, the first page which the user sees is a dashboard shown in Figure 4. On the left side of the page, there is the main menu with three categories. The system statistic is given in the middle of the page where we can have the cumulative statistic for all systems or the individual system. The proposed statistics express how much time the system spent working, powered off or on, etc.

J. Benić, A. Vico, L. Vučetić & Ž. Šitum: IOT based Web application concept for monitoring and control of fluid power systems

321
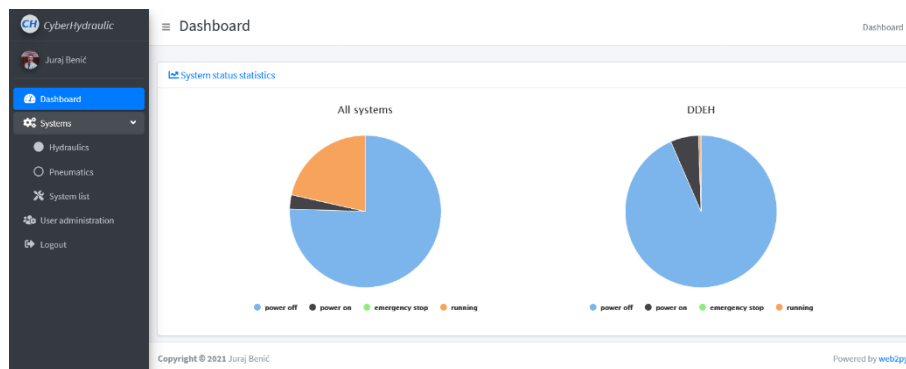
Figure 4: Dashboard.

The web page for system administration is shown in Figure 5. The user with administrative privileges can edit, delete or add a new system to the database. The list of all systems from the database with their basic data is shown in the Table in Figure 5.
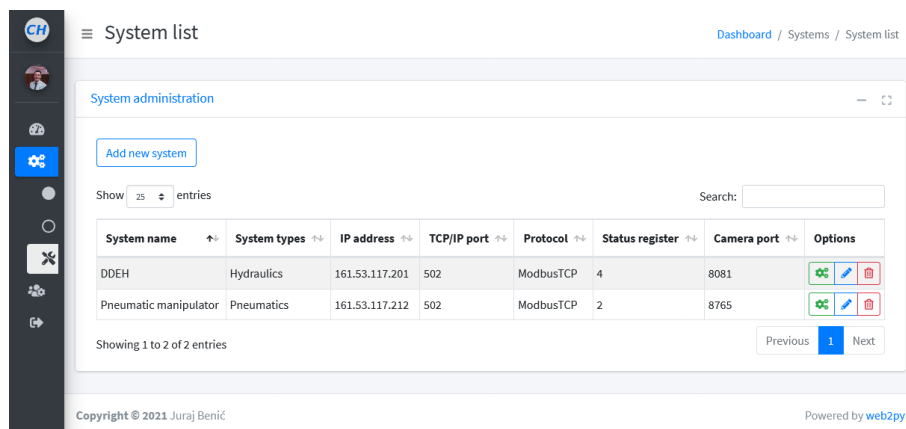
Figure 5: System administration.

By clicking on the green cogs button the web page for system registres appears as shown in Figure 6. Here, the user can add all relevant registres used in a PLC which are needed for remote monitoring and control. For each registres user needs to define the register number from a PLC, name, data type, read/write mode, logging, and description. Next, Tables in the database for the added registres need to be defined. Defined Tables are used for saving continuous logged data and monitored data in the database.

Figure 6: List of system registers for a given system.

The submenus for the hydraulic and pneumatic systems are located under the main menu *systems*. The web page lists all systems depending on a chosen system category as shown in Figure 7. Every system has its card with a basic description, two buttons for history, and a detailed view while system status is updated every 100 ms.

Figure 7: Pneumatic experimental setup.

The detailed system view is shown in Figure 8. The *live charts* are showing all process variables which need to be continuously monitored and they are updated every 100 ms. Live stream video is shown on the card titled *video*. The registres which only need to be monitored are given in the Table on the card *register* monitoring and they are refreshed every 100 ms. System control is done on the

J. Benić, A. Vico, L. Vučetić & Ž. Šitum: IOT based Web application concept for monitoring and control of fluid power systems

323

write registers card where users need to choose the register in which they want to write the value.
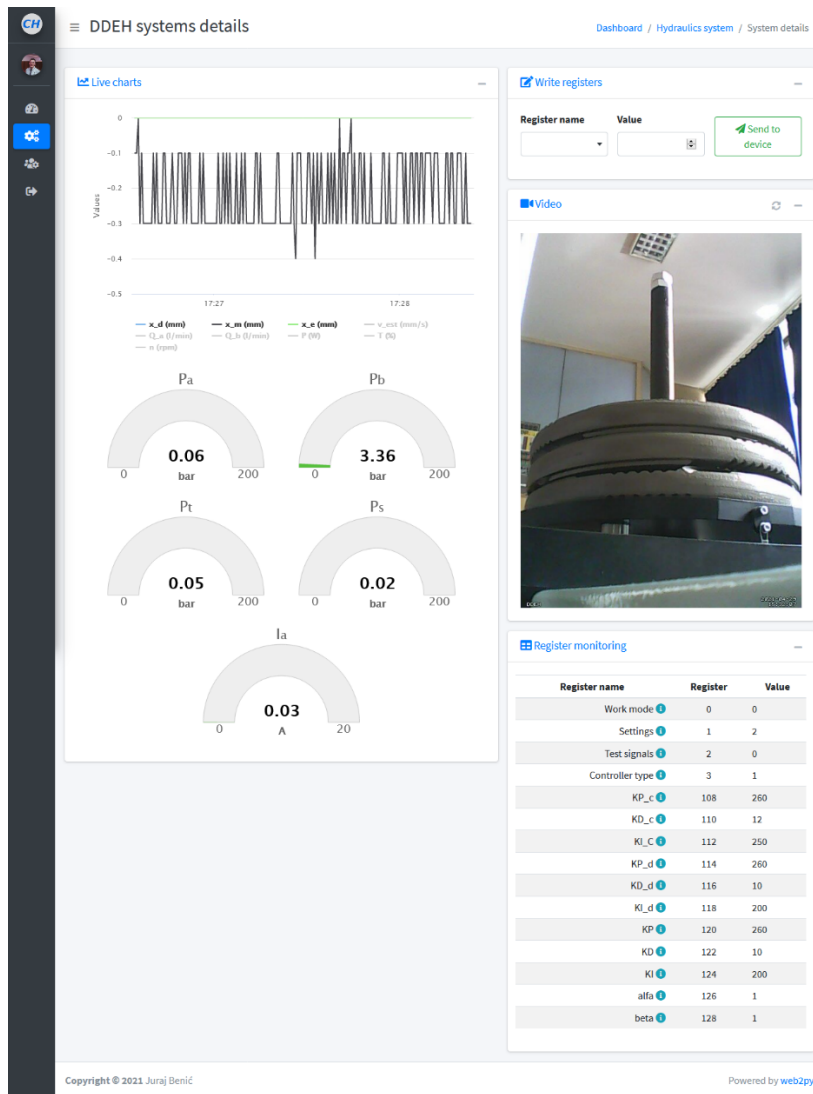
Figure 8: Pneumatic experimental setup.

The history view of logged data is shown in Figure 9. Users can choose between two values and mutually compare them. Their comparison is shown on a line graph and it can easily be exported in CSV, jpeg, png, and other formats.
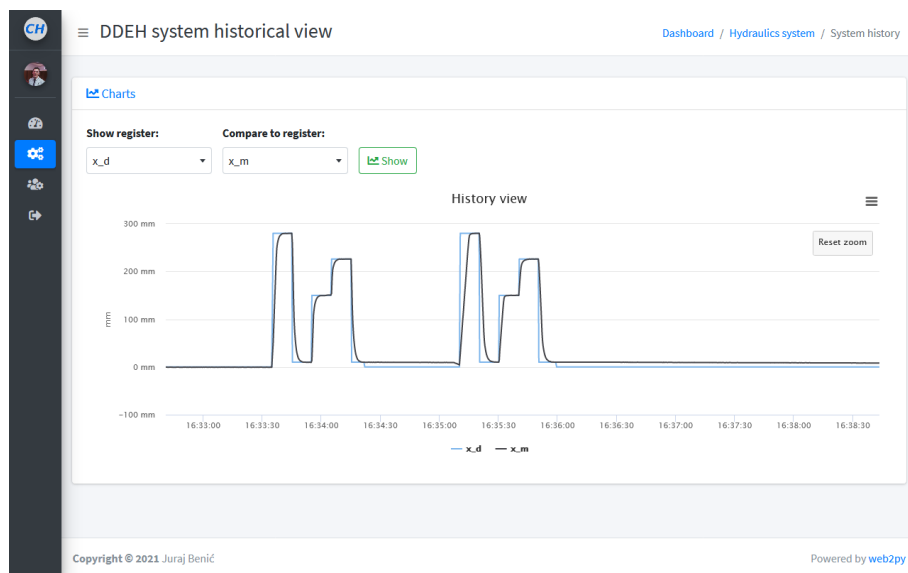
Figure 9: Pneumatic experimental setup.

## 5	Conclusion

The proposed web application is user-friendly and scalable. It is easily integrated into existing systems controlled via PLC due to the use of standard industrial ModbusTCP protocol. Integrated systems are monitored and controlled in real-time. The web application can be expanded with custom statistics dependable on plant requirements. Further work will include the integration of different industrial communication protocols to the web application such as EtherCAT, EtherNet/IP, Powerlink, etc.

J. Benić, A. Vico, L. Vučetić & Ž. Šitum: IOT based Web application concept for monitoring and control of fluid power systems

325

References

[1] Madakam, S., Ramaswamy, R., Tripathi, S. (2015). Internet of Things (IoT): A Literature Review. *Journal of Computer and Communications, 3*, 164-173

[2] Alt, R.M., Murrenhoff, H., Schmitz, K. (2018). A Survey of "Industrie 4.0" in the Field of Fluid Power-Challenges and Opportunities by the Example of Field Device Integration. *Universitätsbibliothek der RWTH Aachen*

[3] Wang, L.H., Wang, Y. (2014). Design of Direct Drive Electro-hydraulic Actuator Based on Internet of Things Technology. *In Advanced Materials Research, 945*, 1601-1605

[4] Pelz, P., Dietrich, I., Schänzle, C., Preuß, N. (2018). Towards digitalization of hydraulic systems using soft sensor networks. *Universitätsbibliothek der RWTH Aachen*

[5] Dabčević, Z., Benić, J., Šitum, Ž. (2021). Web Controlled Pneumatic Press. *Ventil 27, no. 2*, 96-103

[6] Benić, J., Šitum, Ž. (2019). Position Controller for Direct Driven Electro-Hydraulic System. *International che Fluid Power 2019*, 181-194

Conference sponsors

General sponsor

FESTO d.o.o.

Social event sponsor:

HAWE Hidravlika d.o.o.

Conference organization has been sponsored by:

OLMA d.o.o.

BECKHOFF Avtomatizacija d.o.o.

TESNILA Bogadi d.o.o.

POCLAIN Hydraulics d.o.o.

DIMAS PRO d.o.o.

NEVIJA d.o.o.

Media sponsors:

VENTIL   **UM Press**   **IRT3000**

We would like to thank all the sponsors for their support and contribution to the organization of the conference!

Nothing moves without us.
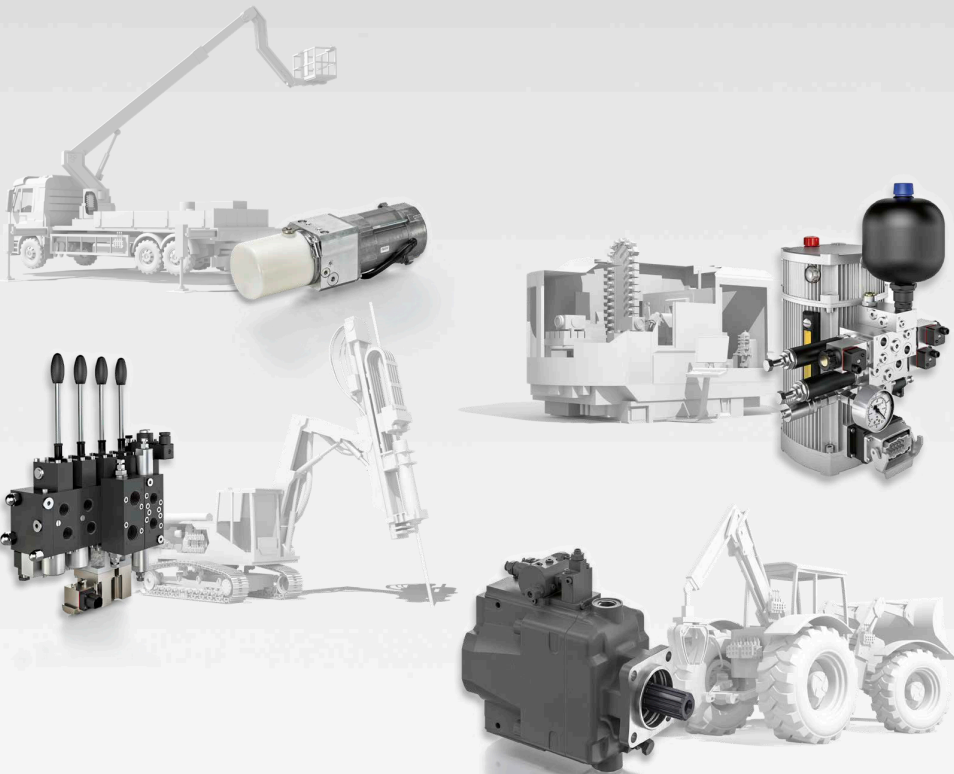
When great things are being moved with hydraulics, HAWE is involved.

HAWE Hydraulik is a leading manufacturer of technologically advanced, high-quality hydraulic components and systems. HAWE products are used wherever high quality, high power and maximum precision is required - whether in machine tools, construction machinery or wind turbines.

www.hawe.com

S pravim mazivom

ne spodrsava

Olma d.o.o., Poljska pot 2, 1000 Ljubljana,
tel.: (01) 58 73 600, e-pošta: order@olma.si

OLMA
www.olma.si

Dimas Pro

DIMAS PRO d. o. o. zastopa vodilnega svetovnega proizvajalca filtrnih elementov podjetje **HY-PRO FILTRATION**. Z njihovo pomočjo, lastnim znanjem in pomočjo kanadskega podjetja **EPT Cleanoil** ter novozelandskega podjetja **TROJAN Dry-Out Systems** nudimo:

- sodobne tehnične rešitve, naprave in šolanja za nego hidravličnih, mazalnih, transformatorskih olj in goriv;
- zamenjavo oljnih filtrnih elementov vseh svetovnih proizvajalcev v izvedbi, ki večinoma zagotavlja nadgrajeno kvaliteto filtriranja, s tem pa daljšo uporabno dobo komponent sistemov in višjo dodano vrednost.;
- elektronsko upravljanje in nadzor mazalnih sistemov (IOT);
- elektronsko analizo in izvajanje meritev olj, idr.

FLUIDNA TEHNIKA
NEVIJA

Gregorčičeva ulica 29a, SI - 2000 Maribor, E-mail: dragan@nevija.si

INŽENIRING s področja hidravlike v industriji in energetiki

Zastopstva:

HÄNCHEN Hydraulik

simply good.

ENERPAC

Visokotlačna hidravlična orodja

I **Strokovni in znanstveni prispevki**

I **Iz prakse za prakso**

I **Ventil na obisku**

I **Novice - zanimivosti**

I **Aktualno iz industrije**

I **Novosti na trgu**

I **Podjetja predstavljajo**

I **Ali ste vedeli**

I **Dogodki**

Spoštovani!

Ventil je znanstveno-strokovna revija in objavlja prispevke, ki obravnavajo razvojno in raziskovalno delo na Univerzi, inštitutih in v podjetjih s področja fluidne tehnike, avtomatizacije in mehatronike. Revija želi seznanjati strokovnjake z dosežki slovenskih podjetij, o njihovih izdelkih in dogodkih, ki so povezani z razvojem in s proizvodnjo na področjih, ki jih revija obravnava. Prav tako želi ustvariti povezavo med slovensko industrijo in razvojno in raziskovalno sfero ter med slovenskim in svetovnim proizvodnim, razvojnim in strokovnim prostorom. Naloga revije je tudi popularizacija področij fluidne tehnike, avtomatizacije in mehatronike še posebno med mladimi. Skrbi tudi za strokovno izrazoslovje na omenjenih področjih.

Revija Ventil objavlja prispevke avtorjev iz Slovenije in iz tujine, v slovenskem in angleškem jeziku. Prispevkom v slovenskem jeziku je dodan povzetek v angleščini, prispevki v angleščini pa so objavljeni z daljšim povzetkom v slovenskem jeziku. Člani znanstveno strokovnega sveta so znanstveniki in strokovnjaki iz Slovenije in tujine. Revijo pošiljamo na več naslovov v tujini in imamo izmenjavo z drugimi revijami v Evropi. Revija je vodena v podatkovni bazi INSPEC.

Štiriindvajsetletno izhajanje revije Ventil pomeni, da je v prostoru neprecenljiva za razvoj stroke. Uredništvo si skupaj z znantveno strokovnim svetom prizadeva za visokokvalitetno raven in relevantnost objav, ki bosta v prihodnosti vse napore usmerila v to, da bo kvalitetna raven še višja. V ta namen vključuje v znantveno strokovni svet priznane znanstvenike, raziskovalce in strokovnjake, ki s svojim znanjem vspodbujajo vsak na svojem področju objavljanje rezultatov razvojnega in raziskovalnega dela. Uredništvo spremlja razvoj stroke in znanstveno raziskovalno delo doma in vtujini preko konferenc, delavnic in seminarjev ter z izmenjavo tuje periodike.

Revija je priznana v tujini, še posebno na področju fluidne tehnike, kar želimo doseči tudi na področju mehatronike in avtomatizacije. Preko objav v reviji se promovirajo dosežki slovenske znanosti in industrijske proizvodnje. Revija je in bo tudi v prihodnje prostor za predstavljanje kvalitetnih razvojnih in raziskovalnih dosežkov slovenske industrije in raziskovalne sfere na področju fluidne tehnike, avtomatizacije in mehatronike.
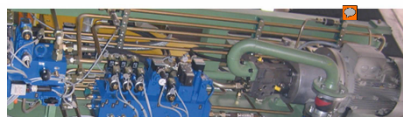
Uredništvo

University of Maribor Press

Fizikalno ozadje delovanja hidravličnih sistemov

Darko Lovrec

Uvod v hidravlično Pogonsko-krmilno tehniko

Darko Lovrec

Hidravlika za mehatronike

Darko Lovrec
Vito Tič

Clarivate Analytics

open Open Access
Publishing in European Networks

doab directory of open access books

Univerza v Mariboru
Digitalna Knjižnica Univerze v Mariboru

dLib DIGITALNA KNJIŽNICA SLOVENIJE

https://press.um.si/

University of Maribor

Faculty of Mechanical Engineering

FT2021